

University of Windsor

Scholarship at UWindor

Electronic Theses and Dissertations

Theses, Dissertations, and Major Papers

10-5-2017

Enzymatic treatment of azo-dyes with soybean peroxidase

Laura Gabriela Cordova Villegas
University of Windsor

Follow this and additional works at: <https://scholar.uwindsor.ca/etd>

Recommended Citation

Cordova Villegas, Laura Gabriela, "Enzymatic treatment of azo-dyes with soybean peroxidase" (2017).
Electronic Theses and Dissertations. 7245.
<https://scholar.uwindsor.ca/etd/7245>

This online database contains the full-text of PhD dissertations and Masters' theses of University of Windsor students from 1954 forward. These documents are made available for personal study and research purposes only, in accordance with the Canadian Copyright Act and the Creative Commons license—CC BY-NC-ND (Attribution, Non-Commercial, No Derivative Works). Under this license, works must always be attributed to the copyright holder (original author), cannot be used for any commercial purposes, and may not be altered. Any other use would require the permission of the copyright holder. Students may inquire about withdrawing their dissertation and/or thesis from this database. For additional inquiries, please contact the repository administrator via email (scholarship@uwindsor.ca) or by telephone at 519-253-3000ext. 3208.

Enzymatic treatment of azo-dyes with soybean peroxidase

By

Laura Gabriela Cordova Villegas

A Dissertation
Submitted to the Faculty of Graduate Studies
through the Department of Civil and Environmental Engineering
in Partial Fulfillment of the Requirements for
the Degree of Doctor of Philosophy
at the University of Windsor

Windsor, Ontario, Canada

2017

© 2017 Laura Gabriela Cordova Villegas

Enzymatic treatment of azo-dyes with soybean peroxidase

by

Laura Gabriela Cordova Villegas

APPROVED BY:

S. Ghosal, External Examiner

Department of Civil Engineering and Applied Mechanics

McGill University

I. Al-Aasm

Department of Earth & Environmental Sciences

R. Seth

Department of Civil and Environmental Engineering

J.K. Bewtra

Department of Civil and Environmental Engineering

N. Biswas, Co-Advisor

Department of Civil and Environmental Engineering

K.E. Taylor, Co-Advisor

Department of Chemistry & Biochemistry

25 August 2017

DECLARATION OF ORIGINALITY

I hereby certify that I am the sole author of this thesis and that no part of this thesis has been published or submitted for publication.

I certify that, to the best of my knowledge, my thesis does not infringe upon anyone's copyright nor violate any proprietary rights and that any ideas, techniques, quotations, or any other material from the work of other people included in my thesis, published or otherwise, are fully acknowledged in accordance with the standard referencing practices. Furthermore, to the extent that I have included copyrighted material that surpasses the bounds of fair dealing within the meaning of the Canada Copyright Act, I certify that I have obtained a written permission from the copyright owner(s) to include such material(s) in my thesis and have included copies of such copyright clearances to my appendix.

I declare that this is a true copy of my thesis, including any final revisions, as approved by my thesis committee and the Graduate Studies office, and that this thesis has not been submitted for a higher degree to any other University or Institution.

ABSTRACT

The presence of azo-dyes in water bodies represents an environmental problem due to their recalcitrant, toxic and in some cases carcinogenic characteristics. In this dissertation, a more complete analysis is presented which includes color removal, dye conversion, total amines (as aniline) and product degradation. Enzymatic treatment with soybean peroxidase (SBP) was studied to decolorize and degrade two impure azo-dyes, Acid Blue 113 (AB113; a di-azo dye) and Direct Black 38 (DB38; a tri-azo dye). A single-step process (direct enzymatic treatment) and a two-step process (zero-valent iron (Fe^0) reduction followed by enzymatic treatment) were compared to obtain the optimal conditions of pH, H_2O_2 concentration, enzyme concentration and reaction time for maximum decoloration, dye and products degradation as well as total amines removal. More than 95% decoloration and dye degradation was achieved for both dyes after single- and two-step processes. A two-step process was preferred for DB38, because, after Fe^0 reduction, the products (aniline and benzidine) were SBP substrates which needed low SBP and H_2O_2 concentrations for 95% removal. The lowest K_M value (data obtained from Michaelis-Menten plot) was for a simple and highly pure reference dye, Crocein Orange G (COG), followed by AB113 and then DB38. Evidence for azo-cleavage of COG due to direct enzymatic treatment was obtained, identified and quantified by high-performance liquid chromatography (HPLC) where aniline was produced. Mass spectrometry was used to confirm the presence of aniline after treatment.

An alternative for reducing the number of experimental runs during optimization and obtain valuable statistical parameters, response surface methodology (RSM; software program Minitab), was used to optimize and characterize the decoloration of AB113 and DB38. These methods showed that the parameters: pH, H₂O₂ and enzyme concentrations were statistically significant in the removal of azo-dye; in addition, the presence of curvature in the response surface, indicated a preference for a second-order model. Decoloration of more than 95% was obtained by the RSM model. For AB113 the optimal response obtained with Minitab model was 5.7 % and the experimental value under the same conditions was 8.0% (2.3% difference) while for DB38 the optimal Minitab response was 3.6% and 5.1% for the experimental value (1.5% difference). Equations were obtained to determine percent color remaining within the study area (for AB113 pH 3.6-5.3; enzyme 1.0-2.0 U/mL; H₂O₂ 1.0-3.0 mM and for DB38 pH 3.0-5.0; enzyme 2.5-3.5 U/mL; H₂O₂ 2.5-3.5 mM). A positive RSM result shows the reduction of experimental runs compared to the optimization of one-parameter-at-a-time which represent diminished analysis time.

DEDICATION

To mom and dad who always encourage me to follow my dreams and were there every step of the process, muchas gracias

Ale, Perla, Martin for the loving support during all these years

ACKNOWLEDGEMENTS

I would like to express my sincere gratitude to Dr. N. Biswas and Dr. K.E. Taylor for the continuous support during my PhD study, for the opportunity to work in their research group, for their patience and immense knowledge which always share with me. Also, I will like to extend my gratitude to Dr. Bewtra for his valuable suggestions and comments.

I would like to express my deep appreciation to the members of my committee, Dr. Seth, Dr. Al-Aasm, Dr. Ghoshal for their time and feedback in my thesis work.

I also want to thank Mr. Bill Middleton for his help and guidance during all my PhD research work, particularly in the lab. I have learned a lot from him. To Dr. Janeen Auld, for her guidance and patience with mass spectrometry.

Thanks to my colleagues and friends, past and present. Dr. Samar Mazloum was my first teacher in the lab. Wei Feng, Miao Chen, Debjani Mukherjee, Baturh Yarkwan, Kayven Beemer for their help and good times. To my volunteer students Sophie Glanz, Kiruthika Baskaran and Daniel Yee, thanks for your help.

I would like to recognize the financial assistance of CONACyT and express my gratitude to the University of Windsor.

A special thanks to my 'sister' Neda Mashhadi. You are my family-far from home, thank you for your support and help during these four years. To my friends in Windsor and México.

I would also like to thank my sister, M.S.M. Alejandra, for her help with statistics calculations and loving support, to my sister Perla and brother-in-law Victor for being always there for me. To my niece Maria José for bringing joy to my life. To my parents for being the most important support through my entire life, and always believe in me. To Martin for his unconditional support, encouragement and help during all these years, which made this journey easier.

TABLE OF CONTENTS

DECLARATION OF ORIGINALITY	iii
ABSTRACT.....	iv
DEDICATION	vi
ACKNOWLEDGEMENTS	vii
LIST OF TABLES	xii
LIST OF FIGURES	xiii
Chapter 1. Introduction	1
1.1 Synthetic dyes	1
1.2 Textile industry	2
1.3 Treatment of azo-dyes	3
1.4 Toxicity of azo-dyes.....	5
1.5 Initiatives and objectives	6
1.6 Scope.....	7
Chapter 2. Literature review	9
2.1 Enzymatic treatment.....	9
2.2 Peroxidases	9
2.2.1 Soybean peroxidase (SBP).....	11
2.2.2 Production of soybeans in Canada and other countries.....	12
2.3 Azo-dyes.....	13
2.3.1 Benzidine-based dyes	15
2.3.2 Benzidine.....	15
2.3.3 Aniline	15
2.4 Enzymatic treatment of textile dyes.....	16
2.5 Zero-valent iron reduction of azo-compounds.....	17
2.5.1 Fe ⁰ reduction process	18
2.6 Response surface methodology (RSM)	19

2.6.1 Second-order model	21
Chapter 3. Materials and methods	24
3.1 Materials	24
3.1.1 Azo-dyes, aniline, benzidine, 3-aminobenzenesulfonic acid	24
3.1.2 Enzymes	24
3.1.3 Reagents.....	24
3.1.4 Buffer and solvents	24
3.1.5 Others	24
3.2 Analytical and laboratory equipment	25
3.2.1 UV-VIS Spectrophotometry.....	25
3.2.2 HPLC (High Performance Liquid Chromatography).....	25
3.2.3 Total Organic Carbon (TOC) analysis.....	25
3.2.4 Sonicator	25
3.2.5 Centrifuge and pH meter	25
3.2.6 Software.....	26
3.3 Analytical methods	26
3.3.1 Soybean Peroxidase (SBP) Activity Assay.....	26
3.3.2 Color reduction	26
3.3.3 Anilines colorimetric assay.....	27
3.3.4 Product determination by HPLC	27
3.3.5 TOC analysis	28
3.3.6 Buffer preparation	28
3.3.7 Enzyme stock solution preparation	28
3.3.8 Batch reactors for color reduction and dye degradation. Single- step process	28
3.3.9 Iron preparation.....	29
3.3.10 Iron pretreatment- enzymatic treatment. Two- step process.....	29
3.3.11 Kinetics.....	30
3.3.12 Product identification after single-step process.....	30
3.3.13 Response-surface methodology	31
3.4 Sources of error	32
Chapter 4. Results and discussion.....	33

4.1 Decoloration with single-step process.....	33
4.1.1 pH optimization.....	33
4.1.2 H ₂ O ₂ optimization.....	35
4.1.3 Enzyme optimization	37
4.1.4 Time dependence	41
4.1.5 Initial rates, first-order model for decoloration.....	42
4.1.6 Michaelis-Menten kinetic studies.....	45
4.2 Two-step process. Products and total amines removal for azo-dyes.....	53
4.2.1. Color reduction after zero-valent iron reduction AB113.....	53
4.2.2 pH optimization, second-step of two-step process. Enzymatic treatment for AB113.....	56
4.2.3 H ₂ O ₂ optimization, second-step of two-step process. Enzymatic treatment for AB113.....	57
4.2.4 Enzyme optimization, second-step of two-step process. Enzymatic treatment for AB113	59
4.2.5. Color reduction after zero-valent iron reduction DB38.....	61
4.2.6. pH optimization, second step enzymatic treatment for DB38	64
4.2.7. H ₂ O ₂ optimization second step enzymatic treatment for DB38	69
4.3 TOC removal for single-step and two-step process.....	71
4.4 COG azo-cleavage evidence.....	73
4.4.1HPLC analysis	74
4.4.2 MS results	78
4.4.4 Other products identified	82
4.5 Optimization for decoloration of azo-dyes using response surface methodology (RSM).....	86
4.5.1. Factorial design for AB113	86
4.5.1.1. Variance analysis (ANOVA)	91
4.5.1.2. Estimate the model and lack-of-fit test	92
4.5.1.3. Second-order search. Box-Behnken design	94
4.5.1.4. Factorial design second order (Box-Behnken design).....	96
4.5.1.5 Contour and surface plots for AB113.....	101
4.5.1.6 Optimized response for AB113	103
4.5.1.7 AB113 second-order design, second approach	105

4.5.1.8 Analysis of variance ANOVA and estimate the model and lack-of-fit test	105
4.5.1.9 Second-order search. Box-Behnken design	107
4.5.1.10 Contour and surface plots second approximation.....	108
4.5.1.11 Optimized response for AB113, second approximation	110
4.5.2. Factorial design for DB38.....	111
4.5.2.1 Variance analysis (ANOVA)	112
4.5.2.2 Estimate the model and lack-of-fit test	113
4.5.2.3 Second-order search. Box-Behnken design	114
4.5.2.4. Countour and surface plos for DB38.....	118
4.5.2.5. Optimum response for DB38	120
4.5.2.6. DB38 second-order design, second approach	121
4.5.2.7 Variance analysis (ANOVA)	122
4.5.2.8. Estimate the model and lack-of-fit test	123
4.5.2.9 Second-order search. Box-Behnken.....	124
4.5.2.10. Countour and surface plos for DB38.....	128
4.5.2.11. Optimum response for DB38	130
Chapter 5. Summary and Conclusions.....	132
5.1 Summary	132
5.2 Conclusions.....	135
Chapter 6. Recommendations	137
REFERENCES	138
APPENDIX A. CALIBRATION CURVES	152
APPENDIX B. 3-ABS ENZYMATIC TREATMENT	158
APPENDIX C. MINITAB EXPERIMENTAL RUNS.....	160
VITA AUCTORIS	168

LIST OF TABLES

Table 1. Area harvested and production of various countries as February, 2017 (USDA, 2017)	13
Table 2. Single-step enzymatic process. Optimal conditions for both dyes	45
Table 3. Kinetic parameter for Michaelis-Menten for azo-dyes.....	51
Table 4. Kinetic parameters for Lineweaver-Burk plot for azo-dyes	51
Table 5. Two-step process optimal conditions for AB113 and DB38.....	71
Table 6. Optimal conditions for aniline formation after enzymatic treatment of 1 mM COG	76
Table 7. Values for the three levels for AB113	89
Table 8. Treatments and combinations for first-order research for AB113 (H ₂ O ₂ in mM, enzyme in U/mL).....	90
Table 9. Treatments used for Box-Behnken design for AB113 (H ₂ O ₂ in mM, enzyme in U/mL)	97
Table 10. Values for the three levels for AB113, second approach (H ₂ O ₂ in mM, enzyme in U/mL)	105
Table 11. Values for the 3 levels for DB38 (H ₂ O ₂ in mM, enzyme in U/mL)	111
Table 12. Treatments and combination for DB38 (H ₂ O ₂ in mM, enzyme in U/mL).....	111
Table 13. Treatment used for Box-Behnken design for DB38 (H ₂ O ₂ in mM, enzyme in U/mL)	115
Table 14. Values for the 3 levels for DB38 (H ₂ O ₂ in mM, enzyme in U/mL)	121
Table 15. Treatments and combination for DB38 (H ₂ O ₂ in mM, enzyme in U/mL).....	121
Table 16. Treatment used for Box-Behnken for DB38 (H ₂ O ₂ in mM, enzyme in U/mL) ...	125
Table 17. Summary for Minitab model and one parameter at the time for both azo-dyes	131
Table C. 1. Order for runs in first-order search for AB113.....	160
Table C. 2. Order for runs in Box-Behnken design with two replicates for AB113.....	161
Table C. 3. Order for runs in first-order search for AB113, second approach.....	162
Table C. 4. Order for runs in Box- Behnken design with two replicates for AB113, second approach	163
Table C. 5. Order for runs first-order search for DB38	164
Table C. 6 Order for runs in Box-Behnken design with two replicates for DB38.....	165
Table C. 7. Order for runs first-order search for DB38, second approach.....	166
Table C. 8. Order for runs in Box- Behnken design with two replicates for DB38, second approach	167

LIST OF FIGURES

Figure 1. Examples of chromophoric groups present in organic dyes.....	2
Figure 2. Area harvested for all years in Canada of soybean. Data reported on 2/2017 ...	12
Figure 3. Azo- dyes used for this thesis work	14
Figure 4. Box-Behnken geometric representation.....	20
Figure 5. RSM for dye decoloration	21
Figure 6. Maximum surface plot	22
Figure 7. Surface with valley	22
Figure 8. Surface with minimax	23
Figure 9. pH optimization for 1 mM AB113 with 2.0 U/mL SBP, 2.5 mM H ₂ O ₂ , 3 hour reaction at room temperature.....	34
Figure 10. pH optimization for 0.5 mM DB38 with 2.0 U/mL SBP, 2.5 mM H ₂ O ₂ , 3 hour reaction at room temperature.....	35
Figure 11. H ₂ O ₂ optimization for 1 mM AB113 at pH 4.0 and 4.6 with 3.0 U/mL of SBP, 3 hour reaction at room temperature	36
Figure 12. H ₂ O ₂ optimization for 0.5 mM DB38 at pH 3.6 with 3.0 U/mL of SBP, 3 hour reaction at room temperature.....	37
Figure 13. Enzyme optimization with for 1 mM AB113 with pH 4.0 and 4.6 with 2.5 mM H ₂ O ₂ , respectively, 3 hour reaction at room temperature	38
Figure 14. Second pH optimization for 1 mM AB113 with 2.0 mM H ₂ O ₂ and 2 U/mL SBP, 3 hour reaction at room temperature	39
Figure 15. Enzyme optimization for 0.5 mM DB38 with pH 3.6, 2.5 mM H ₂ O ₂ or 3 mM H ₂ O ₂ , 3 hour reaction at room temperature	40
Figure 16. Time dependence for 1 mM AB113 using 2.5 mM H ₂ O ₂ and 0.05 U/mL or 1.5 U/mL at pH 4.0, at room temperature	41
Figure 17. Time dependence for 0.5 mM DB38 with 2.5 mM H ₂ O ₂ and 2.0 U/mL or 3 U/mL at pH 3.6, at room temperature	42
Figure 18. First-order reaction for 1 mM AB113	43
Figure 19. First-order reaction for 0.5 mM DB38	44
Figure 20. Initial velocities for AB113. Reactions with 0.125 mM H ₂ O ₂ , 0.0015 U/mL SBP and pH 4.0, at room temperature	45
Figure 21. Initial velocities for DB38. Reactions with 0.125 mM H ₂ O ₂ , 0.0015 U/mL SBP and pH 3.6, at room temperature	46
Figure 22. Initial velocities for COG. Reactions with 0.125 mM H ₂ O ₂ , 0.0025 U/mL SBP and 40 mM pH 8.0, at room temperature	46
Figure 23. Michaelis-Menten plot for AB113.....	48
Figure 24. Michaelis-Menten plot for DB38.	48
Figure 25. Michaelis-Menten plot for COG.....	49
Figure 26. Lineweaver-Burk plot for AB113.....	49

Figure 27. Lineweaver-Burk plot for DB 38.....	50
Figure 28. Lineweaver-Burk plot for COG.....	50
Figure 29. Color reduction after zero-valent iron treatment of 1 mM AB113 using different Fe ⁰ concentrations in the presence of 1 mM sodium sulfite.	53
Figure 30. Azo-cleavage of AB113 by zero-valent iron reduction	54
Figure 31. Time course for decoloration of 1 mM AB113 and formation of 3-ABS (mM) after iron reduction using 1g Fe ⁰	55
Figure 32. pH optimization for 0.8 mM 3-ABS with 1.5 U/mL SBP and 2.5 mM H ₂ O ₂	56
Figure 33. pH optimization for 0.85 mM total amines with 1.5 U/mL SBP and 2.5 mM H ₂ O ₂	57
Figure 34. H ₂ O ₂ optimization for 0.8 mM 3-ABS with 1.5 U/mL SBP at pH 4.0	58
Figure 35. H ₂ O ₂ optimization for 0.85 mM total amines with 2.5 U/mL SBP at pH 4.0.....	58
Figure 36. Enzyme optimization for 0.8 mM 3-ABS with 2.5 mM H ₂ O ₂ at pH 4.0	59
Figure 37. Enzyme optimization for 0.85 mM total amines using 2.5 mM H ₂ O ₂ at pH 4.0	60
Figure 38. Total amines after single-step process for 1 mM AB113 with 2.5 mM H ₂ O ₂ at pH 4.0	61
Figure 39. Color reduction after iron zero-valent of 0.5 mM DB38 using different Fe ⁰ concentrations in the presence of 1 mM sodium sulfite.....	62
Figure 40. Azo-cleavage for DB38 after zero-valent iron reduction	63
Figure 41. Time course of decoloration of 0.5 mM DB38 and formation and subsequent formation of aniline and benzidine after iron reduction using 1 g Fe ⁰	64
Figure 42. pH optimization of 1.5 mM total amines with 0.5 U/mL SBP and 1 mM H ₂ O ₂ .	65
Figure 43. pH optimization of 1.5 mM total amines from 0.5 mM DB38 with 0.5 U/mL SBP and 0.5 mM H ₂ O ₂	65
Figure 44. pH optimization for 0.33 mM aniline and 0.35 mM benzidine with 0.5 U/mL SBP and 1 mM H ₂ O ₂	66
Figure 45. pH optimization for 0.33 mM aniline and 0.35 mM benzidine with 0.5 U/mL SBP and 0.5 H ₂ O ₂	67
Figure 46. pH optimization for 0.33 mM aniline and 0.35 mM benzidine with 0.2 U/mL SBP and 1 mM H ₂ O ₂	68
Figure 47. Enzyme optimization for 0.33 mM aniline and 0.35 mM benzidine with 1 mM of H ₂ O ₂ at pH 5.0.....	68
Figure 48. Enzyme optimization for 1.5 mM total amines with 1 mM of H ₂ O ₂ , pH 5.0.....	69
Figure 49. H ₂ O ₂ optimization for 0.33 mM aniline and 0.35 mM benzidine with 0.6U/mL SBP	70
Figure 50. H ₂ O ₂ optimization for 1.5 mM total amines with 0.6U/mL of SBP	70
Figure 51. TOC remaining for single and two-step processes for AB113 and DB38.....	72
Figure 52. Aniline produced after enzymatic treatment of 1 mM COG with different SBP and H ₂ O ₂ concentrations (mM) at pH 8	74
Figure 53. COG degradation under HPLC and spectroscopy for different SBP and H ₂ O ₂ concentrations (mM) with pH 8.....	75

Figure 54. Degradation of COG with 1 mM spiked aniline with 0.75 U/mL and 0.5, 1.0 and 1.5 mM H ₂ O ₂ at 180 minutes reaction.....	76
Figure 55. Aniline remaining by HPLC in spiked solutions.	77
Figure 56. COG degradation with spiked (1mM) and non-spiked aniline with 0.75 U/mL SBP and 0.5 mM H ₂ O ₂	78
Figure 57. ESI-MS (+) for pure aniline; m/z from 85 to 105.....	79
Figure 58. ESI-MS (+) for aniline produced after enzymatic treatment.....	80
Figure 59. ESI-MS (+) for aniline produced after enzymatic treatment.....	81
Figure 60.ESI-MS (+) for aniline produced after enzymatic treatment	82
Figure 61.ESI-MS (+) for product formed with m/z 184.0725 after enzymatic treatment	83
Figure 62. ESI-MS (+) for product with m/z 275.1168 after enzymatic treatment.....	83
Figure 63. ESI-MS (-) for dye remaining detected (m/z 327.0443)	84
Figure 64. ESI-MS (-) for dimer of the dye product (m/z 325.0283)	85
Figure 65. Flowchart with the general steps used for dimensional reduction step (screening step).....	87
Figure 66. Flowchart with the general steps used for search I or first-order search	88
Figure 67. Geometrical representation of the parameters: pH, enzyme and H ₂ O ₂	89
Figure 68. Cube plot (fitted means) for the response (color remaining).....	90
Figure 69. ANOVA analysis for AB113 (first-order search)	91
Figure 70. Residual plot for % remaining for AB113.....	93
Figure 71. Flowchart for second-order model search steps	95
Figure 72. Geometrical representation of the parameters for search II with Box-Behnken design.....	96
Figure 73. ANOVA analysis for Box-Behnken.....	98
Figure 74. ANOVA analysis without effect of interactions “enzyme*pH” and “enzyme*H ₂ O ₂ ”	100
Figure 75. Contour plots for AB113. Fixed values: a) enzyme 2.0 U/mL, b) H ₂ O ₂ 3.0 mM, c) pH 5.3	101
Figure 76. Surface plots. Fixed values: a) enzyme 2.0 U/mL, b) H ₂ O ₂ 3.0 mM, c) pH 5.3	102
Figure 77. Optimization graph for AB113	104
Figure 78. ANOVA analysis for AB113 (first-order search), second approach.....	105
Figure 79. Residual plot for % remaining for AB113, second approximation.....	106
Figure 80. ANOVA analysis for Box-Behnken, second approach	107
Figure 81. ANOVA analysis without the non-significant interactions.....	107
Figure 82. Contour plot for AB113. Fixed values: a) enzyme 1.5 U/mL, b) H ₂ O ₂ 2.0 mM, c) pH 4.45.....	108
Figure 83. Surface plots. Fixed values: a) enzyme 1.5 U/mL, b) H ₂ O ₂ 2.0 mM, c) pH 4.45	109
Figure 84. Optimization graph for AB113, second approximation	110
Figure 85. ANOVA analysis for DB38.....	112
Figure 86. Residual plots for % remaining for DB38	114
Figure 87. ANOVA analysis for Box-Behnken for DB38.....	116

Figure 88. ANOVA analysis without the effects of “enzyme*enzyme” and “pH *H ₂ O ₂ ” factors	117
Figure 89. Contour plots for DB38. Fixed values: a) enzyme 2.25 U/mL, b) H ₂ O ₂ 2.25 mM, c) pH 4.0	118
Figure 90. Surface plots. Fixed values: a) enzyme 2.25 U/mL, b) H ₂ O ₂ 2.25 mM, c) pH 4.0	119
Figure 91. Optimization graph for DB38	120
Figure 92. ANOVA analysis for DB38.....	122
Figure 93. Residual plots for % remaining for DB38	124
Figure 94. ANOVA analysis for Box-Behnken for DB38.....	125
Figure 95. ANOVA analysis without the main effect of “pH*H ₂ O ₂ ” and “enzyme *H ₂ O ₂ ”	127
Figure 96. Contour plots for DB38. Fixed values: a) enzyme 2.5 U/mL, b) H ₂ O ₂ 2.5 mM, c) pH 3.0.....	128
Figure 97. Surface plots. Fixed values: a) enzyme 2.5 U/mL, b) H ₂ O ₂ 2.5 mM, c) pH 3.0	129
Figure 98. Optimization graph for DB38 (H ₂ O ₂ in mM, enzyme in U/mL)	130
Figure A. 1 Calibration curve for AB113 at 565 nm (spectroscopy).....	152
Figure A. 2 Calibration curve for AB11 at 536nm, pH 3.6 (spectroscopy)	152
Figure A. 3 Calibration curve for DB38 at 520 nm (spectroscopy).....	153
Figure A. 4 Calibration curve AB113 at 565 nm (HPLC)	153
Figure A. 5 Calibration curve DB38 at 520nm (HPLC)	154
Figure A. 6 Calibration curve for total amine test as aniline at 440nm	154
Figure A. 7 Calibration curve for 3-ABS at 235nm (spectroscopy).....	155
Figure A. 8 Calibration curve 3-ABS at 235nm (HPLC)	155
Figure A. 9 Aniline calibration curve at 280 nm (HPLC)	156
Figure A. 10 Benzidine calibration curve at 280 nm (HPLC)	156
Figure A. 11 TOC (mg/L) for different enzyme concentrations (U/mL)	157
Figure B. 1 pH optimization of 1 mM 3-ABS with 1 mM H ₂ O ₂ and 1 U/mL	158
Figure B. 2 Enzyme optimization of 1 mM 3-ABS with 1 mM H ₂ O ₂ , pH 3.6.....	158
Figure B. 3 H ₂ O ₂ optimization of 1 mM 3-ABS with 3 U/mL, pH 3.6.....	159

Chapter 1. Introduction

1.1 Synthetic dyes

Synthetic dyes have been extensively used in different types of industries such as textiles, food, leather, and printing, among others. World trade organizations before 1960s used to give information about worldwide productions of dyes, however this doesn't happen anymore (Zollinger, 2013). As some reviews reported, it is estimated that over 0.7 million tons of synthetic dyes are produced worldwide, from which almost 200,000-280,000 tons are released to the ecosystem from mainly dyeing and finishing operations in the industry (Ali *et al.*, 2013; Chequer *et. al.*, 2013; Husain, 2006). In Canada, there are 1085 textile-manufacturing plants specifically in Quebec and Ontario. The clothing or apparel industry (2465 plants) is the largest single consumer of textiles (Davidson, 2013). United States Environmental Protection Agency (EPA) estimates that 36 plants in the United States generate and manage organic dyes (azo, triarylmethane and anthraquinone dyes) which generates approximately 36,000 metric tons of potentially dangerous waste (United States Environmental Protection Agency, 2005).

Normally, 1 mg/L gives visible color to water bodies; however concentrations up to 300 mg/L have been reported in textile manufacturing processes. Textile dyes represent the most problematic compounds in textile wastewater due to high toxicity, high water solubility, and recalcitrant nature (Pandey *et al.*, 2007). Furthermore, some dyes are potentially carcinogenic, mutagenic and genotoxic (Ali *et al.*, 2013; Kalsoom *et al.*, 2013), and they are aesthetically unacceptable. The possible breakdown products, such as aromatic amines, have a negative impact in the environment and in the living organisms (Weisburger, 2002). For all these reasons it is important to have adequate removal technologies.

In textile industries, due to inefficient dyeing process, large amounts of dyes and other chemicals are released to the environment or to the system that will go to a wastewater treatment facility (Ventura-camargo *et al.*, 2013).

A dye is a chemical which gives color to a material, the color imparted is due to the chromophore group of the dye. Based on this, chromophore group chemical structure, there are around 30 groups of dyes. Dyes can be classified into: azo (mono-azo, di-azo, tri-azo, poly-azo), anthraquinone, triarylmethane, indigoid, and polycyclic aromatic carbonyl dyes (Figure 1). The azo-group is normally connected to an aromatic ring such as benzene or naphthalene. There are several classes of azo-dyes, the most common are: acid, basic, reactive, direct, and mordant (Sudha *et al.*, 2014). Based on the substituents of the dyes they can be water-soluble or insoluble. The reactive dyes are water soluble due to the sulfonate or carboxylate group in their molecule and are used for dyeing fibers like cotton, wool, silk and nylon. On the other hand, water insoluble dyes like disperse dyes contain chloro- or nitro-substituents; this type of dyes is usually used for nylon, acrylic, plastic and polyester (Nam, 1998; Gregory, 1990; Husain, 2006). Direct dyes are used for cotton, rayon, paper, leather and nylon, while acid dyes can be used for nylon, wool, silk, paper, inks, and leather (Husain, 2006). Marechal *et al.* (1997) estimates that around 3000 dyes are available to the industry where half of them belong to azo-dye group.

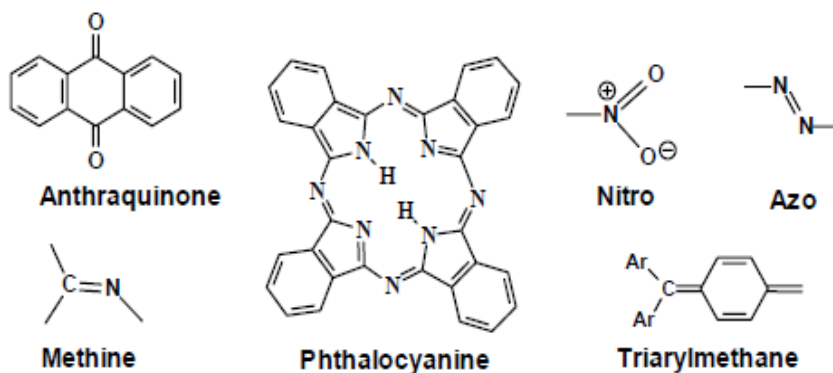


Figure 1. Examples of chromophoric groups present in organic dyes

IARC, 2010

1.2 Textile industry

The textile industry uses natural and man-made fibers to transform into yarns and threads, which will also be transformed into fabrics that will be subjected to dyeing and finishing. A common textile industrial facility includes the processes of: desizing, scouring,

bleaching, mercerizing and dyeing. During the dyeing process, color is added to the fibers, requiring a large amount of water and other compounds like metals, salts surfactants (United States Environmental Protection Agency, 1997; Carmen and Daniela, 2012). During the dyeing of cotton, approximately 1450-4750 ADMI (American Dye Manufacturer's Institute color index) color is discharge on wastewater (Cooper, 1995; Carmen and Daniela, 2012). The most coloured effluents are due to the presence of textile dyes, pigments and other colored compounds and come from dyeing and rinsing steps; they also have high variability in parameters like COD, BOD, pH, salinity and temperature (Carmen and Daniela, 2012).

1.3 Treatment of azo-dyes

To remove color caused by dyes in effluents, several methods have been studied such as membrane filtration processes (including nanofiltration) biological treatment, coagulation/flocculation, reverse osmosis, electrodialysis, ion exchange, sorption techniques and liquid-phase extraction (LPE) (Crini, 2006; Akceylan and Erdemir, 2015). As reviewed by Mohan *et al.* (2002) chemical and physicochemical treatments are effective in removing dyes, but represent a problem due to high cost and regeneration problems. For example, active carbon used in adsorption, results in a toxic sludge which presents a problem of disposal. On the other hand, biological treatment has been an attractive alternative due to several advantages such as lower cost, environmentally friendly, allowing complete mineralization of the dyes, as well as lower production of sludge compared to chemical or physical methods (Mohan *et al.*, 2002; Puvaneswari *et al.*, 2006; Solis *et al.*, 2012). Several microorganisms, such as bacteria, fungi or yeast have been investigated to decolorize textile wastewater, through the release of enzymes by which azo-dyes can be reduced to simpler compounds that can be mineralized easier. These enzymes can be peroxidases, reductases and laccases, among others (Sudha *et al.*, 2014; Neifar *et al.*, 2011). It has been reported that some algae species were able to reduce azo-dyes to aromatic amines which can be further treated. Mohan *et al.* (2002) demonstrate that a *Spirogyra* species was able to decolorize the azo-dye reactive, yellow 22 after 3 days;

the decoloration was done by biosorption, bioconversion and biocoagulation processes. For reductive bio-decolorization processes, the more electron-withdrawing groups an azo-dye has the faster the decoloration will be; also if they are in *ortho*- or *para*-position decoloration is faster than in *meta*-position, since it provides a stronger resonance effect (Solis *et al.*, 2012; Zhang *et al.*, 2012). For oxidative decoloration, the more electro-donating groups and less steric hindrance in the azo-dye favor the decoloration (Zhang *et al.*, 2012).

Physical methods include filtration (ultra-filtration, reverse osmosis) and adsorption processes. These methods are used when they have to be included in an already established plant water system. Adsorption methods, such as activated carbon, are not efficient in the decoloration of dye solutions since they require long times. However, bio-sorption is a promising method, which uses low-cost adsorbents to bind the compound of interest to biomass. Gimenez *et al.* (2014) used fungal biomass (*Lentinus edodes*) which possesses enzymes (lignin, and manganese peroxidases and laccase) immobilized in loofa sponge to bio-sorb several synthetic dyes, where more than 90% removal of dyes was achieved.

Chemical processes include coagulation and flocculation, oxidation or electrochemical methods. Processes involving ozone or photo-Fenton conditions are effective in the decoloration process and have been reported to achieve complete mineralization of dyes. However, such processes have high cost of installation such as ozone generator or high cost of chemicals involve in the coagulation process and it also has high production of sludge (Lokesh and Kiran, 2014). Qiu *et al.* (2014), compare the efficiency of photo-Fenton and UV/TiO₂ processes, both shown to be effective in the removal of an azo-dye (Reactive Black 5). However, the photo-Fenton process was more efficient and faster in the initial stages (before 45 minutes); efficiency depends on factors such as initial concentration of dye, iron, TiO₂, hydrogen peroxide and pH. Ozonation of an azo-dye was investigated by Tizaoui *et al.* (2011) where the stoichiometric ratio was 3 mol O₃/mol of dye. Moreover, when pH was increased to 11, 95% removal was achieved in 3 minutes. Also the ozone inlet concentration played an important role in the decoloration, for example at pH 7 for

90% removal at 25 mg/L of dye, it requires 20 g/m³ NTP in 3.4 minutes, while at 50 mg/L of dye with the same ozone concentration, the time needed was 8.6 minutes (Tizaoui *et al.*, 2011).

A combination of processes has also been reported to increase the efficiency over an individual process. For example, zero-valent iron reduction combined with anaerobic sludge digestion has been proved to increase the efficiency of decoloration approximately 30% of an azo-dye compared to the sum of the individual systems (reactive blue 13). The presence of iron modifies the sludge morphology and structure of the microbial community, the increase of efficiency is due to the more favorable conditions of pH and anaerobic environment after adding zero-valent (ZV) iron as well as the direct chemical removal (Li *et al.*, 2013).

Enzymatic treatment has been successful for dye decoloration. Under mild condition, which is an advantage, besides being able to convert complex chemical compounds into insoluble compounds which can be subsequently removed by conventional filtration (Husain, 2006; Husain, 2010; Ali *et al.*, 2013; Kalsoom *et al.*, 2013).

1.4 Toxicity of azo-dyes

The presence of dyes in aquatic ecosystems presents a public health problem and it is an aesthetic problem. The presence of dyes in water streams results in a diminished in light flux for aquatic organisms (Ventura-Camargo B. *et al.*, 2013). The potential carcinogenicity of azo-dyes is due to the dyes themselves or amines produced by their reduction (Nam, 1998). Most of the dyes can be absorbed through the skin or by inhalation. Benzidine-based dyes are carcinogenic as discussed later. Through discharge in wastewater they are readily available through the food chain (Sudha *et al.*, 2014). In general, azo-dyes are toxic, in terms of genotoxicity, mutagenicity and carcinogenicity to aquatic organisms. In mammals, hepatic azoreductases (liver or intestine flora) are able to reduce azo-dyes into amines which are carcinogenic. Furthermore, they can cause soil pollution and problems with plant growth when discharged on the soil (Puvanewari *et al.*, 2006). Maguire and Tkacz (1991) detected 14 different dyes in the Yamaska River in Quebec during two year measurements, the first study that detected the presence of dyes in the environment.

1.5 Initiatives and objectives

Decoloration of high purity azo-dyes has been studied using enzymatic treatment with horseradish peroxidase (Gholami-Borujeni *et al.*, 2011; Onder *et al.*, 2011), and soybean peroxidase (Ali *et al.*, 2013; Kalsoom *et al.*, 2013) as well as other processes, such as zero-valent iron reduction (Cao *et al.*, 1999; Fan *et al.*, 2009). However, an assessment in the product formation and total amines production should be done in order to determine and compare the effectiveness of both processes in terms of dye, product and color degradation and the concentrations of SBP and H₂O₂ as well as the pH required. Therefore, this dissertation used two impure model compounds of the azo-dyes which were subject to single-step process with SBP in the presence of H₂O₂ and a two-step process using zero-valent iron reduction followed by SBP treatment, in order to determine which is the optimal process based on the parameter requirements and removal efficiency.

Rather than one-parameter-at-a-time optimization, an alternative is to optimize the decoloration of azo-dyes using response surface methodology. This methodology has been used to study the decoloration of dyes with laccase (Daassi *et al.*, 2012; Roriz *et al.*, 2009; Neifar, 2011), *Pseudomonas* (Jadhav *et al.*, 2012; Senthilkumar *et al.*, 2013) and the bacterium *Bacillus subtilis* (Sharma *et al.*, 2009). An advantage of RSM is the lower number of experimental runs needed which represents time and cost savings. However, to our best knowledge RSM with SBP decoloration and comparison with optimization one-parameter-at-a-time has not been done for AB113 and DB38. For this reason, this dissertation uses RSM to obtain optimization parameters for AB113 and DB38 and compare the number of experimental runs versus optimization one-parameter-at-a-time.

An important consideration to any degradation study is the mechanistic pathways. For SBP treatment, mechanism pathways, with azo-dyes have not been extensively studied. The possibility of the azo-splitting by SBP has been qualitatively studied (Kalsoom *et al.*, 2013; Ali *et al.*, 2013; Onder *et al.*, 2011), however, there is no attempt in quantifying the release of the products resulting from azo-cleavage. In this study, an approach to quantify aniline as a product of COG azo-splitting by HPLC was made and the presence of it was confirmed with electro-spray mass spectrometry (EI-MS).

The objectives for this dissertation were:

1. Optimize direct SBP decoloration and degradation in the presence of H_2O_2 of two impure azo-dyes: a di-azo dye, Acid Blue 113, and a tri-azo dye, Direct Black 38
2. Optimize iron reduction followed by SBP-catalyzed degradation for both dyes
3. Develop an experimental design in Minitab 16, for direct decoloration of the azo-dyes
4. Get evidence for azo splitting of a model compound (COG) after enzymatic treatment

1.6 Scope

The scope of this dissertation includes:

1. Optimize direct SBP decoloration and degradation in the presence of H_2O_2 of two impure azo-dyes: a di-azo dye, Acid Blue 113, and a tri-azo dye, Direct Black 38
 - Investigate the SBP capability for direct decoloration and degradation of azo-dyes (AB113 and DB38) with pH, H_2O_2 and enzyme optimization to achieve $\leq 5\%$ color/dye remaining
 - Estimate kinetic parameters (K_M , V_{max} and V_{max}/K_M) for AB113, DB38 and COG with Michaelis-Menten and Lineweaver-Burk plots
 - Determine total organic carbon (TOC) and dye degradation under optimal conditions
 - Optimize total amines (as aniline) removal
2. Optimize iron reduction followed by SBP-catalyzed degradation for both dyes
 - Determine the optimal parameters for $\leq 5\%$ remaining: iron amount (for a fixed volume of solution treated), reaction time, color removal, reduction in product

concentrations and in total amines (as aniline) concentration, dye and TOC for AB113 and DB38 to assess the effectiveness of two-step process

- Compare the optimal conditions for single-step process and two-step process and determine the optimal treatment to achieve $\leq 5\%$ remaining of color, dye degradation and products with the lowest SBP and H_2O_2 concentrations.

3. Develop an experimental design in Minitab 16, for direct decoloration of the azo-dyes

- Develop a RSM for AB113 and DB38 using Box-Behken design in order to compare the optimization results with those for optimization one-parameter at the time (objective 1), and obtain contour and surface plots with the respective second-order equation that models the process and predicts percent color remaining in the area of study

4. Get evidence for azo splitting of a model compound (COG) after enzymatic treatment

- Determine, by HPLC, the formation (qualitative and quantitative analysis) of aniline as a product after single-step enzymatic treatment of the model compound COG (used due to simpler structure and high purity, 90%).
- Use the optimal conditions for aniline formation in HPLC to confirm the presence by EI-MS.
- Identify other possible products by EI-MS for azo-cleavage and/or radical polymerization

Chapter 2. Literature review

2.1 Enzymatic treatment

Aromatic compounds were treated with enzymes for the first time in the early 1980s using horseradish peroxidase (HRP) for the treatment of phenols and anilines compounds (Klibanov and Morris, 1981). Other studies were carried out using laccase for phenolic compounds (Bollag *et al.*, 1979), and since that times studies of enzymatic treatment have increased with time. Enzymatic treatment has several advantages compared to conventional methods, such as simplicity and easy to control, is fast, therefore small footprint, lower sludge production and high activity over a broad range of pH and temperature, as well as the specificity of the enzyme to the substrate. On the other hand, one disadvantage of the enzymatic treatment is the cost of the enzyme; however, advances in the industry make the application of enzyme a practical alternative (Steevensz *et al.*, 2014; Karam and Nicell, 1997). Enzymes are highly specific and can act under mild conditions of pH, temperature and pressure (Al-Ansari *et al.*, 2011).

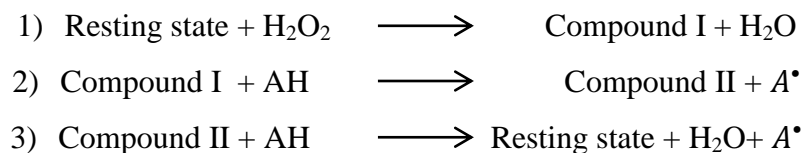
Oxidoreductases have been found to act on an extensive range of substrates. The main oxidoreductases, laccases and peroxidases, are used to treat several classes of compounds, including colored compounds such as dyes.

2.2 Peroxidases

The enzymes generate free radicals that can undergo a series of coupling and/or cleavage reactions. The most common peroxidase is horseradish peroxidase (HRP) (Henriksen *et al.*, 2001).

Peroxidases come from animal, plant, fungi or bacteria kingdoms. They are classified into three families based on their sequence homologies. Class I corresponds to the prokaryotic enzymes such as yeast or chloroplast. Class II peroxidases are secreted fungi, such as lignin or manganese enzymes. Class III are classical secretory plant peroxidases such as SBP, horseradish and peanut enzyme (Dunford, 1999; Al-Ansari *et al.*, 2011).

Peroxidases are hemoproteins which catalyze the oxidation of a broad range of organic and inorganic substrates in the presence of H₂O₂ (Cijzen *et al.*, 1993). The mechanism that they follow is a ping-pong mechanism (Dunford 1999):



From the first equation, native or resting state enzyme forms Compound I a 2-electron oxidation in reaction with H_2O_2 (electron acceptor). Compound I accepts an aromatic compound (AH) which undergoes a one-electron oxidation in the active site of the enzyme, releasing a free radical A^\bullet . Compound I reduced to compound II which can oxidize another aromatic compound releasing a second free radical and the enzyme returns to the resting state. Non-enzymatic coupling of the free radicals forms dimers, trimers, tetramers and oligomers (Nicell *et al.*, 1993; Ibrahim *et al.*, 2001; Al-Ansari *et al.*, 2011). The oligomers formed act as hydrogen donors that allows additional polymerization, forming compounds which are insoluble in water (Fersht, 1977). These compounds can be removed from the solution with processes such as sedimentation and filtration (Kilbanov and Morris, 1981). Peroxidases can catalyze a wide range of substrates in the presence of hydrogen peroxide, the H_2O_2 acts as the electron acceptor (Dunford and Stillman, 1976).

The active site of the enzymes consist of a catalytic site and a binding site, the first one is where the reaction occurs and the second one is where the substrate is held to undergo the reaction (Fersht, 1977; Al-Ansari *et al.*, 2011).

Examples of enzymes used for dye degradation are lignin peroxidase, laccases, horseradish peroxidase, tyrosinase, manganese peroxidase, etc. (Kalsoom *et al.*, 2013).

Inactivation of peroxidase represents a disadvantage in the enzymatic treatment. One possible inactivation can be due to the free radicals present in the process which can return to the active site and forms a covalent bond not allowing the substrate to access the active site stopping the catalytic process (Klibanov *et al.*, 1983). Another possibility is an excess of H_2O_2 or low reducing substrate concentration (Dunford, 1999). Also, the peroxidase can be adsorbed onto the polymerized substrate causing apparent inactivation (Nakamoto and Machida, 1992; Feng *et al.*, 2013).

2.2.1 Soybean peroxidase (SBP)

The soybean seed coats (hulls) are a by-product from crushing operations that are used as animal feed. After a washing process of these hulls with water, SBP can be extracted without compromising the feed value of the hulls. The activity of the SBP varies among the cultivars and seed coats (Buttery and Buzzell, 1968; Buzzell and Buttery, 1969; Gijzen, 1993; Gijzen *et al.*, 1997). Extraction of SBP can also be done with phosphate buffer ($\text{NaH}_2\text{PO}_4/\text{Na}_2\text{HPO}_4$, pH 6.0) followed by filtration and centrifugation (6000 rpm for 15 minutes) process to obtain the final supernatant (Ghaemmaghmi *et al.*, 2010).

SBP has several applications, from polymer and resin industry, baking industry, medical (as a replacement for HRP in ELISA assays) as well as wastewater treatment (Al-Ansari *et al.*, 2011; Sessa *et al.*, 2004). The peroxidase extracted from the hulls has higher activity than the peroxidase found in the root of leaf (Geng *et al.*, 2001). Organic solvents are used sometimes during enzymatic reaction in order to increase the solubility of substrates; however, Geng *et al.* (2001) found that the SBP activity decreases as the concentration of organic solvent increase. SBP is active in the presence of organic solvents such as acetonitrile, acetone, methanol or ethanol. Other authors have also demonstrated that SBP is active in organic solvents (acetone, methanol and ethanol) (Ghaemmaghmi *et al.*, 2010).

SBP (Enzyme Classification 1.11.1.7) is a heterogeneous glycoprotein that belongs to the family of class III (secretory plant peroxidases), is an oxidoreductase enzyme extracted from soybean seed coats (hulls) (Al-Ansari *et al.*, 2011 Dunford, 1999). SBP shows 57% amino acid sequence identity to HRP. The high thermal stability and reactivity and stability at low pH are some of the advantages of SBP compared to other peroxidases. For example, inactivation temperature is 90.5°C compared to HRP that is 81.5°C. Also, Henriksen *et al.* (2001) have demonstrated that SBP has a higher affinity for the haem than HRP isoenzyme C.

The use of soybeans represents an inexpensive source since the hulls are considered a low-value by product, it does not compete with animal feed or other land used, and also it is considered environmentally friendly replacing harsh chemicals (Nicell, 2003; Hailu *et al.*, 2010). The isolation of crude SBP represents a cheaper option that can be used in several applications in bioremediation and biocatalysis (Hailu *et al.*, 2010).

SBP has a molecular weight of 40660 Da, contains 17.7-18.2% carbohydrate, the secondary structure of the enzyme consists of 13 α -helices and 2 β -sheets. Fe (III) protoporphyrin IX, also called heme, is the active site of SBP. The heme consist of four pyrrole rings joined by methene-bridge (carbon atoms labeled α , β , γ and δ) with iron (III) complex at the center (Al-Ansari *et al.*, 2011; Henriksen *et al.*,2001; Dunford 1999). SBP has been used to remove several compounds. Phenolic compounds have been found to be removed by SBP, achieving 95% removal (Caza *et al.*, 1999). Anilines are other group of compounds that have been studied with SBP. Mantha *et al.* (2002) remove efficiently aromatic amines using a two-step process to remove anilines after iron zero-valent treatment of nitroaromatic compounds (nitrobenzene), *o*-, *m*- and *p*-nitrotoluenes where enzymatic treatment was conducted at pH 5.5-8.0, 1.5 mM H₂O₂ and enzyme concentration from 0.01-0.2 U/mL (Mantha *et al.*, 2002).

2.2.2 Production of soybeans in Canada and other countries

Soybeans are currently grown on an estimated 6% of arable land. The global production has increased almost 93% from 1960 to 2008 (17 million metric tons (MMT) to 230 MMT) (Hartman *et al.*, 2011). In Canada, USDA data available estimates that the area harvested up to February 2017 was more than 2,180,000 HA, with a production of 6,450,000 MT (Figure 2).

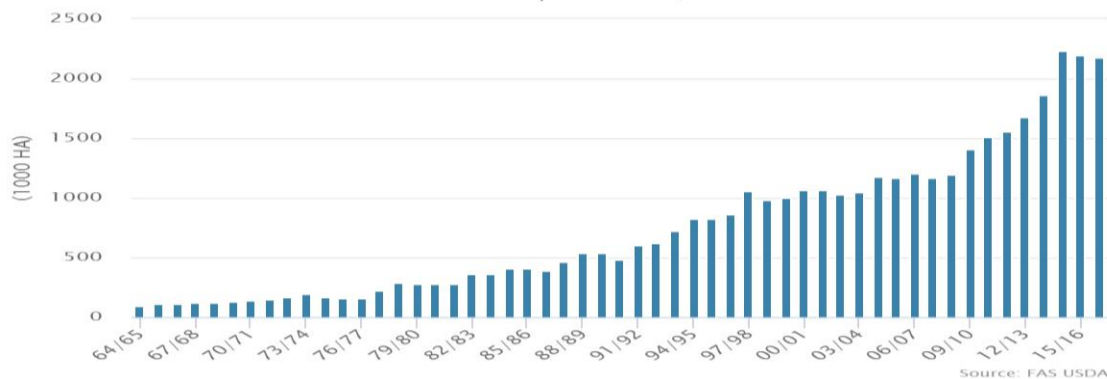


Figure 2. Area harvested for all years in Canada of soybean. Data reported on 2/2017

USDA, 2017

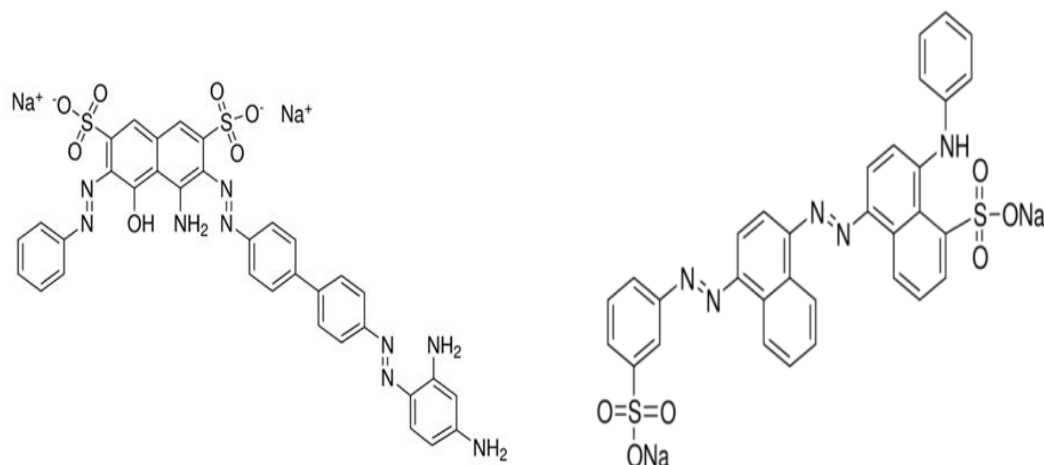
Soybean production has grown in about 23% in the province of Ontario, Quebec, Manitoba and Saskatchewan (USDA, 2017). Other countries production is shown in table 1.

Table 1. Area harvested and production of various countries as February, 2017 (USDA, 2017)

Country	Area harvested (HA)	Production (MT)
United States	33,482,000	117,208,000
Brazil	33,900,000	104,000,000
Argentina	19,000,000	55,500,000
Canada	2,180,000	6,450,000
Bolivia	1,133,000	2,107,000
Mexico	280,000	490,000

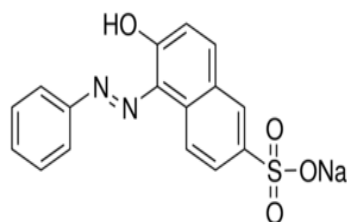
2.3 Azo-dyes

The azo-dyes are characterized by an azo-linkage (-N=N-) (Figure 3) and constitute more than 50% of all dyes produced in the world (Nam, 1998). These azo-dyes are used in several types of industries such as textile, food, printing, leather and paper among others. They are resistant to microbial degradation used in wastewater treatment plants, thus ending up sorbed on the flocs in the sludge (Bandala *et al.*, 2007). They are resistant to degradation on exposure to soil, bacteria and sunlight (Ganesh *et al.*, 1994).



Direct black 38 (Chlorazol black)

Acid blue 113



Crocein Orange G

Figure 3. Azo- dyes used for this thesis work

Acid blue 113 is an azo-dye used for dyeing wool, nylon and silk, blended-rayon fabric, leather and biological coloring of paper (Gupta *et al.*, 2011).

Manufacturers stopped using benzidine-based dyes, such as Direct black 38, in the 1970s (Environment Canada, 2009), however, it is still being imported to the EU (less than 500 kg). This represents a risk for consumers who are in contact with textiles which use this dye. These dyes can be used in dyeing cellulose, wool, silk, leather, plastics, vegetable-ivory buttons, wood flour used as resin filler and aqueous inks. They have also reportedly been used in hair dyes (Echa, 2013).

2.3.1 Benzidine-based dyes

EPA recognizes the potential cancerogenic danger of dyes derived from benzidine. Benzidine is a constituent from the aromatic amines family which is a precursor of synthetic dyes. Dyes derived from benzidine are well-known carcinogens to which the consumer is exposed. Direct black 38 is a benzidine-based dye listed by EPA as a “Benzidine-Based and Congener-Based Dyes with Potential to Degrade to Carcinogenic Amines” (United States Environmental Protection Agency, 2015). Azo-reduction of benzidine-dyes occurs in the human body and the skin, which represent a health problem (Golka *et al.*, 2004).

EPA preliminary risk assessment of these types of derivatives of benzidine and its congeners demonstrate the main hazard concern was the carcinogenic effects to humans (United States Environmental Protection Agency, 1980).

2.3.2 Benzidine

Benzidine is an aromatic amine used since 1850 in the manufacturing process of several dyes, nowadays prohibited in some countries; however, there is still small production in countries such as Germany, India and USA (IARC, 2010). People can be exposed when they come in contact with goods that contain benzidine such as clothes or toys (Garrigós *et al.*, 2002). Benzidine is classified as human carcinogenic by IARC (International Agency for Research of Cancer) (IARC, 2010; IARC 2012) in human bladder.

2.3.3 Aniline

Aniline is an aromatic amine (C_6H_7N). There isn't production of aniline in Canada, nevertheless some is imported which is used mostly in the production of rubber and polymers. In USA it is also used for the production of dyes and in the pharmaceutical industry. It is not expected to last long in the environment due to the short half-life of few weeks (Health Canada, 2013). It is classified as B2 possible human carcinogenic on IRIS system. Acute exposure can affect lungs and cause congestion, chronic effects include formation of methemoglobin that causes cyanosis, can irritate eyes, skin and respiratory tract (United States Environmental Protection Agency, 2002). Break down of azo-dyes to aromatic amines has been studied. Azo-reductase enzyme used to degrade Acid blue 113 give some intermediate metabolites such as aniline and various other after treatment.

Senthilvelan *et al.* (2014) confirmed the presence of these metabolites using GC-MS and MS-ESI.

2.4 Enzymatic treatment of textile dyes

Several authors have investigated the enzymatic treatment of dyes with different enzymes such as bacterial culture of azo-reductases (Senthilvelan *et al.*, 2014), laccase (Daassi *et al.*, 2012), manganese peroxidase detected in culture of *Phlebia tremellosa* (Kirby *et al.*, 2000) and SBP (Ali *et al.*, 2013; Kalsoom *et al.*, 2013), among others. Aromatic dyes can be degraded or transformed using peroxidases from different sources such as soybean, radish, turnip, manganese peroxidase or lignin peroxidase, among others, through a precipitation process or opening the ring of the structure. The use of redox mediators have been used to improve the dye degradation (Husain, 2010).

HRP has been used by several authors to degradate dyes. Ulson de Souza *et al.* (2007) studied decoloration of two dyes (Remazol Turquoise Blue and Lancet Blue 2 R) obtaining approximately 60 and 95% removal, respectively, achieving also a reduction in toxicity after enzymatic treatment, tested for toxicity towards *Daphna magna*. Kulshrestha and Husain (2007) investigate the decoloration of five acid dyes using turnip peroxidase achieving between 62 to 100 % color removal with HOBT (1-hydroxybenzotriazole) as a mediator.

For azo-dyes, Ali *et al.* (2013) studied the mechanism for degradation of azo-dye (Crystal Ponceau 6R, CP6R) with SBP complete degradation of 40 ppm azo-dye under optimal conditions (0.27 μ M SBP, pH 5, H₂O₂ 0.175 mM). Sadhanandam *et al.* (2013) studied the color degradation of Acid blue 113 with HRP, achieving 80% degradation with 0.08 U HRP (where U is measure as 1 μ L of the enzyme solution contained 10 U) in 45 minutes with pH 6.6, they also studied the immobilization of the HRP into beads which require more contact time (4 hours) for approximately 80% removal with a maximum recycle of 3 times. Mazloum (2014) studied the decoloration of two azo-dyes with SBP achieving, under optimal conditions, 85-95% color decoloration, with pH 8, 0.75 U/mL SBP and 3.5 mM H₂O₂.

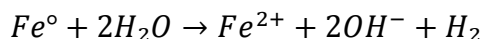
2.5 Zero-valent iron reduction of azo-compounds

The first application of zero-valent iron treatment is reported from 1972 by the patent of Sweeny and Fischer, where they used granular iron to degrade halogenated pesticides. The first studies using zero-valent process were focused on halogenated organics compounds mainly (Gillham and O'Hannesin, 1994; Orth and Gillham, 1995; Chuang *et al.*, 1995). However, since this, other compounds have been studied using zero-valent iron reduction such as dinitrotoluenes and azo-dyes (Patapas *et al.*, 2007; Biswas *et al.*, 2004; Nam and Tratnyek, 2000; Pereira and Freire, 2006). Zero-valent iron is considered an environmentally friendly reducing agent for these kinds of compounds which will be an adequate pre-treatment due to the resistance of azo-dyes to conventional treatment processes. Using zero-valent iron as pretreatment will allow cleaving the azo-molecules into products which are more suitable for treatment under biological processes. Where the dye molecule gets reduced and the iron is oxidized (Junyapoon, 2005). One advantage is the possibility of recycling the iron using magnetic techniques to recover it. New developments have been done trying to increase the surface area of the iron particles (increasing the activity of the Fe^0 with more active sites per surface area) to decrease the reaction time (Fan *et al.*, 2009); this has been done using nanoscale zero-valent iron (NZVI). Fan *et al.* (2009) demonstrated the effective decoloration of azo-dye methyl orange with synthesized NZVI with a size of 20-80 nm, which requires approximately 60 minutes to achieve 90% decoloration. Formation of products such as sulfanilic acid, N,N-dimethyl-*p*-phenylenediamine and N-methyl-*p*-phenylenediamine using GC-MS (Fan *et al.*, 2009) was also demonstrated. Azo-bond cleavage results in loss of the visible absorbance band after iron treatment for azo-dyes due to the formation of aromatic amines after-bond breakage (Nam *et al.*, 2000; Cao *et al.*, 1999; Pereira and Freire 2006). For example, Cao *et al.* (1999) reported a decrease for Acid Orange II in absorbance at 483 nm and an increase in the range from 191-228. These aromatic amines are toxic, thus requiring further treatment (Nam *et al.*, 2000). For this reason, in this thesis work, the concentration of total aromatic amines and of the products after Fe^0 reductions were measured and SBP in the presence of peroxide was used to treat them. Iron reduction has been reported to efficiently decolorize dye solutions. Pereira and Freire (2006) achieved 95% color removal and 70% TOC removal for Remazol Black B under acidic conditions

(pH 3) and 0.5 g/L of recycling iron (250 μm) for 15 minutes. Nam and Tratnyek (2000), studied reduction of 9 azo-dyes using zero-valent iron, for all dyes the reduction follows a first order kinetics.

2.5.1 Fe⁰ reduction process

This has to be done under anaerobic conditions to prevent the corrosion of the iron, where it acts as a strong reducing agent and water is the oxidizing agent. This reaction produces Fe²⁺, OH⁻ and H₂ gas (Reardon, 1995). As follows:



The redox couple of Fe⁰/Fe²⁺ (aqueous) has a standard reduction potential of -0.440 V. This reduction can be used with azo-dyes; the reduction of the azo-bond is thermodynamically favorable producing a colorless solution (Pereira and Freire, 2006). The reduction of azo-dyes results in the formation of aromatic amines which are toxic, for this reason is important to combine iron reduction with another wastewater technique to treat those toxic amines (Larson and Weber, 1994; Feng *et al.*, 1999). It was found the decoloration of dyes under this process follows a first-order equation (Nam and Tratnyek, 2000). Cao *et al.* (1999) determined that the two factors that most influenced the process were the acidity of the solution and the iron surface area. They also suggested that pretreating the iron with HCl increase the acidity and surface area which will improve the reduction process (Cao *et al.*, 1999).

Past studies discovered that it is a surface-mediated process, which is better at low pH and the higher the surface area better the reduction process (Weber, 1996). The reduction process is dominated by the mass-transfer of the dye to the surface of the iron, after reaching the surface they associate in the sites of the iron. Competition might be present between the substrate and other solutes. The sites on the iron surface can be of two types: reactive or non-reactive. The first ones are those where the molecule can break the bonds and a chemical reaction occurs. The non-reactive sites are those where the substrate is only absorbed but no reaction occurs (Junyapoon, 2005).

2.6 Response surface methodology (RSM)

Compared to a conventional optimization method, which requires optimization of one parameter at the time, RSM is less time consuming and laborious (requires fewer experiments) (Roriz *et al.*, 2009; Senthilkumar *et al.*, 2013). Applying RSM to optimize the decoloration of a textile dye allows reduction in process variability, time and can reduce cost by reducing the number of experiments needed to obtain optimal conditions (Daâssi *et al.*, 2012). A proper comparison between the two optimization techniques should be addressed which is one of the objectives in this dissertation work.

The origin of RSM dated from the studies of Box and Wilson 1951, where it developed from theoretical aspects to real case scenarios (Cuesta, 2009).

RSM is the experimental and analytical strategy that combines mathematical and statistical techniques to analyze the effects of several independent variables to find the optimum operating conditions of a process, *i.e.* those that result in "optimal values" of one or more characteristics of product quality. It is a strategy of sequential experimentation and modeling that allows estimation of the optimal conditions of operation of a process and to significantly improve it. The model has to explain at least 70% of the behavior of the response, in terms of R^2 , otherwise is considered a bad prediction (Montgomery and Runger, 2010; Roriz *et al.*, 2009).

An advantage of the response surface is that it shows the estimates of the response at all possible levels of the factors studied. The response surface allows visualization of inspection of the average response for different levels of the factors of interest and evaluation of the sensitivity to them. Software such as Minitab allows easy analysis of polynomial models of first- or second-order and their effects (Montgomery and Runger, 2010; Cuesta 2009).

This methodology has been used by other authors for the decoloration of dyes, using a microbial consortium (Ayed *et al.*, 2010), a fungal system (Papadopoulou *et al.*, 2013) laccase (Daâssi *et al.*, 2012) and other techniques such as electrocoagulation (Singh *et al.*, 2016).

This methodology allows identification and optimization of all interactions, including quadratic effects, that can exist between the factors involved in the process, specifically

the Box-Behnken approach has demonstrated effectiveness in a study of decoloration of dyes requiring fewer points to run (Daâssi *et al.*, 2012). The points of this design are located in the middle of the edges of the cube centered at the origin and, as had been pointed out, it does not include the vertices, such as (1, 1, 1) and (-1, -1, -1) Figure 4 represents the points used for a Box-Behnken methodology:

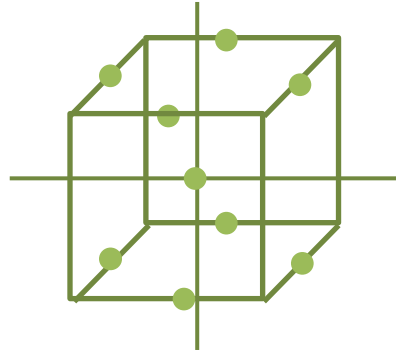


Figure 4. Box-Behnken geometric representation

The second-order model equation is:

$$Y = \beta_0 + \beta_1x_1 + \beta_2x_2 + \beta_3x_3 + \beta_{12}x_1x_2 + \beta_{13}x_1x_3 + \beta_{23}x_2x_3 + \beta_{11}x_1^2 + \beta_{22}x_2^2 + \beta_{33}x_3^2 + \varepsilon$$

Definitions:

- Experimental region: is the space defined by experimentation ranges used by each factor.
- Operability region: is defined by the set of points or conditions where the equipment or process can be operated.
- The optimum point (optimum process performance) is the best possible combination in the entire region of operability (Montgomery and Runger, 2010)

The objective of the RSM is to get the optimum operating conditions to determine the parameters with which the factors achieved the highest percentage of removal of dyes, through the implementation of response surface methodology. A graphical description of the process is shown below (Figure 5).

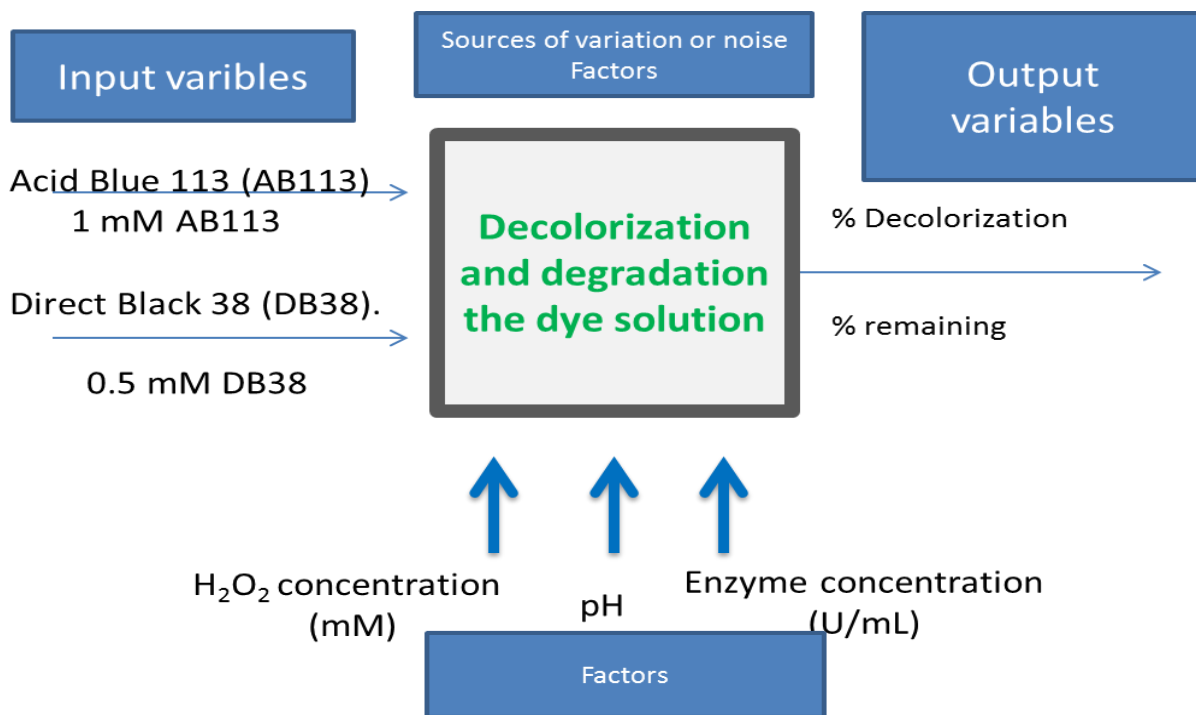


Figure 5. RSM for dye decoloration

Model and design

There is a direct relationship between the type of model that is selected to be adjusted and type of design that should be run. The design depends on the type of behavior expected of the answer. The designs provide treatments for predicting data to fit a model that describes a variable response in an experimental region. For the model, the response surfaces are characterized by fitting it to experimental data. The adjusted model for each design represents an approximation to the unknown reality of the process.

For the optimization process, the surface described by the model is explored, adjusted and validated, to find the combination of levels of the factors that result in the optimum value of the response (Montgomery and Runger, 2010).

2.6.1 Second-order model

The specific form taken by the surface depends on the signs and magnitudes of the coefficients in the model. The three basic types of surface plots are:

Maximum surface plot (mountain). In this type of graph as the color gets darker the response increases (Figure 6) (Minitab 17 support (a), 2017).

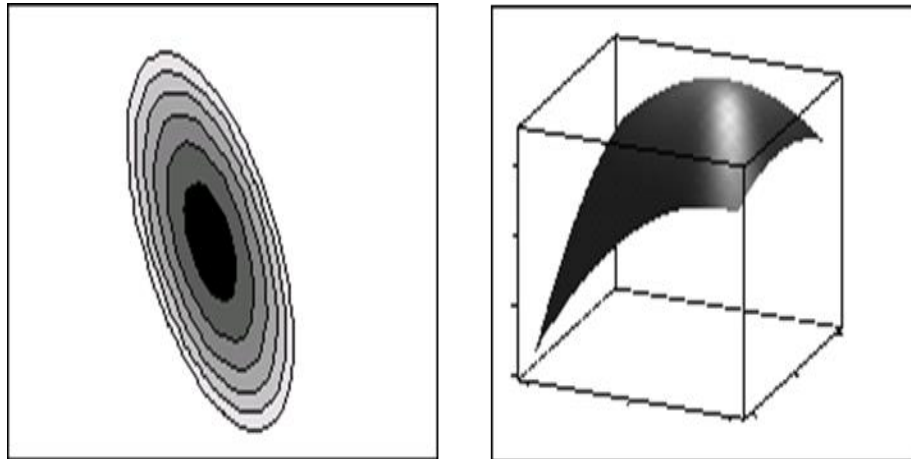


Figure 6. Maximum surface plot

(Minitab 17 support (a), 2017).

Surface with minimum (valley). The response decrease as it approaches the minimum point (Figure 7).

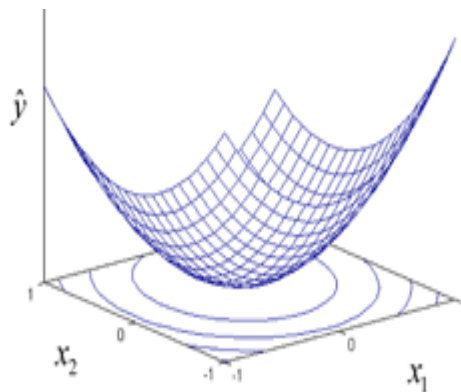


Figure 7. Surface with valley

ReliaSoft (2015)

Surface saddle point (minimax). The intensity of color is related to the response, as the color gets darker the response increases (Figure 8). From the stationary point of the graph if both factors decrease or increase at the same time the response leads to decrease. On the other hand, if one of the factors decreases meanwhile the other increase the response tends to increase (Minitab 17 support (a), 2017).

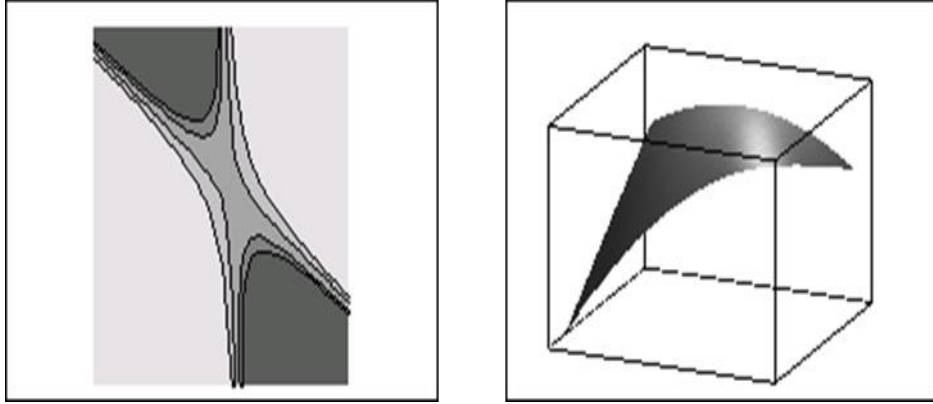


Figure 8. Surface with minimax

(Minitab 17 support (a), 2017).

3.1 Materials

3.1.1 Azo-dyes, aniline, benzidine, 3-aminobenzenesulfonic acid

Acid blue 113 (AB113, 50% purity), direct black 38 (DB38, $\geq 45\%$ purity), 3-aminobenzenesulfonic acid (97% purity) and aniline (99% purity) were purchased from Sigma-Aldrich Chemical Company (Oakville, ON). Crocein Orange G (COG, 90% purity) was purchased from MP Biomedicals (Solon, OH). Benzidine ($>95\%$ purity) was purchased from British drug houses Canada LTD (Toronto, ON).

3.1.2 Enzymes

Crude dry solid SBP (E.C. 1.11.1.7, Industrial Grade lot #18541NX, RZ = 0.750.10. activity 5 U/mg) was obtained from Organic Technologies (Coshocton, OH). Catalase from bovine liver (CAS 9001-05-2, lot #SLBB1797V, activity 2000-5000 U/mg protein) was purchased from Sigma Chemical Company Inc. (Oakville, ON). The enzyme and catalase were stored at -15°C ; the solutions prepared were stored in the fridge at 4°C .

3.1.3 Reagents

Hydrogen peroxide (30% w/v) was purchased from ACP Chemicals Inc. (Montreal, QC). 4-dimethylaminobenzaldehyde (99% pure) was purchased from Sigma-Aldrich (Oakville, ON).

3.1.4 Buffer and solvents

Analytical grade sodium acetate, monobasic and dibasic sodium phosphate, sodium bicarbonate, concentrated hydrochloric acid (HCl), glacial acetic acid were purchased from ACP Chemicals Inc. Sodium carbonate ($>99.5\%$ purity), sodium sulfite ($>98\%$ purity) were purchased from Sigma-Aldrich. HPLC grade acetonitrile was obtained from Fisher Scientific and ammonium acetate HPLC grade was purchased from sigma-Aldrich (Ottawa, ON).

3.1.5 Others

Filtropur S 0.2 syringe filters, for sterile filtration, 0.2 μm pore size were purchased from Sarstedt, Montreal. Iron filings (40-60 mesh, MSDS IX0210, for AB113 experiments),

cobalt chloride, Fisherbrand P8 Qualitative filter paper, magnetic stir bars in different sizes were obtained from Fisher Scientific Company (Ottawa, ON). Iron filings (40-60 mesh, MSDS IX0210, for DB38 experiments) were purchase from Innovating science through Fisher Scientific.

3.2 Analytical and laboratory equipment

3.2.1 UV-VIS Spectrophotometry

An Agilent 8453 UV-Visible spectrophotometer (λ range of 190 -1100 nm and 1 nm resolution) controlled by a Hewlett Packard Vectra ES/12 computer was used. Quartz glass spectrophotometer cuvettes with 10 mm light path type 104-QS were purchased from Hellma (Concord, ON).

3.2.2 HPLC (High Performance Liquid Chromatography)

Product identification and dye degradation measurements were analyzed by an HPLC instrument from Waters Co. (Mississauga, ON) with a Model 2487 dual-wavelength absorbance detector, Model 1525 binary HPLC pump and Model 717 autosampler operated by Breeze 3.3 software. A Waters Symmetry C18 reverse-phase column (5 μ m, 4.6 X 150 mm) was used. For mobile phase ammonium acetate 5 mM and acetonitrile were used.

3.2.3 Total Organic Carbon (TOC) analysis

TOC was determined by a Shimadzu model TOC-L CPH Total Carbon Analyzer. The analyzer gives the TC, IC and TOC in mg/L. Adequate calibration curves were selected from TOC instrument done previously by Bill Middleton, Lab technician.

3.2.4 Sonicator

Mixing during zero-valent iron treatment of azo-dyes was done using a Sonicator SC-101TH (volts 110-120, 50 /60 Hz, 2.3 Amps) from Sonicor Instrument Corporation.

3.2.5 Centrifuge and pH meter

The centrifuge was Corning LSE compact centrifuge (New York, USA). The pH meter used an Oakton pH/CON 700 benchtop meter (pH range -1.99 to 16.00, pH resolution

0.01), with an Orion pH probe (9110DJWP, Ag/AgCl double junction, glass body) (IL., USA).

3.2.6 Software

For the response surface methodology and Michaelis-Menten kinetics adjustment Minitab 17 was used for all dyes.

3.3 Analytical methods

All experiments were run in triplicates, unless otherwise stated, at room temperature and standard deviations were calculated and denoted as error bars (error bars that can't be seen are hidden by the icons).

3.3.1 Soybean Peroxidase (SBP) Activity Assay

A time-based colorimetric measurement developed by Caza *et al.*, 1999 was used to determine the SBP activity, according to the reaction:



SBP was mixed with 2.4 mM 4-AAP (4-aminoantipyrine), 10 mM phenol, 0.2 mM H₂O₂ and pH=7.4 (phosphate buffer, 50 mM), the mixture produce a pink chromophore with a maximum absorption at 510 nm and the enzyme activity can be measured through the absorbance increase over a certain time. As a definition, 1 unit of activity (U) is defined as the number of micromoles of H₂O₂ converted per minute at pH 7.4 at room temperature, under the conditions of the assay.

The test consists of the addition of 50 µL diluted SBP to 950 µL reagent in the cuvette. The formation of the chromophore during the first 30 seconds (cycle time 5 seconds) was monitored by the spectrophotometer and the activity was calculated using the kinetic rate calculation function built into the software.

3.3.2 Color reduction

Stock solutions of DB38 and AB113 were made up at 1 and 2 mM with deionized water, respectively. Then, a 1 mM (AB113) and 0.5 mM (DB38) stock solution were made.

For these new stock solutions, 40-fold and 20-fold dilutions were analyzed by UV-VIS spectrophotometer to determine λ_{\max} for maximum absorbance for both dyes. For calculation of the color remaining after enzymatic treatment and two-step process, initial color (A_i) as well as final color (A_f) were measured at λ_{\max} and percent color remaining was calculated as follows:

$$\text{Percent color remaining} = 100 * \left(\frac{A_f}{A_i}\right)$$

3.3.3 Anilines colorimetric assay

A modified method of Oren *et al.* (1991) was used. Aniline was assayed colorimetric by reaction with *p*-dimethylaminobenzaldehyde.

To 2.25 mL of sample (proper dilutions were made), 0.026 mL of 1 M HCl was added, and then 0.62 mL of ethanol, 0.26 mL of 5% *p*-dimethylaminobenzaldehyde in ethanol, and 0.26 mL of 15.7% citric acid in 6% NaOH were added. The samples were then measured at 440nm. Calibration curves were done with aniline to express the results as total amines as aniline. The spectrophotometer was blanked with the reagent blank (2.25 mL of water, 0.026 mL of 1 M HCl, 0.62 mL ethanol, 0.26 mL of 5% *p*-dimethylaminobenzaldehyde in ethanol, and 0.26 mL of 15.7% citric acid in 6% NaOH) and then measurements were done every minute until the maximum absorbance was reached, to determine the time of the reaction for color development (10 minutes).

3.3.4 Product determination by HPLC

Aniline determination was done with 1 mL/min flow, 60% of 5 mM ammonium acetate and 40% acetonitrile at 280 nm. For 3-aminobenzenesulfonic acid, with 1 mL/min flow the mobile phase was 50% of 5 mM ammonium acetate and 50% acetonitrile at 235 nm. For COG with 1 mL/min flow, the mobile phase was 60% of 5 mM ammonium acetate and 40% acetonitrile at 482 nm.

For DB38 dye was 0.7 mL/min with 50% of 5 mM ammonium acetate 5 mM and 50% acetonitrile at 520 nm. For AB113 it was used 0.5 mL/min with 50% of 5 mM ammonium acetate 5 mM and 50% acetonitrile at 565 nm.

3.3.5 TOC analysis

TOC analyses were done on batch reactor experiments run under the optimum conditions for direct enzymatic treatment and the two-step process in order to compare both processes. Since optimum pH was, for both dyes, in the low range (3.6 and 4.0) pH was adjusted with HCl to avoid the carbon from acetate-acetic acid buffers. Samples were collected and micro-filtered, after proper dilution they were measured. The instrument was allowed to run 3 milli-Q water injections. Three injections were used for each reading and the average was recorded. TOC of distilled water was measured before the sample analysis.

3.3.6 Buffer preparation

The buffers used in this study were prepared based on Gomori's methods (Gomori, 1955). Sodium phosphate buffer (pH range from 6.0-8.0) acetate buffer (pH from 3.0-5.6), and carbonate-bicarbonate buffer (pH 9.2 and 10.0) were used.

3.3.7 Enzyme stock solution preparation

SBP stock solution was prepared by weighing 1.4 g solid enzyme and mixing with 100 mL distilled water for 24 hours; then the mixture was centrifuged for 25 min at 4000 rpm. The supernatant was taken and stored at 4 °C. Catalase stock was prepared as 0.5 g/100 mL mixing for 4 hours then stored at 4 °C.

3.3.8 Batch reactors for color reduction and dye degradation. Single- step process

A total volume of 20 mL was used for batch reactors to determine the decoloration and degradation of the dyes. Parameters optimized were: pH, H₂O₂ concentration, enzyme concentration, and reaction time. The initial concentrations of dye were 1 mM for AB113 and 0.5 mM DB38. Buffer concentration was the same for all experiments, 40 mM, using acetate (pH 3.5-5.0) or phosphate buffers (pH 6.0-8.0). Reactors were continuously mixed during 3 hours, unless otherwise stated, using a Teflon-coated magnetic stir bar. At the end of the reaction, 100 µL of catalase solution was add to break down the H₂O₂ remaining to stop the reaction. AB113 samples were microfiltered and measured, DB38 samples where first centrifuged (25 minutes for 5000 rpm) then microfiltered and measured. TOC measurements were done only for samples obtained under optimal reaction conditions.

3.3.9 Iron preparation

All the iron used in this research was pre-treated by soaking the filings with 10% HCl for 20 minutes to remove metal oxides from the surface; this allows the substrate to have a higher surface area for contact during the process (Agrawal and Tratnyek, 1996). Then, the iron was washed four times with 15 mM carbonate buffer (pH 9.5) and 1 mM sodium sulfite (to make the solution anaerobic) this to remove the metal oxides and all chlorides. After this, it was washed again four times with a 20 mM sodium sulfite solution (with 0.1% w/w cobalt chloride with respect to sodium sulfite) to remove excess alkalinity and prevent contact with oxygen. The final iron was stored in the 20 mM sodium sulfite solution with 0.1% w/w cobalt chloride to preserve anaerobic conditions.

3.3.10 Iron pretreatment- enzymatic treatment. Two- step process

First, reactors were set up to decolorize AB113 and DB38 using iron filings (previously conditioned as described in 3.3.9) by azo cleavage obtaining products like aniline and benzidine for DB38 and 3-aminobenzenesulfonic acid for AB113. The amount of iron was optimized for maximum decoloration; varying the amount of iron and reaction time in a 40 mL glass vials with screw cap. The amount of iron (1, 1.5 or 2 g) was added to the vial and sodium sulfite (with 1% w/w cobalt chloride) to make anaerobic conditions. Since Fe^{+2} and sodium sulfite (Na_2SO_3) from the zero-valent iron reduction can interfere with the enzymatic treatment, the reaction solution was aerated before SBP treatment to precipitate Fe^{+2} as Fe^{+3} and Na_2SO_3 as Na_2SO_4 . For these experiments tap water was used, taking advantage of its buffering capacity (it was left overnight to dissipate any chlorine). The samples were mixed in a sonicator water bath and samples were measured every 15 minutes. The vials were allowed to settle the iron by placing them on a magnet and then the experiment was microfiltered and measured to determine color remaining (UV-Vis spectrophotometer) aniline, benzidine and 3-aminobenzenesulfonic acid formation (HPLC), as well as total amines (as aniline) using the modified method of Oren *et al.* 1991 (section 3.3.3).

Once the measurements were done, 20 mL batch reactors were set up with the products obtained before. The initial conditions were: for AB113, 0.85 mM of total amines and 0.8 mM 3-aminobenzenesulfonic acid; for DB38, 0.33 mM aniline and 0.35 mM benzidine as well as 1.5 mM amines as aniline. Optimization for pH, H_2O_2 and enzyme concentration

were done in order to remove aniline, benzidine, 3-aminobenzenesulfonic acid and total amines as aniline, the optimization process was done as described for the single-step process. TOC measurements were done only for samples obtained under optimal reaction conditions.

3.3.11 Kinetics

Initial velocities were measured for AB113, DB38 and COG varying the substrate concentrations and SBP but keeping the same H₂O₂ concentration. Individual batches with 10 mL total volume were run with 40 mM optimum buffer for each substrate (pH 3.6, 4.0, and 8.0 for DB38, AB113 and COG, respectively). The monitoring was done until adequate data was obtained to determine the initial rate (around 10-15% conversion). Samples were measured in the spectrophotometer at optimum pH for each substrate; all samples were microfiltered before measured. Minitab 17 was used to calculate the Michaelis-Menten equation. Lineweaver-Burk plot was done with Microsoft excel 2010, to provide estimates K_M and V_{max} .

3.3.12 Product identification after single-step process.

COG (Figure 3) was used as a model azo-dye for product identification after enzymatic treatment for its high purity (90%) and simpler structure to avoid any interference.

First, HPLC was used to identify a possible product from azo-cleavage of COG, aniline. Several concentrations of SBP and H₂O₂ were tested in order to determine the amount of aniline formed. HPLC technique is described in section 3.3.4. Spiked solutions with pure aniline (1 mM) were compared to non-spiked solutions for aniline concentrations.

Second, EI-MS (instrument Xevo G2-XS Tof) analysis was conducted in order to confirm the presence of aniline after enzymatic treatment; it was run in positive and negative modes with untreated and treated dye sample and appropriated blanks and standards samples. The measurements were completed using electrospray ionization in both positive and negative modes (ESI (+) and ESI (-)). All measurements were of a 1 μ L injection into a sample loop with a constant flow of 50:50 water: acetonitrile with 0.1% formic acid. For ESI (+), solutions were prepared in 50:50 H₂O:CH₃CN with 0.1% formic acid and for ESI (-) no acid was included for the sample solution.

3.3.13 Response-surface methodology

First, a tentative first-order model (the first-order stage) was sought with the parameters defined by literature review as those most likely to significantly affect the color removal of azo-dyes by enzymatic treatment (pH, enzyme and H₂O₂ concentrations) (Mazloun, 2014). This is to confirm the significant influence of the selected factors on the response variable to optimize and preliminarily characterize the surface type of response, running a first-order design with points to the center, to detect the presence of curvature, which will identify if the system is a second-order model.

After this a more complete controlled study of the significant factors was done. This study will allow confirmation of the influence of the factors in maximizing the percent removal of the dye, and to estimate the regression model that best describes the behavior of the effect of these factors and their interactions, and to determine if the surface shows curvature. To achieve these objectives, a full factorial design by 2³ repetitions at the center was proposed and developed with 2 replicates of each treatment (as recommended for a design 2³) (Gutiérrez and De la Vara Salazar, 2008), with 3 repetitions at center and three levels for each factor .

Due to the presence of curvature, the next step was to do the search II or second-order model, the main objective of this stage is to model the behavior of the process in a very precise and relatively small region, to determine the combination of factors most likely to be considered optimal. To characterize and analyze in more detail the curvature detected within the experimental region, the number of experiments were increased, for this, additional points which are located in the middle of the edges of the cube centered at the origin were selected and run, to study main effects, double interactions and quadratic effects to be included in the fitted model. The second-order model was obtained, according to the analysis of variance (ANOVA), the significant linear, quadratic and interaction effects were identified and those terms that were not significant were eliminated and the adjusted R² of the model was calculated, then the one which has the best fit was chosen to represent the response surface. It is preferred to select the model with all terms because a hierarchical model provides greater stability.

A Box-Behnken design was used, since it requires fewer runs, compared to other designs like central composite design (CCD), and consequently resource consumption was

reduced and treatments levels were easier to obtain. After this, the model was analyzed with a confidence level of 95% for the 3 factors and their interactions, checking the p-value as well as the capacity predictor (fitted R^2). Subsequently mathematical model was found. ANOVA was used to compare statistically the adjusted design against the previous second-order design and choose the one that best describes the surface of the experimental region.

Once the model was properly fitted to the second-order model, debugged and validated, the surface described by the model was explored to find the combination of levels in which the factors result in an optimal value of the response. The response surface allows visual inspection of the average response in a certain area (the design area) of the factors of interest and evaluation of the sensitivity to these factors. Surface and contour plots for the experimental area were obtained and analyzed.

Using the integrate option in Minitab 17 for response optimization, the best combination of values was found for the factors that are in the experimental region, following the fitted model, to obtain the lowest possible percent dye remaining. This function allows identification of the combination of factors that optimize the response (Minitab support (d), 2017)

3.4 Sources of error

The experiments done in this investigation are affected by systematic and random errors. All experiments were run in the presence of blanks as well as standards run in between samples to ensure precision of the machines. All experiments were run in triplicates, unless otherwise stated, to reduce human error. All graphs show the standard deviation as error bars, those graphs in which error bars that can't be seen are hidden by the icons (standard deviation less than 1%). SBP activity was checked daily since it is affected by the room temperature and reagent age (the experiments were done 1 hour after preparing the enzyme reagent). Equipment such as pipettes, balance, pH meter were calibrated before use.

4.1 Decoloration with single-step process

A single-step process was developed to decolorize AB113 and DB38 (section 3.3.8) based on absorbance decrease at the maximum absorption wavelength. The maximum wavelength for AB113 was 565 nm in all buffers; with the exception of pH 3.6 at which it is 536 nm, therefore, a separate calibration curve was determined for this pH (see Appendix A, Figure A.1 and A.2). The maximum wavelength reported by the producer (Sigma-Aldrich) is 565 nm. For DB38 the maximum wavelength was 520 nm, independent of the buffer and pH, therefore the same calibration curve was used for all pHs (see Appendix A, Figure A.3). The optimization is done respect to efficiency in terms of color reduction. Optimizations for pH and peroxide concentration were done under stringent conditions with respect to enzyme concentration (where the % remaining was between 25% to 40%) to provide easier discerning of the optimal point or range for the varied parameter. The figures for pH, H₂O₂ and SBP optimizations for both azo-dyes show lines that do not represent a model fit but are simply a visual aid.

4.1.1 pH optimization

Dye degradation using enzymatic treatment has been proven to be pH dependent (Kalsom *et al.*, 2013, Mazloun *et al.*, 2014; Chiong *et al.*, 2016) which is different for each enzymatic reaction, depending on the substrate and reaction conditions. The optimum pH is the one that satisfy the required ionization states of the critical amino acids residues (histidine and arginine) present in the enzyme, which value guarantees the best conformational state of the enzyme for the catalysis (Al-Ansari *et al.*, 2011). For AB113, different pHs were tested (range 3.6 to 8.0) with the same concentration of enzyme, H₂O₂, and buffer. As be seen in Figure 9, the optimal pH is located in the range from 3.5 to 4.5; specifically the optimum pH was 4.0. It was decided to study the pHs of 4.0 and 4.6 since the difference of % remaining was only 2.7%, for enzyme and H₂O₂ optimization.

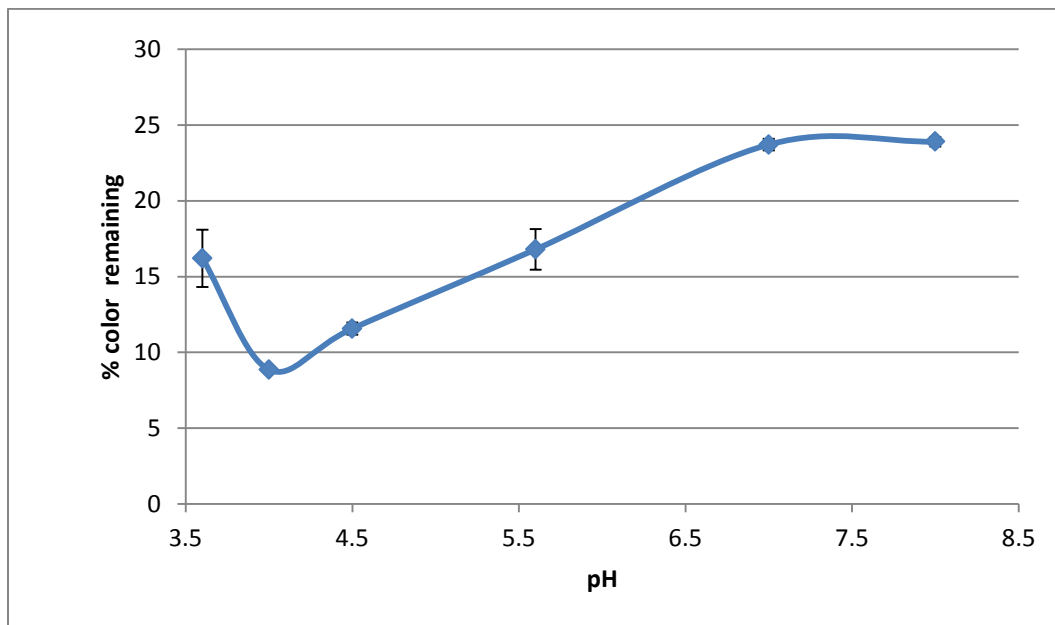


Figure 9. pH optimization for 1 mM AB113 with 2.0 U/mL SBP, 2.5 mM H₂O₂, 3 hour reaction at room temperature

For DB38, also different pHs were tested (range 2.6 to 8.0) seen in Figure 10. As it can be seen (Figure 10) the lowest percent remaining was obtained in the acidic pH range specifically 3.6 and 4.0. For further experiments a pH of 3.6 was chosen.

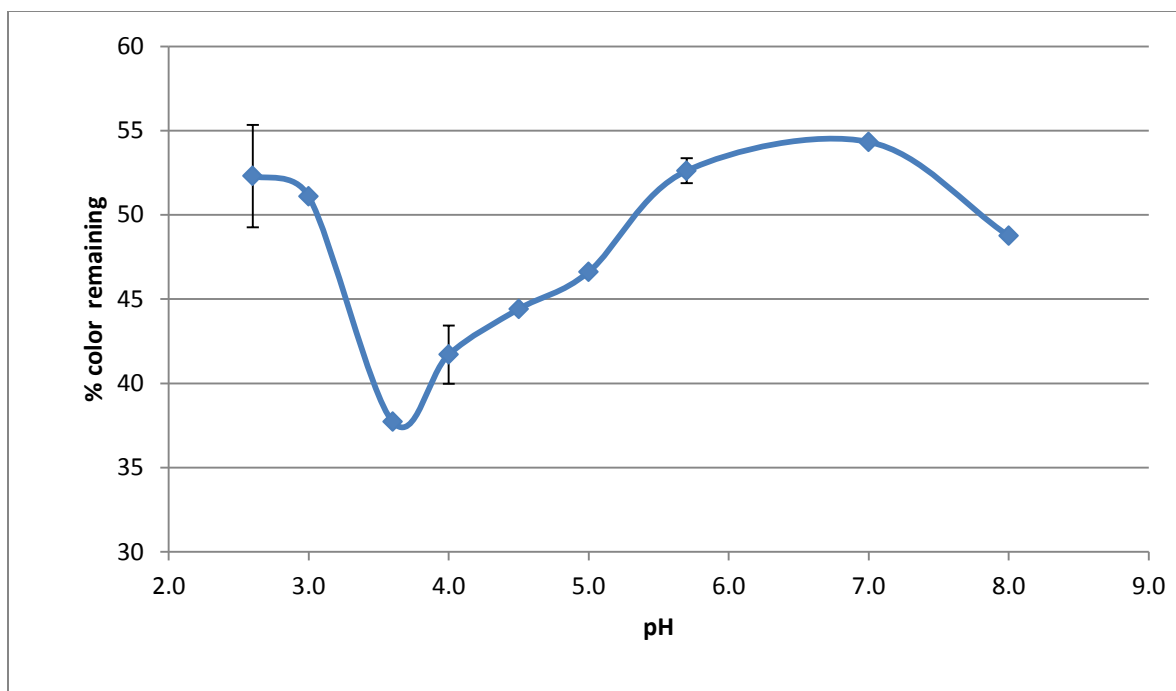


Figure 10. pH optimization for 0.5 mM DB38 with 2.0 U/mL SBP, 2.5 mM H₂O₂, 3 hour reaction at room temperature

As seen in Figures 9 and 10, the behavior for both azo-dyes is similar, where the best performance is at acidic conditions. Other authors have found same tendency regarding pH optimization of azo-dyes with peroxidases: Kalsom *et al.* (2013) found that the optimum pH for Trypan Blue was in the acidic range using SBP. The optimum pH was 4.0 but pH 3.0 and 5.0 showed almost the same behavior. Ulson de Souza *et al.* (2007) found that the optimum pH range for Remazol Turquoise Blue was 4.0–5.0 using HRP. Sadhanandam *et al.* (2013) decolorize AB113 with HRP; it was found that the optimum pH was 6.6. However, pH 4.0 and 9.0 had similar results. Chiong *et al.* (2016) also studied an azo-dye (methyl orange) with SBP achieving a maximum of 81.4% decoloration pH 5.0, with higher pH the decoloration decreased. Thus the best performance was under acidic conditions (Kalsom *et al.*, 2013; Ulson de Souza *et al.*, 2007; Sadhanandam *et al.*, 2013; Chiong *et al.*, 2016; section 4.1.1).

4.1.2 H₂O₂ optimization

H₂O₂ is a major factor in the enzymatic reaction, since it is a co-substrate that initiates the enzyme mechanism. If the H₂O₂ is in excess it can cause enzyme inhibition and if it is at low enough concentration, it acts as a limiting factor (Dunford, 1999).

For AB113, different concentrations of H₂O₂ were tested with 3 U/mL of enzyme at pH 4.0 and 4.6 as shown in Figure 11.

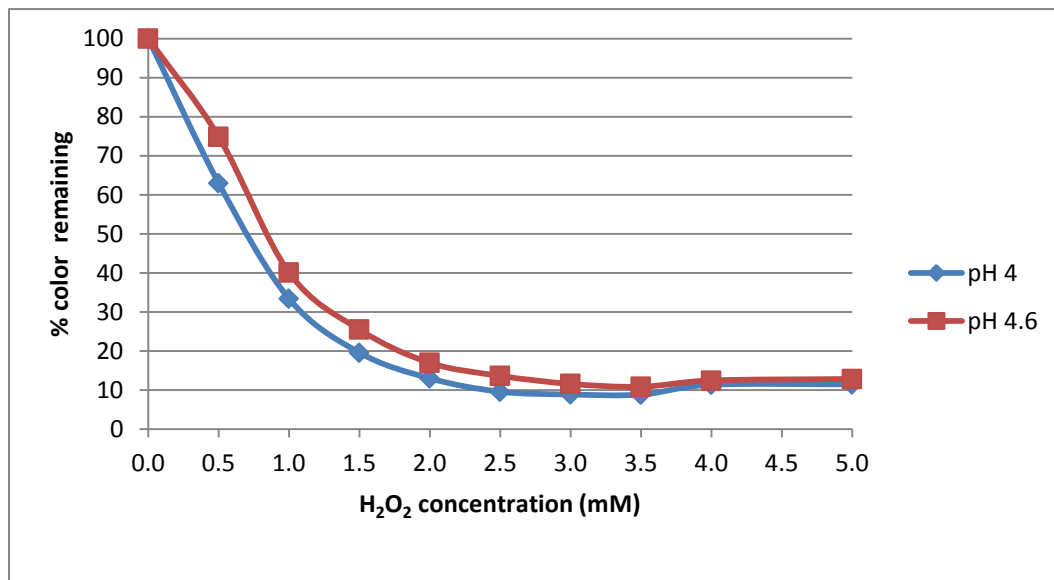


Figure 11. H₂O₂ optimization for 1 mM AB113 at pH 4.0 and 4.6 with 3.0 U/mL of SBP, 3 hour reaction at room temperature

As seen in Figure 11 for AB113, the two different pHs, reached the lowest percent remaining and then a plateau phase is presented, meaning that after that point no more significant removal can be achieved, even at higher H₂O₂ concentrations the % remaining start to increase in around 2.5%. This can be explained because the H₂O₂ is a stoichiometric co-substrate of the SBP, when the concentration of H₂O₂ is low, it limits the extent of reaction but if it is too high the H₂O₂ (and the substrate concentration is low) can oxidize the enzyme causing its inactivation (Ali *et al.*, 2013; Steevensz *et al.*, 2014).

The 10-20% dye remaining can also be due to an artifact of the colorimetric methods, the dyes DB38 and AB113 are only 45 and 50 % pure, respectively, which can lead to colored products interfering in the spectrometry measurement.

For both pH 3.6 and 4.0 the lowest remaining percentage was achieved with 2.5 mM showing 9.0 and 14% color remaining, respectively.

For DB38, also different concentrations of H₂O₂ were tested with same amount of enzyme (3.0 U/mL) with pH 3.6. As seen in Figure 12, the concentration required was 2.5 mM for a 3% color remaining, after this, as for AB113, no significant increase was achieved.

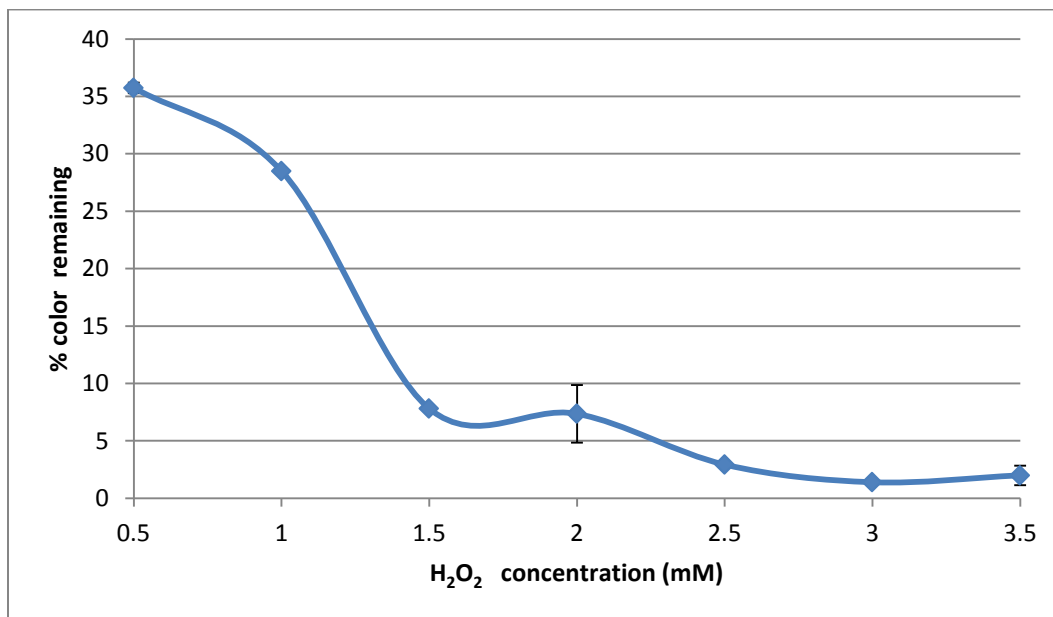


Figure 12. H₂O₂ optimization for 0.5 mM DB38 at pH 3.6 with 3.0 U/mL of SBP, 3 hour reaction at room temperature

Kalsoom *et al.* (2013) found that when 64 μ M H₂O₂ was used to decolorize 10-40 mg/L (0.011 mM- 0.046 mM) of dye, a maximum percent degradation of 60% was achieved. For more than 90% degradation a step-wise addition of H₂O₂ was required (total time required was 15 minutes with addition of H₂O₂ every 3 minutes). Chiong *et al.* (2016), found for methyl orange dye (30 mg/L or 0.09 mM) an optimum of 2 mM H₂O₂ achieved approximately 80% decoloration.

4.1.3 Enzyme optimization

As mentioned above, pH 4.0 and pH 4.6 (pH optimization; Figure 9) are the pH optima, with 2.7% difference; for this reason enzyme optimization was done at both pHs as for H₂O₂ optimization.

There is an optimal ratio of enzyme and substrate to achieve the maximum removal (Kalsoom *et al.*, 2013). For AB113, different concentrations of enzyme were tested at pHs 4.0 and 4.5 and using the optimum H₂O₂ concentration found before (2.5 mM, respectively) (Figure 13). The best performance, 6% remaining, was achieved. The striking feature of these curves is that the first 60-85% color removal was achieved with 0.10 U/mL SBP, while additional color removal was only achieved to a plateau level with 10-fold more enzyme concentration.

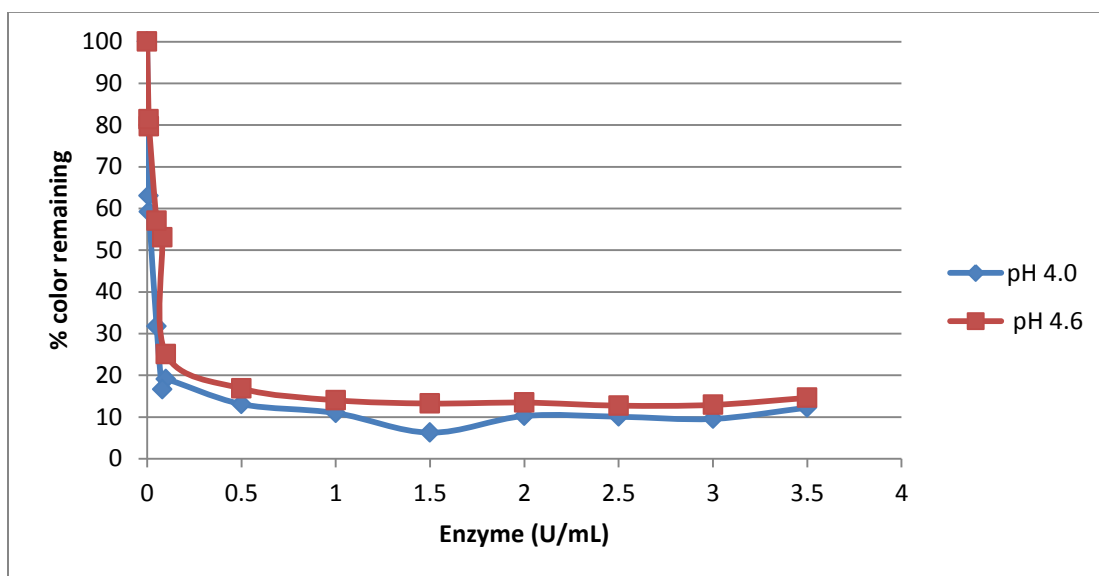


Figure 13. Enzyme optimization with for 1 mM AB113 with pH 4.0 and 4.6 with 2.5 mM H₂O₂, respectively, 3 hour reaction at room temperature

As it can be observed, as the enzyme concentration increase the color removal increase (% remaining decrease), but after certain concentration there is no change in the % remaining, this can be because there are not enough dye molecules to continue the reaction, which means there is no need to add more concentration of enzyme or as explain in section 4.1.2 due to the possible artifact cause by the impurities of the dye.

A last experiment was run to confirm the optimum pH (due to the results in section 4.1.1) and, as seen in Figure 14, the optimum pH was again pH 4.0.

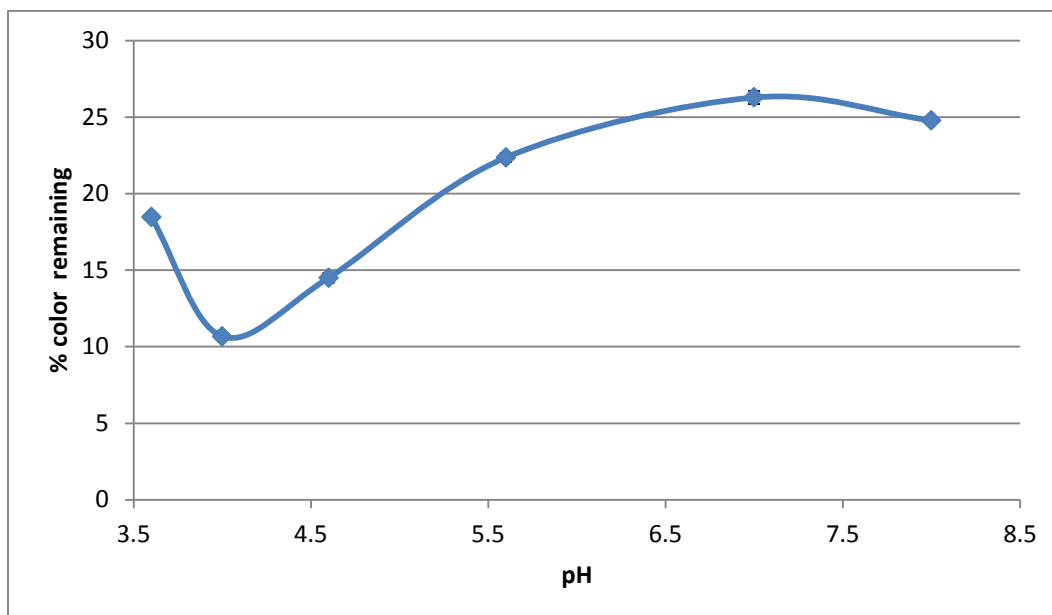


Figure 14. Second pH optimization for 1 mM AB113 with 2.0 mM H₂O₂ and 2 U/mL SBP, 3 hour reaction at room temperature

For DB38, different concentrations of enzyme were tested (Figure 15) with 2.5 mM and 3 mM H₂O₂ (as they were 1% different in the optimization), achieving 3% color remaining with 3 U/mL and 2.5 mM H₂O₂, higher concentration of enzyme does not modify the % color remaining in a linear manner.

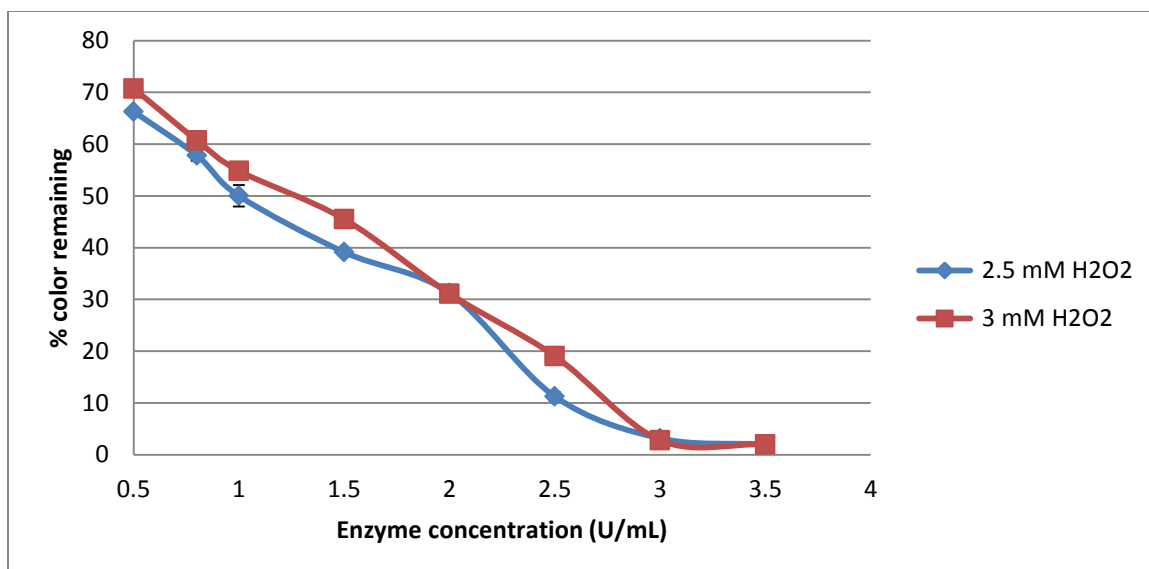


Figure 15. Enzyme optimization for 0.5 mM DB38 with pH 3.6, 2.5 mM H₂O₂ or 3 mM H₂O₂, 3 hour reaction at room temperature

Chiong *et al.* (2016) needed 0.186 U/mL (0.5 mL of 0.373 U/mL SBP) of SBP at pH 5 with 2 mM H₂O₂ to treat 0.09 mM (30 mg/L) methyl orange dye during one hour reaction (where one unit of enzymatic activity (U) is the amount of enzyme that catalyses 1.0 μ mol of H₂O₂ per min at 25 °C and pH 6.0. The substrate concentration used in this thesis is 6 to 12 times more that the used by Chiong *et al.* (2016) which result in higher concentration of SBP needed.

To explain the possible artifact of the color remaining, an HPLC analysis was done at the optimal conditions for both dyes. Under HPLC (for AB113) with pH 4, 2.5 mM H₂O₂ and 1.5 U/mL it was achieve 3 % dye remaining while by spectroscopy, under the same conditions, it was 6% color remaining. For DB38 at pH 3.6, 3 mM H₂O₂, 3 U/mL the dye degradation by HPLC was less than 2% remaining while by spectroscopy was 2.39%, since this percentage remaining where lower than 5%, other conditions were tested to prove that the percentage dye degradation was higher (HPLC) than the color reduction (spectroscopy). For pH 3.6, 3 U/mL and 1.0 mM H₂O₂ HPLC dye degradation was 26.3% and spectroscopy was 28.1 % remaining (See Appendix A, Figures A.4 and A.5)

There was no color removal by the enzyme in the absence of hydrogen peroxide, for both dyes. This situation indicates that the decolorization occurs exclusively as a function of the catalytic activity of the enzyme.

4.1.4 Time dependence

Figure 16, shows the time dependence for AB113 decoloration using 2.5 mM H₂O₂ and 1.5 U/mL SBP as well as 0.05 U/mL SBP with pH 4. For the optimal conditions, with 1.5 U/mL, the decoloration is done under the first minutes of reaction, for this reason stringent condition of SBP was used. Under these conditions reactions is complete at 60 minutes, after this time there is no change in the percent remaining presumably due to enzyme inactivation as seen in Figure 16.

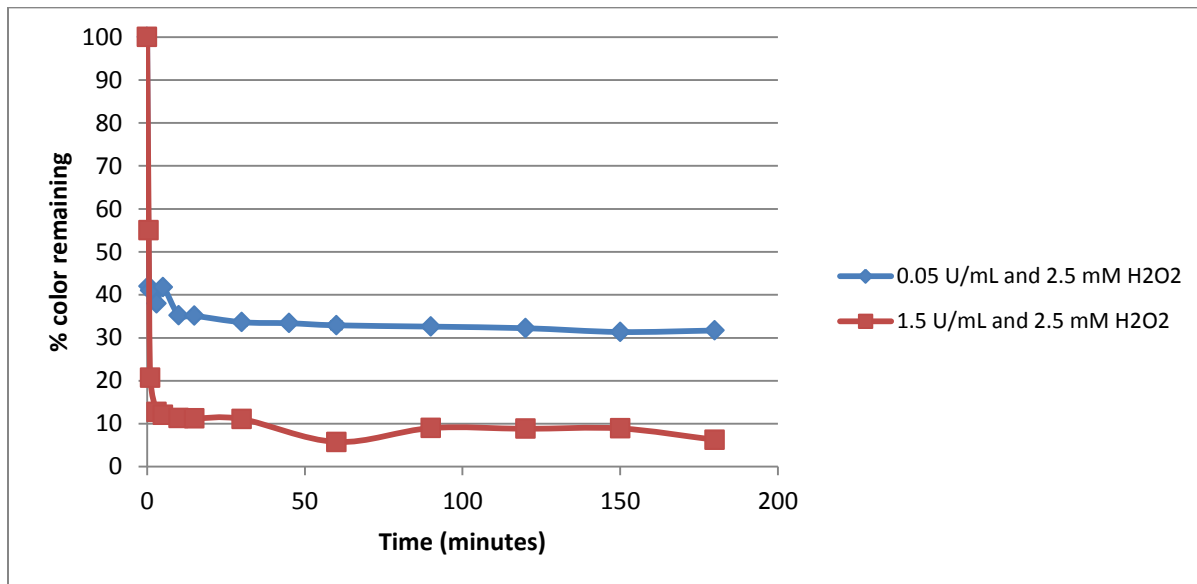


Figure 16. Time dependence for 1 mM AB113 using 2.5 mM H₂O₂ and 0.05 U/mL or 1.5 U/mL at pH 4.0, at room temperature

As done for AB113, for DB38 2.5 mM H₂O₂ and 2.0 U/mL and 2.5 mM H₂O₂ and 3.0 U/mL were used to determine the time dependence of the reaction (Figure 17); is seen, the reaction was largely complete in the first minutes of the reaction. At 120 minutes with 2.0 U/mL SBP, another small decrease was observed, after that it remains stable under stringent conditions; this 3% decrease might be a systematic error. For optimal conditions, after 4 minutes' reaction, less than 5% color was achieved.

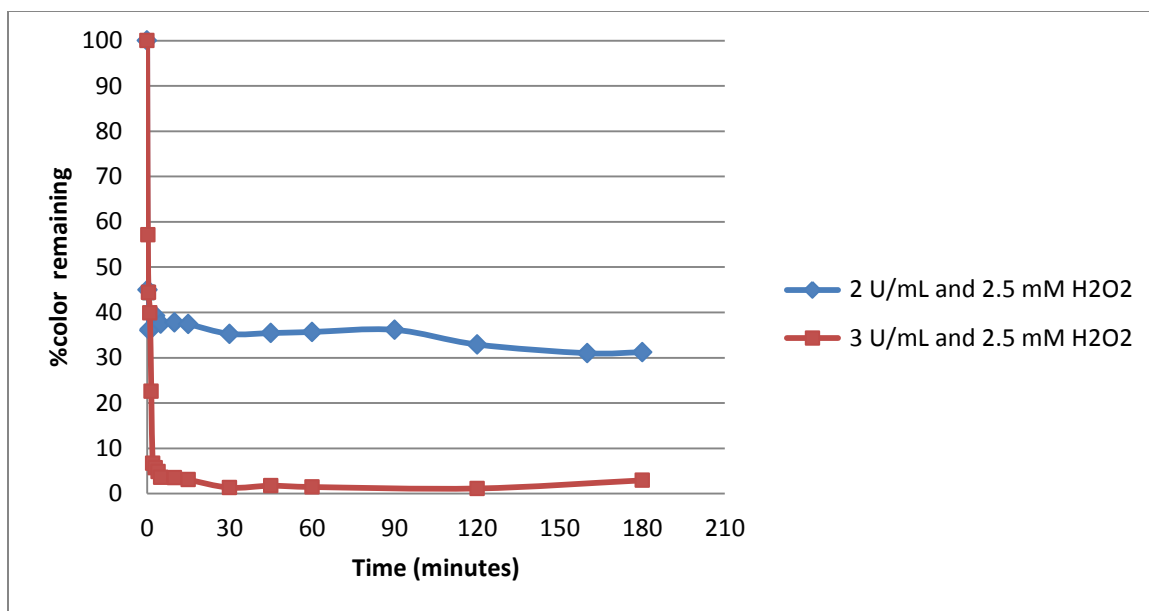


Figure 17. Time dependence for 0.5 mM DB38 with 2.5 mM H₂O₂ and 2.0 U/mL or 3 U/mL at pH 3.6, at room temperature

Figure 17 and 18 show that the reactions are faster in the first stages. Onder *et al.* (2011) studied the decoloration of naphthol blue black by HRP, founding that the decoloration was fast, during the first 5 minutes 80-90% of dye was decolorize. Chiong *et al.* (2016), found that after 60 minutes reaction there was no further increase in dye degradation, caused by the saturation of enzyme active sites. Gholami-borujeni *et al.* (2013) found that after 70 minutes there was not significant change in the dye degradation of Acid Blue 25 with HRP.

4.1.5 Initial rates, first-order model for decoloration

The apparent first-order rate constant and half-life of AB113 was calculated by plotting the percent color remaining during the first seconds of the reaction against the Ln of percent remaining. As seen in Figure 18 the reaction can be fit to a first-order reaction with a R² of 0.9844. The equation of best fit was:

$$\% \text{ color remaining} = e^{(-0.00132t+3.7952)}$$

Half-life of the substrate means the time at which the substrate is decreased by half of the original value and can be calculated for both dyes using the first order reaction. The half-life for AB 113 was calculated with the formula:

$$t_{1/2} = 0.693/k$$

Where $t_{1/2}$ was 525 ± 35.6 seconds or 8.76 ± 0.594 minutes

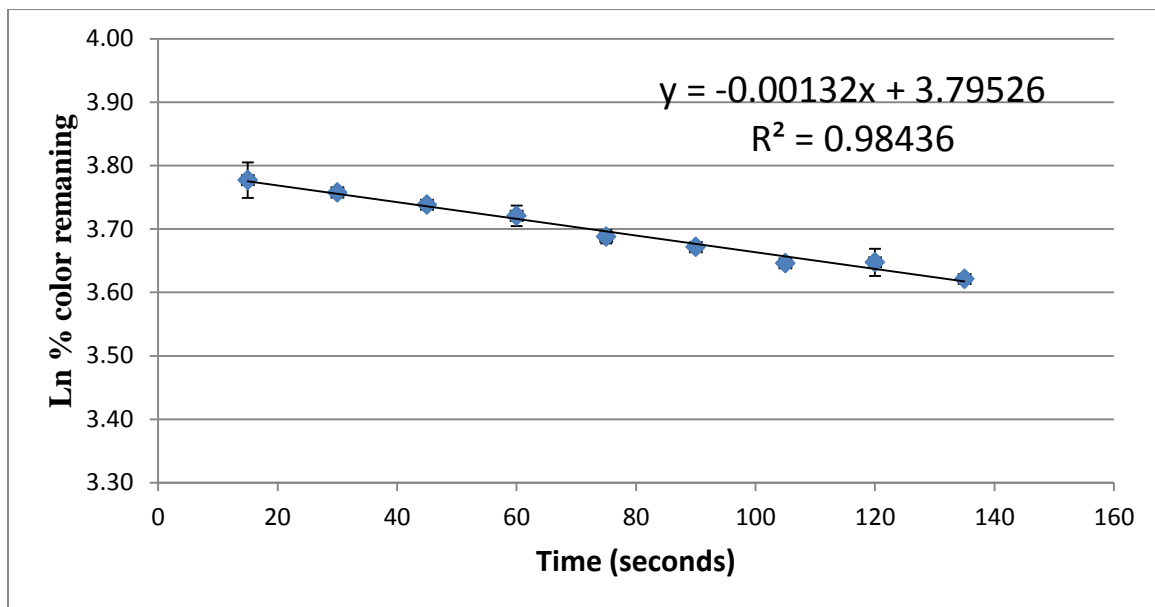


Figure 18. First-order reaction for 1 mM AB113

Conditions: 0.05 U/mL, 2.5 mM H₂O₂ and pH 4. At room temperature. Obtained value: $k = -0.00132 \pm 0.000063$

For DB38, Figure 19, the reaction can be also fit to a first-order reaction with a R^2 of 0.9835. The half-life for DB38 was 127 ± 11.8 seconds or 2.12 ± 0.196 minutes. The equation of best fit was:

$$\% \text{ color remaining} = e^{(-0.00544t+3.7686)}$$

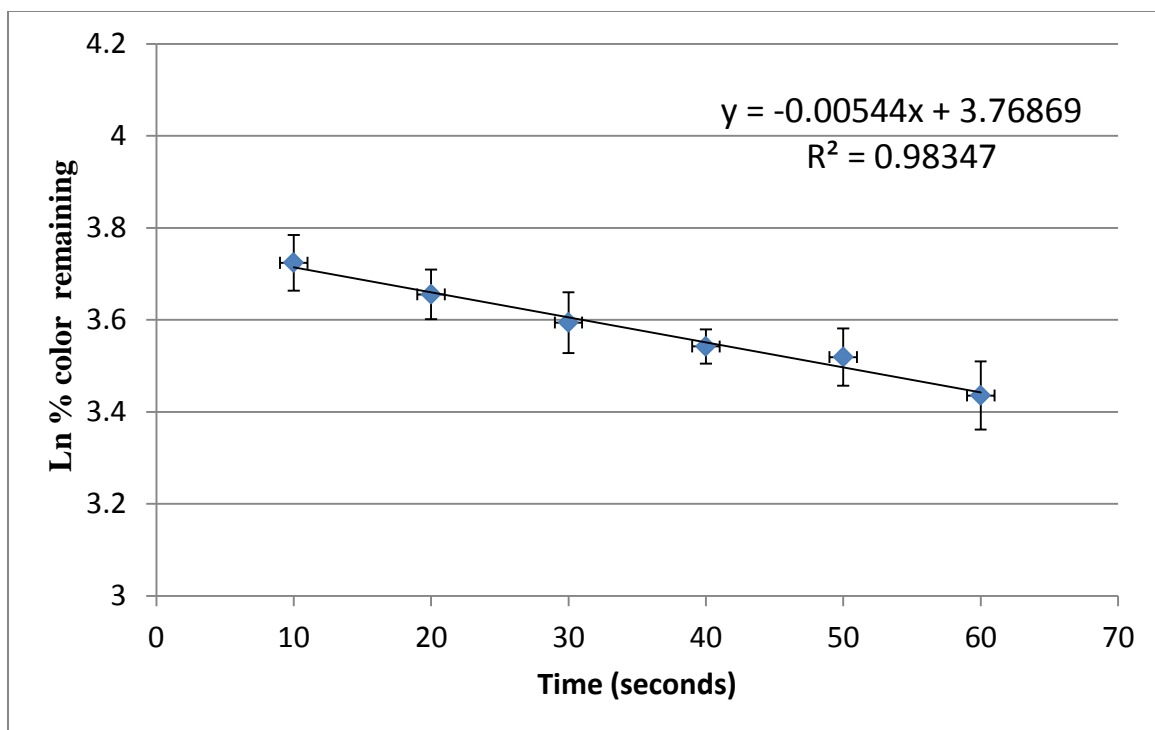


Figure 19. First-order reaction for 0.5 mM DB38

Conditions: 2.0 U/mL SBP, 2.5 mM H₂O₂ and pH 3.6, at room temperature. Obtain value: $k = -0.00544 \pm 0.00035$

Gholami-Borujeni *et al.* (2011) determined that the enzymatic reaction of HRP with and azo-dye (acid orange 7), was a first-order reaction with an $R^2=0.93$. The half-life of DB38 is 2.12 minutes which is faster than for AB113 (8.76 minutes) with more enzyme concentration for DB38 (40 times more). Table 2 shows the final conditions for maximum direct enzymatic treatment.

Table 2. Single-step enzymatic process. Optimal conditions for both dyes

Dye	Initial concentration	H ₂ O ₂ (mM)	SBP (U/mL)	% remaining	Optimum pH
AB113	1 mM	2.5	1.5	5.20	4.0
DB38	0.5 mM	2.5	3	3.16	3.6

4.1.6 Michaelis-Menten kinetic studies

Kinetic parameters allow having an understanding of the affinity of SBP for the different dyes (substrates). Initial velocities were calculated from the plots of different initial concentrations (mM) against time (seconds) (progress curves, Figures 20-22). The curves were adjusted to polynomials of second-order using Microsoft Excel program. All reactions were done at the optimum pH for each dye AB113, DB38 and COG. For AB113 and DB38 the measurements were done every 30 seconds and for DB38 and for COG every 60 seconds.

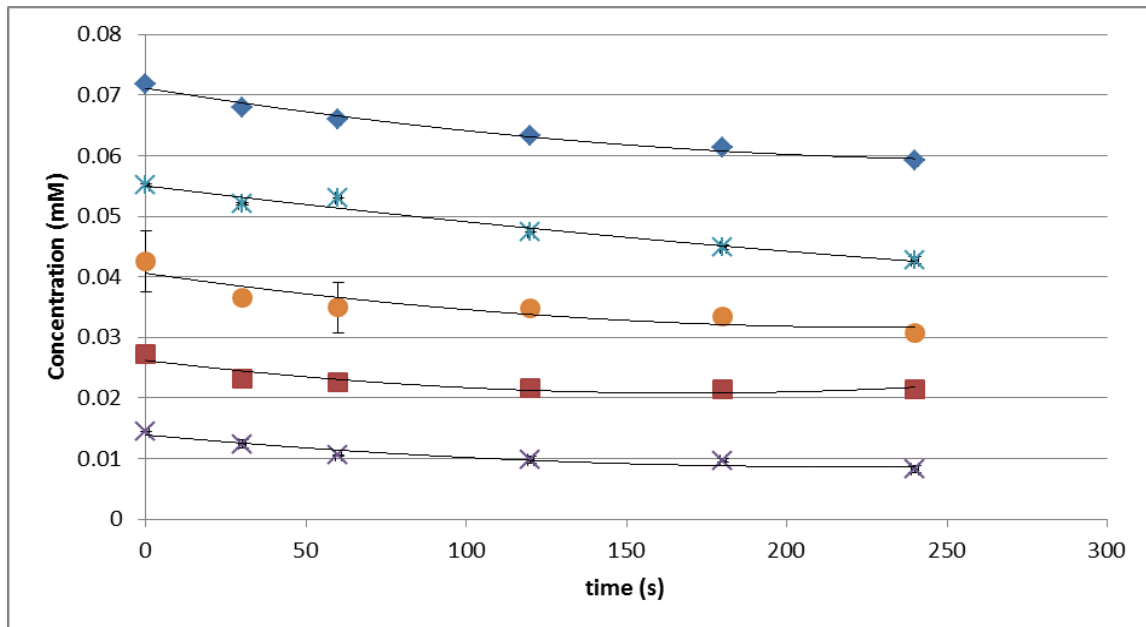


Figure 20. Initial velocities for AB113. Reactions with 0.125 mM H₂O₂, 0.0015 U/mL SBP and pH 4.0, at room temperature

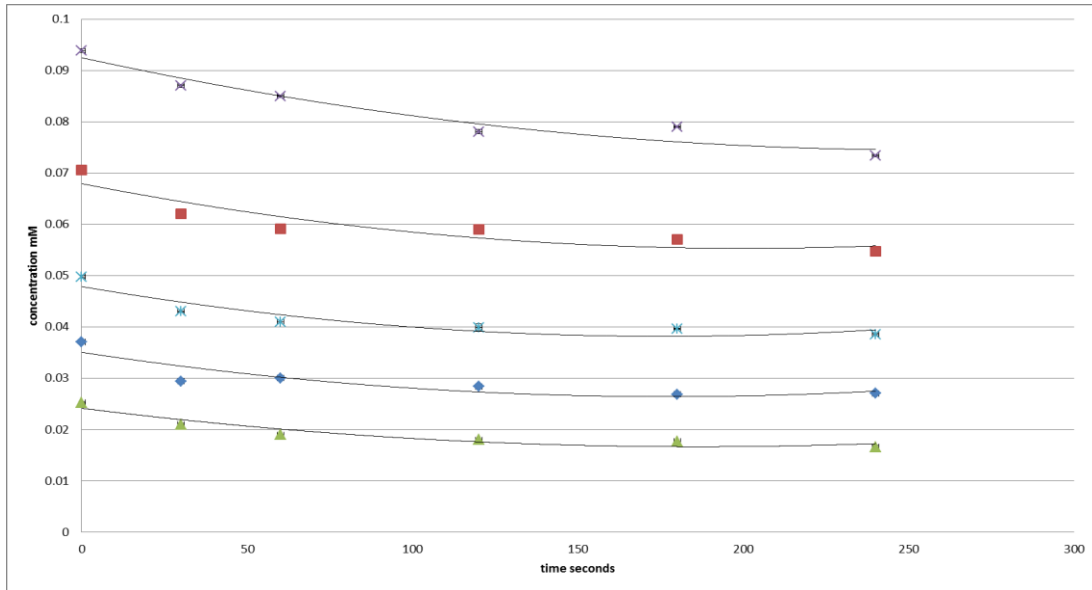


Figure 21. Initial velocities for DB38. Reactions with 0.125 mM H₂O₂, 0.0015 U/mL SBP and pH 3.6, at room temperature

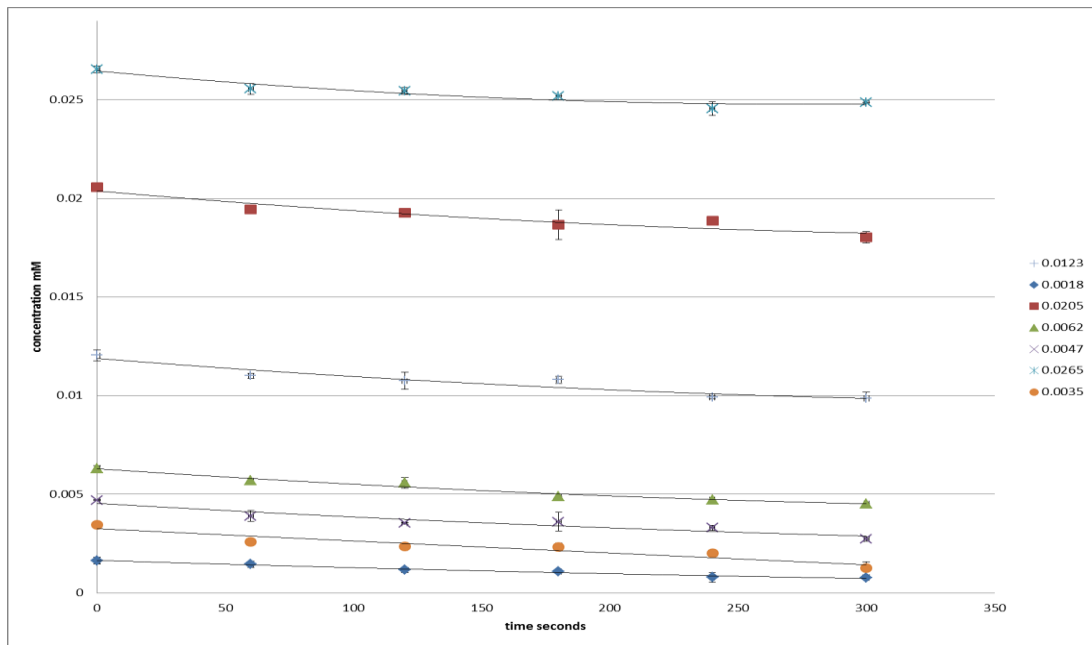


Figure 22. Initial velocities for COG. Reactions with 0.125 mM H₂O₂, 0.0025 U/mL SBP and 40 mM pH 8.0, at room temperature

Once the initial velocities were obtained, the rate ($\mu\text{M/s}$) was plotted against the initial substrate concentration and fitted to the Michaelis-Menten model directly (Figures 23-25)

and to its Lineweaver-Burk lineal transform (Figures 26-28) to obtain the kinetic parameters K_M and V_{max} .

The Michaelis-Menten equation is as follows:

$$v = \frac{V_{max} * Cs}{K_M + Cs}$$

Where v is the velocity of the reaction, Cs is the concentration of the substrate, V_{max} (maximum initial velocity) which is maximum rate achieve when the enzyme is saturate with the substrate, K_M (Michaelis-Menten constant) is the concentration of the substrate at half of the rate V_{max} .

One transformation of the Michaelis-Menten equation to facilitate the calculation of the kinetics factors is the Lineweaver-Burk plot which equation is:

$$\frac{1}{v} = \left(\frac{1}{V_{max}} \right) + (K_M + V_{max}) \left(\frac{1}{Cs} \right)$$

For this equation it was necessary to plot the reciprocal of the initial velocity against the reciprocal of the substrate concentration and adjust to a straight line, V_{max} was determined as the reciprocal of the intercept of the line in the $1/v$ axis and K_M was determined by multiplying the slope of the line K_M/V_{max} by V_{max} .

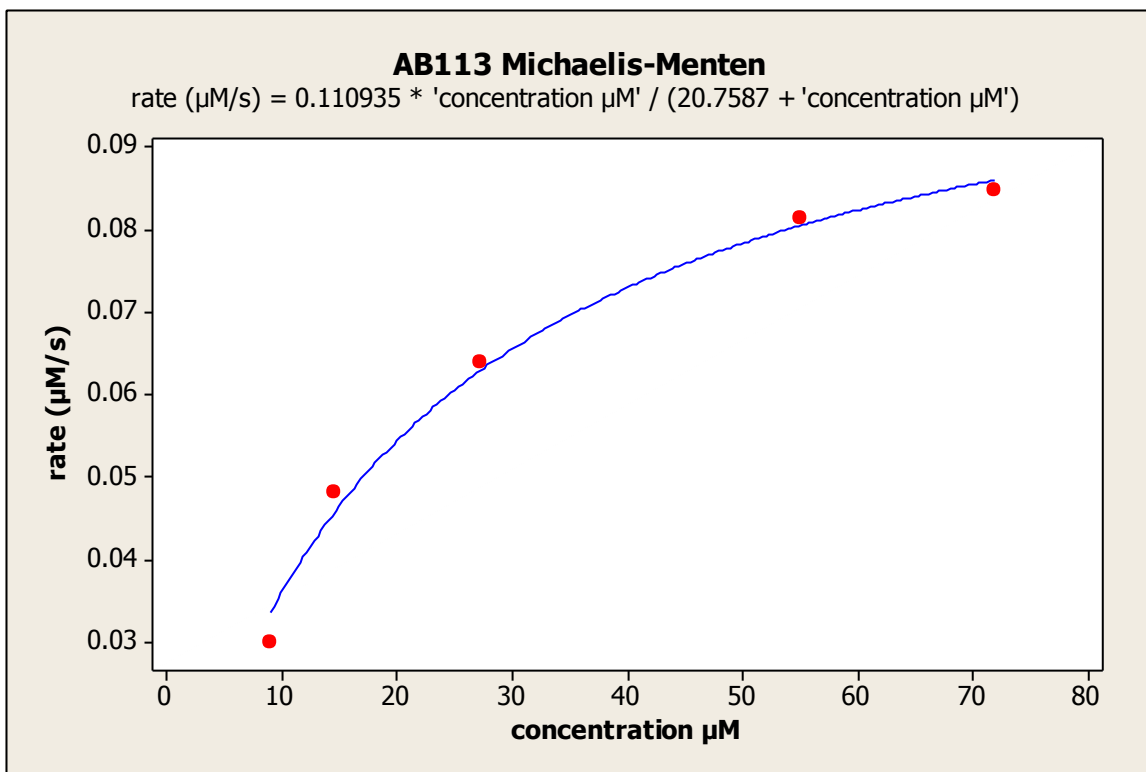


Figure 23. Michaelis-Menten plot for AB113

Obtained values: $V_{\max} = 0.11093 (\mu\text{M/s}) \pm 0.0055$, $K_M = 20.758 \mu\text{M} \pm 2.78$ $S = 0.0027995$ (reactions with 0.125 mM H_2O_2 , 0.0015 U/mL and pH 4, at room temperature)

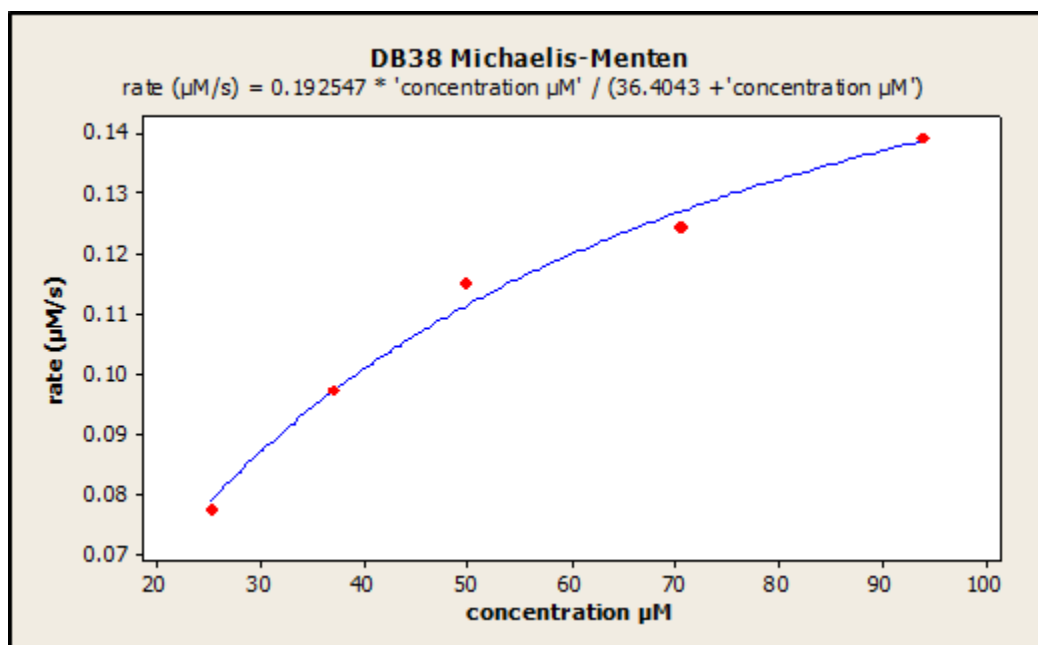


Figure 24. Michaelis-Menten plot for DB38.

Obtained values: $V_{\max} = 0.193 (\mu\text{M/s}) \pm 0.009$, $K_M = 36.4 \mu\text{M} \pm 4.3$, $S = 0.0029712$ (reactions with 0.125 mM H_2O_2 , 0.0015 U/mL and pH 3.6, at room temperature)

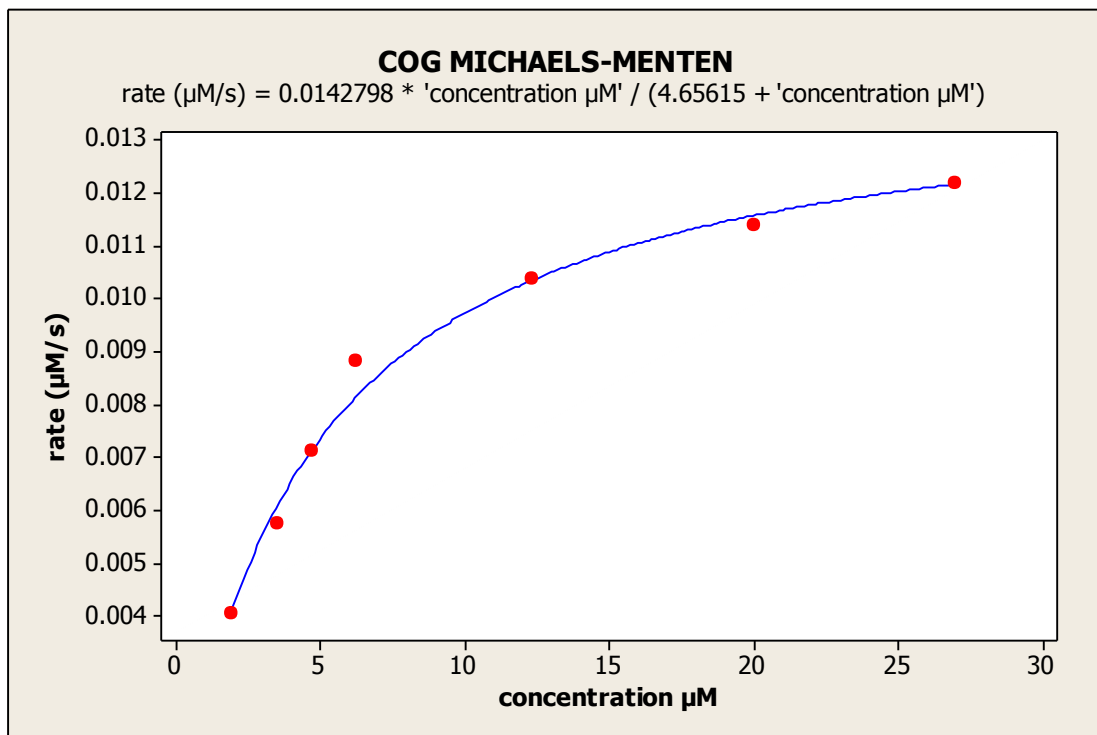


Figure 25. Michaelis-Menten plot for COG

Values obtained: $V_{\max} = 0.0142 (\mu\text{M/s}) \pm 0.0004$, $K_M = 4.66 \mu\text{M} \pm 0.45$, $S = 0.0003568$ (reactions with $0.125 \text{ mM H}_2\text{O}_2$, 0.0025 U/mL and $40 \text{ mM pH } 8$, at room temperature)

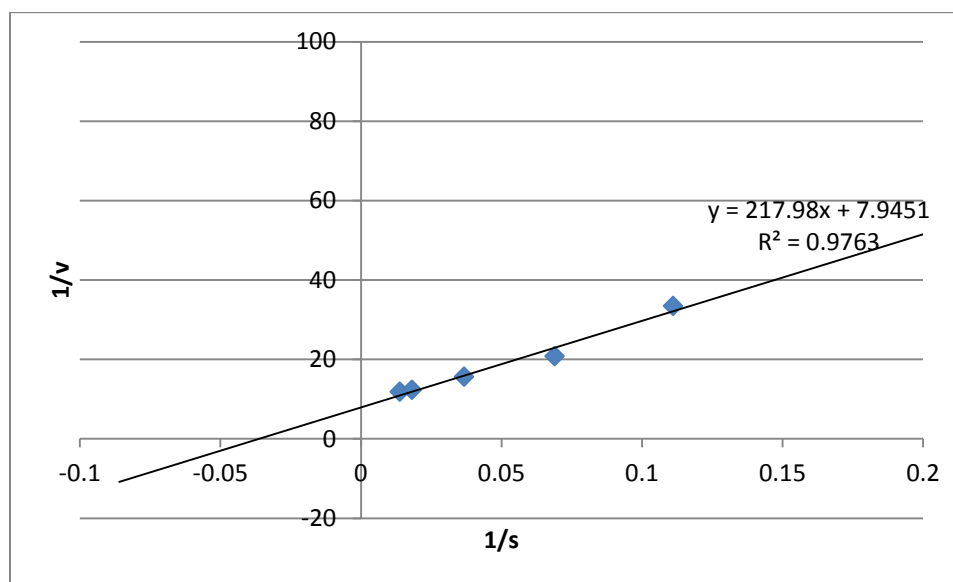


Figure 26. Lineweaver-Burk plot for AB113

Obtained values: $V_{\max} = 0.126 \pm 0.014$, $K_M = 26.3$, $R^2 = 0.9763$ (reactions with $0.125 \text{ mM H}_2\text{O}_2$, 0.0015 U/mL and $40 \text{ mM pH } 4$, at room temperature)

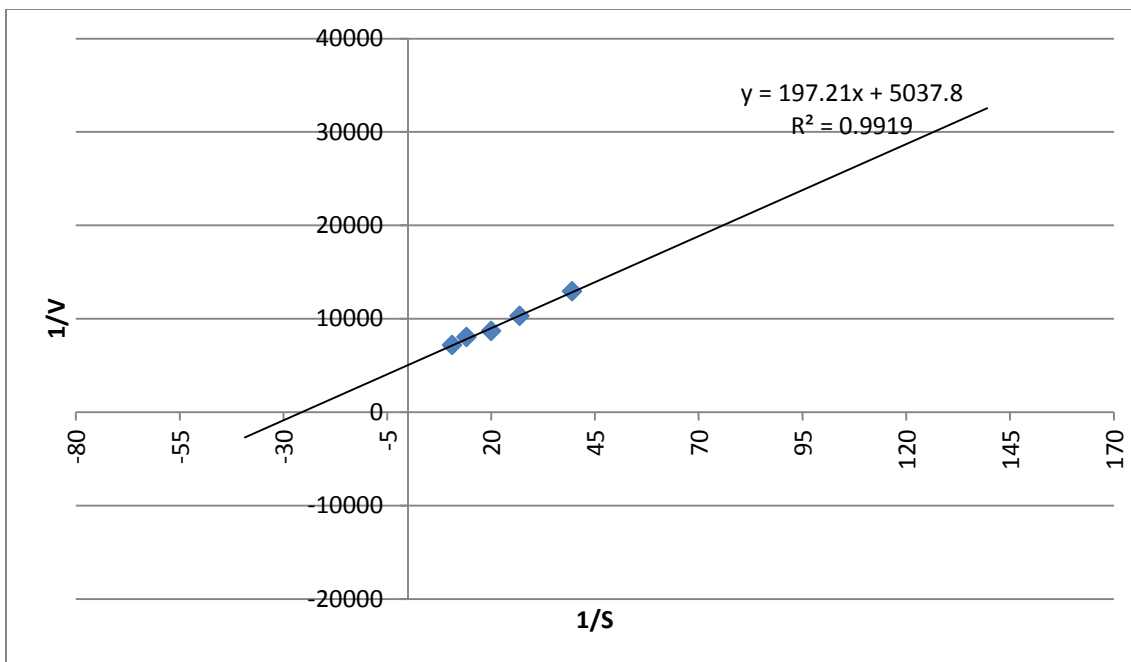


Figure 27. Lineweaver-Burk plot for DB 38.

Obtained values: $V_{\max} = 0.198 \pm 0.0099$, $K_M = 35.7$, $R^2 = 0.9919$ (reactions with 0.125 mM H_2O_2 , 0.0015 U/mL and 40 mM pH 3.6, at room temperature)

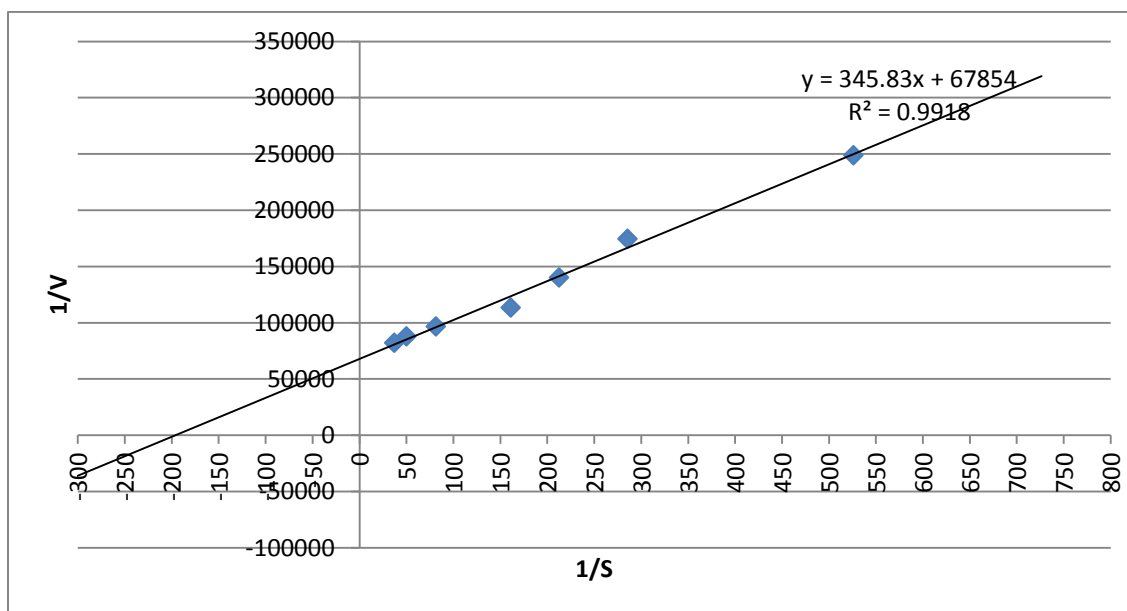


Figure 28. Lineweaver-Burk plot for COG.

Obtained values: $V_{\max} = 0.015 \pm 0.00077$, $K_M = 5$, $R^2 = 0.9918$ (reactions with 0.125 mM H_2O_2 , 0.0025 U/mL and 40 mM pH 8, at room temperature)

Table 3 and 4 show the summary of the kinetic parameters for Michaelis-Menten and Lineweaver-Burk plot, respectively.

Table 3. Kinetic parameter for Michaelis-Menten for azo-dyes

Summary of kinetic parameters fit to Michaelis-Menten equation							
Dye	K_M (μM)	V_{\max} ($\mu\text{M/s}$)	V_{\max}/K_M (s)	enzyme (U/mL)	H_2O_2 (mM)	s	pH
COG	4.7 ± 0.45	0.014 ± 0.00045	0.0030 ± 0.00030	0.0025	0.125	0.00036	8.0
AB113	21 ± 2.8	0.11 ± 0.0055	0.0053 ± 0.00074	0.0015	0.125	0.0028	4.0
DB38	36 ± 4.3	0.19 ± 0.0090	0.0053 ± 0.00067	0.0015	0.125	0.00297	3.6

Table 4. Kinetic parameters for Lineweaver-Burk plot for azo-dyes

Summary of kinetic parameters with Lineweaver-Burk plot							
Dye	K_M (μM)	V_{\max} ($\mu\text{M/s}$)	V_{\max}/K_M (s)	enzyme (U/mL)	H_2O_2 (mM)	R^2	pH
COG	5.1 ± 0.34	0.015 ± 0.0008	0.0029	0.0025	0.125	0.9918	8.0
AB113	27 ± 3.9	0.13 ± 0.016	0.0046	0.0015	0.125	0.9782	4.0
DB38	39 ± 2.7	0.20 ± 0.0094	0.0051	0.0015	0.125	0.9919	3.6

The kinetic parameter of K_M is an indicator of the affinity of the SBP to the substrate, in this case, the azo-dyes. The lower the K_M value the higher the affinity (better binding of enzyme to the respective substrate). Also, higher the V_{\max} indicates the reaction is faster.

Based on direct Michaelis-Menten plots it can be observed that the lowest K_M value is for COG followed by AB113 and then DB38. Using a double-reciprocal plot, Lineweaver-Burk plot, has the same trend, and the values are close to those predicted by Michaelis-Menten equation. The K_M value for AB113 is the one that deviates from 21 to 27 for Michaelis-Menten and Lineweaver-Burk, respectively. DB38 has the higher catalytic

efficiency (V_{\max}/K_M), using Lineweaver–Burk plot. The R^2 values ranges from 0.9782-0.9919. It can be observed a good correlation between both types of analysis. For Michaelis-Menten equation the “s value” is presented. “S value” is calculated by Minitab software. This value is known as “standard error of the regression or the standard error of the estimate”, which represents the distance from the observed values to the regression line. Studies such as the ones performed by Spiess and Neumeyer (2010), that shows how using R^2 or R^2_{adj} values for non-linear models can lead to wrong conclusions, where only between 28-43% of the time is the true model selected. Packages like Minitab does not calculate R^2 for non-linear models, instead it use the “s value” (Spiess and Neumeyer, 2010). The smaller the “s value” is the best (Minitab support 17 (b), 2017). Lineweaver-Burk plots introduce error by taking reciprocals, for this it is not the best option for parameter estimation.

Preethi *et al.* (2013) determined the kinetic parameters for AB113 for free and immobilized HRP, using the Lineweaver-Burk plots, the K_M value for free HRP was 0.068 mmol/L, and for immobilized was 0.425 mmol/L. The V_{\max} value for free HRP was 0.067 mmol/L.min and for immobilized was 0.048 mmol/L.min. Free HRP has higher affinity to AB113 than immobilized which can be due to the lower enzyme activity of immobilized HRP. Other authors have studied the kinetic parameters of azo-dyes. Rodriguez *et al.* (1999), determined that the K_M value for Reactive Blue dye was 3500-3900 μM using laccase, the variation depends on the purified enzyme activity (168/170 U/mg). Others authors, have also investigated other azo-dyes with laccase. With crude enzyme, direct black 22, K_M value was 102 μM and V_{\max} was 0.001 $\mu\text{mol}/\text{min}$ (Michniewicz *et al.*, 2008).

4.2 Two-step process. Products and total amines removal for azo-dyes

A two-step process was conducted, for both azo-dyes, in order to compare the effectiveness and requirements against the single-step process (described in section 4.1). After zero-valent iron treatment three parameters were measured: a product from azo-splitting (depending on the dye), total amines (as aniline) (see Appendix A. Figure A.6) and dye decoloration. Dye degradation by HPLC and TOC were measured under the optimal conditions to confirm the level of mineralization of the dye.

4.2.1. Color reduction after zero-valent iron reduction AB113

For the two-step process, iron reduction (as described in section 3.3.10) was done, followed by enzymatic treatment where the parameters pH, H₂O₂ and SBP concentrations were optimized. First, color reduction was optimized using different concentrations of zero-valent iron (Fe⁰) (Figure 29).

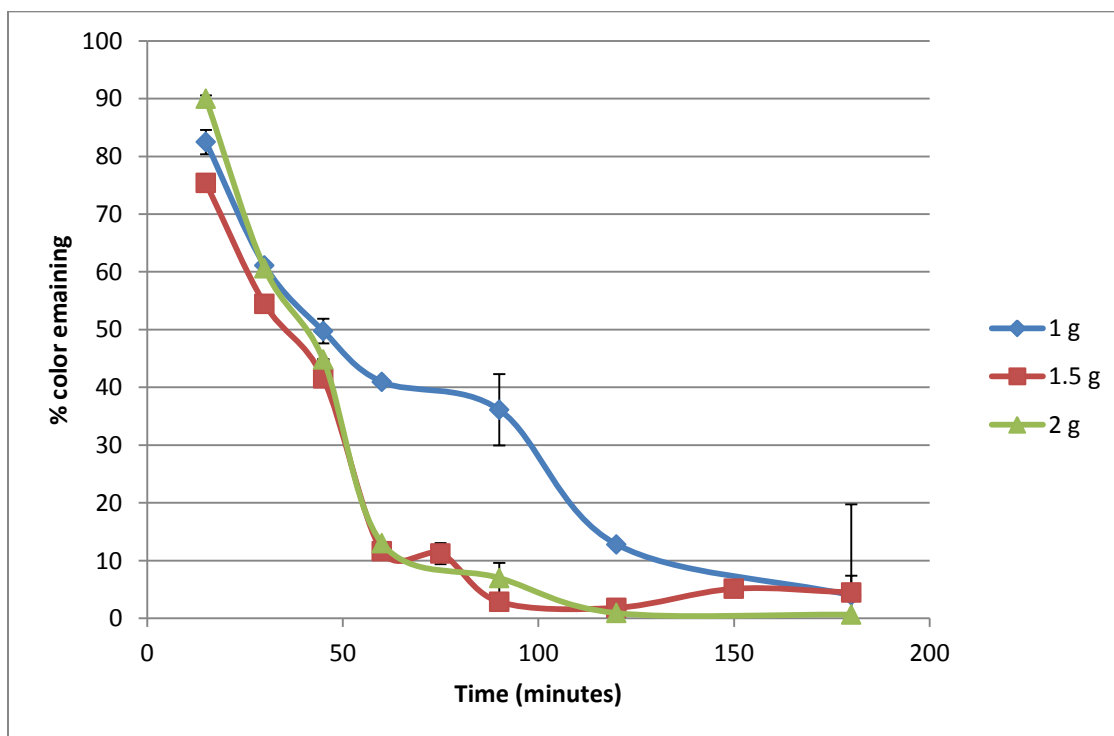


Figure 29. Color reduction after zero-valent iron treatment of 1 mM AB113 using different Fe⁰ concentrations in the presence of 1 mM sodium sulfite.

After this optimization, it was decided to choose the conditions around 90% color removal. It was chosen for AB113, 1.5 g of iron and 60 minutes reaction time for this first stage (11.7 % color remaining).

For AB113, after iron reduction, three parameters were measured: 3-aminobenzenesulfonic acid also named metanilic acid (3-ABS) (see Appendix A. Figures A.5 and A.6), which is produced after azo-cleavage of AB113 with zero-valent iron (Figure 30) (see Appendix A, Figures A.7 and A.8), total amines (as aniline) and color reduction.

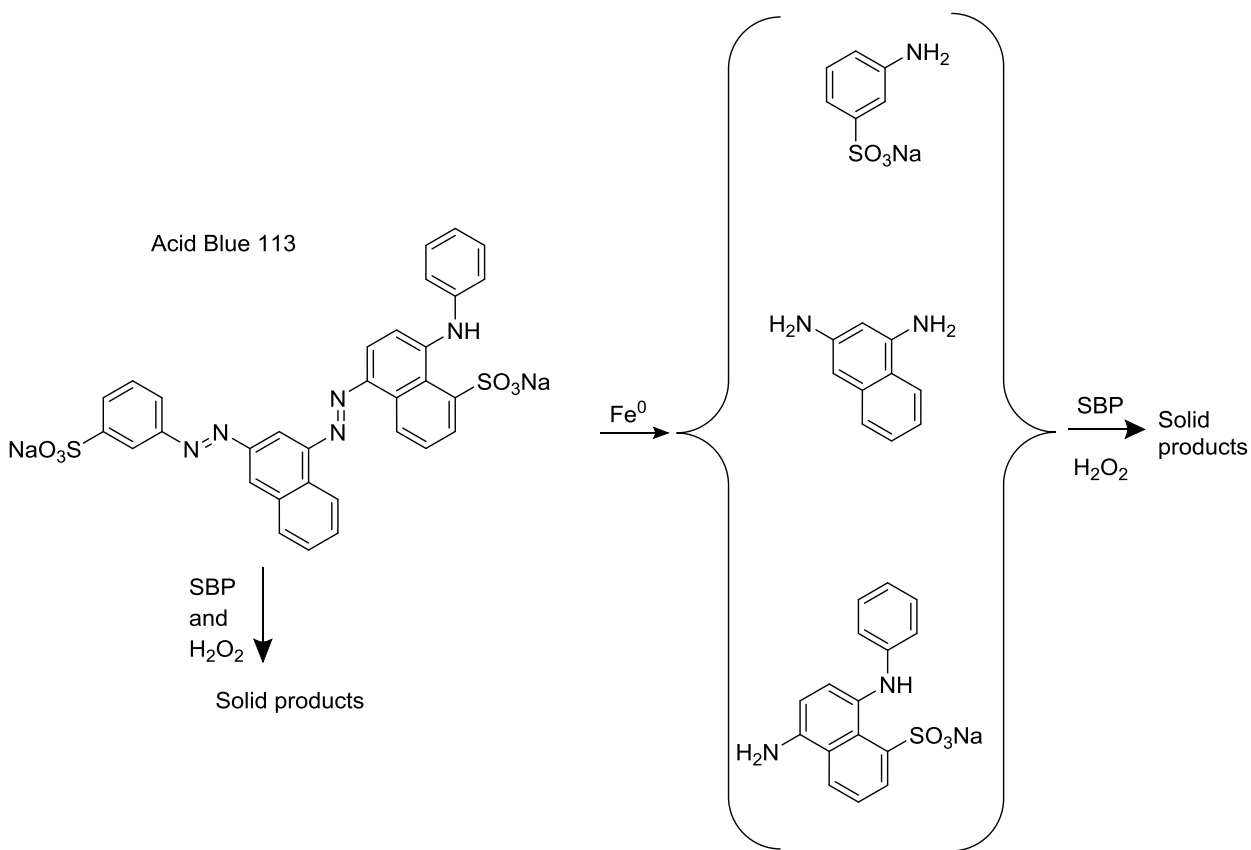


Figure 30. Azo-cleavage of AB113 by zero-valent iron reduction

The formation of 3-ABS and the dye concentration were measured with time, as seen in Figure 31, the concentration of 3-ABS was proportional to the color removal of azo-dye

AB113. The mass balance between AB113 and 3-ABS produced, reached 99% after 120 minutes, suggesting the disappearance of AB113 due to reduction by Fe^0 .

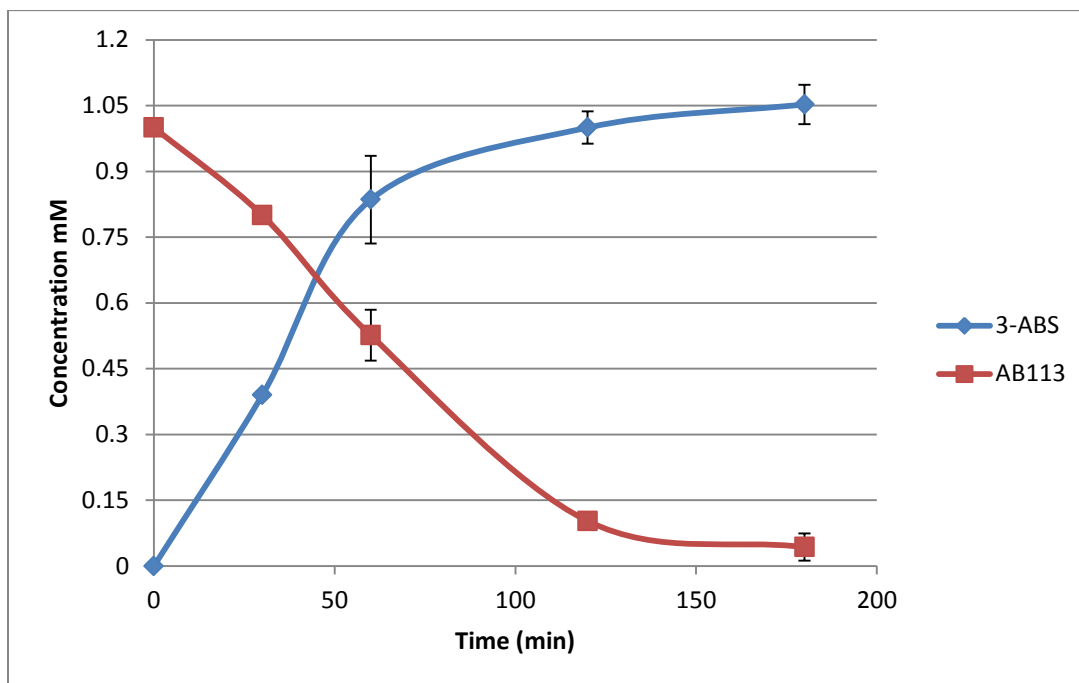
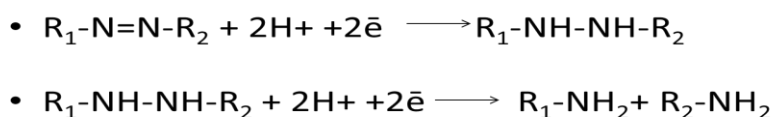


Figure 31. Time course for decoloration of 1 mM AB113 and formation of 3-ABS (mM) after iron reduction using 1g Fe^0

Similar behavior has been reported by other authors. Nam and Tratnyek (2000) reported the formation of sulfanilic acid as a product from iron reduction of Orange II by Fe^0 in 10 minutes, result of the azobenzene reduction of the dye (reductive cleavage of the azo-bond). This reaction might be a step-wise reaction. Where two electrons will be first transferred, from the Fe^0 , to transform the azo-dye into a hydrazo-intermediate, then the azo-linkage will be further reduced with two more electrons, generating the substituted aniline (Nam, 2000; Weber, 1996; Gooding *et al.*, 1996) as seen below:



4.2.2 pH optimization, second-step of two-step process. Enzymatic treatment for AB113

After iron reduction of 1 mM AB113, with 1.5 g Fe⁰ for 60 minutes, the concentrations obtained were: 1.14 mM of 3-ABS, 0.10-0.15 mM AB113, 1.2 mM of total amines. For enzymatic treatment (starting with 11.7% color remaining), batch reactor concentrations where, on average: 0.80 mM initial concentration of 3-ABS, 0.85 mM of total amines as aniline and 0.10 mM of AB113, all parameters were measured every time and the percent remaining was calculated based on those measurements. Figure 32 shows the pH optimization for the enzymatic-step, based on the 3-ABS formation. As seen in Figure 32, the optimum pH was 4.0, based on decoloration and 3-ABS remaining. Optimum pH of pure 3-ABS was found to be in the range of 3.6-4.0 (see Appendix B). All the optimizations were done under stringent conditions as established on section 4.1.

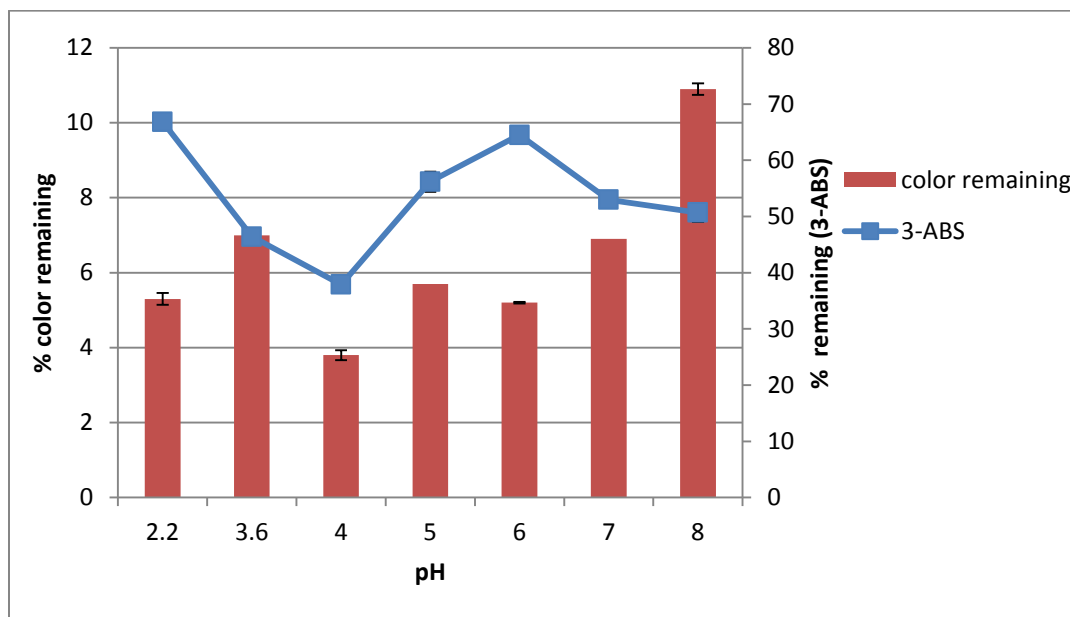


Figure 32. pH optimization for 0.8 mM 3-ABS with 1.5 U/mL SBP and 2.5 mM H₂O₂

As seen in Figure 33, pH optimization based on the total amines was also done. The optimum pH was also 4.0 for AB113 under those conditions. For this reason, further experiments were done at pH 4.0.

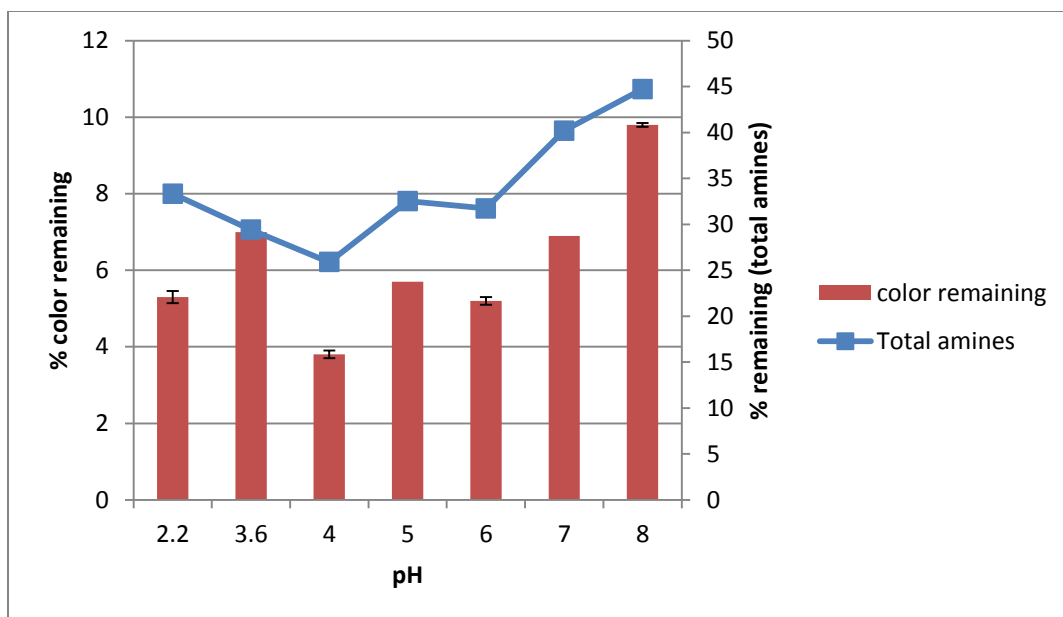


Figure 33. pH optimization for 0.85 mM total amines with 1.5 U/mL SBP and 2.5 mM H₂O₂

4.2.3 H₂O₂ optimization, second-step of two-step process. Enzymatic treatment for AB113

Figures 34 and 35 show the H₂O₂ optimization for 3-ABS and total amines, respectively. As seen in these figures, the color remaining is (with exception of 1.5 mM H₂O₂) less than 5% which is the target percent for this thesis work. However, the lowest 3-ABS percent remaining was with 2.5 mM H₂O₂ to achieve 25% and for total amines 2.5-3.0 mM H₂O₂ to achieve 0.2 mM final concentration of total amines (26.2% amines remaining).

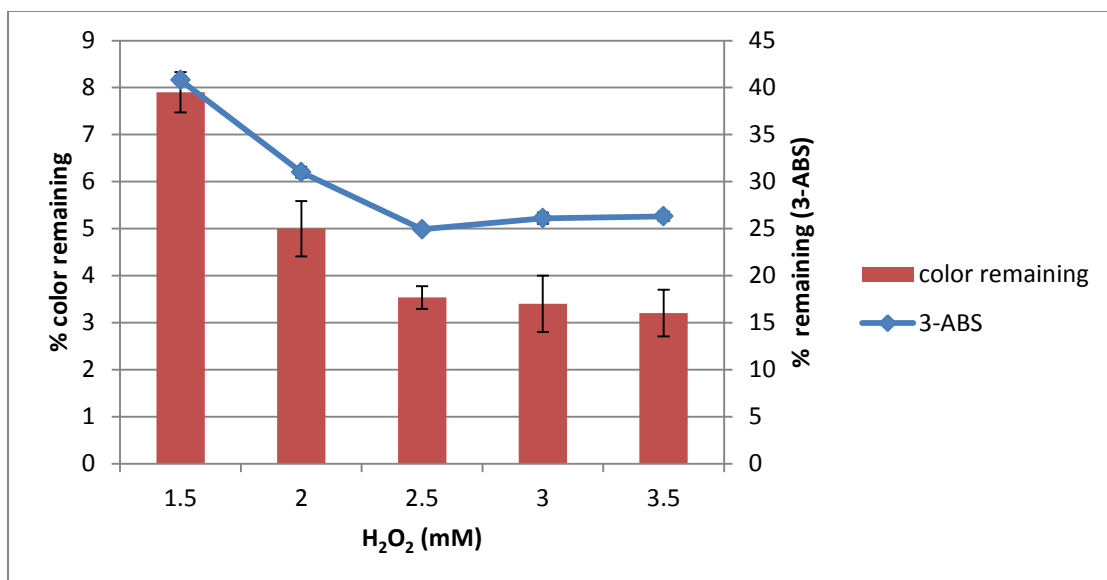


Figure 34. H₂O₂ optimization for 0.8 mM 3-ABS with 1.5 U/mL SBP at pH 4.0

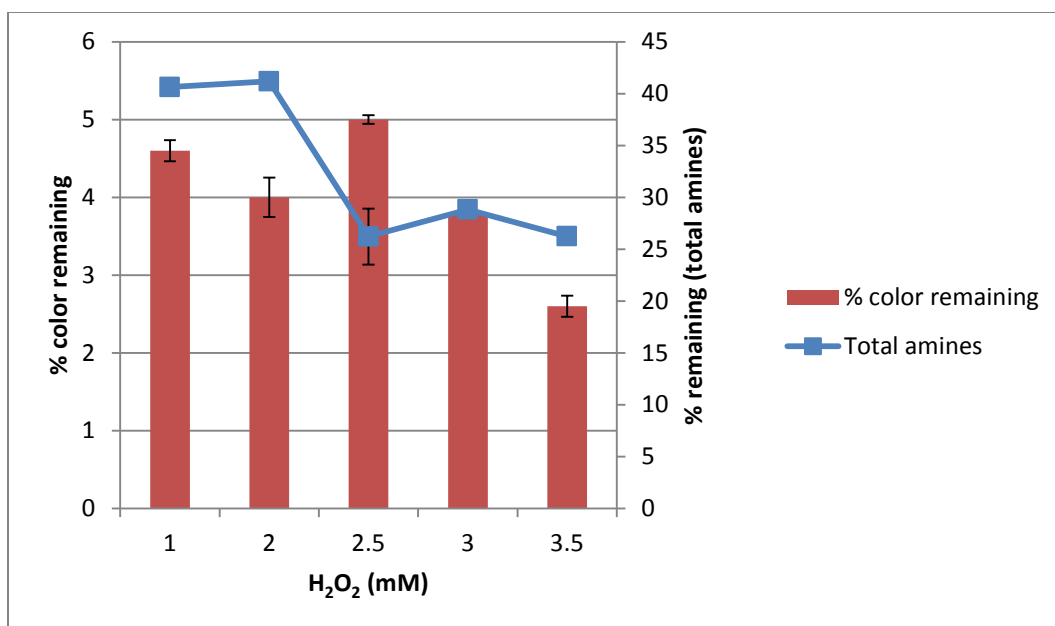


Figure 35. H₂O₂ optimization for 0.85 mM total amines with 2.5 U/mL SBP at pH 4.0

The optimum concentration for H₂O₂ for both parameters was 2.5 mM H₂O₂, same as for the single-step process.

4.2.4 Enzyme optimization, second-step of two-step process. Enzymatic treatment for AB113

For enzyme optimization, several concentrations of enzyme were tested at optimum pH and H₂O₂ concentration. As seen in Figure 36, the minimum percent remaining for 3-ABS was 21% with 1.5 U/mL.

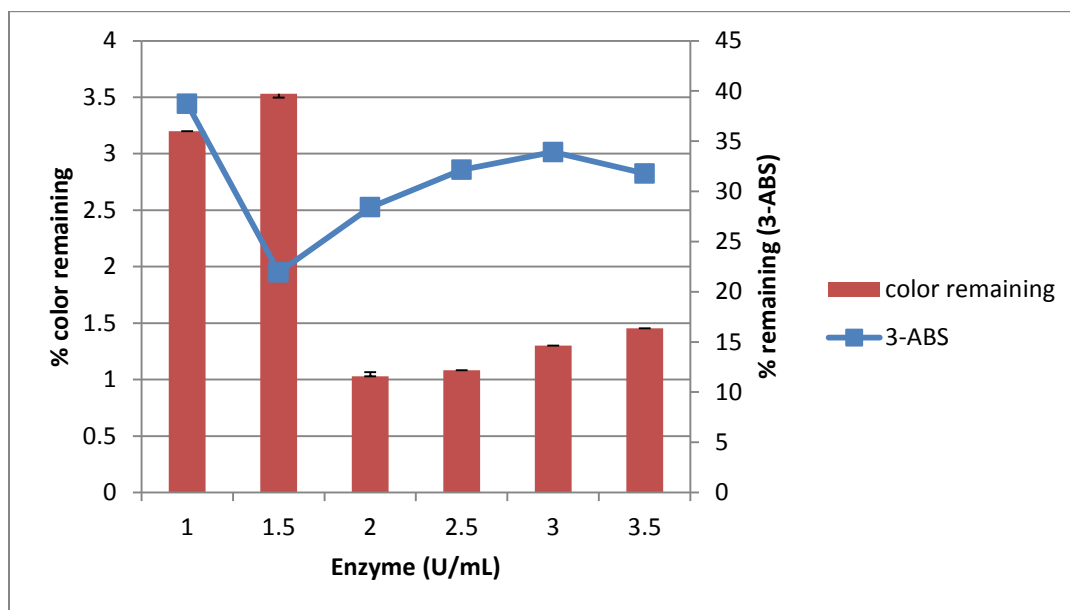


Figure 36. Enzyme optimization for 0.8 mM 3-ABS with 2.5 mM H₂O₂ at pH 4.0

For total amines, Figure 37 shows the lowest percent remaining achieved was 26% remaining with 2.5 U/mL.

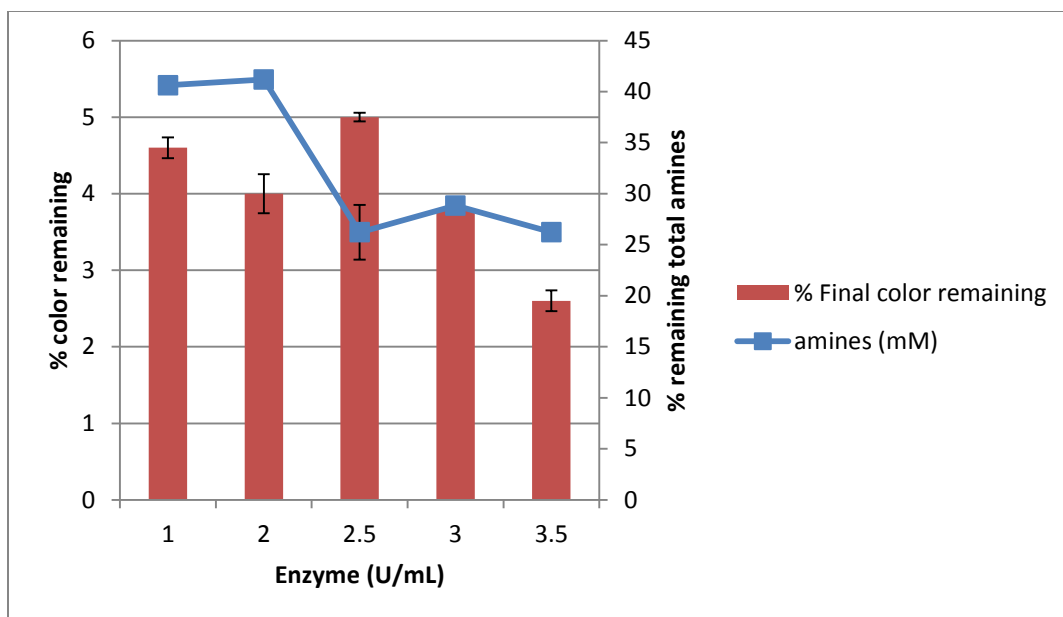


Figure 37. Enzyme optimization for 0.85 mM total amines using 2.5 mM H₂O₂ at pH 4.0

In summary, the two-step process for AB113 requires pH 4.0, with 2.5 mM H₂O₂ and 1.5 U/mL SBP for 21% remaining of 3-ABS. For total amines, optimal conditions were pH 4.0 with 2.5 mM H₂O₂ and 2.5 U/mL for 26% remaining based on total amines (0.2 mM). For both conditions, color reduction and dye degradation are at less than 5% remaining. Even though the optimum color reduction is reached with this two-step process, the appearance of products after iron reduction, such as 3-ABS and total amines are high and even under optimal conditions approximately 20% is remaining for both components. The product 3-ABS is a substrate which requires high amounts of SBP and H₂O₂ and does not reach high removal efficiencies; pure 3-ABS (1 mM) required 1 mM H₂O₂ and 3 U/mL to achieve around 26% remaining (see Appendix B). Another consideration is that after the single-step process the final concentration of total amines is 0.7 mM under optimal conditions for color removal, less than 5% color remaining (1.5 U/mL and 2.5 mM H₂O₂ at pH 4.0). The starting dye has a concentration of 0.5 mM total amines, which means that after enzymatic reaction some product compounds are formed as amines, this can be due a possible azo-bond breakage during the enzymatic treatment. Other processes, like anaerobic decoloration of Disperse Blue 79, have shown a similar behavior of an increase of total amines after treatment indicating the azo-bond cleavage

for that process (Melgoza *et al.*, 2004). To obtain more amine removal with a single-step process, higher enzyme concentration should be used (Figure 38). At pH 4.0, 2.5 mM of H₂O₂ and 2.5 U/mL SBP lowest amines remaining can be achieved (0.17 mM). It should be noted, that the azo-dye concentrations used in this thesis for AB113 and DB38 is in the high range (682 mg/L and 391 mg/L). Studies using real wastewater have found concentrations in the range of 0-600 mg/L from a cotton textile dyeing wastewater treatment plant at Yixing, Jiangsu Province, China (Dai *et al.*, 2016). Concentrations of 200 mg/L were used in another study, where the concentration was selected as approximately the same found in real wastewater in Argentina (Durruty *et al.*, 2015). As reviewed by Pandey *et al.* (2007) and Lade *et al.* (2015), wastewater containing 10–200 mg/L of dyes are high colored wastewater.

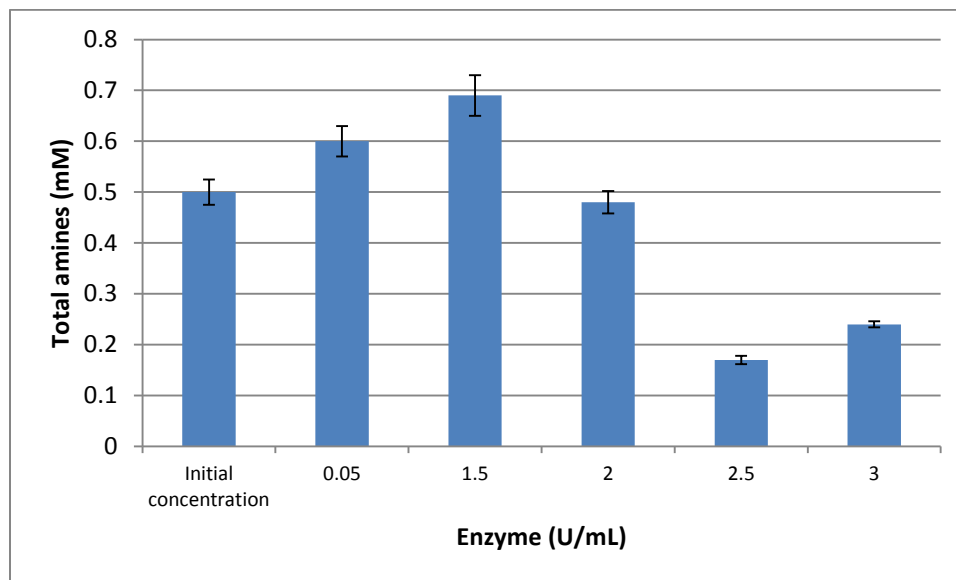


Figure 38. Total amines after single-step process for 1 mM AB113 with 2.5 mM H₂O₂ at pH 4.0

4.2.5. Color reduction after zero-valent iron reduction DB38

As for AB113, first color reduction was optimized using different concentrations of Fe⁰ (Figure 39).

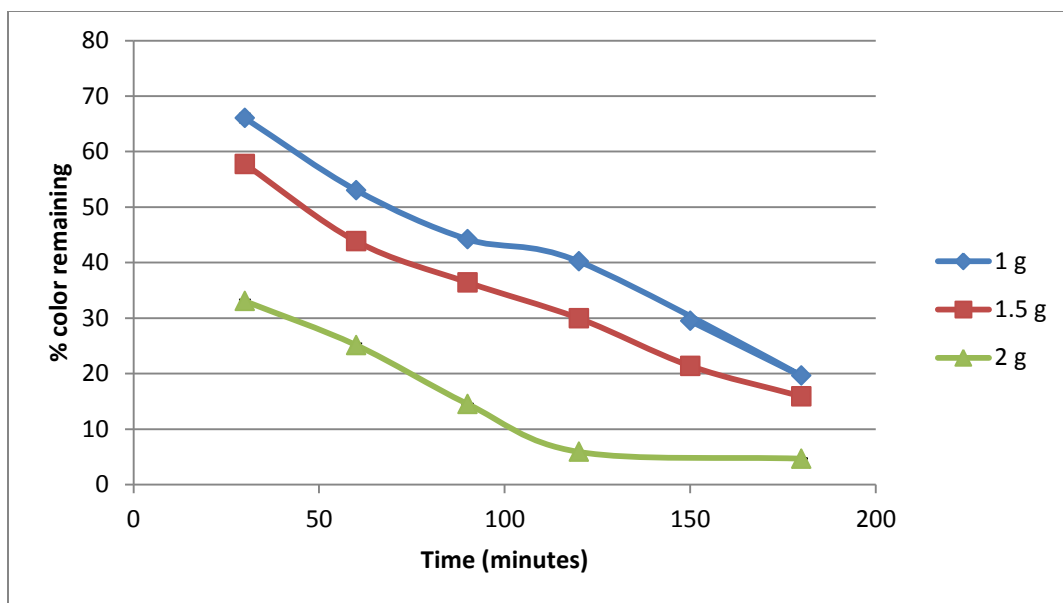


Figure 39. Color reduction after iron zero-valent of 0.5 mM DB38 using different Fe⁰ concentrations in the presence of 1 mM sodium sulfite.

For DB38, 2.0 g and 120 minutes for 0.5 mM DB38 were selected, followed by enzymatic treatment where pH, H₂O₂ and enzyme optimizations were done. After iron reduction aniline and benzidine are produced as result of the azo-reduction process (Figure 40) (see Appendix A.9 and A.10).

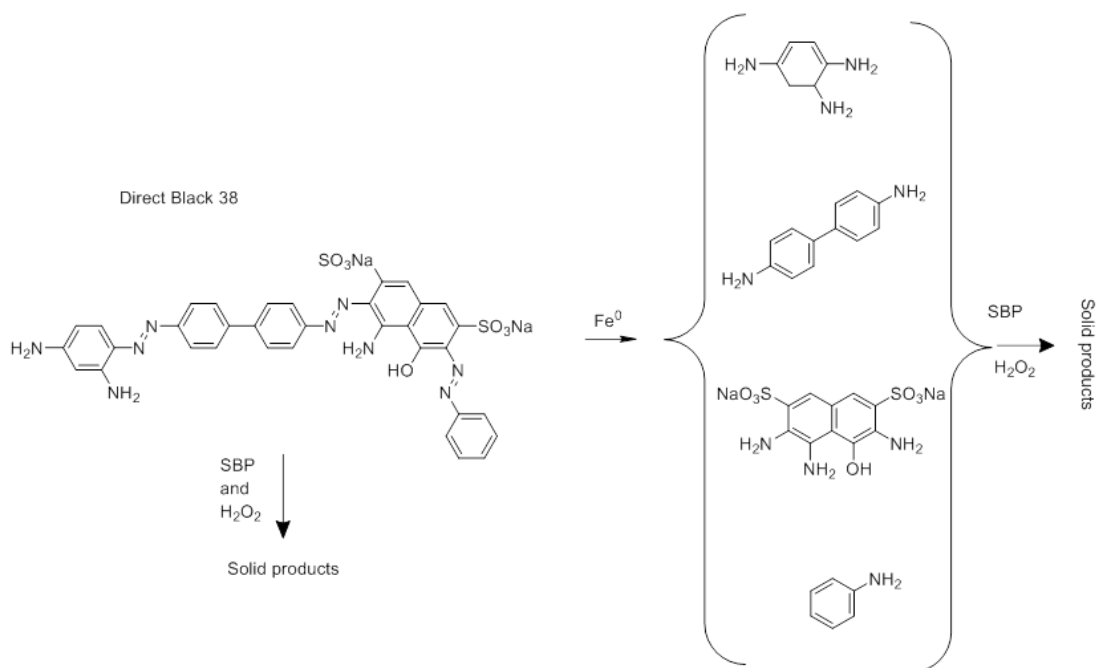


Figure 40. Azo-cleavage for DB38 after zero-valent iron reduction

After iron reduction process the color remaining was 5.6%, 0.45 mM aniline, 0.48 mM benzidine and 2.0 mM total amines. Thus for enzymatic treatment the initial conditions were 0.33 mM for aniline, 0.35 mM for benzidine and 1.5 mM total amines. Figure 41 shows the aniline and benzidine produced after azo-cleavage of DB38 with Fe^0 . This behavior is the same as describe by AB113 in this dissertation work and other authors (Nam, 2000; Samar 2014)

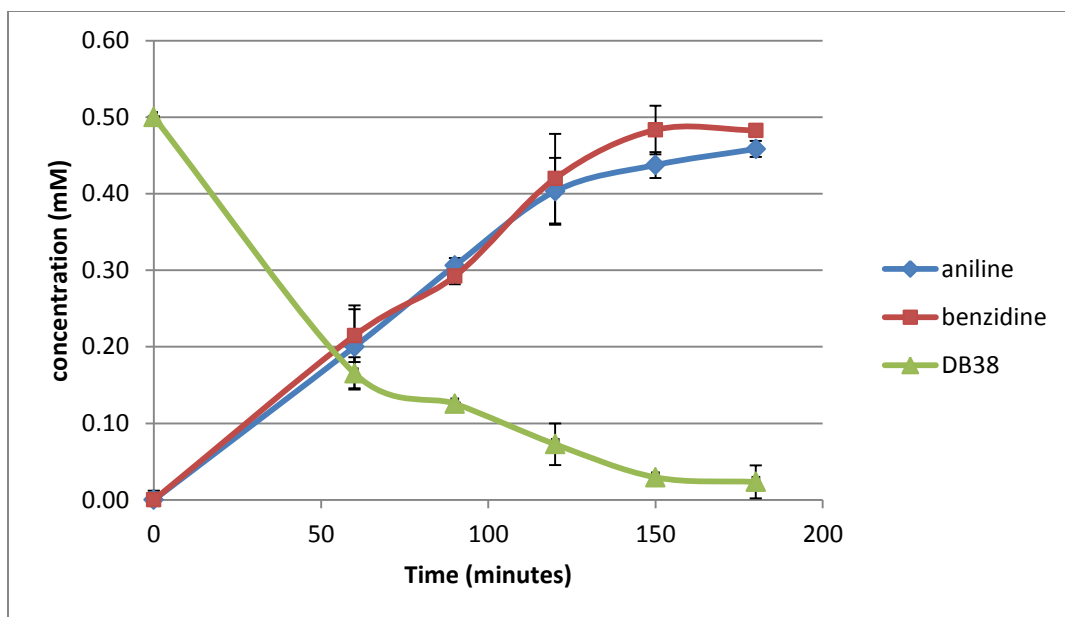


Figure 41. Time course of decoloration of 0.5 mM DB38 and formation and subsequent formation of aniline and benzidine after iron reduction using 1 g Fe⁰

4.2.6. pH optimization, second step enzymatic treatment for DB38

Color removal is not presented for DB38 graphs as the initial concentration (for the enzymatic process) was already 5% color remaining. Figure 42 shows the pH optimization based on total amines.

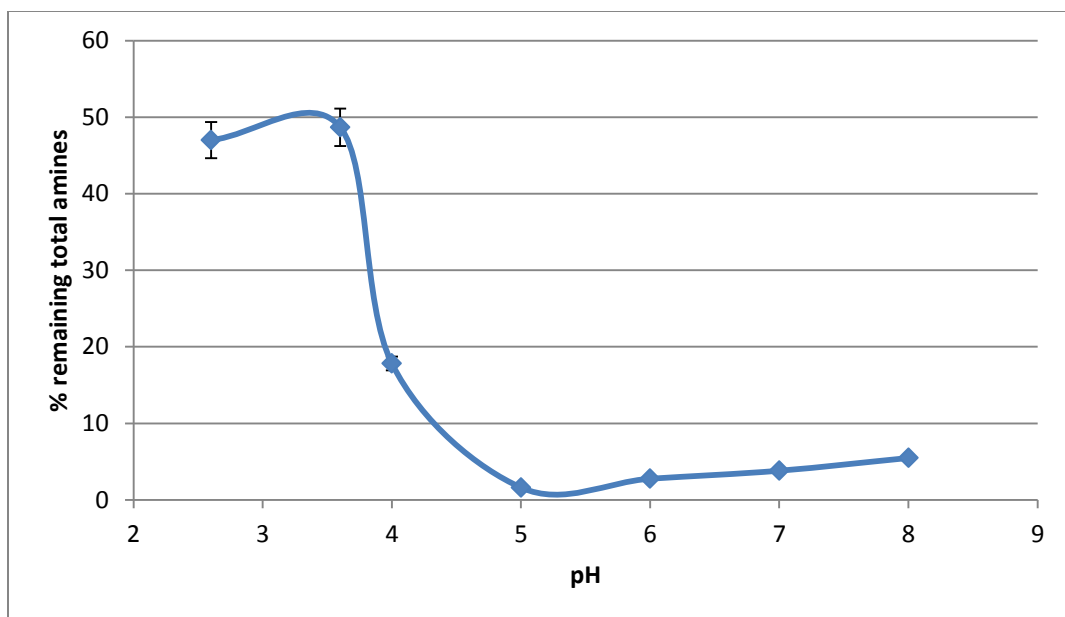


Figure 42. pH optimization of 1.5 mM total amines with 0.5 U/mL SBP and 1 mM H₂O₂

As seen in Figure 42, for pH 5.0, 6.0, 7.0 and 8.0 the total amines remaining are less than 5% , for this reason another pH optimization was done to create more stringent conditions and determinate the optimum pH (Figure 43).

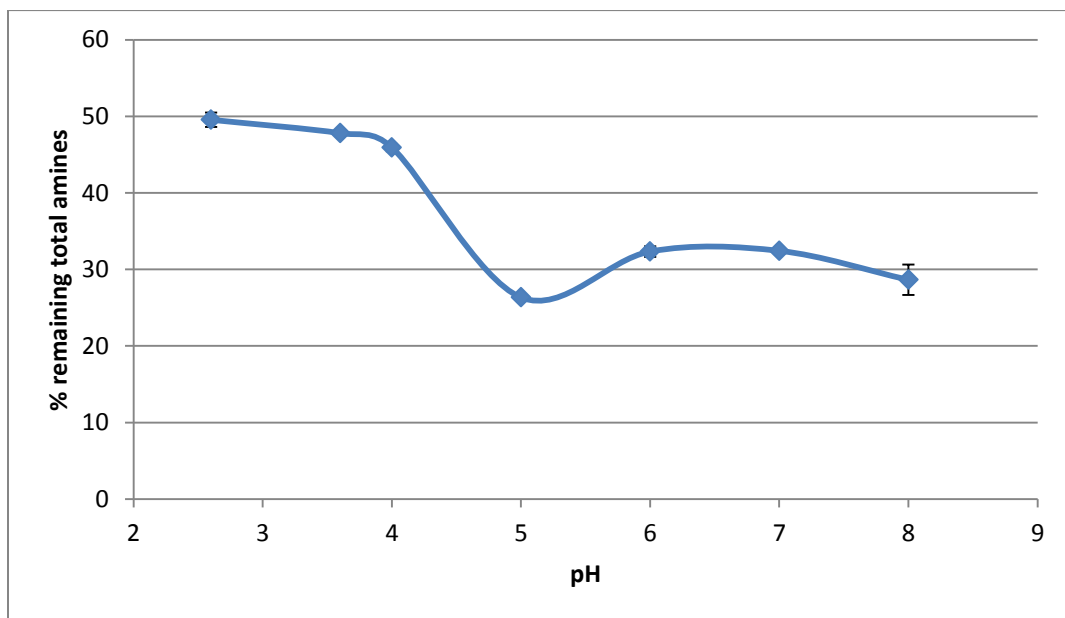


Figure 43. pH optimization of 1.5 mM total amines from 0.5 mM DB38 with 0.5 U/mL SBP and 0.5 mM H₂O₂

It can be observed that the optimum pH for total amines was 5.0. Authentic aniline and benzidine optimum pHs have been reported as pH 5.0 (Mazloun, 2014; Altahir *et al.*, 2015).

Figure 44 and 45 shows the pH optimization for products aniline and benzidine. As seen in Figure 44, the optimum range was 5.0-7.0 with less than 8% remaining. As done for total amines, more stringent conditions were chosen to determinate the optimal pH. Figure 45 show that the optimum pH was 5.0.

Since this pH (pH 5.0) was optimum for total amines, aniline and benzidine further experiments were done with this pH.

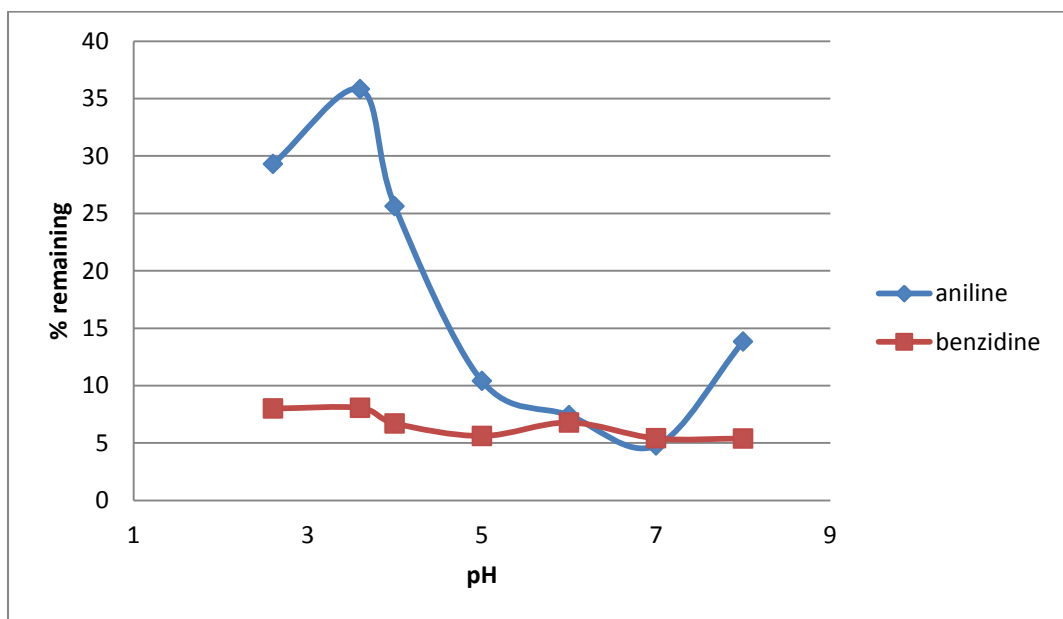


Figure 44. pH optimization for 0.33 mM aniline and 0.35 mM benzidine with 0.5 U/mL SBP and 1 mM H₂O₂

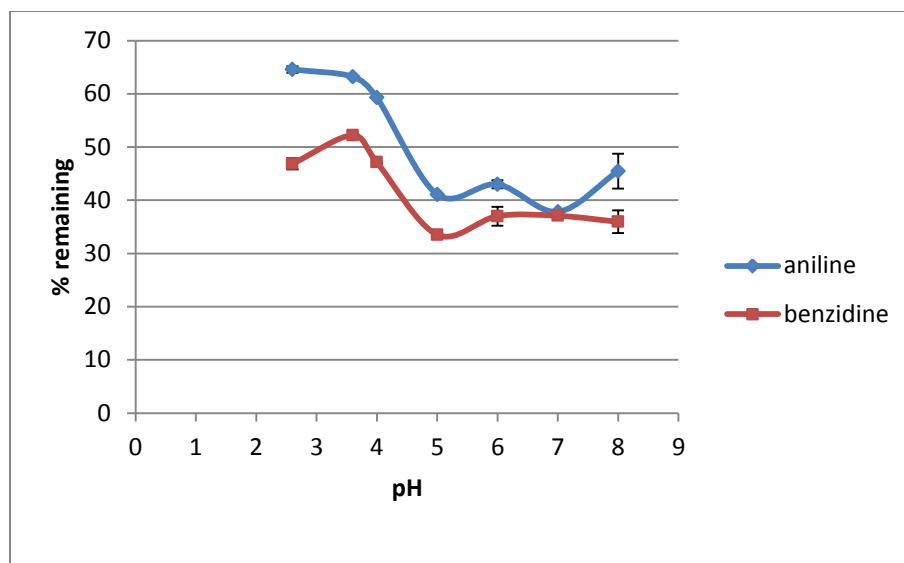


Figure 45. pH optimization for 0.33 mM aniline and 0.35 mM benzidine with 0.5 U/mL SBP and 0.5 H₂O₂

As seen under the conditions in Figure 45, benzidine appears as well as aniline after enzymatic treatment. However, benzidine is not the “limiting factor” (since it requires less enzyme and peroxide concentration than aniline). It is noticed that aniline is a substrate which requires more enzyme and H₂O₂ concentrations than benzidine. Benzidine has been proven to be an enzyme substrate where 0.1 mM pure benzidine requires 0.43 mU/mL SBP, and 0.15 mM H₂O₂ at pH 5 for single-step enzymatic treatment (Altahir *et al.*, 2015). Aniline, has been proven to be also a SBP substrate where 0.6 U/mL of SBP and 1.5 mM H₂O₂ at pH 5.0 for around 95% removal. In Figure 45 seen to have run out H₂O₂, for this reason a final pH optimization was done with lower amount of enzyme and higher amount of H₂O₂, to prove the behavior mention above which indicates that the control factor will be aniline (Figure 46).

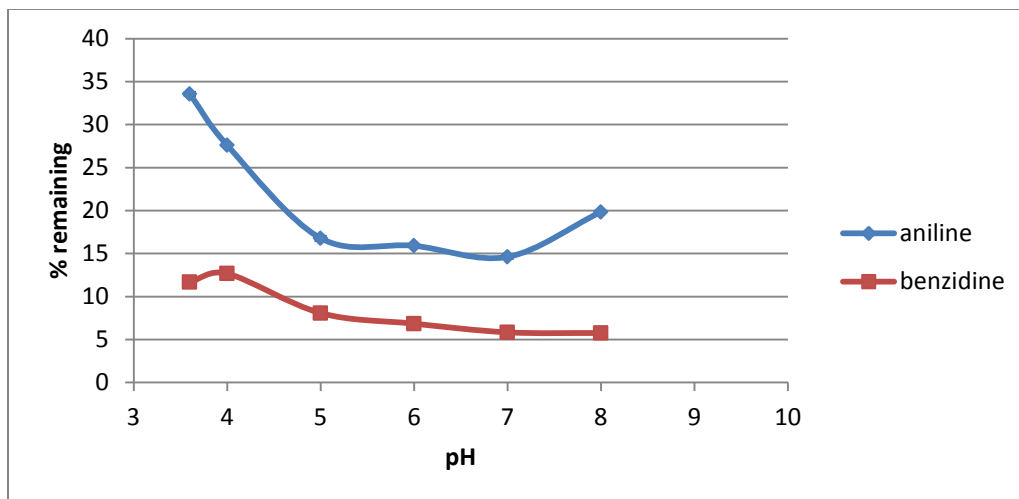


Figure 46. pH optimization for 0.33 mM aniline and 0.35 mM benzidine with 0.2 U/mL SBP and 1 mM H₂O₂

Even though, the aniline is confirmed to be the “limiting factor”, benzidine will be measured after every experiment.

Figure 47 shows the enzyme optimization for the products aniline and benzidine, where for all the concentrations benzidine were less than 5% remaining, as for aniline 0.6 U/mL is required.

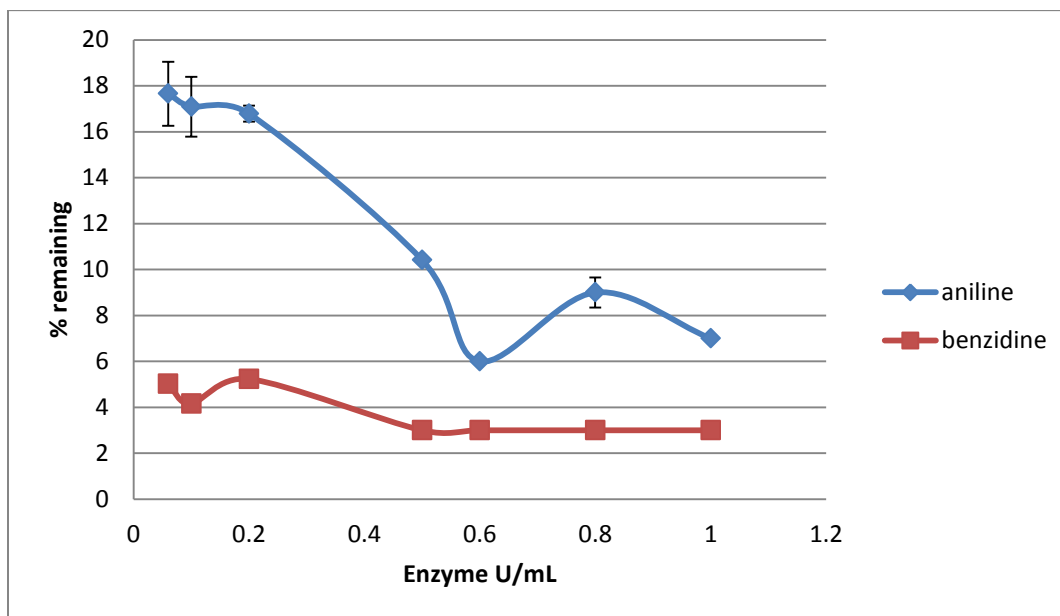


Figure 47. Enzyme optimization for 0.33 mM aniline and 0.35 mM benzidine with 1 mM of H₂O₂ at pH 5.0

As seen in Figure 48, the optimum enzyme concentration for total amines is in the range of 0.5-0.6 U/mL SBP for less than 5% remaining. However, with 0.1-0.3 the % remaining was close to 5% (5.9 % - 5.3 %).

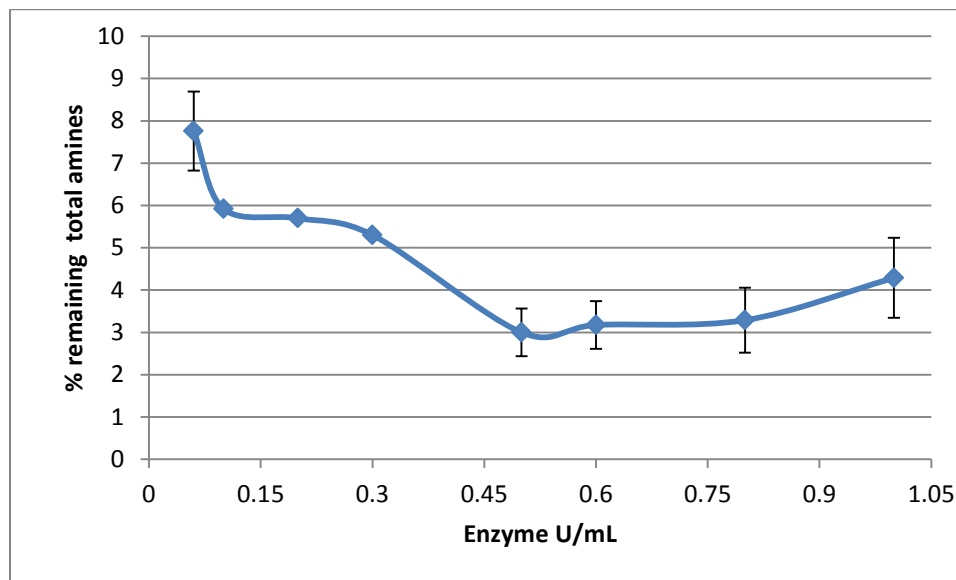


Figure 48. Enzyme optimization for 1.5 mM total amines with 1 mM of H₂O₂, pH 5.0

Since for aniline the optimum enzyme concentration is 0.6 U/mL and for total amines is in that same range, 0.6 U/mL was chosen for H₂O₂ optimization for both parameters.

4.2.7. H₂O₂ optimization second step enzymatic treatment for DB38

Figures 49 and 50 show the H₂O₂ optimization for aniline and benzidine and for total amines, respectively. As seen in the other optimizations, all the parameters measured follow the same behavior. Thus, 1.1 mM H₂O₂, 0.6 U/mL SBP at pH 5.0 were needed to achieve less than 5% remaining of aniline, benzidine and total amines. Under these conditions more than 95% color removal was achieved as well as 98% dye degradation.

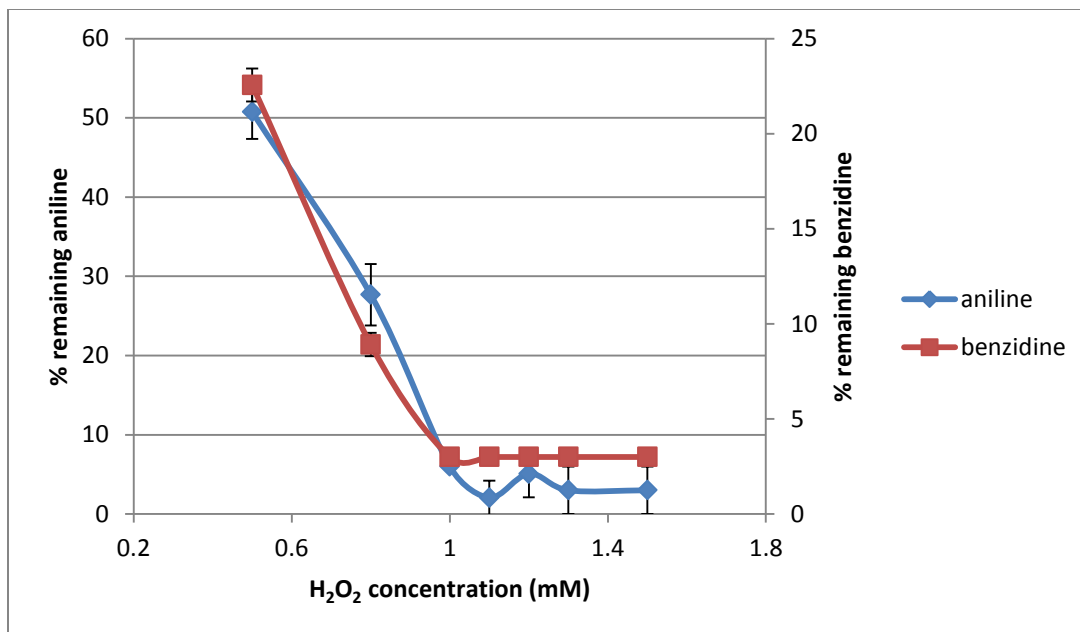


Figure 49. H₂O₂ optimization for 0.33 mM aniline and 0.35 mM benzidine with 0.6U/mL SBP

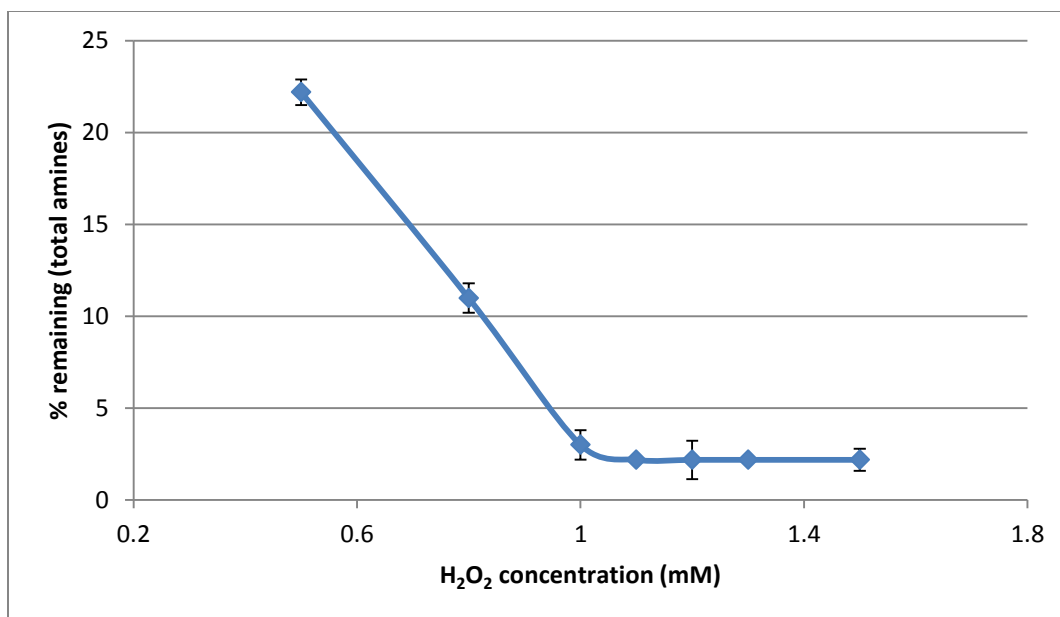


Figure 50. H₂O₂ optimization for 1.5 mM total amines with 0.6U/mL of SBP

Table 5 shows the optimal conditions for the two-step process for both azo-dyes. For both dyes after Fe⁰ reduction, in terms of total amines assuming that 1 mole of AB113 should produce 5 moles of amines and that 1 mole of DB 38 should produce 9 moles of amines, the yields achieved are in the range of 22-24%. It should be noted that the amines

measured in this thesis work are amines as aniline which might be the reason for not achieving the 100% mass balance. A similar mass balance have been detected, Elisangela *et al.*(2009) measure aromatic amines as aniline-2-sulfonic acid, obtaining mass balance from 40-100% for mono and diazo dyes with *Staphylococcus arlettae* strain VN-11. However, a mass balance for AB113 and the 3-ABS produced was 110% and for DB38 for aniline and benzidine produced were 90 and 96%, respectively.

Table 5. Two-step process optimal conditions for AB113 and DB38

Azo-dye	Fe ⁰ conditions	SBP (U/mL)	H ₂ O ₂ (mM)	pH	Color remaining %	Dye remaining %	Total amines remaining %	Product remaining %
AB113	1.5 g /60min	1.5	2.5	4.0	≤ 5	≤ 5	NA	21*
AB113	1.5 g /60min	2.5	2.5	4.0	≤ 5	≤ 5	26	31*
DB38	2 g/ 120 min	0.6	1.1	5.0	≤ 5	≤ 3	≤ 5	≤ 5**

* 3- aminobenzenesulfonic acid

** Aniline and benzidine

4.3 TOC removal for single-step and two-step process

The total organic carbon value is indicative of mineralization of the dyes under single (enzymatic treatment) or two-step process (iron reduction then enzymatic treatment). To confirm that some of the dye was being mineralized to CO₂, TOC analyses were carried out on untreated solution as well as under the optimal conditions for decoloration and degradation with single and two-step processes. The TOC data was converted into TOC remaining using the initial % TOC value of the untreated samples for both processes (see Appendix, Figure A.11).

By one-step enzymatic reaction under the optimal conditions for dye decoloration and degradation, for AB113 the average TOC remaining was 70% while for DB38 was 22.6%. For the two-step process under optimal conditions, the TOC remaining for AB113 was 31.9 % and for DB38 was 10.4% (Figure 51).

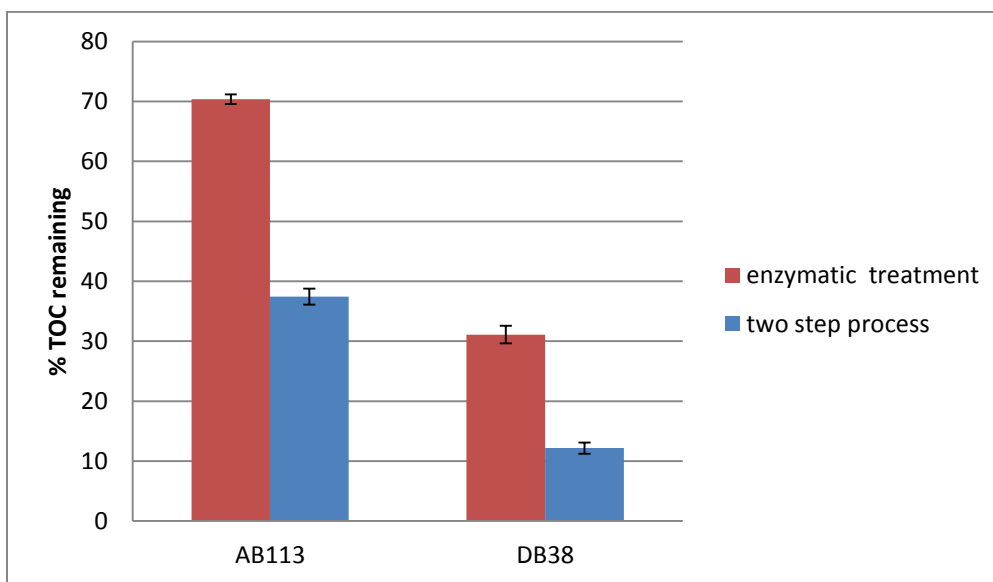


Figure 51. TOC remaining for single and two-step processes for AB113 and DB38.

Single-step: AB113 1.5 U/mL, 2.5 mM H₂O₂ and pH 4.0; DB38 3U/mL, 3mM H₂O₂ and pH 3.6. Two-step process: AB113, 2.5 U/mL, 3 mM H₂O₂ and pH 4.0; DB 38, 0.6 U/mL and 1.1 mM H₂O₂ and pH 5.0

Ali *et al.* (2013) used SBP with a redox mediator to degrade the azo-dye Crystal Ponceau 6R, CP6R. For a sample with 100% dye decoloration of 400 ppm CP6R (0.80 mM), 35% TOC remaining was achieved. Matto and Husain (2007) demonstrated the decoloration of direct dyes with salt fractionated turnip proteins in the presence of redox mediators Hydroxybenzotriazole and Violuric acid, achieving TOC remaining between 10-30%.

Based on this thesis work and past work in the same research group (Mazloun, 2014), the two-step process is observed to work generally better for azo-dyes for which the purity is low and the products after iron reduction process are substrates for the enzyme. DB38 with purity $\geq 45\%$ or AR4 (Acid Red 4) with 45% purity (Mazloun, 2014) worked better with iron reduction process as a pretreatment. DB38 products aniline and benzidine are substrates of enzyme which requires low concentration of SBP and H₂O₂, similar behavior was seen for *o*-anisidine product of AR4. Even though AB113 purity was only 50%, the product like 3-ABS is not a good substrate for SBP.

4.4 COG azo-cleavage evidence

Several authors have found evidence that suggests an azo-cleavage with peroxidases (Onder *et al.*, 2011; Kalsoom *et al.*, 2013; Ali *et al.*, 2013; López *et al.*, 2004). Onder *et al.* (2011) used HPLC-UV-ESI-MS to identify possible products of the enzymatic reaction of HRP with azo-dye naphthol blue black. The results suggest that decoloration of the dye was via reductive cleavage of the azo-bond. Kalsoom *et al.* (2013) used HPLC-DAD and LC-MS/MS to develop a mechanism of degradation of a diazo Trypan dye with SBP. It was found that SBP degradation was via symmetrical azo-cleavage and following radical-initiated ring opening of the metabolites. Ali *et al.* (2013), studied mono-azo Crystal Ponceau 6R (CP6R azo-dye) in the presence of a mediator HOBt, with SBP, using MS/MS they analyzed several metabolites finding that both symmetric and asymmetric azo-bond cleavage were involved in the dye degradation. López *et al.* (2004) used NMR and EI-MS and HPLC to identify the products (intermediates and final products) of the enzymatic reaction of azo-dye Orange II with MnP. The authors found products which suggest symmetrical and asymmetrical azo-cleavage occurred in their enzymatic system. In none of these cases was a mass balance attempted, thus there is no knowledge as to how important the azo- cleavage pathway is relative to phenolic/aniline polymerization.

In this thesis work, it was tried to identify a possible product for azo-cleavage for COG and determine under which conditions this product was produced and quantify it by HPLC and confirms its identity by EI-MS. COG was used for this study since the purity was 90%, in order to avoid any interference of the impurities. Assuming a symmetrical azo-bond cleavage, aniline would be produced after treatment with SBP, thus for this, aniline was used as a target product.

4.4.1 HPLC analysis

Several concentrations of enzyme and H₂O₂ were tested with 1mM COG at pH 8 detecting the amount of aniline released by HPLC, to get evidence of azo-splitting catalyzed by SBP during a 3-hour reaction. pH 8 has been demonstrated to be optimal for COG with SBP but not for aniline treatment (pH 5), which allowed detection of aniline after enzyme treatment (Mazloun, 2014). Aniline is a SBP substrate, which might be formed in greater amount but it reacts with the SBP, nevertheless the pH used (pH 8) is not optimal for aniline-SBP treatment which might be the reason why some aniline remain in the batch. As it can be seen (Figure 52) the highest amount of aniline released was around 0.025 mM, which was achieved during the first minutes of reaction persist for 3 hours.

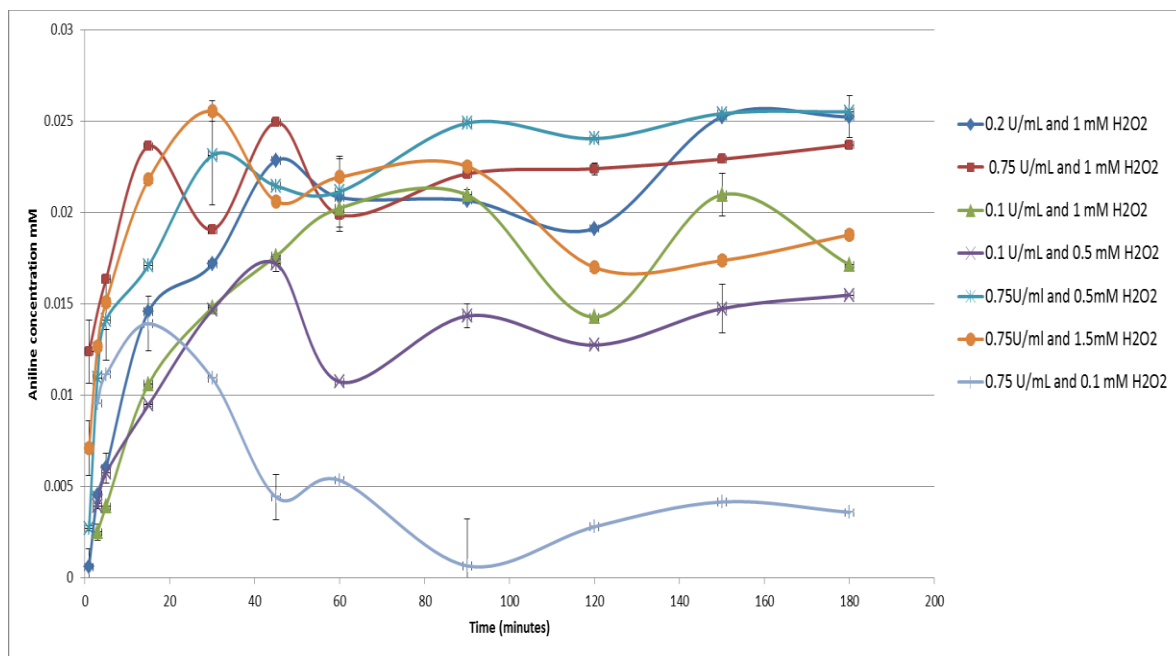


Figure 52. Aniline produced after enzymatic treatment of 1 mM COG with different SBP and H₂O₂ concentrations (mM) at pH 8

Figure 53 shows the degradation of COG under HPLC and spectroscopy techniques for the different concentrations of enzyme and H₂O₂ used in samples from Figure 52. The best conditions for aniline production in Figure 52, 0.75 U/mL and 0.5 mM H₂O₂ (0.026

mM aniline formed) are seen in Figure 53 to achieve dye degradation to about 41% and 32% remaining by spectroscopy and HPLC, respectively. Similar final aniline concentration was achieved with 0.75 U/mL and 1 mM H₂O₂ (0.237 mM aniline formed) for 18% dye remaining by spectroscopy and 10 % by HPLC and 0.2 U/mL and 1 mM H₂O₂ (0.0252 mM aniline formed) for 21% and 12% dye remaining by spectroscopy and HPLC, respectively (Table 6).

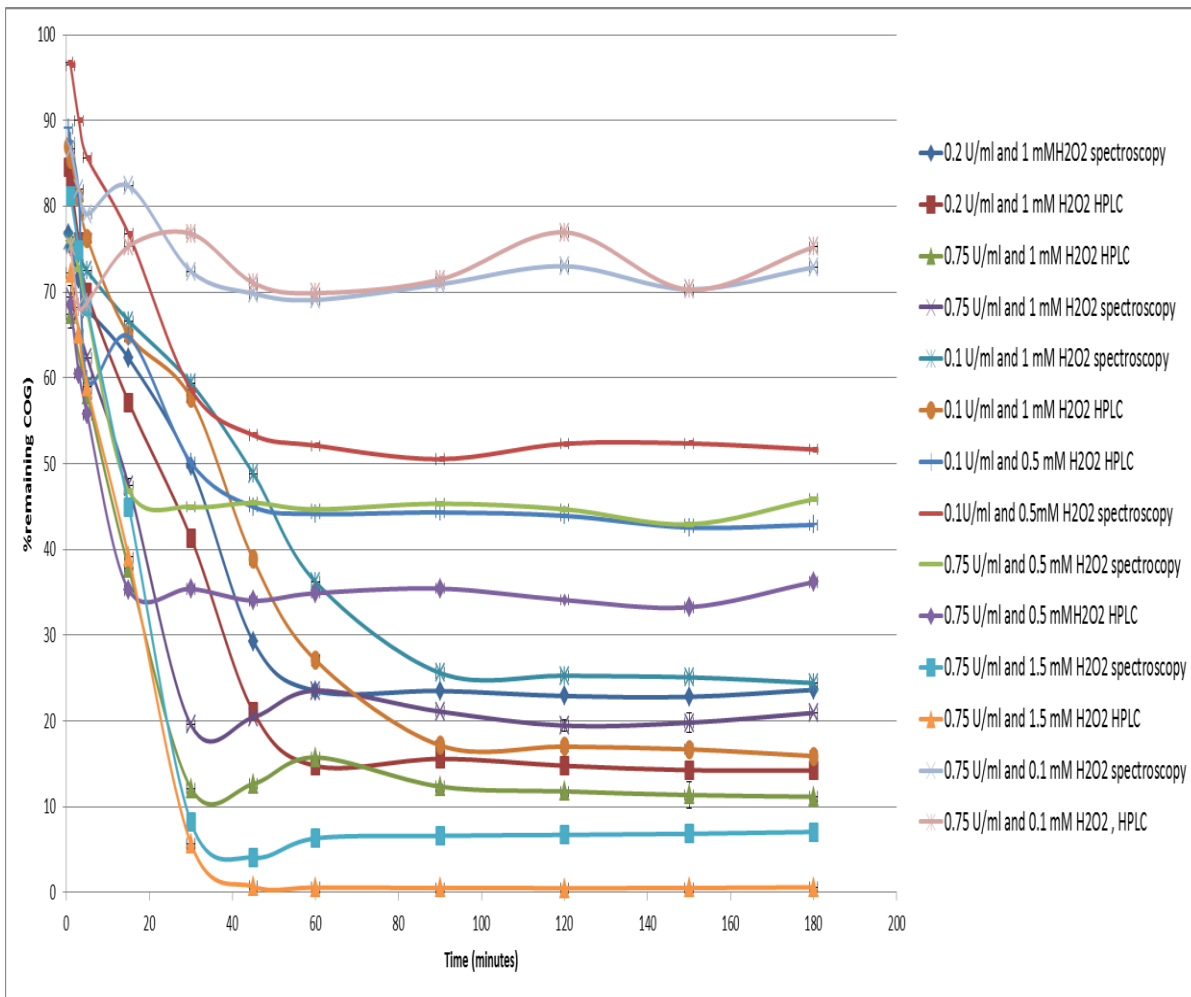


Figure 53. COG degradation under HPLC and spectroscopy for different SBP and H₂O₂ concentrations (mM) with pH 8

Table 6. Optimal conditions for aniline formation after enzymatic treatment of 1 mM COG

	Sample 1	Sample 2	Sample 3
Enzyme U/mL (SBP)	0.75	0.2	0.75
H ₂ O ₂ (mM)	0.5	1	1
Color of dye using spectrophotometer (mM)	0.4126	0.2126	0.1886
Dye concentration based on HPLC measurement (mM)	0.3258	0.128	0.10051
Concentration of aniline found using HPLC measurement (mM)	0.026	0.0252	0.0237

For further experiments the conditions used were with the optimal conditions to achieve the highest release of aniline as well as the lowest COG concentration.

A spiked initial solution containing the COG dye plus 1 mM aniline was also tested with 0.75 U/mL SBP and 0.5, 1.0 and 1.5 mM H₂O₂. First, Figure 54 shows the degradation estimated by spectroscopy and HPLC for COG. As it can be seen, 0.75 U/mL and 1.5 mM H₂O₂ was needed to degrade more than 90% of dye and around 85% color removal. Increasing the amount of H₂O₂ enhanced the dye degradation.

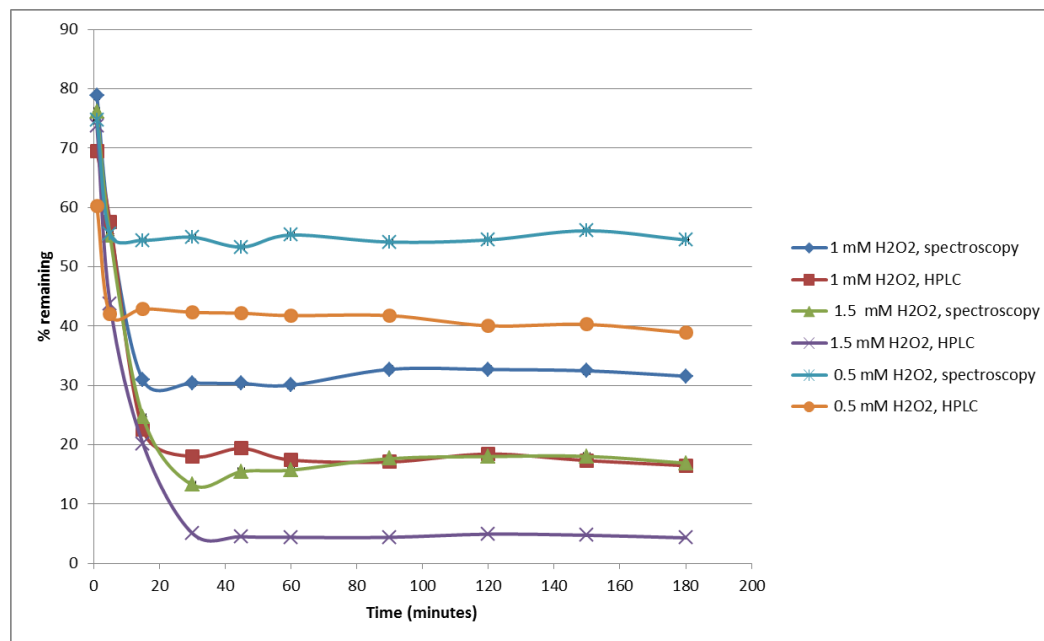


Figure 54. Degradation of COG with 1 mM spiked aniline with 0.75 U/mL and 0.5, 1.0 and 1.5 mM H₂O₂ at 180 minutes reaction.

As seen in Figure 55 the removal of aniline from the spiked solution occurred in the first minutes of reaction and after that it remains constant, same behavior was observed in this thesis work for AB113. Also it should be noted that not all aniline was removed, proving that the conditions are not the optimal for aniline removal, as the pH used was pH 8. However, it is proven that the aniline was removed competition with COG.

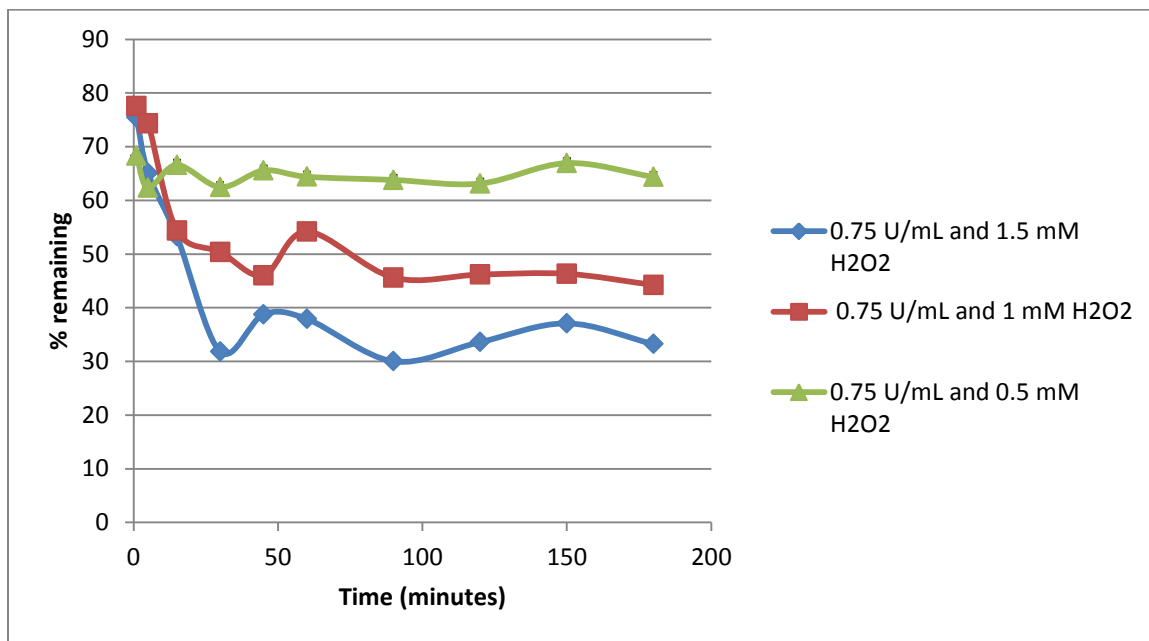


Figure 55. Aniline remaining by HPLC in spiked solutions.

Initial concentrations: aniline 1 mM, 0.75 U/mL SBP and 0.5, 1.0 and 1.5 mM H₂O₂, 3 hour reaction

Figure 56, compares the degradation of COG determined by HPLC and spectroscopy with a spiked and non-spiked aniline solution.

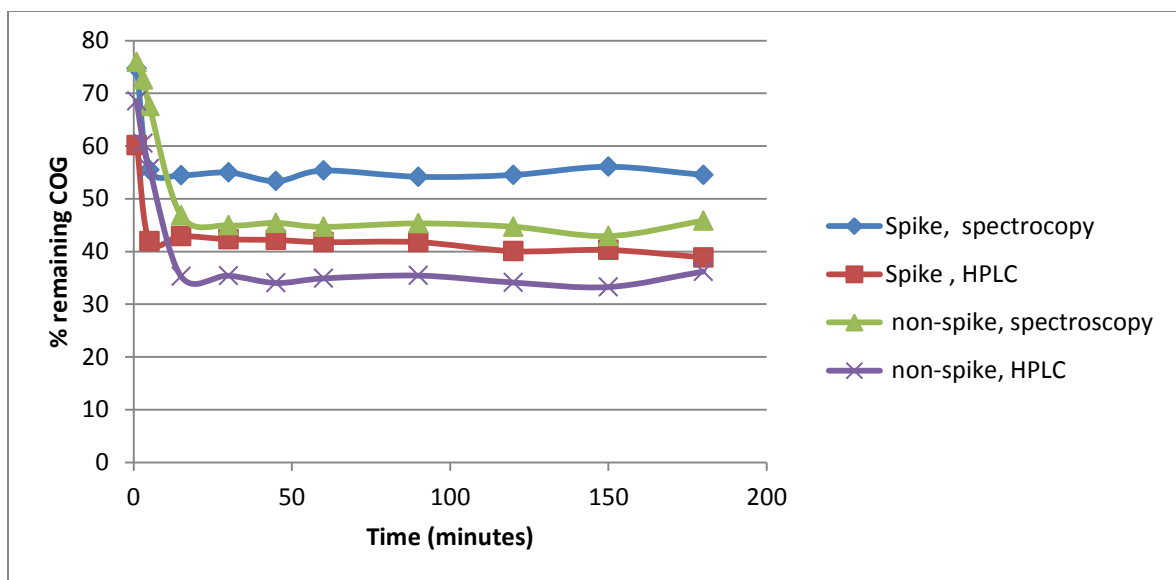


Figure 56. COG degradation with spiked (1mM) and non-spiked aniline with 0.75 U/mL SBP and 0.5 mM H₂O₂

From Figure 56 it can be seen, that the presence of aniline (a second substrate for SBP which competes with COG by HPLC diminished the removal efficiency for COG by 20%, for color as well as dye degradation by HPLC.

4.4.2 MS results

EI-MS data shown below were taken for the samples which produced more aniline based on the HPLC results shown above as well as more dye decoloration and degradation (Table 6). The sample used was 1 mM COG with pH 8, 1mM H₂O₂ and 0.75 U/mL SBP. First measurements showed the presence of aniline; however the phosphate buffer used, created some interference in the product peaks. For this reason, it was decided to lower the phosphate buffer concentration from 40 mM to 10 mM to avoid that interference. Figure 57 shows the mass spectrum for pure aniline in water. The figures shown in this chapter are the same mass spectrum with different peaks number of ions detected at the largest peak display.

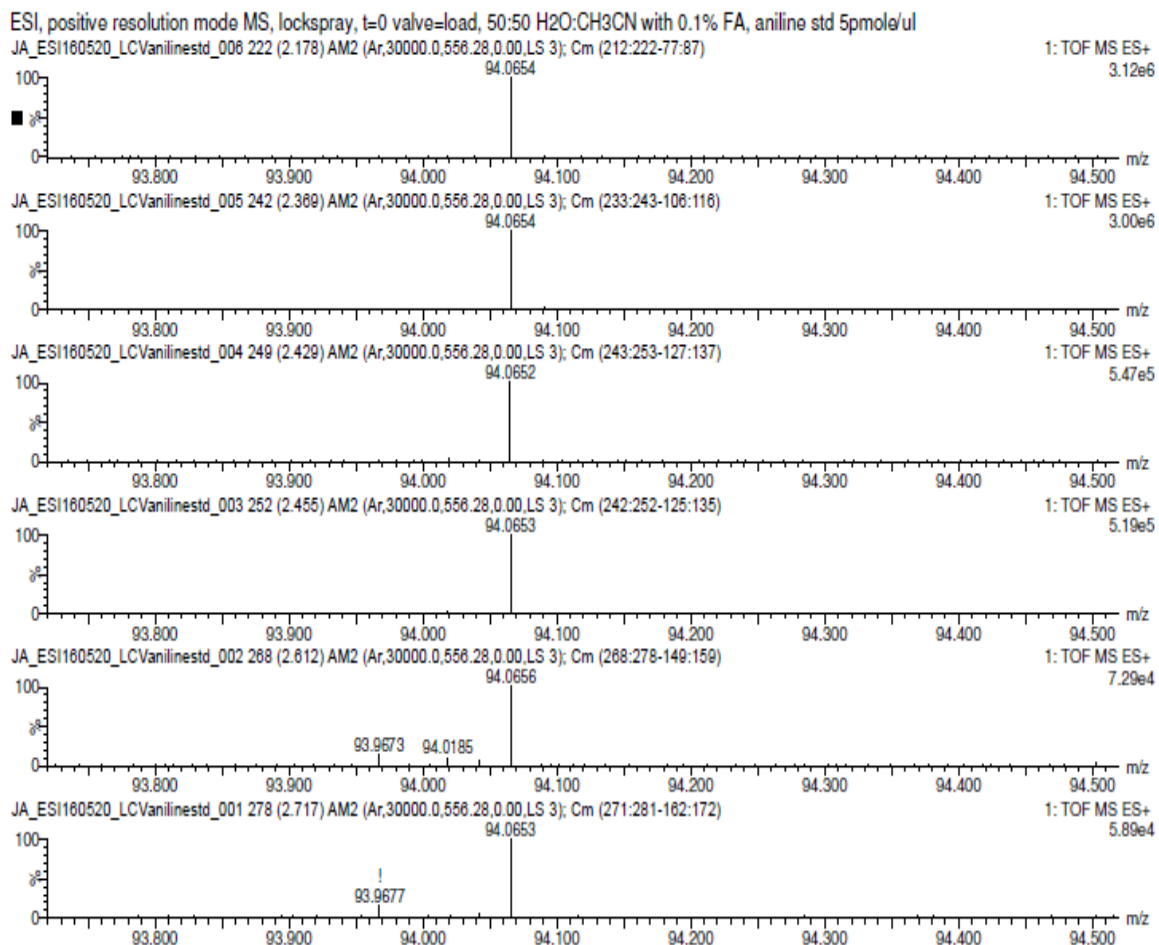


Figure 57. ESI-MS (+) for pure aniline; m/z from 85 to 105.

Figure 58 shows a mass chromatograph of the products after enzymatic treatment with 1mM sample COG, pH 8 (40mM), 1mM H₂O₂ and 0.75 U/L, resulting in 18% color remaining, 10% color remaining degradation by HPLC and 0.0237 mM of aniline formation (based on HPLC measurement).

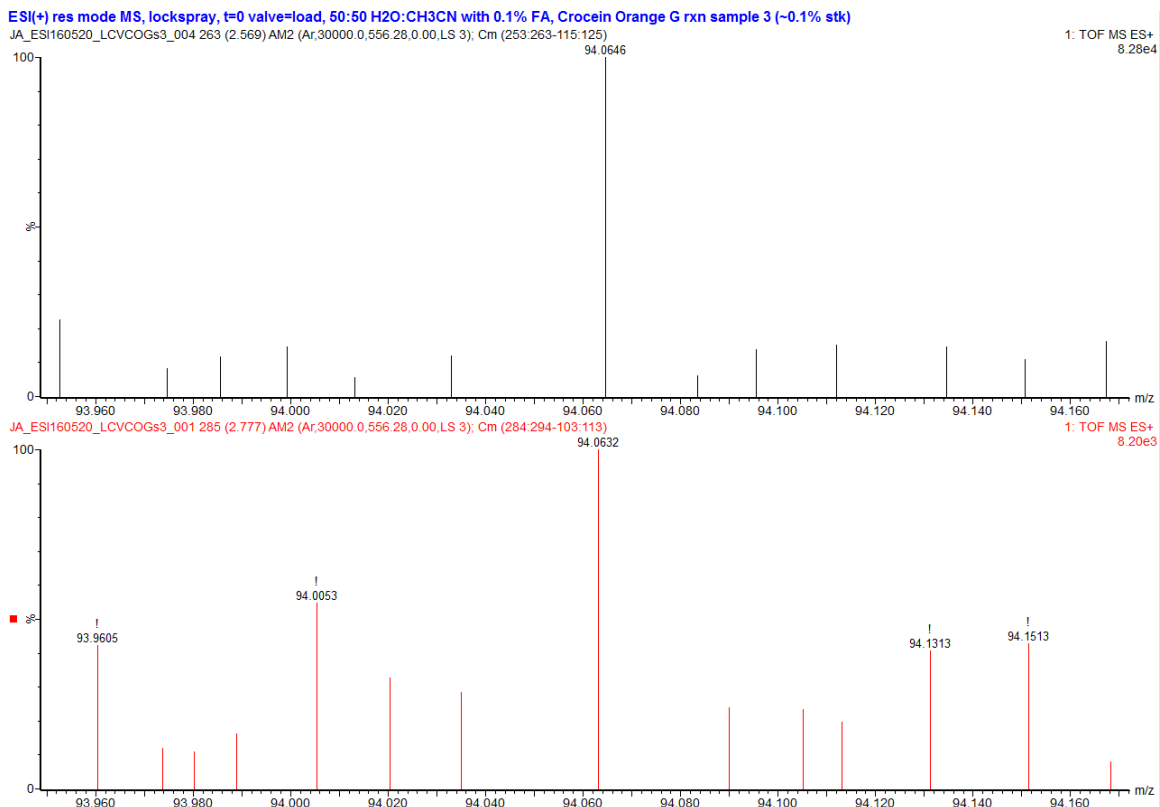


Figure 58. ESI-MS (+) for aniline produced after enzymatic treatment

Conditions: 1 mM COG , pH 8 (40 mM), 1 mM H₂O₂ and 0.75 U/L

Figure 59 shows the mass spectrum after enzymatic treatment of 1 mM COG with 0.2 U/mL and 1 mM H₂O₂, getting 21% color remaining and 12.8% dye remaining (HPLC) with 0.0252 mM aniline formation (based on HPLC measurement).

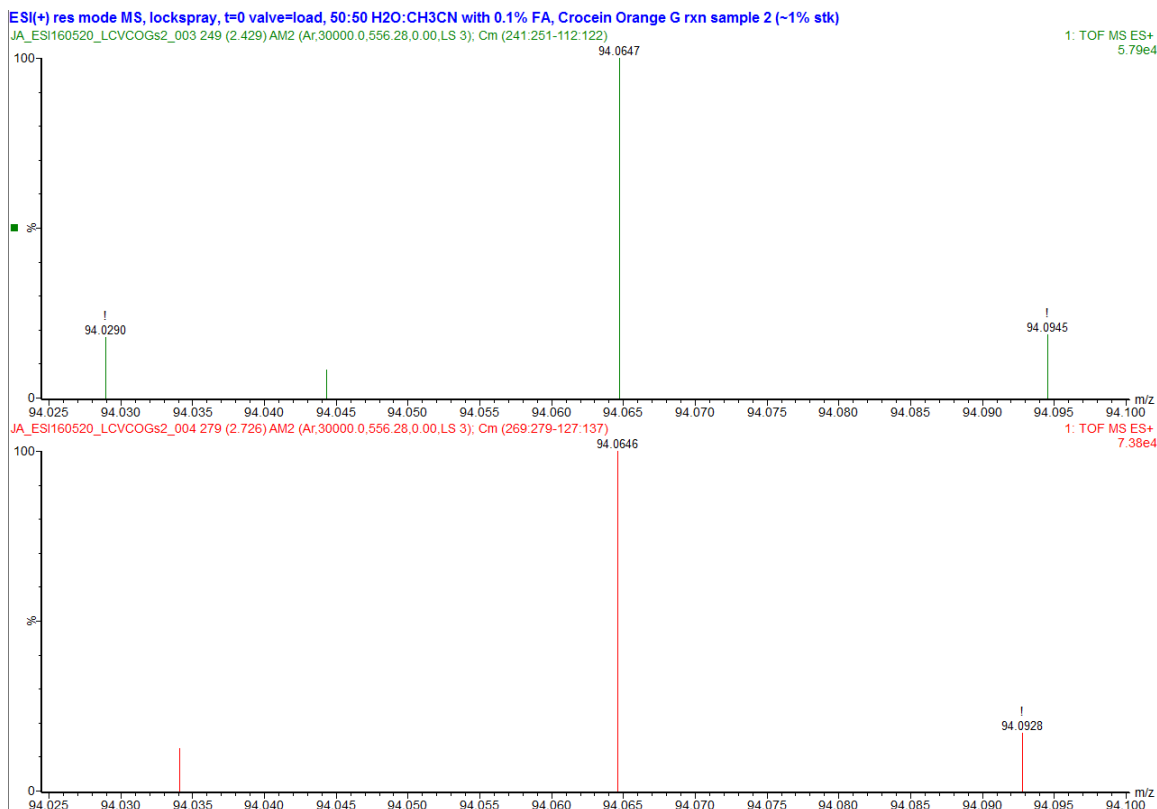


Figure 59. ESI-MS (+) for aniline produced after enzymatic treatment

Conditions: 1 mM COG under pH 8 (40 mM), 1 mM H₂O₂ and 0.2 U/L

As it can be seen, there was evidence that support the premise that there is azo-splitting bond during enzymatic treatment, because aniline was present after the treatment as shown in HPLC analysis. The peaks from Figure 58 and 59 are weak peaks (low intensity) which created the need to modify the approach for the measurements in order to determine the possible presence of aniline after treatment. An approach is needed to reduce the amount of phosphate buffer (pH 8) present in the sample, because it interferes in the MS peaks, masking other possible products.

Figure 60 shows the products after enzymatic treatment with the same conditions as for Figure 58 but in 10 mM buffer, the mass spectrum shows the presence of aniline after enzymatic treatment. The two panels show samples under the same conditions of SBP and H₂O₂ but they are different samples measured in different days.

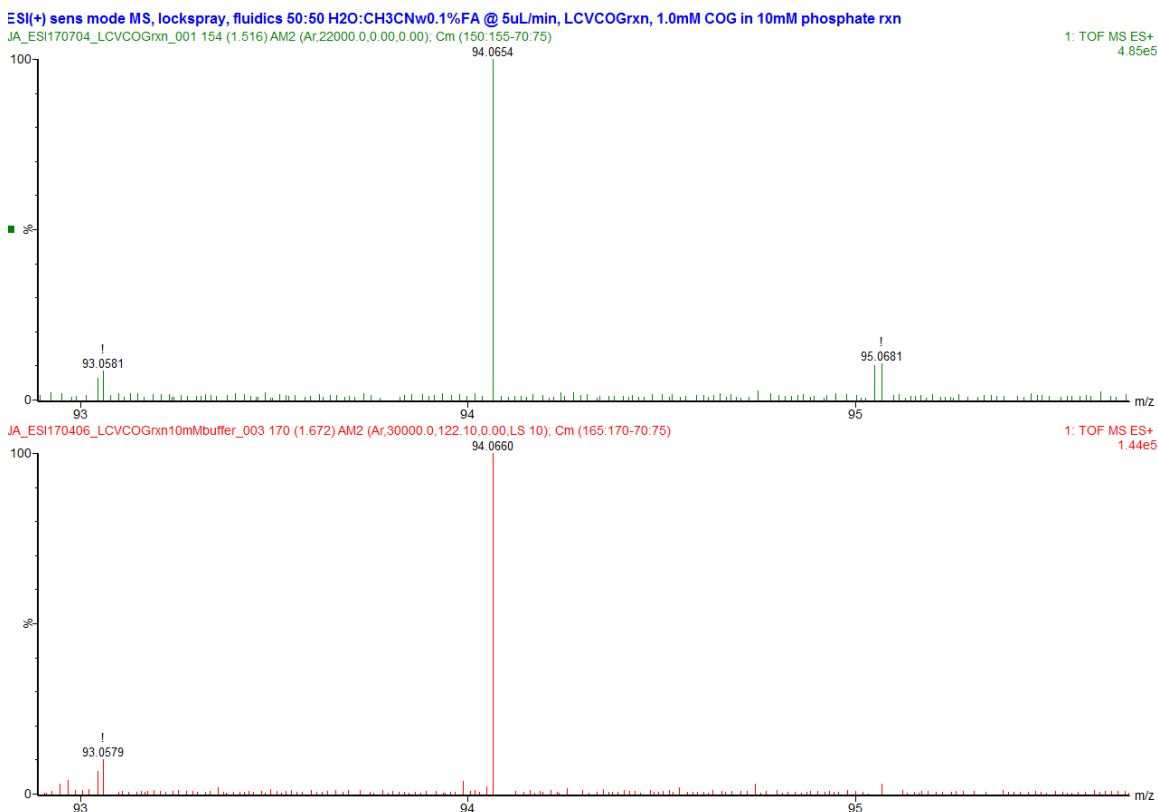


Figure 60.ESI-MS (+) for aniline produced after enzymatic treatment

Conditions: 1 mM COG, 1 mM H₂O₂, 0.75 U/mL SBP with 10 mM pH 8 phosphate buffer

4.4.4 Other products identified

Peaks were found that suggest the presence of other aniline compounds, however, this required further analysis. A possible product with m/z 184.0725 has been identified which suggest the presence of the compound C₁₂H₁₀NO which is the protonated hydrolysis product of aniline dimer (Figure 61).

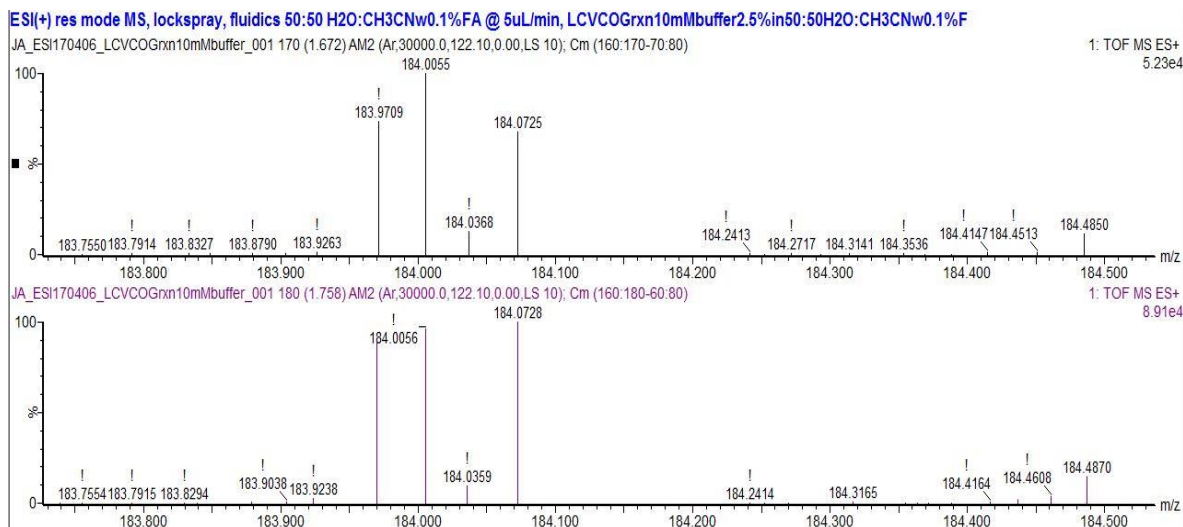


Figure 61.ESI-MS (+) for product formed with m/z 184.0725 after enzymatic treatment

Conditions: 1 mM COG, 1 mM H₂O₂, 0.75 U/mL SBP with 10 mM pH 8 phosphate

A product with m/z 275.1168 suggests the presence of a compound with the formula C₁₈H₁₄N₂O which can be the protonated hydrolysis product of aniline trimmer (Figure 62).

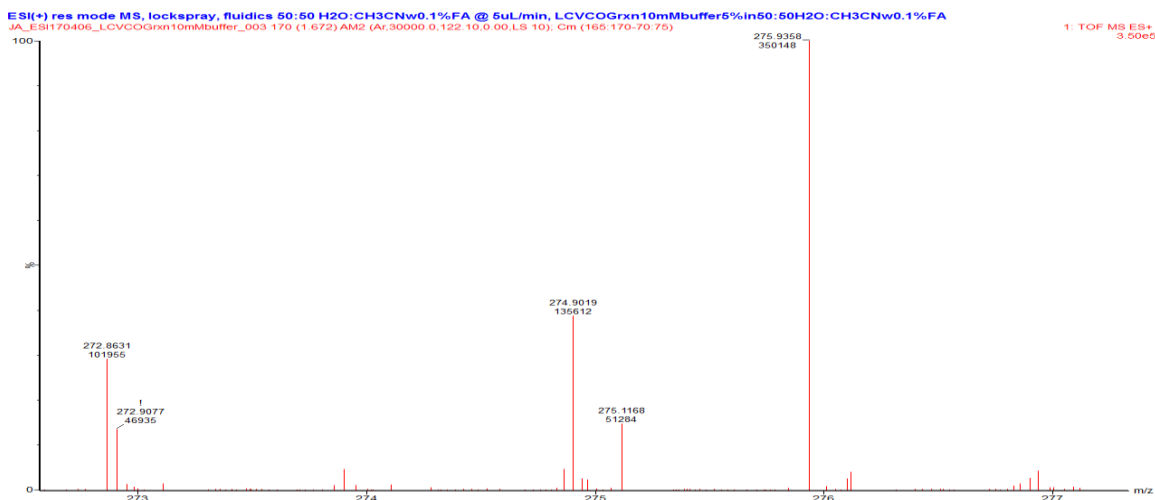


Figure 62. ESI-MS (+) for product with m/z 275.1168 after enzymatic treatment

Conditions: 1 mM COG, 1 mM H₂O₂, 0.75 U/mL SBP with 10 mM pH 8

This same type of products has been found were the oxidation of aniline dimer and trimer is easy oxidize at bench scale or as a possible oxidation process in the ES emitter by the electrochemical process of the ESI, which can oxidize the dimer or trimer of aniline that can be subsequently hydrolyzed (Kertesz and Van Berkel, 2002).

Some dye was still present on the samples after treatment as shown in Figure 63.

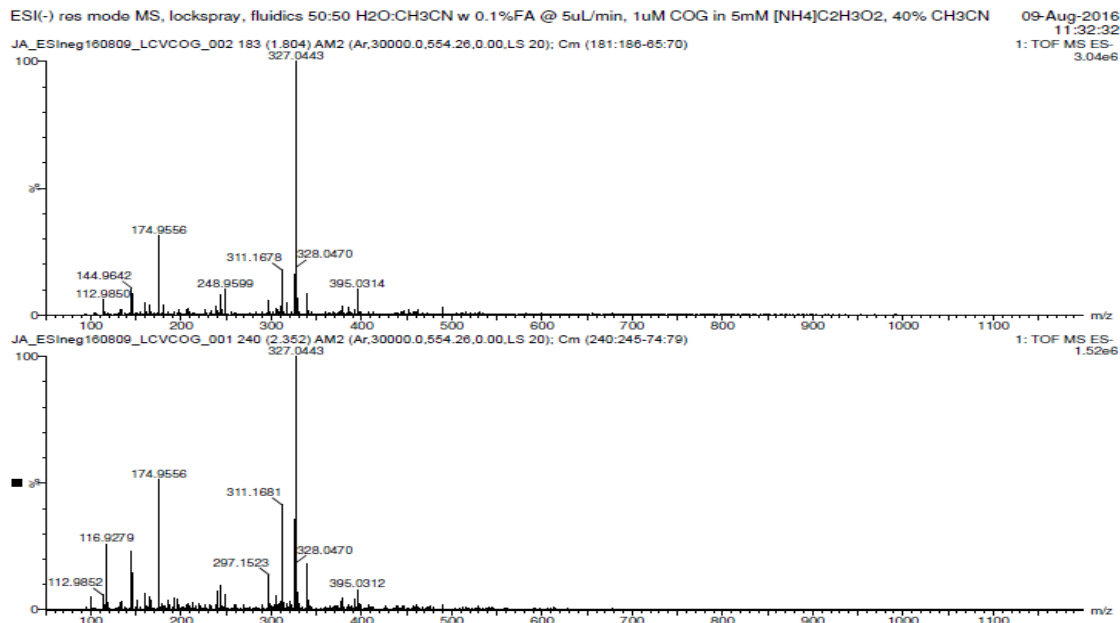


Figure 63. ESI-MS (-) for dye remaining detected (m/z 327.0443)

Conditions: 1 mM COG, 1 mM H₂O₂, 0.75 U/mL SBP with 10 mM pH 8 phosphate buffer

The presence of a peak at 325.0283 shows the possibility of a dimer of the dye with molecular formula C₃₂H₂₀N₄O₈S₂ with a charge state of -2 due to the sulphate groups present (Figure 64).

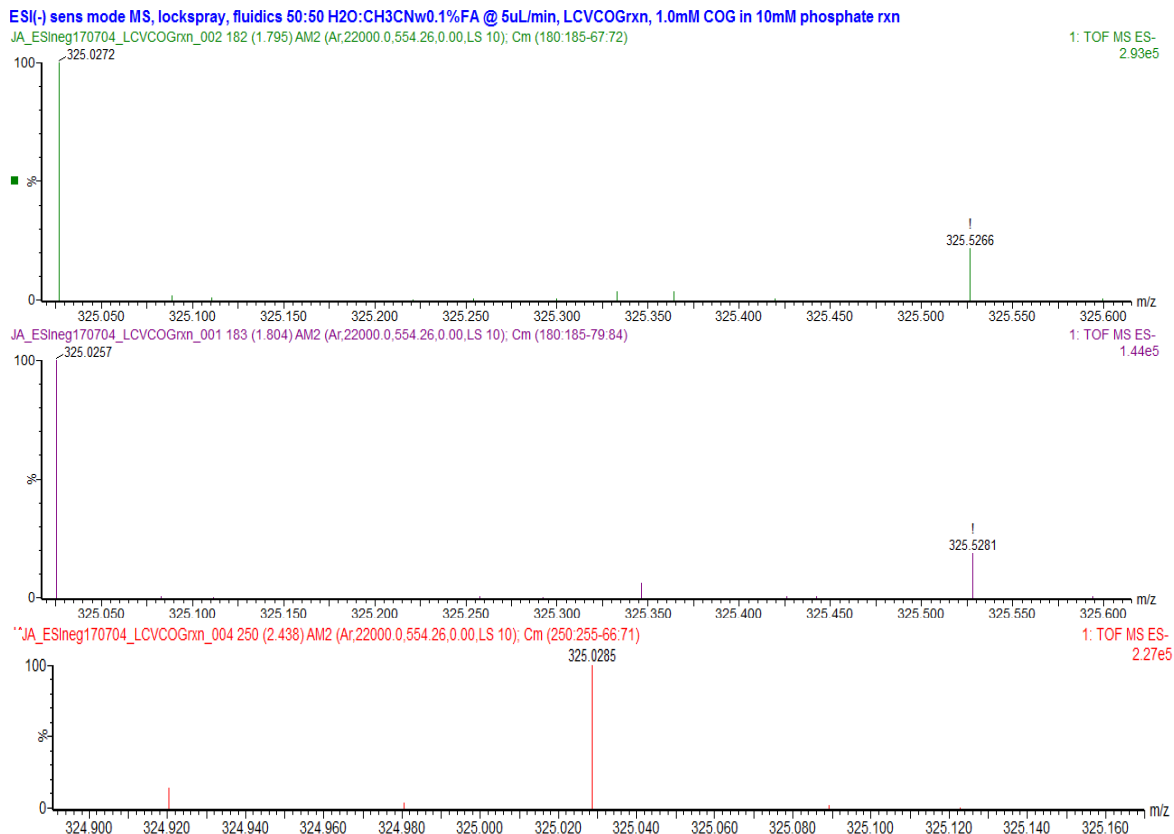


Figure 64. ESI-MS (-) for dimer of the dye product (m/z 325.0283)

Conditions: 1 mM COG, 1 mM H₂O₂, 0.75 U/mL SBP with 10 mM pH 8 phosphate buffer

As mentioned before the MS measurements should be considered as an evidence that suggest the presence of the products, however, it is required another technique such as MS-MS or HPLC/MS that increase the sensitivity of the instrument allowing the confirmation of any of the products.

4.5 Optimization for decoloration of azo-dyes using response surface methodology (RSM)

RSM is a set of experimental strategies to explore the space between the process variables and the response. RSM allows development of an approximation of the relationship among the factors and finds the level of optimum response *i.e.*, those that result in "optimal values" of one or more characteristics of product quality and describes the response near the optimum point (Myers *et al.*, 2016); in this case the conditions for the maximum decoloration. It also allows for the interaction between/among parameters, in contrast to one-parameter-at-a-time optimization. This methodology is less time-consuming and allows detection of the optimal point by evaluating all possible interactions in contrast to the conventional method where one parameter is modified at a time leaving the other parameters constant (Karthikeyan *et al.*, 2010). In this chapter the decoloration of AB113 and DB38 was done using RSM methodology in the program Minitab 17.

4.5.1. Factorial design for AB113

The first step in the RSM was the screening of parameters that affect the response value (color remaining). It was done based on literature review (Mazloum, 2014; Ali *et al.*, 2013; Gholami-Borujeni *et al.*, 2011). Flowcharts shown in Figure 64, 65 and 70 were prepared based on Montgomery and Runger, 2010. Essentially this step (screening step) consists in selecting from many factors those that most significantly affect the response variable or variables that are intended to be optimized (Figure 65). It is complicated and costly to manipulate many factors and it is known that when handling information with more than four factors the effects tend to get confused and it requires more experiments to be run (Natrella, 2010). Thus the parameters selected for optimization were: pH, H₂O₂ and enzyme concentrations.

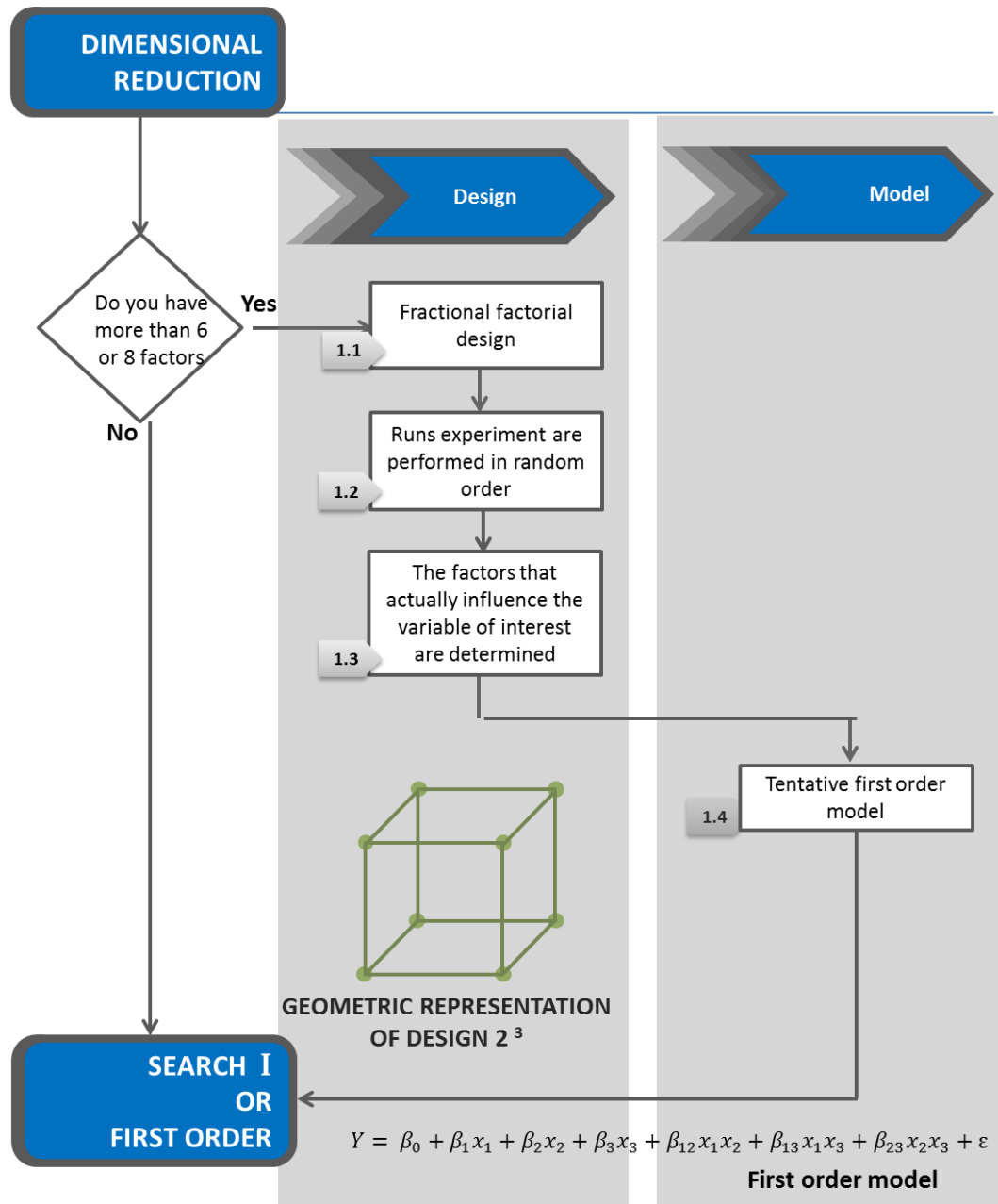


Figure 65. Flowchart with the general steps used for dimensional reduction step (screening step)

After doing the screening, the first-order search was done following the steps in Figure 66. The search I or first-order search applies when you have few factors ($k \leq 5$) and it is known that they influence the response variable. The main objective of this stage is to confirm the significant influence of selected factors on the response variable to be optimized and to characterize the surface type response, running a first-order design with

center points, to detect the presence of curvature (Montgomery and Runger, 2010; Myers *et al.*, 2016).

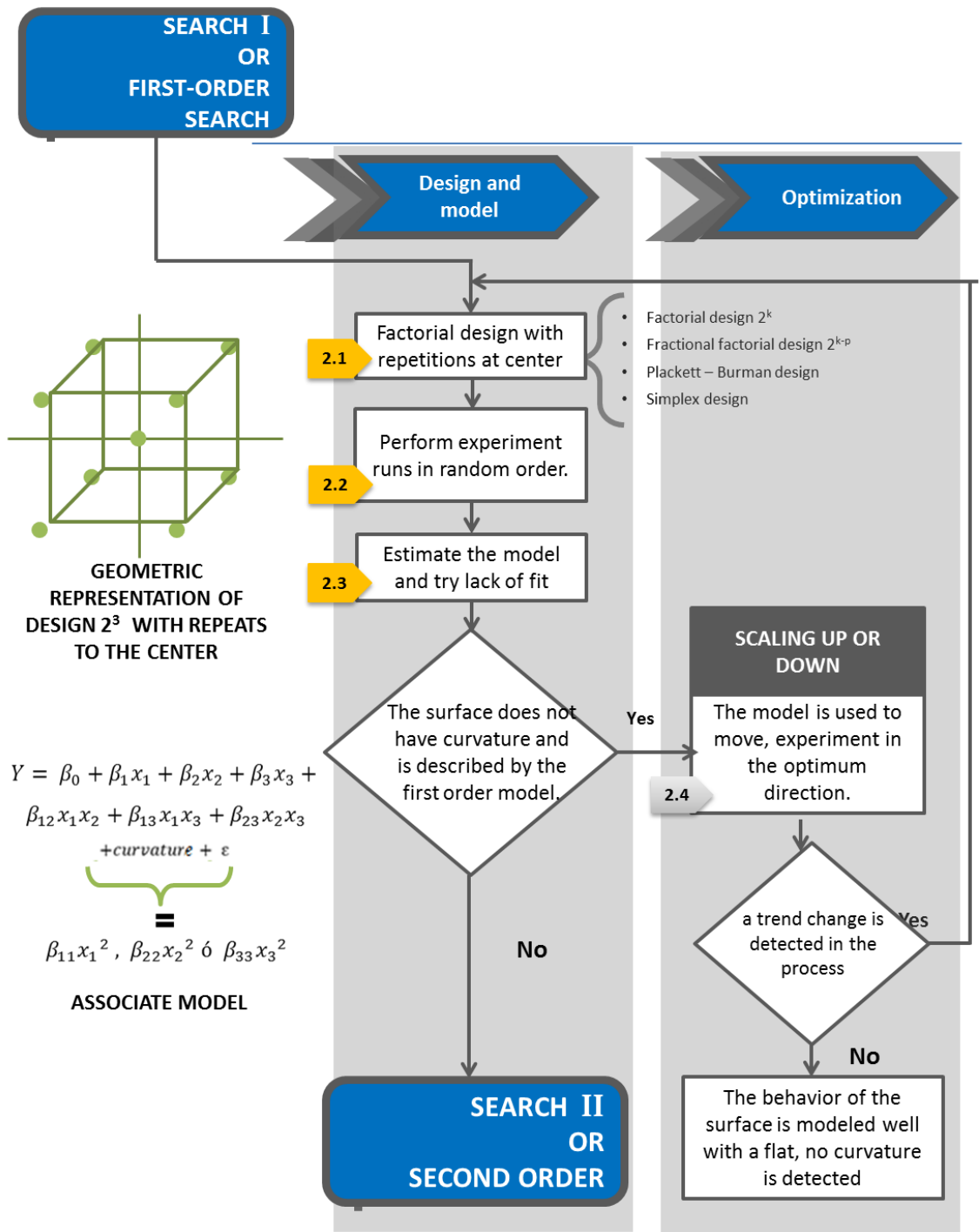


Figure 66. Flowchart with the general steps used for search I or first-order search

The first-order search was proposed and developed with a full factorial design by 2^3 with two replicates of each treatment (Gutiérrez and De la Vara Salazar, 2008), with three repetitions at the center and the levels of each factor were chosen as shown in Table 7 for AB113. Figure 67 shows the geometrical representation of the parameters.

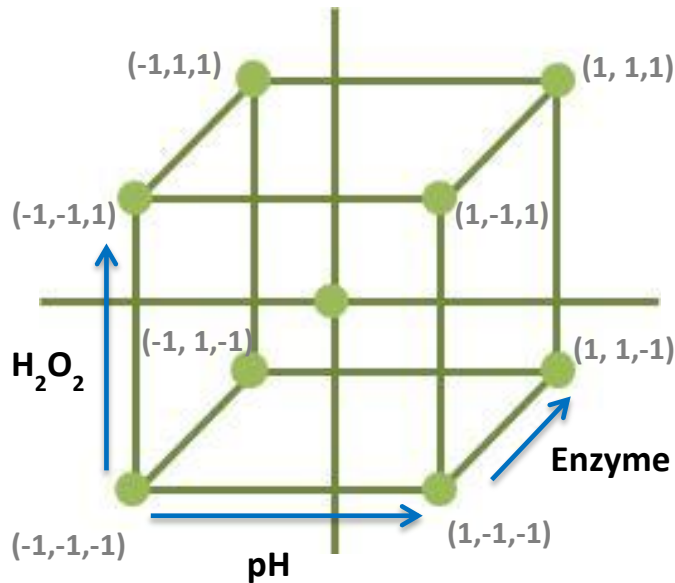


Figure 67. Geometrical representation of the parameters: pH, enzyme and H_2O_2

Table 7 shows the actual values for the 3 levels chosen for AB113, pH, H_2O_2 and enzyme.

Table 7. Values for the three levels for AB113

Factor	Levels		
	-1	0	1
pH	3.6	5.3	7.0
H_2O_2	1.0	2.0	3.0
Enzyme	1.0	1.5	2.0

The Table 8 shows the combinations of the parameters for the different treatments (H_2O_2 in mM, enzyme in U/mL).

Table 8. Treatments and combinations for first-order research for AB113 (H₂O₂ in mM, enzyme in U/mL).

Treatments	pH	H ₂ O ₂	Enzyme
(-1,-1,-1)	3.6	1.0	1.0
(1,-1,-1)	7.0	1.0	1.0
(-1,1,-1)	3.6	3.0	1.0
(1, 1,-1)	7.0	3.0	1.0
(-1,-1,1)	3.6	1.0	2.0
(1,-1,1)	7.0	1.0	2.0
(-1,1,1)	3.6	3.0	2.0
(1,1,1)	7.0	3.0	2.0
(0,0,0)	5.3	2.0	1.5

The experimental runs were carried out in random order (see Appendix C, Table C.1)

Figure 68 is a geometrical representation of the fitted means obtained for the steps in search I.

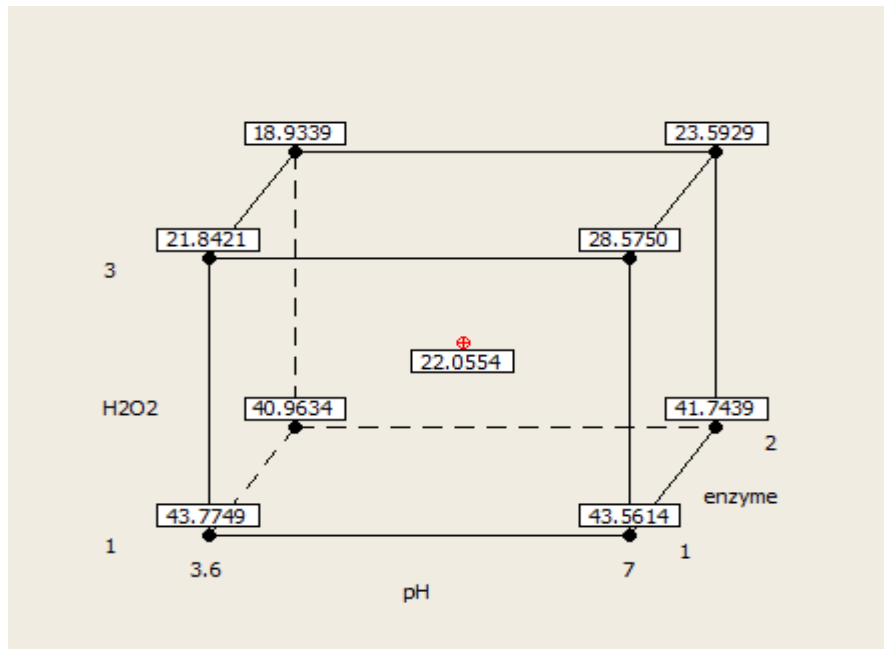


Figure 68. Cube plot (fitted means) for the response (color remaining)

4.5.1.1. Variance analysis (ANOVA)

In order to analyze the results of the first-order search an ANOVA was obtained in order to evaluate the statistical confidence of the model developed. Figure 69 shows the ANOVA analysis for the decoloration of AB113 for the search I.

Source	DF	fit SS	fit Ms	F	P
Principal effects	3	1561.03	1561.03	20862.87	0.000
pH	1	35.75	35.75	1433.54	0.000
H ₂ O ₂	1	1486.09	1486.09	59584.07	0.000
enzyme	1	39.18	39.18	1571.00	0.000
2-interactions	3	32.25	32.25	30.95	0.000
pH*H ₂ O ₂	1	29.29	29.29	1174.57	0.007
pH*enzyme	1	0.29	0.29	11.69	0.000
H ₂ O ₂ *enzyme	1	2.66	2.66	106.61	0.000
3-Interactions	1	2.35	2.35	94.34	0.000
pH*H ₂ O ₂ *enzyme	1	2.35	2.35	94.34	0.000
Curvature	1	295.65	295.65	11854.06	
Residual error	10	0.25	0.25		
Pure error	10	0.25	0.25		
Total	18				

S = 0.157928 R-Squared = 99.99% R-Squared (fit) = 99.98%

Figure 69. ANOVA analysis for AB113 (first-order search)

In Figure 69, DF is the degrees of freedom, the Fit Ms is the fitted mean squares measure, the Fit SS fitted sums of squares and F-value is the Fisher value. For this thesis work the p-value will be analyze.

The results presented are for the quantitative analysis of the experiment in which it is found statistically, with a significance level of 0.05 (α level) or confidence level of 95%, the hypothesis test is statistically significant, that means that the pH, H₂O₂ and enzyme factors are significantly influential on the % remaining dye in the solution, because of the values obtained from p-value of each factor was 0.000, less than 0.05 (significance level).

Furthermore double interactions among these factors also obtained p-value = 0.000 thus prove to be significantly influential on the % remaining dye: likewise the double

interaction of pH and enzyme, due to its p-value=0.007, which is less than 0.05 significance level.

Another aspect of the p-value to consider is the curvature which also happens to be significant, since its value is 0.000, which indicates that curvature is present because at least one of the three quadratic terms is active.

In addition, an R-Squared = 99.98% which indicates that the fitted model explains 99.98% of the percentage remaining, which means that the model has a good fit; it has a high predictive capacity. Is necessary to validate if the effect of curvature (second-order stage) is present in the experimental region, meaning that towards the center of the experimental region, the % remaining is significantly higher or significantly lower than the rest of the experimental region. It has been recommended that the fitted R-Squared be at least 75% to continue consideration of the methodology; otherwise, it is very likely that the procedure will lead us by a wrong path and waste resources, this standard will be used for all the next sections (Montgomery and Runger, 2010).

4.5.1.2. Estimate the model and lack-of-fit test

The fitted equation for this step (first-order search) is as follows:

$$\begin{aligned} \text{Remaining} = & 64.0844 - 1.8278 \text{ pH} - 16.2197 \text{ H}_2\text{O}_2 - 5.4396 \text{ enzyme} \\ & + 1.4726 \text{ pH} * \text{ H}_2\text{O}_2 + 0.74348 \text{ pH} * \text{ enzyme} + 1.57577 \text{ H}_2\text{O}_2 \\ & * \text{ enzyme} - 0.45114 \text{ pH} * \text{ H}_2\text{O}_2 * \text{ enzyme} - 10.8180(\text{CtPt}) \end{aligned}$$

Where *CtPt* is the center point. An analysis of the residuals provides information that statistically validates the quality of the fit for the regression model and thus it is possible to check whether the model is appropriate. Graphics (Figure 70) are often used to complete the model diagnosis are as follows:

- In the normal probability plot it can be seen that the normality assumption on the errors is reasonably well met, because the points in this chart tend to conform to the straight line.

- In the graph of residuals *versus* predicted (*Versus* FITS), points do not follow any pattern and, therefore, are distributed more-or-less randomly across the graph, which means that the model fits the same way along the Y values
- As the plot of the residuals against the values of X (*Versus* Order), points show no pattern, the pattern does not follow any trend over the values of X
- The histogram shows a normal distribution with a classical bell-shape. The frequency counts are grouped in the middle and decrease in the tails

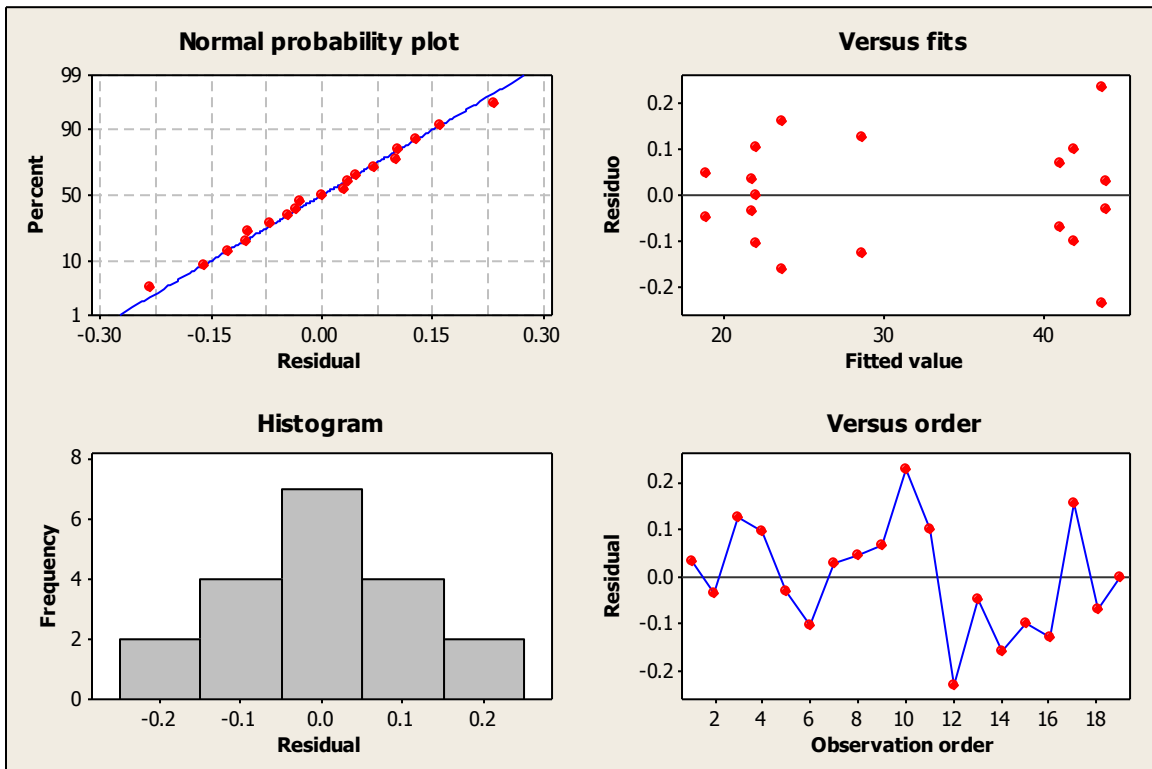


Figure 70. Residual plot for % remaining for AB113

After the first-order research the second-order model was done as shown in the next section.

4.5.1.3. Second-order search. Box-Behnken design

Statistically it was confirmed (first-order stage) that the pH, H₂O₂ and enzyme are highly influential factors for decolorization and degradation of azo-dyes, corroborating the conclusion in the first-order stage of dimensional reduction. The primary objective of the second-order stage is to model the behavior of the process in a very precise and relatively small region, to determine the combination of factors most likely to be considered optimal candidates. This is indicated by the presence of curvature obtain in the first-order stage. It also allows to determine the interactions between/among parameters. Second-order search was conducted as shown in Figure 71.

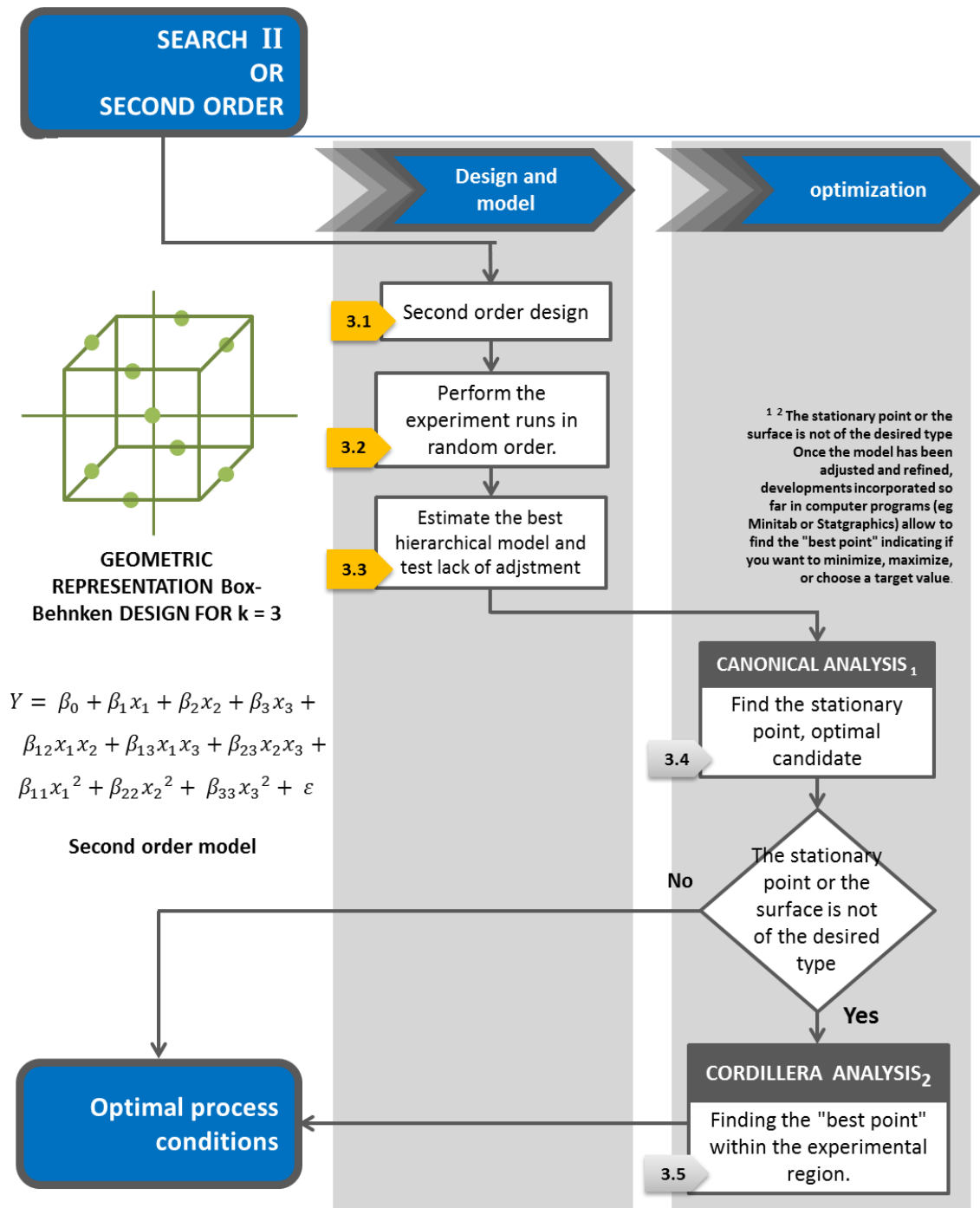


Figure 71. Flowchart for second-order model search steps

It began by characterizing the behavior of the process, with detection of the interactions of the factors that influence the removal of the dye in solution, and thus the factors that should be considered within the model describing the expected behavior. The design proposed allowed detection of curvature within the experimental region, so it was

concluded that the process under study does not have a linear behavior, it has a quadratic behavior. This information permits moving to the next of stage Search II.

4.5.1.4. Factorial design second order (Box-Behnken design)

Second-order design was based on increasing the experiments developed in the previous step (Search I) using Box-Behnken design (Montgomery and Runger, 2010).

This was defined from the levels set in the full factorial design with 2^3 repetitions at the center, the model was fitted and validated in the previous stage, and the design points are located in the middle of the cube edges (Figure 72). Table 9 shows the combinations for the design. The runs were performed in random order (see Appendix C, Table C.2.)

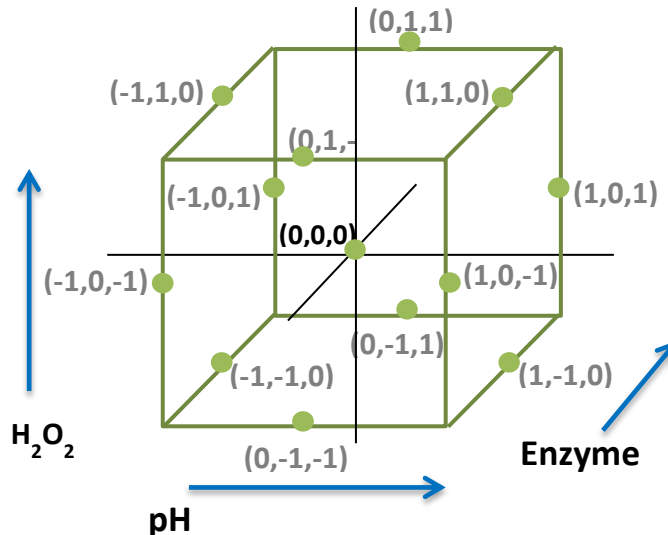


Figure 72. Geometrical representation of the parameters for search II with Box-Behnken design

Table 9. Treatments used for Box-Behnken design for AB113 (H₂O₂ in mM, enzyme in U/mL)

Standard order	Treatments	pH	H ₂ O ₂	Enzyme
1	(-1,-1, 0)	3.6	1	1.5
2	(1, -1, 0)	7	1	1.5
3	(-1, 1, 0)	3.6	3	1.5
4	(1, 1, 0)	7	3	1.5
5	(-1, 0, -1)	3.6	2	1
6	(1, 0, -1)	7	2	1
7	(-1, 0, 1)	3.6	2	2
8	(1, 0, 1)	7	2	2
9	(0,-1,-1)	5.3	1	1
10	(0, 1, -1)	5.3	3	1
11	(0,-1, 1)	5.3	1	2
12	(0, 1, 1)	5.3	3	2
13	(0, 0, 0)	5.3	2	1.5
14	(0, 0, 0)	5.3	2	1.5
15	(0, 0, 0)	6	1.5	1

The Box-Behnken design requires fewer runs than other designs like central composite design (CCD) and consequently resource consumption is reduced and treatments levels are easy to obtain, unlike CCD axial points whose levels should be rounded to produce a range of variation (Daâssi *et al.*, 2012; Minitab support (c), 2017). In summary, the Box-Behnken design had a total of 30 runs with 6 center points. Other authors have done similar experiments using the Box-Behnken design: Daâssi *et al.* (2012) did a total of 52 runs; Garg *et al.* (2015) did 17 experimental runs.

To estimate the best hierarchic model and test lack-of-fit the ANOVA analysis was done for the Box-Behnken design (Figure 73).

Source	DF	fit SS	fit MS	F	P
Regression	9	2719.46	302.16	153.93	0.000
Lineal	3	2218.84	739.61	376.77	0.000
pH	1	12.98	12.98	6.61	0.018
H ₂ O ₂	1	2198.63	2198.63	1120.01	0.000
enzyme	1	7.24	7.24	3.69	0.069
2-interaction	3	483.01	161.00	82.02	0.000
pH*pH	1	110.50	110.50	56.29	0.000
H ₂ O ₂ *H ₂ O ₂	1	344.51	344.51	175.50	0.000
enzyme*enzyme	1	28.43	28.43	14.48	0.001
Interaction	3	17.61	5.87	2.99	0.055
pH*H ₂ O ₂	1	16.35	16.35	8.33	0.009
pH*enzyme	1	1.15	1.15	0.59	0.453
H ₂ O ₂ *enzyme	1	0.11	0.11	0.06	0.813
Residual error	20	39.26	1.96		
Lack-of-fit	3	36.64	12.21	79.34	0.000
Pure error	17	2.62	0.15		
Total	29				

S = 1.40109 R-squared. = 98.58% R-squared (fitted) = 97.94%

Figure 73. ANOVA analysis for Box-Behnken

The analysis of variance of the second-order model with a confidence level of 95% shows the pH and H₂O₂ factors to be significantly influential on the % remaining of the dye in solution, likewise for the interactions that these two factors form and the quadratic effects (pH)², (enzyme)² and (H₂O₂)², because to the p-values for each of the effects was 0.000 and 0.001, less than 5% significance level .

Otherwise, the main effect of the enzyme factor is not significant in the % remaining dye since a p-value of 0.069 greater than 0.05 was obtained, likewise for the interaction of the enzyme factor and the pH factor, which has a p-value of 0.453 and for the H₂O₂ and enzyme factors with a p-value of 0.813. But it is important to note, as seen in Figure 73, the value obtained for the pure quadratic effect of the enzyme which influences the amount of dye remaining in solution, with p-value of 0.001. Therefore, the influence of the enzyme factor in the percentage remaining cannot be ruled out.

The model has a high predictive capacity, R² to 97.94% which indicates that the fitted model explains 97.94% of the amount of dye remaining, thus the model has a good fit. Daâssi *et al.* (2012) found correlation coefficient (R²) of 0.864, 0.663 and 0.776 using

Box-Behnken design for three different dyes: reactive black 5 (diazoic), indigo carmine (indigoid) and aniline blue (anthraquinone) using laccase with an HBT mediator system. In another paper, Jadhav *et al.* (2012), found a higher fitted R^2 of 0.9984 for decoloration of Remazol Orange (a sulphonated azo-dye) by *Pseudomonas aeruginosa* BCH.

According to the results of the analysis of variance, three terms could be eliminated from the model, the main factor of the enzyme and double interaction of pH and enzyme factors as well as H_2O_2 and enzyme, so the mathematical model equation is expressed as follows:

$$Y = \beta_0 + \beta_1x_1 + \beta_2x_2 + \beta_3x_3 + \beta_{11}x_1^2 + \beta_{22}x_2^2 + \beta_{33}x_3^2 + \beta_{12}x_1x_2 + \beta_{13}x_1x_3 + \beta_{23}x_2x_3 + \varepsilon$$

$$Y = \beta_0 + \beta_1x_1 + \beta_2x_2 + \beta_{11}x_1^2 + \beta_{22}x_2^2 + \beta_{33}x_3^2 + \beta_{12}x_1x_2 + \varepsilon$$

$$\begin{aligned} x_1 &= \text{pH} \\ x_2 &= H_2O_2 \text{ (mM)} \\ x_3 &= \text{enzyme (U/mL)} \\ Y &= \% \text{ de remaining} \end{aligned}$$

The model is no longer hierarchical by eliminating one of the three simple terms (X_3) that make up the higher-order terms that are in the model.

In response surface models hierarchic is preferred as they have a more robust design that facilitates exploration of representing surfaces. Eliminating effects or terms of the model should be less strict than in analysis of variance, and allow some non-significant terms to remain in the model to achieve the hierarchy. Since the double interaction of enzyme factor is significant it cannot be ruled out of the equation.

If the “enzyme*pH” and “enzyme* H_2O_2 ” are eliminated, the ANOVA analysis is as shown in Figure 74. It is necessary to examine the ANOVA without those two terms and compare to the full design to select the one that fits best (Figure 74).

Source	DF	fit SS	fit MS	F	P
Regression	7	2718.20	388.31	210.81	0.000
Lineal	3	2218.84	739.61	401.53	0.000
pH	1	12.98	12.98	7.04	0.014
H ₂ O ₂	1	2198.63	2198.63	1193.61	0.000
enzyme	1	7.24	7.24	3.93	0.060
2-interaction	3	483.01	161.00	87.41	0.000
pH*pH	1	110.50	110.50	59.99	0.000
H ₂ O ₂ *H ₂ O ₂	1	344.51	344.51	187.03	0.000
enzyme*enzyme	1	28.43	28.43	15.43	0.001
3-interaction	1	16.35	16.35	8.88	0.007
pH*H ₂ O ₂	1	16.35	16.35	8.88	0.007
Residual error	22	40.52	1.84		
Lack-of- fit	5	37.91	7.58	49.24	0.000
Pure error	17	2.62	0.15		
Total	29				

S = 1.35720 R-squared = 98.53% R-squared (fitted) = 98.06%

Figure 74. ANOVA analysis without effect of interactions “enzyme*pH” and “enzyme*H₂O₂”

Analysis of variance was done to compare statistically the fitted design against the previous second-order design (Figure 73) and choose the one that best describes the surface of the experimental region is performed.

As seen, both models (Figure 73 and 74) have the same adjustment quality because both R² values were 97.94% and 98.06%, respectively.

Besides that, with a confidence level of 95%, all main effects of the factors, quadratic effects pure and double interactions are significantly influential on the % remaining dye solution, except the main effect of the factor of the enzyme, which also in the previous model was not influential in the response, however, the double interactions of enzyme are significant.

So any model could be used to characterize the response surface, in this case study, the full quadratic model was taken, *i.e.*, the first generated. Also, the pure quadratic effect of enzyme and interaction of this factor with H₂O₂ influence the amount of dye remaining in solution. For these reasons, it was decided to keep the X₃ term. The % remaining of the dye is described by the second-order model

$$Y = \beta_0 + \beta_1x_1 + \beta_2x_2 + \beta_3x_3 + \beta_{11}x_1^2 + \beta_{22}x_2^2 + \beta_{33}x_3^2 + \beta_{12}x_1x_2 + \beta_{13}x_1x_3 + \beta_{23}x_2x_3 + \varepsilon$$

In the equation ε is the residual error.

Where the following equation is valid for the experimental region studied:

$$\begin{aligned} \text{Remaining} = & 98.0111 - 14.6712 * pH - 43.8575 * H_2O_2 + 24.0870 * enzyme \\ & + 1.33849 * pH * pH + 6.83021 * H_2O_2 * H_2O_2 - 7.84821 * enzyme \\ & * enzyme + 0.84096 * pH * H_2O_2 - 0.44597 * pH * enzyme. 23810 \\ & * H_2O_2 * enzyme \end{aligned}$$

4.5.1.5 Contour and surface plots for AB113

Figure 75 shows the contour plots and Figure 76 the surface plots for AB113. Each figure demonstrates the effect of two factors while the other factors were fixed at different levels, pH at intermediate level (zero level; pH 5.3), and H₂O₂ and enzyme at the higher level (+1 level; 3.0 mM and 2.0 U/mL, respectively).

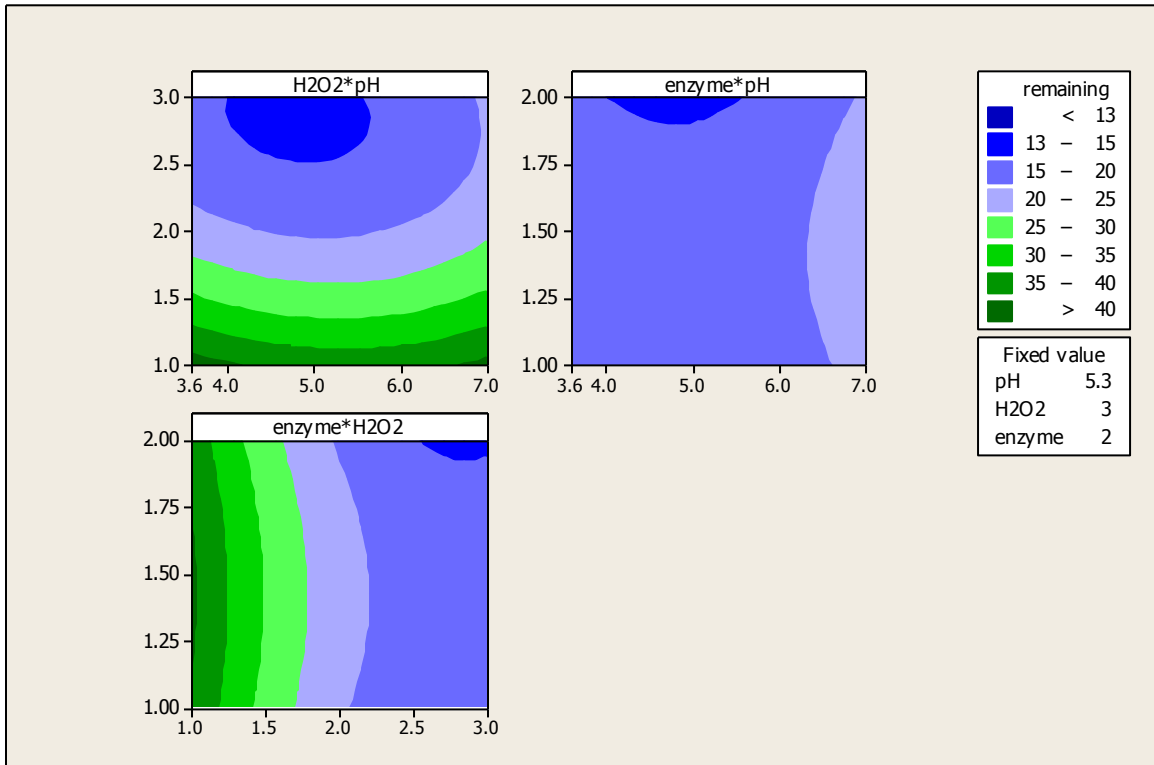


Figure 75. Contour plots for AB113. Fixed values: a) enzyme 2.0 U/mL, b) H₂O₂ 3.0 mM, c) pH 5.3

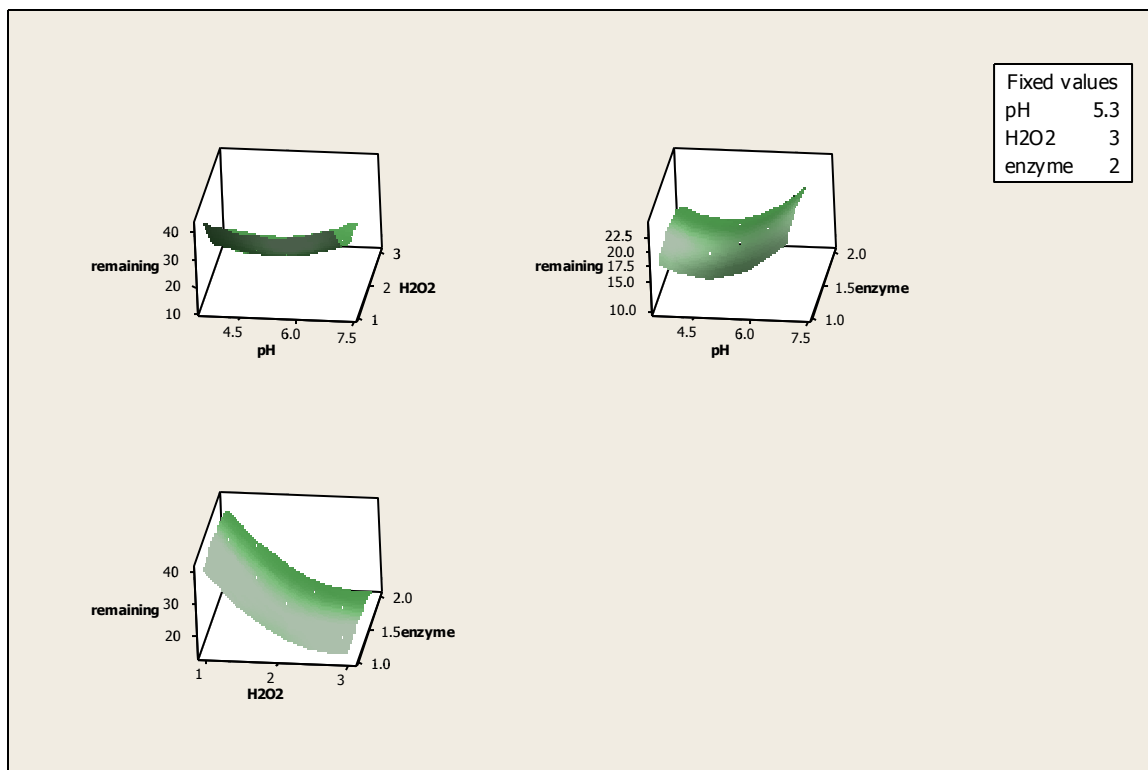


Figure 76. Surface plots. Fixed values: a) enzyme 2.0 U/mL, b) H₂O₂ 3.0 mM, c) pH 5.3

In this case study, the process of removal of an azo-dye from solution is significantly influenced by three factors (pH, H₂O₂ and enzyme) whereby the response surface cannot be graphed fully at once because they are in four dimensions.

For k=3 factors, it is possible to plot the surface by the three graphs with two factors varied each time and with the third constant.

We can analyze the results using the response surfaces and the respective contour graphs in order to locate on a three-dimensional region, calculated based on the fitted second-order model and statistically validated. An advantage of the response surface is that an estimate of the response at all possible levels of the factors studied can be calculated. For each of the three combinations of the factors generated; pH-H₂O₂, pH-enzyme and H₂O₂-enzyme, are plotted the estimated value of the average percentage of remaining dye solution.

The response surface of the combination of pH and H₂O₂ factors, with constant enzyme at 2 U/mL take the form known as simple minimum, as the color gets darker the response

increase (the % color remaining decrease). As it can be seen in Figure 75, the maximum color removal is at acid pH, more specifically between 4.0 and 5.3 approximately. Other studies of enzymatic treatment with SBP of azo-dyes have been also proven to have optimal color removal at acid pH, Ali *et al.* (2013) demonstrates that SBP works better at pH 3.0-5.0 for the azo-dye CP6R, Kalsoom *et al.* (2013) demonstrate that the optimal pH for Trypan blue with SBP was pH 4.0.

The combination of pH-enzyme with 3.0 mM H₂O₂ constant has a minimum point at acid pH and which increases as it goes to basic pH.

Finally, the response surface represented by factors H₂O₂-enzyme, with pH 5.3 as constant takes the form of descending slope, the response has a minimum but this is outside the current experimental region, that is, it can be inferred that the true surface is a valley but its maximum depression is not observed, only one side.

The graphs collectively show that the percentage of color remaining tends to be lower when the pH approaches the acidic range, H₂O₂ is approximately equal to 2.5 mM and enzyme approaches 2.0 U/mL. Notably, the expected average of the response variable obtained from the graphs is a function of two factors only, thus, to really know the optimal point it would be necessary to analyze the pattern of the second-order model and validate the surface, to consider the three factors simultaneously as is done in the next step of the process to get the optimal point.

4.5.1.6 Optimized response for AB113

The optimum response represents the best combination of values for the factors that are in the experimental region, following the fitted model, to obtain the lowest % remaining possible (Figure 77).

The best point in the experimental region is given by:

$$\begin{aligned}x_1 &= pH = 4.5 \\x_2 &= H_2O_2 = 3.0 \text{ mM} \\x_3 &= Enzyme = 2.0 \text{ U/mL} \\Y &= 10.06 \% \text{ remaining}\end{aligned}$$

To validate the model obtained, three validation runs at this point were done obtaining an average of $11 \pm 0.2\%$ remaining dye. The optimum conditions, give in section 4.1.5, with the optimization of one-factor at the time were: pH 4.0, 2.5 mM H₂O₂, 1.5 U/mL for 5.2% color remaining. The second-order model is adequate to describe the response surface in the design space and equations can be used to predict response in the area explored.

In already established processes such as this, it is expected that the optimal point is "not far" from the usual conditions of operation or possibly within the experimental region. Figure 77, shows the optimal point obtained, the graph shows the effect of each factor (columns) on the response (row), the red line represent the optimal value which are in red numbers, meanwhile the blue lines and numbers represents the response.

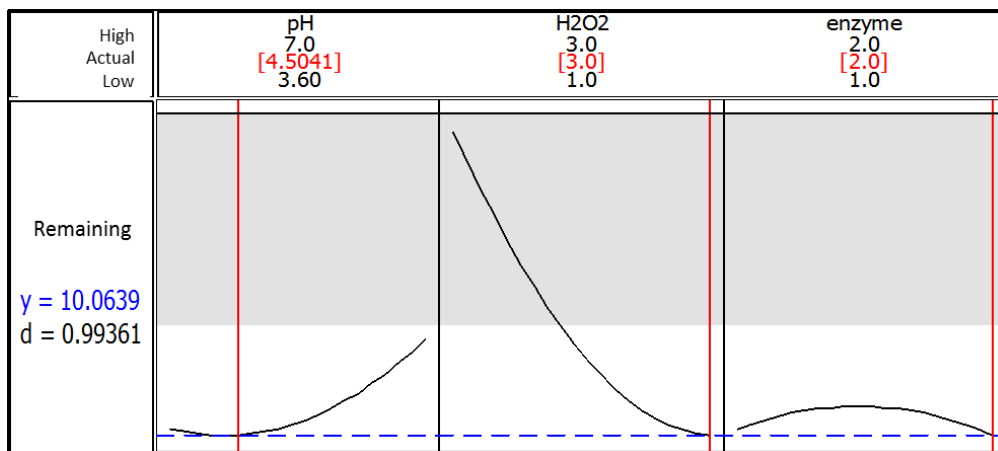


Figure 77. Optimization graph for AB113

A good approximation was achieved with the second-order design. However, 5% remaining is the goal, for this reason a new range of pH was used to find a lower color remaining by decreasing the area explored and moving the initial ranges of the parameters.

4.5.1.7 AB113 second-order design, second approach

In order to get a lower color remaining response the parameters were redefined in the vicinity of the center point and the practical operational experimental area, the values for the parameters were changed as shown in Table 10. Where, the intermediate pH value from the first approach was taken as the highest value in order to reduce the experimental area.

Table 10. Values for the three levels for AB113, second approach (H₂O₂ in mM, enzyme in U/mL)

Factor	Levels		
	-1	0	1
pH	3.6	4.4	5.3
H ₂ O ₂	1.0	2.0	3.0
Enzyme	1.0	1.5	2.0

4.5.1.8 Analysis of variance ANOVA and estimate the model and lack-of-fit test

First, as done before (section 4.5.1), the first-order search was conducted (Appendix C, Table C.3) and the ANOVA analysis is shown in Figure 78.

Source	DF	fit SS	fit MS	F	P
Principal effects	3	2650.12	883.37	1389.84	0.000
pH	1	115.50	115.50	181.73	0.000
H ₂ O ₂	1	2519.16	2519.16	3963.48	0.000
enzyme	1	15.46	15.46	24.33	0.001
2-Interactions	3	42.19	14.06	22.13	0.000
pH*H ₂ O ₂	1	38.80	38.80	61.04	0.000
pH*enzyme	1	3.20	3.20	5.03	0.049
H ₂ O ₂ *enzyme	1	0.20	0.20	0.31	0.590
3-Interactions	1	0.29	0.29	0.46	0.0513
pH*H ₂ O ₂ *enzyme	1	0.29	0.29	0.46	0.513
Curvature	1	879.05	879.05	1383.05	0.000
Residual error	10	6.36	0.64		
Pure error	10	6.36	0.64		
Total	18				

R-squared = 99.82% R-squared (fitted) = 99.68%

Figure 78. ANOVA analysis for AB113 (first-order search), second approach

The fitted equation for this first-order search was as follows:

$$\begin{aligned} \text{Remaining} = & 57.9380 - 0.12034 \text{ pH} - 2.60619 \text{ H}_2\text{O}_2 - 4.25918 \text{ enzyme} \\ & - 2.30891 \text{ pH} * \text{H}_2\text{O}_2 + 0.41554 \text{ pH} * \text{enzyme} - 1.19290' \text{ H}_2\text{O}_2 \\ & * \text{enzyme} + 0.31795 \text{ pH} * \text{H}_2\text{O}_2 * \text{enzyme} - 18.6536(\text{CtPt}) \end{aligned}$$

As seen in Figure 78, all the individual parameters were significant with 95% confidence (less than 5% significance level), except the double interaction of H₂O₂ and enzyme factors as well as the triple interaction.

Figure 79 shows the analysis of the residuals for the first-order search. As seen in the graphs the points tend to follow a straight line (normal probability plot), the Gaussian form is present (histogram), the residuals against the values of X (versus order) points show no pattern, as well as the graph of versus fit the points which doesn't follow any specific pattern but tend to cluster on the lower extreme which means that the model fits on the lower Y values.

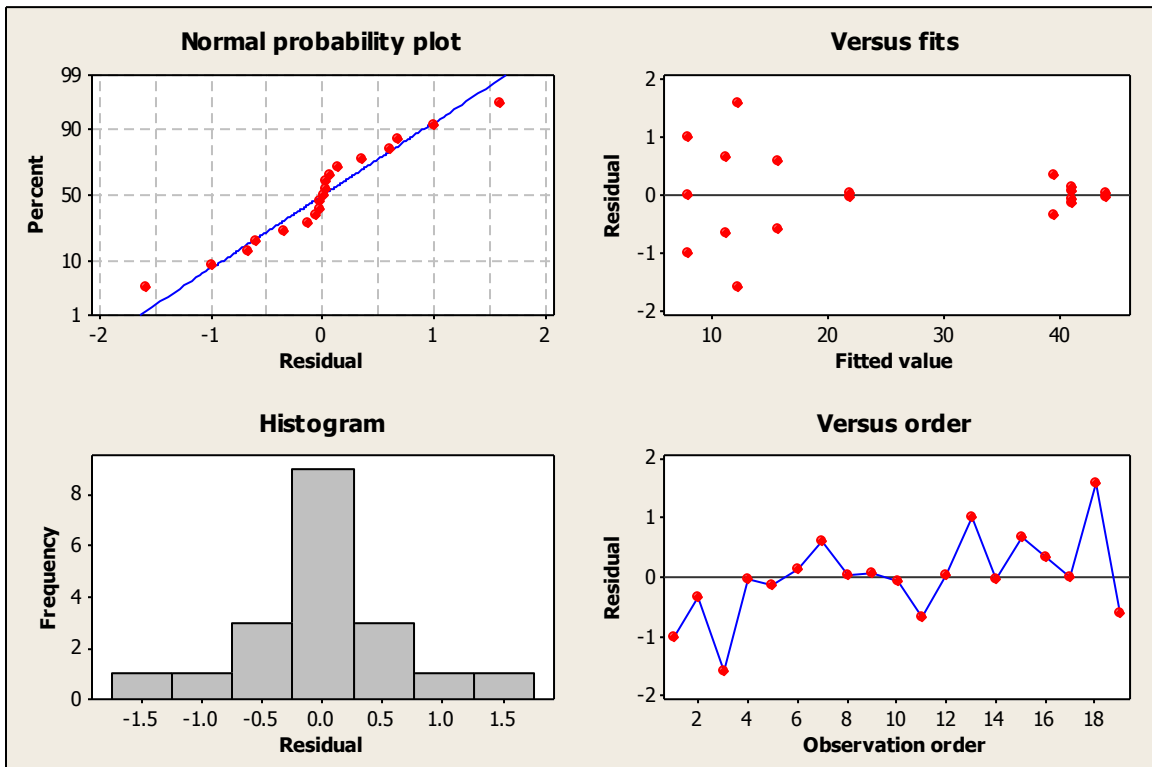


Figure 79. Residual plot for % remaining for AB113, second approximation

4.5.1.9 Second-order search. Box-Behnken design

As done in section 4.5.1.3, a second-order search was conducted (Appendix C, Table C.4.). Figure 80 shows the ANOVA analysis for Box-Behnken design

Source	DF	fit SS	fit MS	F	P
Regression	9	3883.53	431.50	590.29	0.000
Lineal	3	2553.32	851.11	1164.30	0.000
pH	1	4.58	44.58	60.99	0.000
H ₂ O ₂	1	2507.96	2507.96	3430.86	0.000
enzyme	1	0.78	0.78	1.06	0.315
2-interaction	3	1320.01	440.00	601.92	0.000
pH*pH	1	569.93	569.93	779.66	0.000
H ₂ O ₂ *H ₂ O ₂	1	842.48	842.48	1152.51	0.000
enzyme*enzyme	1	39.70	39.70	54.31	0.000
Interaction	3	10.21	3.40	4.65	0.013
pH*H ₂ O ₂	1	0.23	0.23	0.31	0.584
pH*enzyme	1	8.98	8.98	12.28	0.002
H ₂ O ₂ *enzyme	1	1.00	1.00	1.37	0.256
Residual error	20	14.62	0.73		
Lack-of-fit	3	8.77	2.92	8.50	0.001
Pure error	17	5.85	0.34		
Total	29				

R-squared = 99.62% R-squared(fitted) = 99.46%

Figure 80. ANOVA analysis for Box-Behnken, second approach

As seen in Figure 80 the individual factors of enzyme as well as “pH * H₂O₂” and “H₂O₂*enzyme” were not significant since the p-values were more than 0.05. It was necessary to do the ANOVA analysis without these terms (as done in section 4.5.1.3), in this case enzyme was not ruled out since the double interaction “enzyme * enzyme” was significant (Figure 81).

Source	DF	fit SS	fit MS	F	P
Regression	7	3765.52	537.93	496.94	0.000
Lineal	3	2478.33	826.11	763.16	0.000
pH	1	44.58	44.58	41.18	0.000
H ₂ O ₂	1	2433.35	2433.35	2247.94	0.000
enzyme	1	0.40	0.40	0.37	0.550
2-interaction	3	1278.21	426.07	393.61	0.000
pH*pH	1	522.81	522.81	482.97	0.000
H ₂ O ₂ *H ₂ O ₂	1	843.16	843.16	778.92	0.000
enzyme*enzyme	1	39.85	39.85	36.81	0.000
interaction	1	8.98	8.98	8.30	0.009
pH*enzyme	1	8.98	8.98	8.30	0.009
Error residual	22	23.81	23.81	1.08	
Lack-of-fit	5	15.45	3.09	6.28	0.002
Pure error	17	8.37	8.37	0.49	
Total	29				

R-squared = 99.37% R-squared(fitted) = 99.17%

Figure 81. ANOVA analysis without the non-significant interactions

Based on Figures 80 and 81, a full quadratic model is preferred as the R^2 are almost the same (99.46 and 99.17, respectively).

The equation for a full quadratic design is as follows:

$$\begin{aligned} \text{Remaining} = & 329.342 - 106.838 * pH - 55.0634 * H_2O_2 - 14.8751 * enzyme \\ & + 12.159 * pH * pH + 10.6811 * H_2O_2 * H_2O_2 + 9.2745 * enzyme \\ & * enzyme + 0.197789 * pH * H_2O_2 - 2.49289 * pH * enzyme \\ & - 0.70734 * H_2O_2 * enzyme \end{aligned}$$

4.5.1.10 Contour and surface plots second approximation

Figure 82 and 83 show the contour and surface plots, respectively. Each figure demonstrates the effect of two factors while the other factors were fixed at the respective intermediate levels (zero level) (pH 4.45, 2 mM H_2O_2 and 1.5 U/mL SBP).

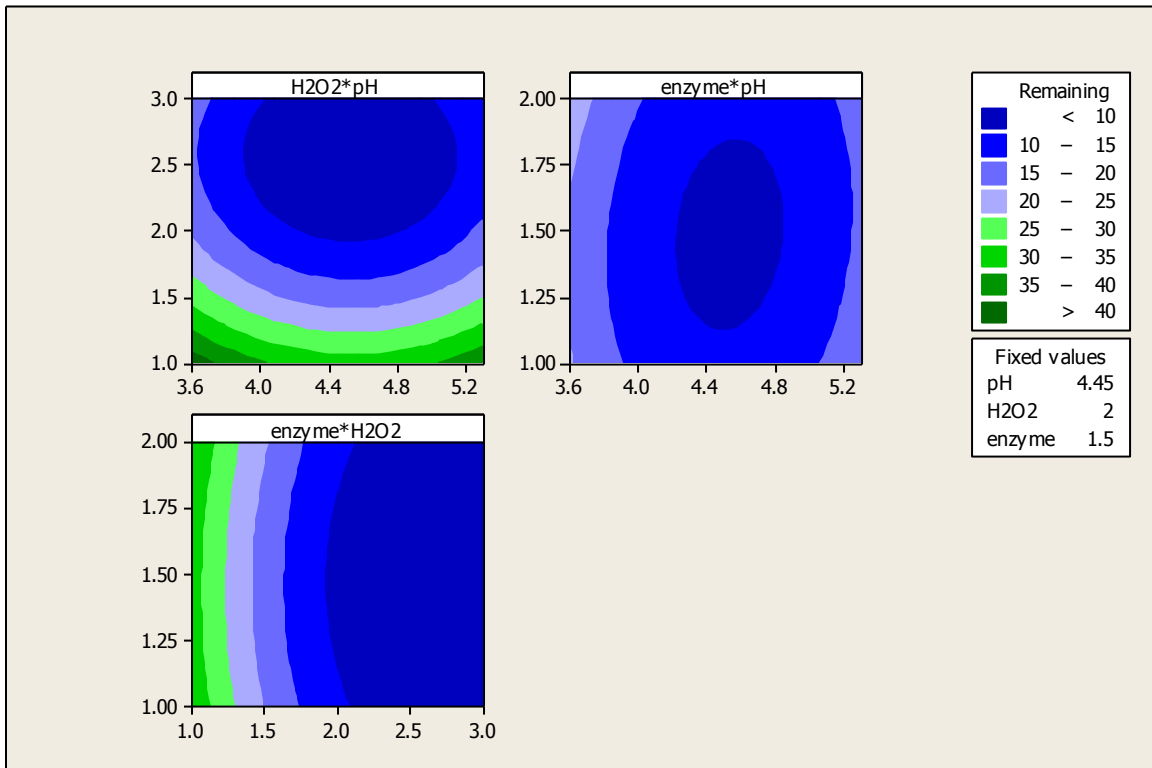


Figure 82. Contour plot for AB113. Fixed values: a) enzyme 1.5 U/mL, b) H_2O_2 2.0 mM, c) pH 4.45

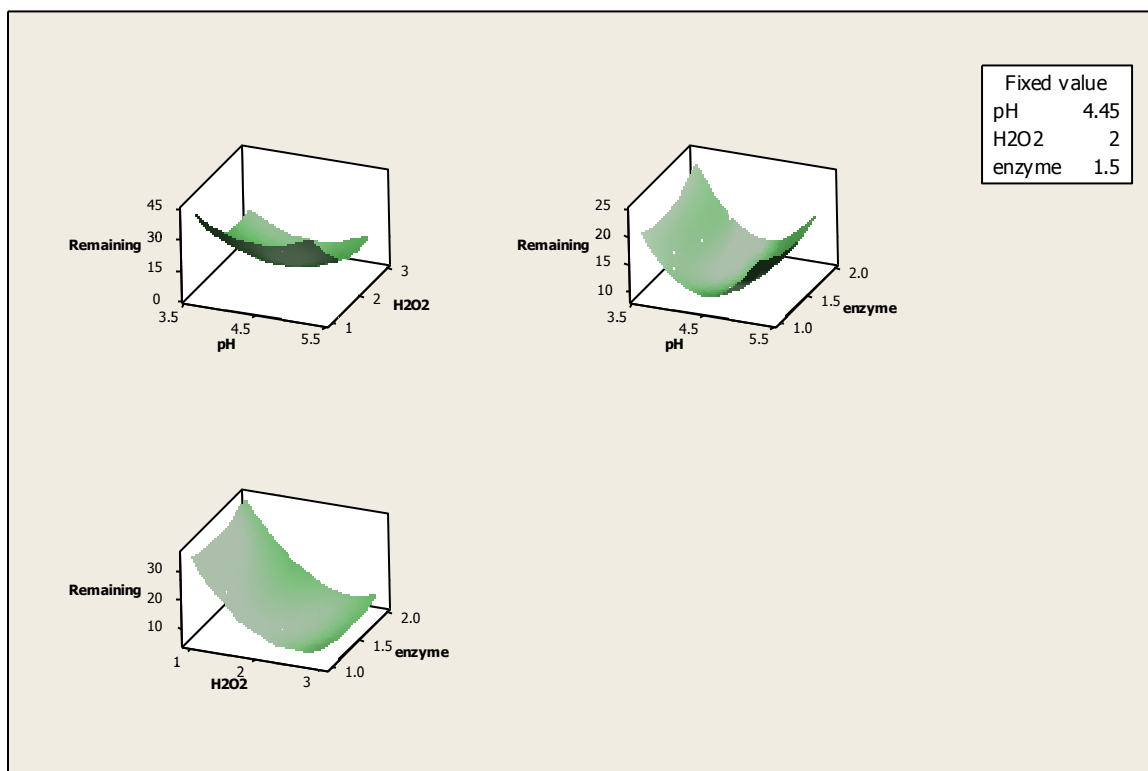


Figure 83. Surface plots. Fixed values: a) enzyme 1.5 U/mL, b) H₂O₂ 2.0 mM, c) pH 4.45

As seen in Figures 82 and 83, the plot of H₂O₂ and pH with a fixed enzyme value of 1.5 U/mL has a minimum value in the darker color and the % color remaining increases as it gets far from that zone which is in the acidic range of 4.0-4.8 and 2.0 mM H₂O₂ or lower concentrations. The same behavior, with presence of a minimum can be seen for enzyme against pH with 2.0 mM H₂O₂ as fixed value, where is more notably in the middle area, when the enzyme is in the range of 1.25- 1.75 U/mL the optimum response is reached. Finally, the response surface represented by factors H₂O₂-enzyme (same behavior as found in the first approach, Figure 75 and 76), at pH 4.45 as constant, takes the form of a descending slope, the response has a minimum but this is outside the current experimental region, that is, it can be inferred that the true surface is a valley but its maximum depression is not observed only one side, where the optimal zone is after >2.0 mM H₂O₂ which there is no further change in the % remaining.

4.5.1.11 Optimized response for AB113, second approximation

The optimum response represents the best combination of values for the factors that are in the experimental region, following the fitted model, to obtain the lowest % remaining possible (Figure 84). As it can be seen, the factors (columns) have an optimum value to reach the lowest % remaining of 5.7% (row).

The best point in the experiment region is given by:

$$\begin{aligned}
 x_1 &= \text{pH} = 4.43 \\
 x_2 &= \text{H}_2\text{O}_2 = 2.57 \text{ mM} \\
 x_3 &= \text{Enzyme} = 1.52 \text{ U/mL} \\
 Y &= 5.67 \% \text{ remaining}
 \end{aligned}$$

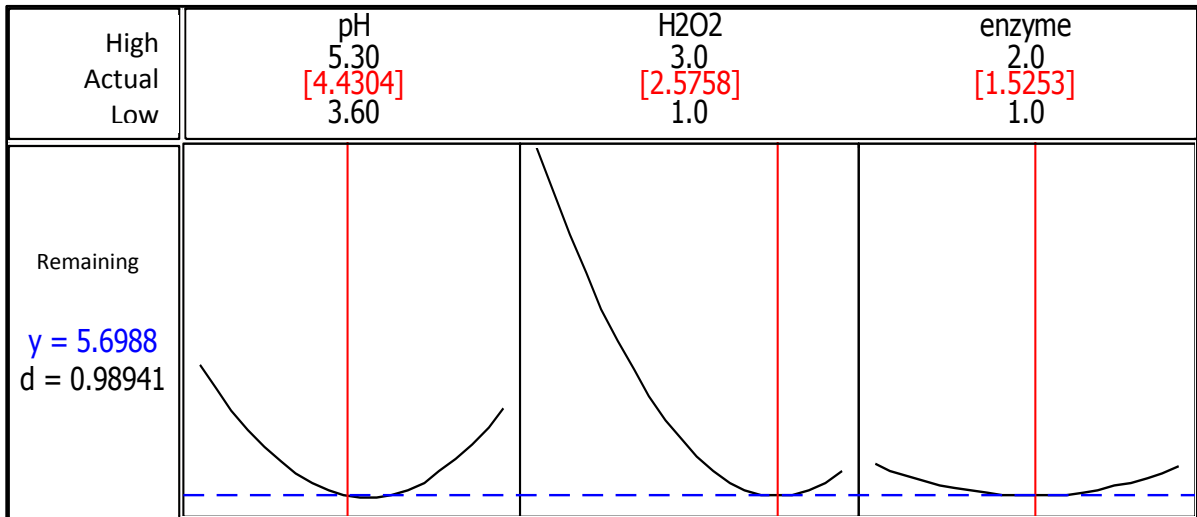


Figure 84. Optimization graph for AB113, second approximation

To validate the model obtained, three validation runs at this point were done obtaining an average of 8.1 ± 0.13 , difference of 2.4 % with Minitab model.

4.5.2. Factorial design for DB38

As done for AB113, a full factorial design by 2^3 repetitions at the center was completed for DB38 as seen in Table 11.

Table 11. Values for the 3 levels for DB38 (H₂O₂ in mM, enzyme in U/mL)

Factor	Levels		
	-1	0	1
pH	3.0	4.0	5.0
H ₂ O ₂	1.50	2.25	3.00
Enzyme	1.50	2.25	3.00

Table 12 shows the combinations of the parameters for the different treatment in this first step of analysis.

Table 12. Treatments and combination for DB38 (H₂O₂ in mM, enzyme in U/mL)

Treatments	pH	H ₂ O ₂	Enzyme
(-1,-1,-1)	3.00	1.50	1.50
(1,-1,-1)	5.00	1.50	1.50
(-1,1,-1)	3.00	3.00	1.50
(1, 1,-1)	5.00	3.00	1.50
(-1,-1,1)	3.00	1.50	3.00
(1,-1,1)	5.00	1.50	3.00
(-1,1,1)	3.00	3.00	3.00
(1,1,1)	5.00	3.00	3.00
(0,0,0)	4.00	2.25	2.25

The experimental runs were conducted in random order (Appendix C, Table C.5)

4.5.2.1 Variance analysis (ANOVA)

The experimental results were analyzed by an ANOVA. Figure 85 shows the ANOVA analysis for the first-order stage of the analysis for DB38.

Source	DF	fit SS	fit MS	F	P
Principal effects	3	1653.61	551.20	460.55	0.000
ph	1	110.60	110.60	92.41	0.000
enzyme	1	1536.97	1536.97	1284.20	0.000
H ₂ O ₂	1	6.03	6.03	5.04	0.051
2-Interactions	3	997.01	332.34	277.68	0.000
ph*enzyme	1	949.24	949.24	793.12	0.000
ph*H ₂ O ₂	1	26.95	26.95	22.52	0.001
enzyme*H ₂ O ₂	1	20.83	20.83	17.40	0.002
3-Interactions	1	83.82	83.82	70.03	0.000
ph*enzyme*H ₂ O ₂	1	83.82	83.82	70.03	0.000
Curvature	1	338.02	338.02	282.43	0.000
Residual error	9	0.77	1.20		
Pure error	9	10.77	1.20		
Total	17				
R-squared. = 99.65%		R-squared (fitted) = 99.34%			

Figure 85. ANOVA analysis for DB38

It was found statistically, with a confidence level of 95%, that the factors of pH and enzyme are significantly influential on the % remaining dye in the solution, because the p-value obtained for each factor was 0.000, less than 5% significance level (α level). The p-value of H₂O₂ was more than 0.05, which shows it is not significantly influential, however further analysis should be done as it is on the limit with a value 0.051, also the double interaction (H₂O₂)² is significant, which indicates that the H₂O₂ cannot be eliminated as being non-significantly influential in the % remaining dye. In this first-order stage, double interactions between pairs of factors also obtained p-values of 0.000 thus proving to be significantly influential on the % remaining dye; likewise with the triple interaction (less than 0.05 significance level).

The curvature p-value 0.000 also happens to be significant, meaning that at least one of the three quadratic terms is active; causing the curvature.

In addition, an R-squared of 99.34% for the fit indicates that the fitted model explains 99.34% of the % remaining dye response; thus the model has a good predictive capacity. As mentioned for AB113, it is recommended that an R-squared value be at least 75% to continue with this methodology. It is, however, necessary to validate if there is an effect of curvature in the experimental region, meaning that towards the center of the

experimental region, the % remaining dye is higher or lower than the rest of the experimental region.

4.5.2.2 Estimate the model and lack-of-fit test

The results from the ANOVA were fitted to the equation for a first-order search as follows:

$$\begin{aligned} \text{Remaining} = & 223.816 - 37.1832 \text{ pH} - 33.4431 \text{ H}_2\text{O}_2 - 95.3315 \text{ enzyme} \\ & + 7.4245 \text{ pH} * \text{H}_2\text{O}_2 + 19.4249 \text{ pH} * \text{enzyme} + 18.3040 \text{ H}_2\text{O}_2 \\ & * \text{enzyme} - 4.06891 \text{ pH} * \text{H}_2\text{O}_2 * \text{enzyme} - 13.7891 \text{ CtPt} \end{aligned}$$

An analysis of the residuals, Figure 86, was done to validate the fit of the regression model.

- The points in the normal probability plot tend to conform to a straight line which indicates that the assumption on the errors is reasonably well met
- In the graph of residuals *versus* predicted (Versus FITS), points do not follow any pattern indicating a more or less random distribution across the graph
- As the plot of the residuals against the values of X (*Versus* Order), points show no pattern, so the pattern does not follow any trend over the values of X
- The histogram is a type of bi-modal histogram, showing that the distribution of points has two peaks; this is due to % remaining values obtained which were in lower or higher extremes because of the ranges used.

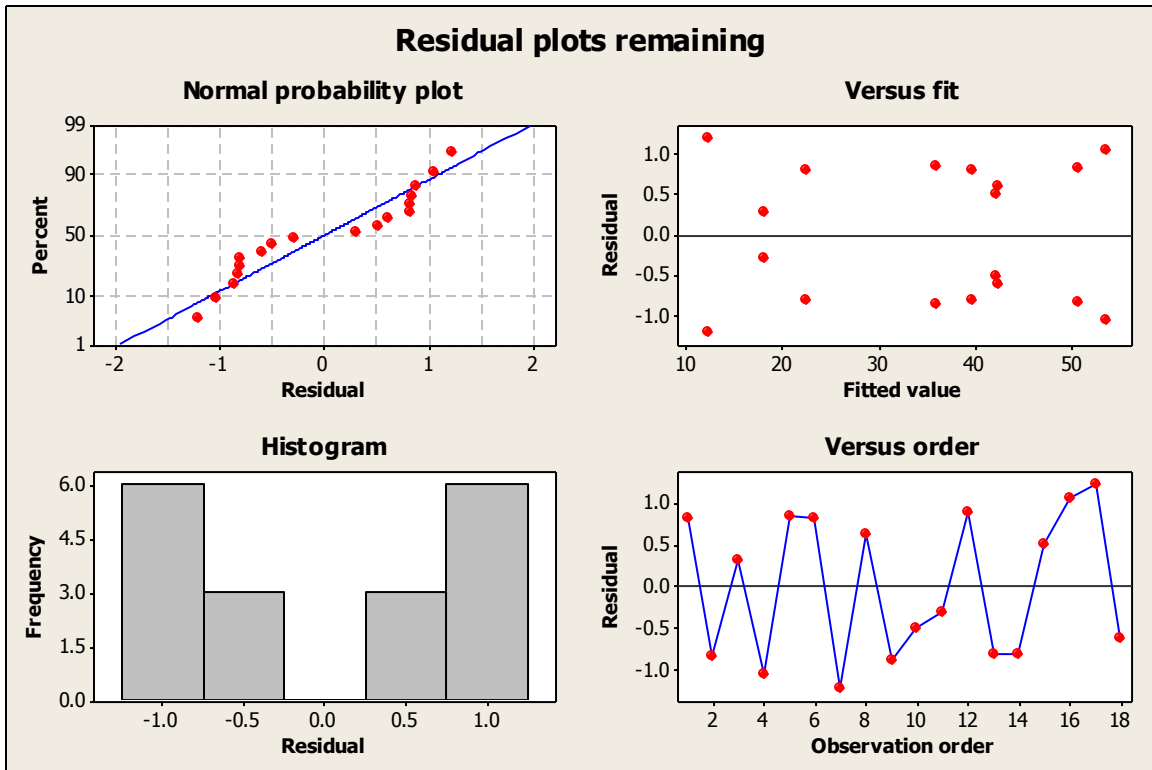


Figure 86. Residual plots for % remaining for DB38

After this step, the second-order model regression analysis was conducted using a Box-Behnken design.

4.5.2.3 Second-order search. Box-Behnken design

Based on the results for AB113, Box-Behnken design model was used for the RSM to determine the optimal levels of the parameters involved. A total of 30 runs were done with 6 center points. The treatments for DB38 are as shown in Table 13.

Table 13. Treatment used for Box-Behnken design for DB38 (H₂O₂ in mM, enzyme in U/mL)

Standard order	Treatments	pH	H ₂ O ₂	Enzyme
1	(-1,-1, 0)	3.00	1.50	2.25
2	(1, -1, 0)	5.00	1.50	2.25
3	(-1, 1, 0)	3.00	3.00	2.25
4	(1, 1, 0)	5.00	3.00	2.25
5	(-1, 0, -1)	3.00	2.25	1.50
6	(1, 0, -1)	5.00	2.25	1.50
7	(-1, 0, 1)	3.00	2.25	3.00
8	(1, 0, 1)	5.00	2.25	3.00
9	(0,-1,-1)	4.00	1.50	1.50
10	(0, 1, -1)	4.00	3.00	1.50
11	(0,-1, 1)	4.00	1.50	3.00
12	(0, 1, 1)	4.00	3.00	3.00
13	(0, 0, 0)	4.00	2.25	2.25
14	(0, 0, 0)	4.00	2.25	2.25
15	(0, 0, 0)	4.00	2.25	2.25

The runs were performed in random order (see Appendix C, Table C.6.). An ANOVA analysis was done to analyze significance of the different parameters (Figure 87).

Source	DF	fit SS	fit MS	F	P
Model	9	3347.59	371.95	87.81	0.000
Linear	3	1555.99	518.66	122.45	0.000
pH	1	1555.91	1555.91	367.32	0.000
Enzyme	1	74.84	74.84	17.67	0.000
H ₂ O ₂	1	69.61	69.61	16.43	0.001
2-interaction	3	1617.81	539.27	127.31	0.000
pH*pH	1	1503.77	1503.77	355.01	0.000
Enzyme*enzyme	1	1.67	1.67	0.39	0.537
H ₂ O ₂ *H ₂ O ₂	1	178.16	178.16	42.06	0.000
Interaction	3	265.18	88.39	20.87	0.000
pH*Enzyme	1	207.51	207.51	48.99	0.000
pH*H ₂ O ₂	1	0.17	0.17	0.04	0.844
Enzyme*H ₂ O ₂	1	57.50	57.50	13.57	0.001
Error	20	84.72	4.24		
Lack-of- fit	3	70.55	23.52	28.22	0.000
Pure error	17	14.17	0.83		
Total	29				

R-squared. = 97.53% R-squared(fitted) = 96.42%

Figure 87. ANOVA analysis for Box-Behnken for DB38

The analysis of variance for the second-order model indicated statistically, with a confidence level of 95% (5% significance level), that the pH, enzyme and H₂O₂ factors were significantly influential on the % remaining dye in solution, likewise, interactions of pairs of these factors showed quadratic effects (pH)² and (H₂O₂)², from p-value obtained 0.000.

However, other pair of factors, “enzyme*enzyme” and “pH*H₂O₂” are not significantly influential on the % remaining dye, with p-value of 0.537 and 0.844.

However, the main effects are significant which means an analysis should be conducted without these quadratic terms to determine which model fits better. As mentioned above for a response surface, an hierarchic model is preferred because it has more stable behavior in exploring the surface.

The model has a high predictive capacity, R² for the fit of 96.42 %, thus indicating that the regression model explains 96.42 % of the % remaining response, which means that the model is a good fit.

According to the results of the analysis of variance, the double interactions of enzyme*enzyme and pH *H₂O₂ factors could be eliminated from the model, so the mathematical model equation is expressed as follows:

$$Y = \beta_0 + \beta_1x_1 + \beta_2x_2 + \beta_{11}x_1^2 + \beta_{22}x_2^2 + \beta_{33}x_3^2 + \beta_{12}x_1x_2 + \beta_{23}x_2x_3 + \varepsilon$$

$$Y = \beta_0 + \beta_1x_1 + \beta_2x_2 + \beta_{11}x_1^2 + \beta_{22}x_2^2 + \beta_{33}x_3^2 + \beta_{12}x_1x_2 + \beta_{23}x_2x_3 + \varepsilon$$

$$x_1 = pH$$

$$x_2 = H_2O_2 \text{ concentration (mM)}$$

$$x_3 = \text{Enzyme concentration (U/mL)}$$

$$Y = \% \text{ color remaining}$$

For this reason it is necessary to re-analyze the results for this model without these effects (Figure 88).

Source	DF	fit SS	fit MS	F	P
Regression	7	3345.76	477.97	121.49	0.000
Lineal	3	1770.54	590.18	150.01	0.000
pH	1	1723.29	1723.29	438.02	0.000
Enzyme	1	147.88	147.88	37.59	0.000
H ₂ O ₂	1	86.86	86.86	22.08	0.000
Cuadrado	2	1616.14	808.07	205.39	0.000
pH*pH	1	1504.97	1504.97	382.53	0.000
H ₂ O ₂ *H ₂ O ₂	1	176.56	176.56	44.88	0.000
Interaction	2	265.01	132.51	33.68	0.000
pH*enzyme	1	207.51	207.51	52.75	0.000
Enzyme*H ₂ O ₂	1	57.50	57.50	14.61	0.001
Residual error	22	86.55	3.93		
Lack-of-fit	5	72.39	14.48	17.37	0.000
Pure error	17	14.17	0.83		
Total	29				

R-squared = 97.48 R-squared(fitted) = 96.68%

Figure 88. ANOVA analysis without the effects of "enzyme*enzyme" and "pH *H₂O₂" factors

The ANOVA was done to compare the fitted design with the preceding second-order design (that including the two quadratic effects) and choose the one that best describes the surface of the experimental region.

Both models have the almost the same R² values for the 96.42 and 96.68, respectively.

Furthermore, with a confidence level of 95%, all main effects of the factors, pure quadratic effects and double interactions are significantly influential on the % remaining dye solution as the full quadratic ANOVA.

So either model could be used to characterize the response surface in this case study. Thus, as for AB113, a full quadratic model was taken as follows.

$$\begin{aligned} \text{Remaining} = & 369.709 - 130.700 * pH - 32.752 * enzyme - 31.588 * H_2O_2 \\ & + 14.27 * pH * pH + 0.845 * enzyme * enzyme + 8.732 * H_2O_2 \\ & * H_2O_2 + 6.791 * pH * enzyme + 0.193 * pH * H_2O_2 - 4.766 \\ & * enzyme * H_2O_2 \end{aligned}$$

4.5.2.4. Countour and surface plos for DB38

Figures 89 and 90 shows the contour and surface plots for DB38, as for AB113, two factors are demonstrated while the other is fixed at intermediate level (zero level). It can be seen that as the pH gets close to 4.0, enzyme 3.0 U/mL with 2.25 mM H₂O₂ the % remaining is below 10%.

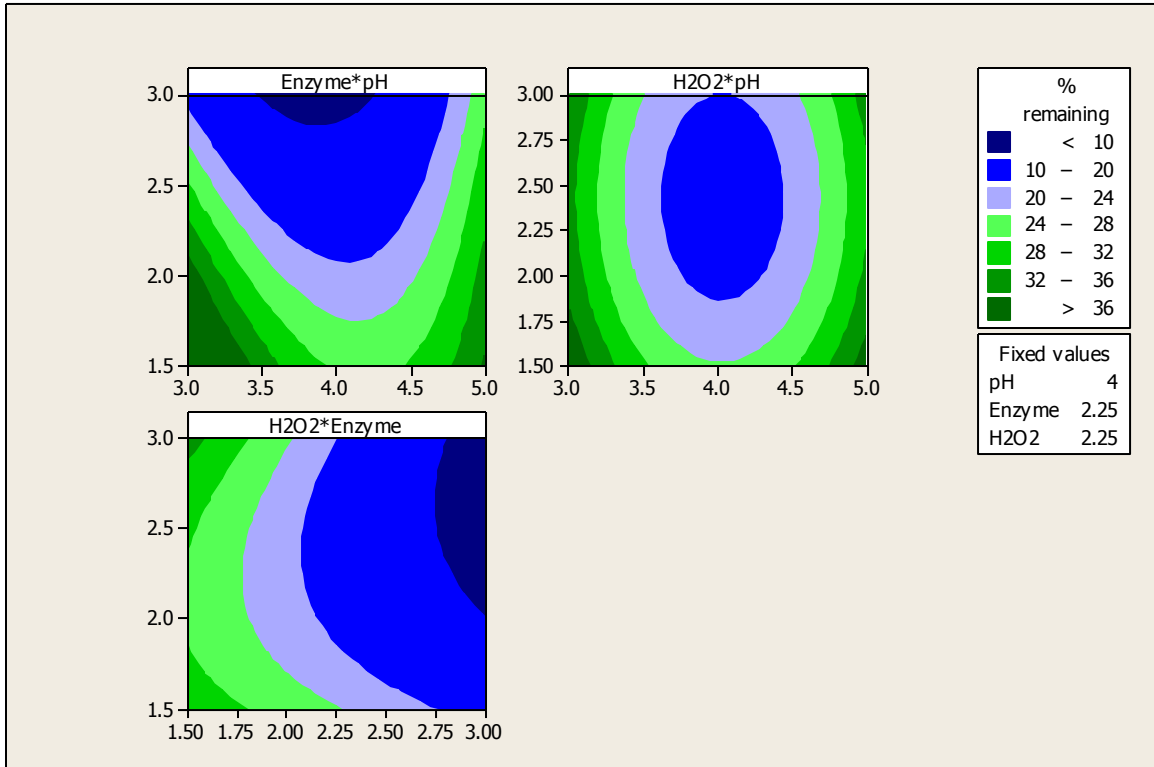


Figure 89. Contour plots for DB38. Fixed values: a) enzyme 2.25 U/mL, b) H₂O₂ 2.25 mM, c) pH 4.0

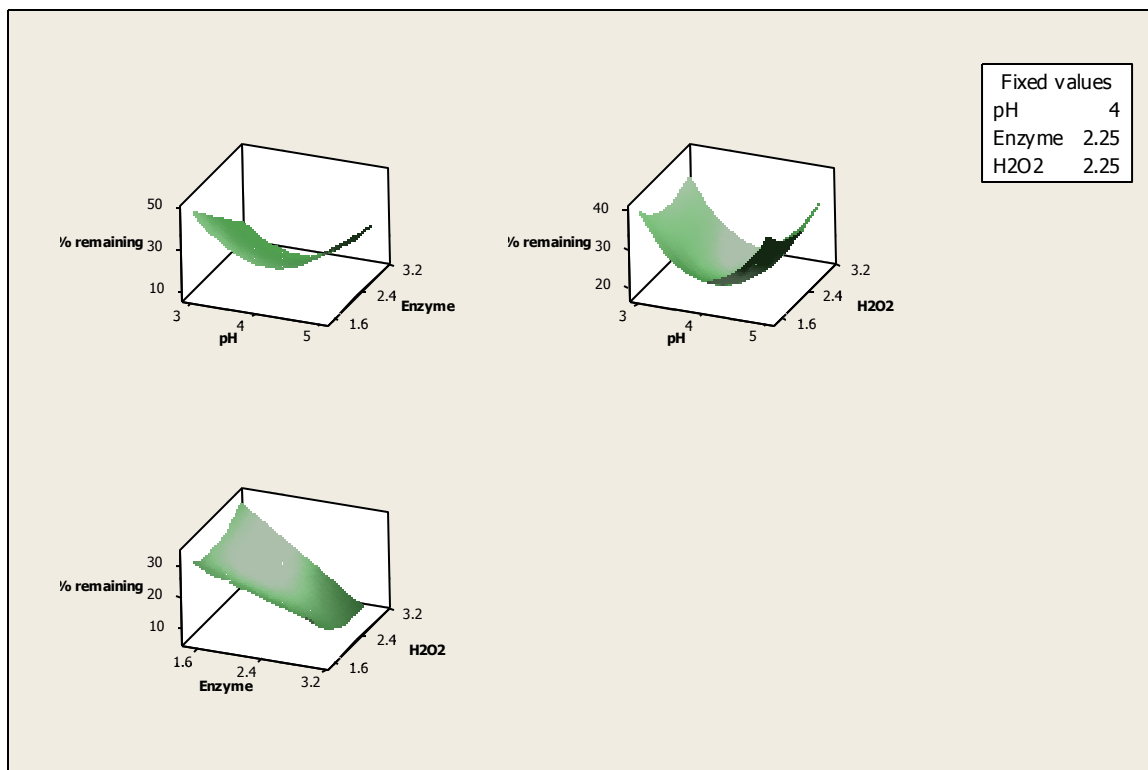


Figure 90. Surface plots. Fixed values: a) enzyme 2.25 U/mL, b) H₂O₂ 2.25 mM, c) pH 4.0

The graph of pH against enzyme seems to have a minimum where the lowest % remaining point is reached in the experimental region, as it gets far from the middle point in the valley of the graph. The minimum point of the response is shown in the region of pH 4.0. For the surface plots, the pH against H₂O₂ graph has a minimum point in the experimental region showing a valley in the surface (where the optimum response as it represents is, because it represents the lowest % remaining). The graph of H₂O₂ against enzyme takes the form of descending slope; the response has a minimum outside the experimental region. The region has a maximum in the % remaining in the lower concentrations of enzyme and H₂O₂ and the response continues to decrease as it reaches 3.0 U/mL of enzyme.

4.5.2.5. Optimum response for DB38

The optimum response represents the best combination of values for the factors that are in the experimental region, from the regression model, to obtain the lowest % remaining possible (Figure 91).

The best point in the experiment region is given by:

$$\begin{aligned}
 x_1 &= \text{pH} = 3.84 \\
 x_2 &= \text{H}_2\text{O}_2 = 2.74 \text{ mM} \\
 x_3 &= \text{Enzyme} = 3.0 \text{ U/mL} \\
 Y &= 5.6 \% \text{ remaining}
 \end{aligned}$$

To validate this data three experimental runs were done obtaining a % remaining of $6.9 \pm 0.41\%$ remaining using this values for the different factors.

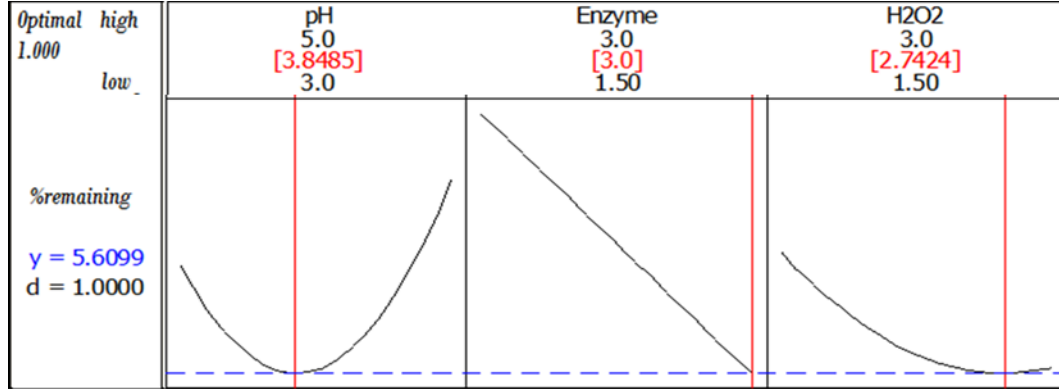


Figure 91. Optimization graph for DB38

To study a different range of H_2O_2 and enzyme another design was done, to be able to see the behavior of the surface if the optimal points are not in the corner of the design space.

4.5.2.6. DB38 second-order design, second approach

As done for the first approach (section 4.5.2), a full factorial design by 2^3 repetitions at the center was completed. Table 14 shows the values for the 3 levels chosen, pH, H₂O₂ and enzyme, where the lower and higher point of H₂O₂ and enzyme increase to avoid the optimal point to be on the corner of the experimental region.

Table 14.Values for the 3 levels for DB38 (H₂O₂ in mM, enzyme in U/mL)

Factor	Levels		
	-1	0	1
pH	3.0	4.0	5.0
H ₂ O ₂	2.5	3.0	3.5
Enzyme	2.5	3.0	3.5

Table 15 shows the combinations of the parameters for the different treatment in this first step of analysis.

Table 15.Treatments and combination for DB38 (H₂O₂ in mM, enzyme in U/mL)

Treatments	pH	H ₂ O ₂	Enzyme
(-1,-1,-1)	3.0	2.5	2.5
(1,-1,-1)	5.0	2.5	2.5
(-1,1,-1)	3.0	3.5	2.5
(1, 1,-1)	5.0	3.5	2.5
(-1,-1,1)	3.0	2.5	3.5
(1,-1,1)	5.0	2.5	3.5
(-1,1,1)	3.0	3.5	3.5
(1,1,1)	5.0	3.5	3.5
(0,0,0)	4.0	3.0	3.0

The experimental runs were conducted in random order (see Appendix C, Table C.7)

4.5.2.7 Variance analysis (ANOVA)

The experimental results were analyzed by an ANOVA. Figure 92 shows the ANOVA analysis for the first-order stage of the analysis for DB38.

Source	DF	fit SS	fit MS	F	p
Principal effects	3	2406.82	802.27	367.15	0.000
pH	1	1340.65	1340.65	613.53	0.000
H ₂ O ₂	1	29.12	29.12	13.33	0.004
enzyme	1	1037.04	1037.04	474.59	0.000
2-Interactions	3	524.46	174.82	80.00	0.000
pH*H ₂ O ₂	1	8.24	8.24	3.77	0.081
pH*enzyme	1	513.74	513.74	235.11	0.000
H ₂ O ₂ *enzyme	1	2.49	2.49	1.14	0.311
3-Interactions	1	0.10	0.10	0.05	0.833
pH*H ₂ O ₂ *enzyme	1	0.10	0.10	0.05	0.833
Curvature	1	1256.38	1256.38	574.97	0.000
Residual error	10	21.85	2.19		
Pure error	10	21.85	2.19		
Total	18				

R-squared = 99.48% R-squared (fitted) = 99.07%

Figure 92. ANOVA analysis for DB38

It was found statistically, with a confidence level of 95% that the main factors of pH, H₂O₂ and enzyme are significantly influential on the % remaining dye in the solution, because of the p-value obtained of each factor was 0.000, less than 5% significance level (α level). On the other side, double interactions of “pH* H₂O₂” and “H₂O₂ *enzyme” as well as the triple interaction were non-significant as the p-value was more than 0.05.

The curvature p-value 0.000 also happens to be significant, meaning that at least one of the three quadratic terms is active; causing the curvature.

In addition, an R-squared of 99.07% for the fitted indicates that the fitted model explains 99.07 % of the % remaining dye response, thus the model has a good predictive capacity.

As mentioned for AB113, it is recommended that an R-squared value be at least 75% to continue with this methodology.

4.5.2.8. Estimate the model and lack-of-fit test

The results from the ANOVA were fitted to the equation for a first-order search as follows:

$$\begin{aligned} \text{Remaining} = & 185.558 - 26.2738 \text{ pH} - 3.9411 \text{ H}_2\text{O}_2 - 62.3332 \text{ enzyme} \\ & + 0.47630 \text{ pH} * \text{H}_2\text{O}_2 + 10.3743 \text{ pH} * \text{enzyme} + 0.30005 \text{ H}_2\text{O}_2 \\ & * \text{enzyme} - 0.31952 \text{ pH} * \text{H}_2\text{O}_2 * \text{enzyme} - 22.3006 \text{ (CtPt)} \end{aligned}$$

An analysis of the residuals (Figure 93) was done to validate the fit of the regression model.

- The points in the normal probability plot tend to conform to a straight line which indicates that the assumption on the errors is reasonably well met
- In the graph of residuals *versus* predicted (*Versus* FITS), points tend to cluster on the extremes of the fitted value which means that the model fits on the extremes values of Y
- As the plot of the residuals against the values of X (*Versus* Order), points show no pattern, so the pattern does not follow any trend over the values of X
- The histogram shows a type of bi-modal histogram, showing that the distribution of points has two peaks, as found in the first search (section 4.4.2.2.)

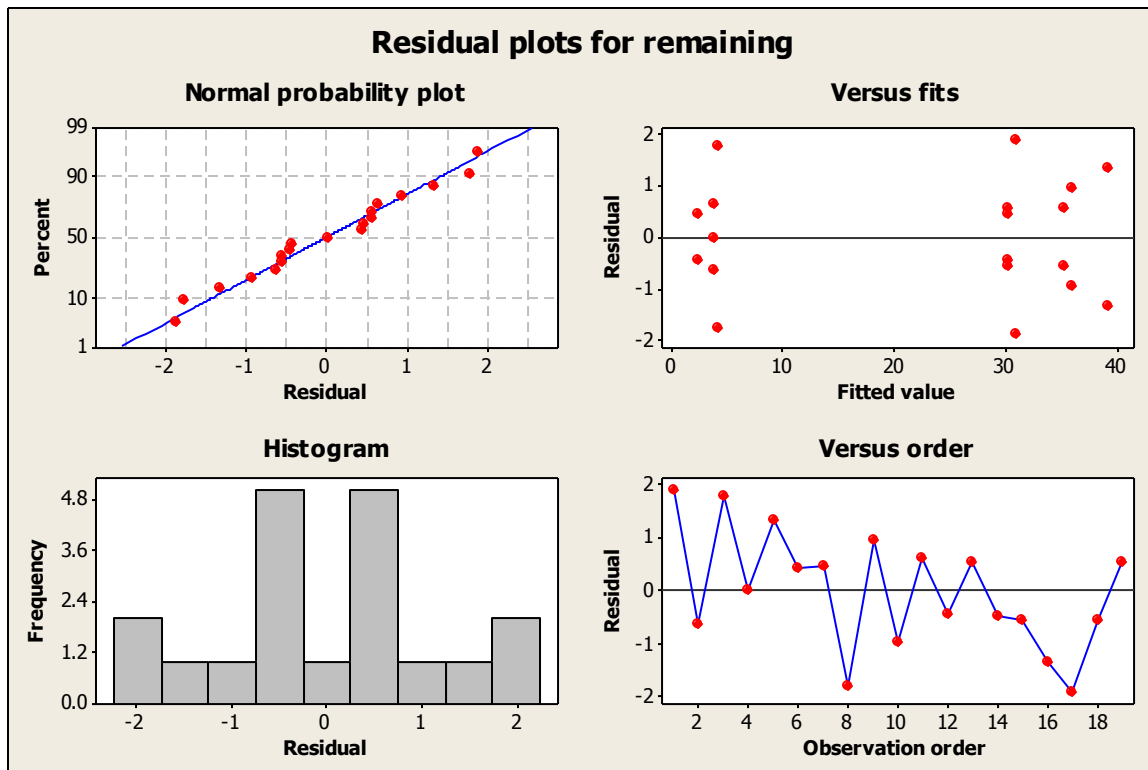


Figure 93. Residual plots for % remaining for DB38

After this step, the second-order model regression analysis was conducted using a Box-Behnken design.

4.5.2.9 Second-order search. Box-Behnken

Box-Behnken design was used as a design model for the RSM to determine the optimal levels of the parameters involved. A total of 30 runs were done with 6 center points. The treatments for DB38 are as shown in table 16.

Table 16. Treatment used for Box-Behnken for DB38 (H₂O₂ in mM, enzyme in U/mL)

Standard order	Treatments	pH	H ₂ O ₂	Enzyme
1	(-1,-1, 0)	3.0	2.5	3.0
2	(1, -1, 0)	5.0	2.5	3.0
3	(-1, 1, 0)	3.0	3.5	3.0
4	(1, 1, 0)	5.0	3.5	3.0
5	(-1, 0, -1)	3.0	3.0	2.5
6	(1, 0, -1)	5.0	3.0	2.5
7	(-1, 0, 1)	3.0	3.0	3.5
8	(1, 0, 1)	5.0	3.0	3.5
9	(0,-1,-1)	4.0	2.5	2.5
10	(0, 1, -1)	4.0	3.5	2.5
11	(0,-1, 1)	4.0	2.5	3.5
12	(0, 1, 1)	4.0	3.5	3.5
13	(0, 0, 0)	4.0	3.0	3.0
14	(0, 0, 0)	4.0	3.0	3.0
15	(0, 0, 0)	4.0	3.0	3.0

The runs were performed in random order (see Appendix C, Table C.8.). An ANOVA analysis was done to analyze the different parameters (Figure 94).

Source	DF	fit SS	fit MS	F	P
Regression	9	1408.97	156.552	101.67	0.000
Lineal	3	888.84	296.281	192.41	0.000
pH	1	482.07	482.072	313.06	0.000
H ₂ O ₂	1	1.72	1.722	1.12	0.303
enzyme	1	405.05	405.051	263.04	0.000
Double	3	444.98	148.327	96.32	0.000
pH*pH	1	375.60	375.602	243.92	0.000
H ₂ O ₂ * H ₂ O ₂	1	54.63	54.634	35.48	0.000
enzyme*enzyme	1	59.93	59.925	38.92	0.000
Interaction	3	75.15	25.049	16.27	0.000
pH* H ₂ O ₂	1	1.57	1.566	1.02	0.325
pH*enzyme	1	73.03	73.029	47.43	0.000
H ₂ O ₂ *enzyme	1	0.55	0.552	0.36	0.556
Residual error	20	30.80	1.540		
Lack-of-fit	3	23.32	7.773	17.67	0.000
Pure error	17	7.48	0.440		
Total	29				

R-squared = 97.86% R-squared (fitted) = 96.90%

Figure 94. ANOVA analysis for Box-Behnken for DB38

The analysis of variance of the second-order model was fitted statistically, with a confidence level of 95%, the pH and enzyme factors found to be significantly influential on the % remaining of the dye in solution; likewise for interactions of these two factors form and quadratic effects (pH)², (enzyme)² and (H₂O₂)², due to the p-values of each being 0.000, implying >95% confidence in the interactions.

Otherwise, the main effect of H₂O₂ as well as the interaction “pH*H₂O₂” and “enzyme *H₂O₂” are not significant in the % remaining dye since the respective p-values of 0.303, 0.325 and 0.556 are greater than 0.05. However, the double interaction of H₂O₂ is significant which means that the main effect of H₂O₂ cannot be ruled out, however, an analysis without the interactions terms pH*H₂O₂” and “enzyme *H₂O₂” was done to determine which model fits better. As mention before for response surfaces, an hierarchic model is preferred because they are a more robust design.

The model has a high capacity predictive, R² to 96.90%, indicating that the fitted model explains 96.90 % of the amount of remaining, which means that the model has a good fit According to the results of the analysis of variance, the double interaction of enzyme*enzyme and pH*H₂O₂ factors could be eliminated from the model, so the mathematical model equation is expressed as follows:

$$Y = \beta_0 + \beta_1x_1 + \beta_2x_2 + \beta_3x_3 + \beta_{11}x_1^2 + \beta_{22}x_2^2 + \beta_{33}x_3^2 + \beta_{12}x_1x_2 + \beta_{13}x_1x_3 + \beta_{23}x_2x_3 + \varepsilon$$

$$Y = \beta_0 + \beta_1x_1 + \beta_3x_3 + \beta_{11}x_1^2 + \beta_{22}x_2^2 + \beta_{33}x_3^2 + \beta_{13}x_1x_3 + \varepsilon$$

$$x_1 = pH = \text{pH}$$

$$x_2 = \text{H}_2\text{O}_2 \text{ concentration (mM)}$$

$$x_3 = \text{Enzyme concentration (U/mL)}$$

$$Y = \% \text{ color remaining}$$

For this reason it is necessary to analyze the results for this model without these effects (Figure 95).

Source	DF	fit SS	fit MS	F	P
Regression	7	1406.85	200.979	134.33	0.000
Linear	3	888.84	296.281	198.02	0.000
pH	1	482.07	482.072	322.20	0.000
H ₂ O ₂	1	1.72	1.722	1.15	0.295
enzyme	1	405.05	405.051	270.72	0.000
Squared	3	444.98	148.327	99.14	0.000
pH*pH	1	375.60	375.602	251.04	0.000
H ₂ O ₂ *H ₂ O ₂	1	54.63	54.634	36.52	0.000
enzyme*enzyme	1	59.93	59.925	40.05	0.000
interaction	1	73.03	73.029	48.81	0.000
pH*enzyme	1	73.03	73.029	48.81	0.000
Residual error	22	32.92	1.496		
Lack-of-fit	5	25.44	5.088	11.57	0.000
Pure error	17	7.48	0.440		
Total	29				
R-squared. = 97.71%		R-squared(fitted) = 96.99%			

Figure 95. ANOVA analysis without the main effect of “pH*H₂O₂” and “enzyme *H₂O₂”

The ANOVA was done to compare the fit of the fitted design against the previous second-order design (Figure 94) and choose the one that best describes the surface of the experimental.

Both models have the almost the same quality of fit 96.90 and 96.99%, respectively.

In addition, with a confidence level of 95%, all main effects of the factors and the pure quadratic effects and double interactions, except for H₂O₂, are significantly influential on the % remaining dye solution as before.

Thus, any model could be used to characterize the response surface in this case study, as for AB113 and the first approach of DB38, a full quadratic model was taken, the first generated.

$$\begin{aligned}
 \text{Remaining} = & 397.092 - 72.3485 * pH - 99.4488 * enzyme - 65.0108 * H_2O_2 \\
 & + 7.14181 * pH * pH + 11.3947 * enzyme * enzyme + 10.8800 \\
 & * H_2O_2 * H_2O_2 + 6.04272 * pH * enzyme + 0.88497 * pH * H_2O_2 \\
 & - 1.05098 * enzyme * H_2O_2
 \end{aligned}$$

4.5.2.10. Countour and surface plos for DB38

Figures 96 ad 97 show the contour and surface plots for DB38, to demonstrate two factors while the other is fixed at low level (-1 level).

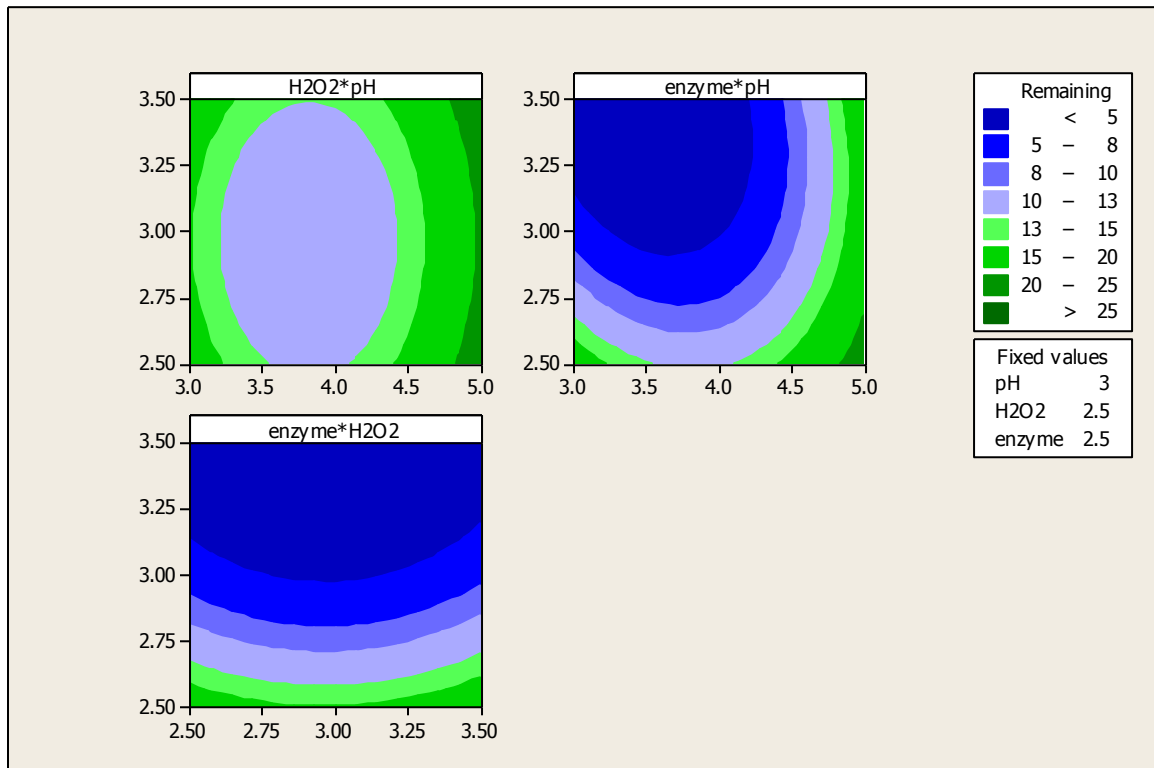


Figure 96. Contour plots for DB38. Fixed values: a) enzyme 2.5 U/mL, b) H₂O₂ 2.5 mM, c) pH 3.0

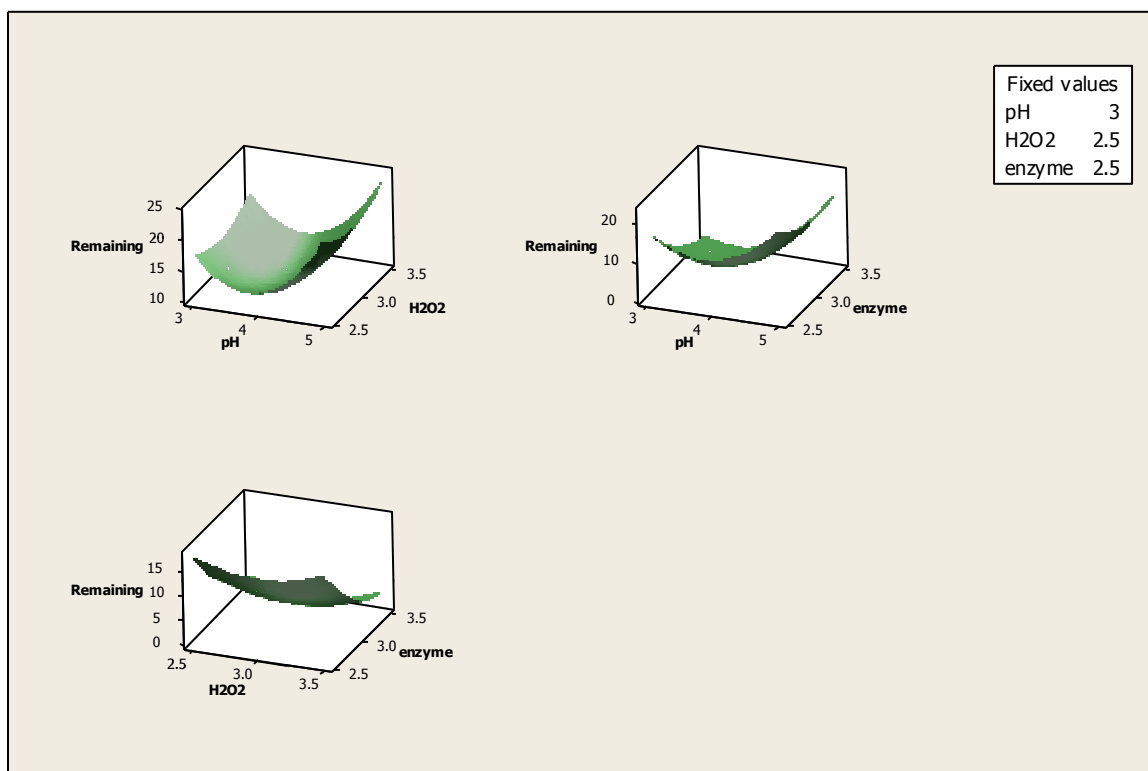


Figure 97. Surface plots. Fixed values: a) enzyme 2.5 U/mL, b) H₂O₂ 2.5 mM, c) pH 3.0

Analyzing Figures 96 and 97, for the contour and surface plots of H₂O₂ against pH, the graph have a minimum (lower % remaining) between pH 3.5 and 4.0 in the experimental region and the response increases as it moves away from that point. The graphs of enzyme against pH also seem to have a minimum point in the experimental region where the minimal remaining response is located in the left extreme of the region of acidic pH. As seen in Figure 96, the optimal enzyme region begins from 3.0 U/mL and shows no change in % remaining with higher values of enzyme. The graph of H₂O₂ against enzyme at pH 3.0 has the optimal values in the upper part of the graph as it can be observed in Figure 96 and 97 it has a simple maximum, independent of the H₂O₂ concentration if the optimal enzyme values are ≥ 3 U/mL.

4.5.2.11. Optimum response for DB38

The optimum response represents the best combination of values for the factors that are in the experimental region, which is shown in Figure 98.

The best point in the experiment region is given by:

$$x_1 = pH = 3.68$$

$$x_2 = H_2O_2 = 2.92 \text{ mM}$$

$$x_3 = Enzyme = 2.84 \text{ U/mL}$$

$$Y = 3.63 \text{ \% remaining}$$

To validate this data experimental runs were done obtaining a % remaining of $5.1 \pm 0.13\%$ remaining using these values for the different factors. The optimum conditions with the optimization of one factor at the time were pH 3.6, 2.5 mM H_2O_2 , 3 U/mL, achieving 3% remaining. Thus, this second approach obtained a lower optimum % remaining for both the Minitab estimation as well as the experimental run. Figures 96 and 97, also gives a better representation of the optimal region.

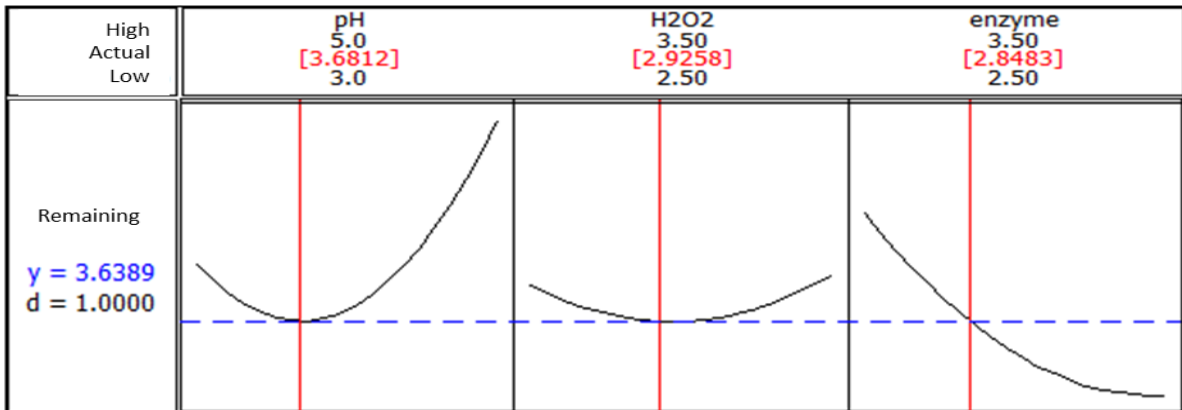


Figure 98. Optimization graph for DB38 (H_2O_2 in mM, enzyme in U/mL)

Table 17 shows the summary of the Minitab model and the optimization one parameter at the time. The % remaining showed for Minitab model is the actual experimental value obtained from the conditions of Minitab, the values predicted for AB113 was 5.6% and 3.6 % for DB38.

Table 17. Summary for Minitab model and one parameter at the time for both azo-dyes

Dye	Minitab model					One parameter at the time			
	H ₂ O ₂ (mM)	Enzyme (U/mL)	pH	%remaining *	%remaining **	H ₂ O ₂ (mM)	Enzyme (U/mL)	pH	%remaining
AB113	2.57	1.52	4.4	8.08	5.67	2.5	1.5	4	5.2
DB38	2.92	2.84	3.68	5.1	3.63	3	3	3.6	3.16

* Experimental value obtained using the Minitab model conditions

** Value predicted by Minitab

Chapter 5. Summary and Conclusions

5.1 Summary

Enzymatic treatment with SBP in the presence of H_2O_2 is an effective method for decoloration and degradation of azo-dyes and their possible products as demonstrated with two impure azo-dyes. In this dissertation a single-step process and two-step process with Fe° reduction were conducted to compare the optimal conditions required for both processes. To determine the effectiveness a complete study of color, dye, total amines (as aniline) and product reductions were conducted by UV-spectroscopy and HPLC. For the single-step process, buffered batch reactions over 3 hour reaction at room temperature showed: AB113 at 1.0 mM required 2.5 mM H_2O_2 and 1.5 U/mL SBP at pH 4.0 to achieve 95% color reduction (spectroscopy), 97% dye conversion (HPLC) and 30% TOC removal; DB38 required 2.5 mM H_2O_2 and 3 U/mL SBP at pH 3.6 to achieve 98% color reduction (spectroscopy), 98% dye degradation (HPLC) and 70% TOC removal. A two-step process was also conducted, where zero-valent iron (Fe°) was used as a pretreatment followed by enzymatic treatment. For the iron reduction step, unbuffered solutions were used and the parameters measured were: color reduction, dye degradation, TOC, total amines (as aniline), a representative Fe° product (by HPLC, 3-ABS for AB113 and aniline/benzidine for DB38) remaining. For AB113, 1.5 g Fe° (for 40 mL of 1 mM dye) and 60 minutes' reaction with Fe° followed by 1.5 U/mL SBP and 2.5 mM H_2O_2 at pH 4.0 were required for greater than 95% color and dye removal (spectroscopy and HPLC measurements) 69% TOC, and 80% of 3-ABS removal. For maximum removal of total

amines (74 %) the same conditions were needed as mentioned above, but a higher SBP concentration was needed (2.5 U/mL).

For DB38, 2 g Fe° (for 40 mL of 0.5 mM dye) and 120 minutes' reaction with Fe° followed by 0.6 U/mL SBP and 1.1 mM H_2O_2 at pH 5.0 were required for greater than 95% color and dye removal (spectroscopy and HPLC, respectively) as well as total amines and aniline/benzidine removal, and 88% TOC removal. The improved conditions for DB38 in the two-step process are due to the formation of products such as aniline and benzidine which are good substrates of SBP, but not 3-aminobenzenesulfonic acid. Thus, in order to choose a single- or two-step process for a given dye, it is necessary to determine if the products of azo cleavage due to Fe° reduction are good SBP substrates (such as aniline/benzidine), otherwise a single-step process is preferred.

With the one-step process, kinetic studies, fitting to the Michaelis-Menten model, were conducted (direct enzymatic treatment) for AB113, DB38 and COG. The lowest K_M value was for COG (4.7 μM) followed by AB113 and DB38 (20.75 and 36.4 μM , respectively). For catalytic efficiency the order obtained was: AB113=DB38>COG, the lower efficiency for COG is due to the lower V_{max} value compared to the other two-azo dyes.

Possible azo-cleavage was detected and also quantified by HPLC and confirmed with ESI-MS for COG after direct enzymatic treatment. The evidence for azo-cleavage of COG to aniline after direct enzymatic treatment with different concentrations of H_2O_2 and SBP was quantified by HPLC and found by the maximum aniline concentration of 0.025 mM and 85%-90% COG degradation from 1.0 mM COG. Spiked and non-spiked solutions were analyzed to determine that the presence of aniline (alternative substrate of

the enzyme) diminished the removal efficiency of the azo-dye COG by around 20%, proving the competition of the two substrates. Evidence supporting the azo-cleavage and formation of aniline product was found by ESI-MS in positive mode, where the optimal conditions obtained by HPLC for the formation of aniline were analyzed, detecting a peak which supports the presence of aniline after treatment. Peaks suggesting the presence of hydrolysis products of the corresponding aniline dimers and trimers were also found supporting the azo-cleavage process. On the other hand, a peak was obtained that suggest the presence of a doubly charged COG dimer. With these results, it is suggested that both direct radical polymerization and azo-cleavage pathways occurred for COG with SBP.

A RSM was developed to statistically analyze the relationship among the parameters that affect the percent color remaining, as well as to obtain the optimal response for the lowest concentration remaining ($\leq 5\%$) and compared to an optimization one-parameter-at-a-time as established in objective 3 of this dissertation. For AB113 the optimal response (conditions: pH 4.4, 2.5 mM H₂O₂ and 1.52 U/mL SBP) obtained with the Minitab model was 2.4% above the experimental value (for the Minitab model the response was 5.7% and the experimental was 8.1 ± 0.13). For DB38 the optimal response (conditions: pH 3.68, 2.92 mM H₂O₂ and 2.84 U/mL SBP) obtained was 1.5% above the experimental value (for the Minitab model the response was 3.6% and the experimental was $5.1 \pm 0.13\%$). Thus it was demonstrated that RSM is an effective methodology to statistically determine the optimal response for decoloration of azo-dye and proper experimental validation should be done as presented. Also, it demonstrates that RSM required a smaller number of experiments (49 experimental runs) to be conducted compared to a

conventional optimization of one-parameter-at-a-time (81 experimental runs) if the appropriate range of values for the parameters are chosen, which represents time and cost savings. Also, the RSM equation and contour/surface plots allow exploration of the interactions of parameters and their influence on the response in the area studied.

5.2 Conclusions

A more complete study compared to the literature review (with respect to the parameters measured) was done in order to determine the conditions where a single- or two-step process is preferred, determining important parameters such as total amines, dye, color and product reduction aiming to achieve 95% removal and seeking the treatment with lower concentration of SBP and H₂O₂.

Enzymatic treatment with SBP was proven to effectively decolorize and remove azo-dyes and their possible toxic byproducts from water under optimal conditions. It can be concluded that a two-step process (with Fe⁰ reduction as pretreatment) was determined to be preferable because the products of Fe⁰ reduction, such as aniline and benzidine, were good SBP substrates showing more than 95% removal of the dye and products. On the other hand, a single-step process is preferred for azo-dyes which products after zero-valent iron, such as 3-ABS, were poor enzyme substrates. This conclusion is useful in considering removal of other azo-dyes present in wastewater.

In order to reduce time and cost based on the number of experimental runs, RSM, using Box-Behnken design, was found to be an appropriate and effective statistical technique to optimize the decoloration of azo-dyes. The reduction in the number of experimental runs, almost 50%, is an advantage of RSM when compared to an optimization of one factor at a time, also important statistics parameters were obtained such as contour/surface plots and model equations.

Aniline formation during SBP treatment was determined under different H₂O₂ and SBP conditions for the mono-azo-dye, COG was quantified by HPLC. The confirmation of

azo-splitting was obtained by ESI-MS, showing the presence of products such as aniline, plus the protonated hydrolysis products of aniline dimer and trimer. At the same time, ESI-MS confirmed the existence of a radical polymerization pathway by showing the presence of doubly-charged COG dimer in the reaction mixture.

Chapter 6. Recommendations

1. Toxicity studies after single enzymatic treatment and two-step process using Fe° pre-treatment are recommended to understand the possible impacts of the products from both processes and to determine the environmental impact.
2. Other products after Fe° reduction of both dyes should be determined, analyzed and quantified if they are SBP substrates and to what extent. Due to the lack of standards for the other products they were not measured in this dissertation, however, a model compound with the highest structural similarities to represent the parent compound should be investigated.
3. The azo-cleavage products by enzymatic treatment should be further investigated by identifying and analyzing the products in the solution and precipitate of enzymatic treatment by HPLC-MS and/or MS/MS which might increase the sensitivity for the compounds. A quantitative study should be carried out in order to obtain the mass balance and determine the ratio between the azo-cleavage pathway and the direct phenolic/anilino polymerization pathway. Qualitative evidence for both pathways was obtained with this dissertation.
4. RSM was used for a single-step process measuring the decoloration of the azo-dyes, obtaining a diminish in the number of experimental runs. However, the application of RSM was not studied for the two-step process. The RSM can be used to optimize the two-step process and compare with the optimization one-parameter-at-a-time in order to decrease the number of experimental runs and obtain the mathematical models.
5. For future industrial applications, the matrix effect of real wastewater should be analyzed at each site to optimize the parameters pH, H_2O_2 and enzyme concentrations.
6. The effect of additives can be included in the enzymatic treatment to improve the processes. The literature has reported that the used of additives reduce the enzyme concentration. This would be necessary for future industrial applications.
7. Cost analysis for both processes should be conducted to determine which can be more cost-efficient for industrial applications of the processes.

REFERENCES

- Agrawal, A., and Tratnyek, P. G. (1996). Reduction of nitro aromatic compounds by zero-valent iron metal. *Environmental Science and Technology*, 30(1), 153-160. doi:10.1021/es950211h
- Al-Ansari, M. M., Saha, B., Mazloun, S., Taylor, K. E., Bewtra, J. K., and Biswas, N. (2011). Soybean peroxidase applications in wastewater treatment. *Soybeans: Cultivation, uses and nutrition* (pp. 189-221)
- Ali, L., Algaithi, R., Habib, H. M., Souka, U., Rauf, M. A., and Ashraf, S. S. (2013). Soybean peroxidase-mediated degradation of an azo dye- A detailed mechanistic study. *BMC Biochemistry*, 14(1) doi:10.1186/1471-2091-14-35
- Altahir B., Feng W., Jasim H., Taylor K., Biswas N., Bewtra J., Jassim S. (2015). Soybean peroxidase-catalysed removal of benzidines from water. *Journal of Environmental Engineering and Science*, 10(4), 73-80
- Akceylan, E., and Erdemir, S. (2015). Carcinogenic direct azo-dye removal from aqueous solution by amino-functionalized calix[4]arenes. *Journal of Inclusion Phenomena and Macrocyclic Chemistry*, 82(3), 471-478. doi:10.1007/s10847-015-0518-7
- Ayed, L., Achour, S., Khelifi, E., Cheref, A., and Bakhrouf, A. (2010). Use of active consortia of constructed ternary bacterial cultures via mixture design for congo red decolorization enhancement. *Chemical Engineering Journal*, 162(2), 495-502. doi:10.1016/j.cej.2010.05.050
- Bandala, E. R., Peláez, M. A., García-López, A. J., Salgado, M. d. J., and Moeller, G. (2008). Photocatalytic decolourisation of synthetic and real textile wastewater containing benzidine-based azo dyes. *Chemical Engineering and Processing: Process Intensification*, 47(2), 169-176. doi:10.1016/j.cep.2007.02.010
- Biswas, M. M., Biswas, N., Bewtra, J. K. and Taylor, K. (2004) Removal of reactive azo dyes from water by Fe⁰ reduction followed by peroxidase-catalysed polymerisation. Water Environment Federation 10th Annual Industrial Wastes Technical and Regulatory Conference.
- Bollag, J. M., Sjoblad, R. D., and Liu, S. Y. (1979). Characterization of an enzyme from rhizoctonia praticola which polymerizes phenolic compounds. *Canadian Journal of Microbiology*, 25(2), 229-233. Doi: 10.1139/m79-035
- Buzzell R.I. and Buttery B.R. (1969) Inheritance of peroxidase activity in soybean seed coats. *Crop Science* 9(3), 387-388.

Buzzell R.I. and Buttery B.R. (1968) Peroxidase activity in seeds of soybean varieties. *Crop Science* 8(6),722–725.

Cao, J., Wei, L., Huang, Q., Wang, L., and Han, S. (1999). Reducing degradation of azo dye by zero-valent iron in aqueous solution. *Chemosphere*, 38(3), 565-571. doi:10.1016/S0045-6535(98)00201-X

Carmen, Z., and Daniela, S. (2012). Textile organic dyes—characteristics, polluting effects and separation/elimination procedures from industrial effluents—a critical overview. In *Organic Pollutants Ten Years After the Stockholm Convention-Environmental and Analytical Update* (pp. 55-81). InTech: Croatia.

Caza, N., Bewtra, J. K., Biswas, N., and Taylor, K. E. (1999). Removal of phenolic compounds from synthetic wastewater using soybean peroxidase. *Water Research*, 33(13), 3012-3018. doi:10.1016/S0043-1354(98)00525-9

Crini, G. (2006). Non-conventional low-cost adsorbents for dye removal: A review. *Bioresource Technology*, 97(9), 1061-1085. doi:10.1016/j.biortech.2005.05.001

Cooper P. (1995). *Color in dyehouse effluent*. West Yorkshire, England: Society of Dyers and Colourists. Alden Press, Oxford

Chequer, F. M., de Oliveira, D. P., Ferraz, E. R., de Oliveira, G. A. R., Cardoso, J. C., and Zanoni, M. V. (2013). *Textile dyes: dyeing process and environmental impact* (pp. 151-176). INTECH Open Access Publisher.

Chiong, T., Lau, S. Y., Lek, Z. H., Koh, B. Y., & Danquah, M. K. (2016). Enzymatic treatment of methyl orange dye in synthetic wastewater by plant-based peroxidase enzymes. *Journal of Environmental Chemical Engineering*, 4(2), 2500-2509. doi:10.1016/j.jece.2016.04.030

Chuang, F., Larson, R. A., and Wessman, M. S. (1995). Zero-valent iron-promoted dechlorination of polychlorinated biphenyls. *Environmental Science and Technology*, 29(14), 2460-2463. Doi: 10.1021/es00009a044

Cuesta, C. A. (2009). *Metodología de Superficies de Respuesta, gran alternativa para incrementar la productividad de sus procesos*. Cali, Colombia: Centro de Ingeniería de la Calidad.

Daâssi, D., Frikha, F., Zouari-Mechichi, H., Belbahri, L., Woodward, S., and Mechichi, T. (2012). Application of response surface methodology to optimize decolourization of dyes by the laccase-mediator system. *Journal of Environmental Management*, 108, 84-91. doi:10.1016/j.jenvman.2012.04.039

Dai, R., Chen, X., Luo, Y., Ma, P., Ni, S., Xiang, X., & Li, G. (2016). Inhibitory effect and mechanism of azo dyes on anaerobic methanogenic wastewater treatment: Can redox mediator remediate the inhibition? *Water Research*, 104, 408-417. doi:10.1016/j.watres.2016.08.046

Dunford, H.B. (1999) *Heme Peroxidases*. New York: John Wiley and Sons

Dunford, H. B., and Stillman, J. S. (1976). On the function and mechanism of action of peroxidases. *Coordination Chemistry Reviews*, 19(3), 187-251.

Durruty, I., Fasce, D., González, J. F., & Wolski, E. A. (2015). A kinetic study of textile dyeing wastewater degradation by penicillium chrysogenum. *Bioprocess and Biosystems Engineering*, 38(6), 1019-1031. doi:10.1007/s00449-014-1344-9

ECHA.European Chemical Agency . (2009): *Screening Assessment for the Challenge – 2,7-Naphthalenedisulfonic acid, 4-amino-3-[[4'-[(2,4-diaminophenyl)azo]][1,1'-biphenyl]-4-yl]azo]-5-hydroxy-6-(phenylazo)-, disodium salt (Direct Black 38)*. Retrieved from : <https://echa.europa.eu/>

Elisangela, F., Andrea, Z., Fabio, D. G., de Menezes Cristiano, R., Regina, D. L., and Artur, C. (2009). Biodegradation of textile azo dyes by a facultative staphylococcus arlettae strain VN-11 using a sequential microaerophilic/aerobic process. *International Biodeterioration and Biodegradation*, 63(3), 280-288. doi:10.1016/j.ibiod.2008.10.003

Fan, J., Guo, Y., Wang, J., and Fan, M. (2009). Rapid decolorization of azo dye methyl orange in aqueous solution by nanoscale zerovalent iron particles. *Journal of Hazardous Materials*, 166(2-3), 904-910. doi:10.1016/j.jhazmat.2008.11.091

Feng, W., Nansheng, D., and Helin, H. (2000). Degradation mechanism of azo dye C. I. reactive red 2 by iron powder reduction and photooxidation in aqueous solutions. *Chemosphere*, 41(8), 1233-1238. doi:10.1016/S0045-6535(99)00538-X

Feng, W., Taylor, K. E., Biswas, N., and Bewtra, J. K. (2013). Soybean peroxidase trapped in product precipitate during phenol polymerization retains activity and may be

recycled. *Journal of Chemical Technology and Biotechnology*, 88(8), 1429-1435.
doi:10.1002/jctb.4075

Fersht, A. (1977) *Enzyme Structure and Mechanism. 2nd edition*. San Francisco: W H Freeman and Co.

Ganesh, R., Boardman, G. D., and Michelsen, D. (1994). Fate of azo dyes in sludges. *Water Research*, 28(6), 1367-1376.

Garg, S. K., Tripathi, M., and Lal, N. (2015). Response surface methodology for optimization of process variable for reactive orange 4 dye discoloration by *Pseudomonas putida* SKG-1 strain and bioreactor trial for its possible use in large-scale bioremediation. *Desalination and Water Treatment*, 54(11), 3122-3133.
doi:10.1080/19443994.2014.905975

Garrigós, M. C., Reche, F., Marín, M. L., and Jiménez, A. (2002). Determination of aromatic amines formed from azo colorants in toy products. *Journal of Chromatography A*, 976(1-2), 309-317. doi:10.1016/S0021-9673(02)01162-7

Geng, Z., Rao, K. J., Bassi, A. S., Gijzen, M., and Krishnamoorthy, N. (2001). Investigation of biocatalytic properties of soybean seed hull peroxidase. *Catalysis today*, 64(3), 233-238. ISSN: 0920-5861

Ghaemmaghami, F., Alemzadeh, I., and Motamed, S. (2010). Seed coat soybean peroxidase: Extraction and biocatalytic properties determination. *Iranian Journal of Chemical Engineering*, 7(2), 28-38

Gholami-Borujeni, F., Faramarzi, M. A., Nejatizadeh-Barandozi, F., & Mahvi, A. H. (2013). Oxidative degradation and detoxification of textile azo dye by horseradish peroxidase enzyme. *Fresenius Environmental Bulletin*, 22, 739-744.

Gijzen, M., Huystee, R. Van and Buzzell, R. (1993) Soybean seed coat peroxidase. *Plant Physiology*, 103, 1061–1066.

Gijzen, M. (1997). A deletion mutation at the ep locus causes low seed coat peroxidase activity in soybean. *Plant Journal*, 12(5), 991-998. Doi: 10.1046/j.1365-313X.1997.12050991.x

Gijzen, M., van Huystee, R., and Buzzell, R. I. (1993). Soybean seed coat peroxidase (a comparison of high-activity and low-activity genotypes). *Plant physiology*, 103(4), 1061-1066.

- Gillham, R. W., and O'Hannesin, S. F. (1994). Enhanced degradation of halogenated aliphatics by Zero-Valent iron. *Groundwater*, 32(6), 958-967. doi:10.1111/j.1745-6584.1994.tb00935.x
- Gimenez, G. G., Ruiz, S. P., Caetano, W., Peralta, R. M., and Matioli, G. (2014). Biosorption potential of synthetic dyes by heat-inactivated and live lentinus edodes CCB-42 immobilized in loofa sponges. *World Journal of Microbiology and Biotechnology*, 30(12), 3229-3244. doi:10.1007/s11274-014-1750-9
- Golka, K., Kopps, S., and Myslak, Z. W. (2004). Carcinogenicity of azo colorants: influence of solubility and bioavailability. *Toxicology letters*, 151(1), 203-210
- Gooding, J. J., Compton, R. G., Brennan, C. M., & Atherton, J. H. (1996). The mechanism of the electro-reduction of some azo dyes. *Electroanalysis*, 8(6), 519-523.
- Gomori G., (1955) Preparation of buffers for use in enzyme studies. *Methods in Enzymology* (1), New York. Academic Press
- Gregory, P. (1990) *The classification of dyes by chemical structure. In The Chemistry and Application of Dyes*. New York: Plenum Publishing
- Gupta, V. K., Gupta, B., Rastogi, A., Agarwal, S., and Nayak, A. (2011). A comparative investigation on adsorption performances of mesoporous activated carbon prepared from waste rubber tire and activated carbon for a hazardous azo dye-acid blue 113. *Journal of Hazardous Materials*, 186(1), 891-901. doi:10.1016/j.jhazmat.2010.11.091
- Gutiérrez H., and De la Vara Salazar R., (2008) *Análisis y diseño de experimentos*. México. Mc Graw Hill.
- Hailu, G., Weersink, A., and Cahlik, F. (2010). Examining the prospects for commercialization of soybean peroxidase. *AgBioForum*, 13(3), 263-273.
- Hartman, G. L., West, E. D., and Herman, T. K. (2011). Crops that feed the world 2. soybean-worldwide production, use, and constraints caused by pathogens and pests. *Food Security*, 3(1), 5-17. doi:10.1007/s12571-010-0108-x
- Health Canada (2013) Environmental and Workplace Health. Available at: <http://www.hc-sc.gc.ca/ewh-semt/pubs/contaminants/psl1-lsp1/aniline/index-eng.php>
- Henriksen, A., Mirza, O., Indiani, C., Teilum, K., Smulevich, G., Welinder, K. G., and Gajhede, M. (2001). Structure of soybean seed coat peroxidase: A plant peroxidase with unusual stability and haem-apoprotein interactions. *Protein Science*, 10(1), 108-115.

Husain, Q. (2006). Potential applications of the oxidoreductive enzymes in the decolorization and detoxification of textile and other synthetic dyes from polluted water: A review. *Critical Reviews in Biotechnology*, 26(4), 201-221. doi:10.1080/07388550600969936

Husain, Q. (2010). Peroxidase mediated decolorization and remediation of wastewater containing industrial dyes: A review. *Reviews in Environmental Science and Biotechnology*, 9(2), 117-140. doi:10.1007/s11157-009-9184-9

Ibrahim, M. S., Ali, H. I., Taylor, K. E., Biswas, N., and Bewtra, J. K. (2001). Enzyme-catalyzed removal of phenol from refinery wastewater: Feasibility studies. *Water Environment Research*, 73(2), 165-172. Retrieved from <http://www.jstor.org/stable/25045478>

International Agency for Research on Cancer. (2010). *Some aromatic amines, organic dyes, and related exposures* (Vol. 99). IARC Press, International Agency for Research on Cancer.

International Agency for Research on Cancer (2012) *Chemical agents and related occupations. A review of human carcinogens*. (100F). IARC Press, International Agency for Research on Cancer

Davidson W.A.B. (2013, December) Textile industry. Retrieved from: <http://www.thecanadianencyclopedia.ca/en/article/textile-industry/>

Jadhav, S.B., Surwase S.N., Phugare S.S., Jadhav J.P. (2012). Response surface methodology mediated optimization of Remazol Orange decolorization in plain distilled water by *Pseudomonas aeruginosa* BCH. *International Journal of Environmental Science and Technology*, 10(1), 181–190. doi:10.1007/s13762-012-0088-9

Junyapoon, S. (2005). Use of zero-valent iron for wastewater treatment. *Science Technology*, 5(3), 587-595.

Kalsoom, U., Ashraf, S. S., Meetani, M. A., Rauf, M. A., and Bhatti, H. N. (2013). Mechanistic study of a diazo dye degradation by soybean peroxidase. *Chemistry Central Journal*, 7(1) doi:10.1186/1752-153X-7-93

Karam, J., and Nicell, J. A. (1997). Potential applications of enzymes in waste treatment. *Journal of Chemical Technology and Biotechnology*, 69(2), 141-153.

Karthikeyan, K., Nanthakumar, K., Shanthi, K., & Lakshmanaperumalsamy, P. (2010). Response surface methodology for optimization of culture conditions for dye decolorization by a fungus, *aspergillus niger* hm11 isolated from dye affected soil. *Iranian Journal of Microbiology*, 2(4), 214-223. Retrieved from www.scopus.com

Kertesz, V., & Van Berkel, G. J. (2002). Surface-assisted reduction of aniline oligomers, N-phenyl-1,4-phenylenediimine and thionin in atmospheric pressure chemical ionization and atmospheric pressure photoionization. *Journal of the American Society for Mass Spectrometry*, 13(2), 109-117. doi:10.1016/S1044-0305(01)00337-3

Kirby, N., Marchant, R., and McMullan, G. (2000). Decolourisation of synthetic textile dyes by *phlebia tremellosa*. *FEMS Microbiology Letters*, 188(1), 93-96. doi:10.1016/S0378-1097(00)00216-0

Klibanov, A. M., and Morris, E. D. (1981). Horseradish peroxidase for the removal of carcinogenic aromatic amines from water. *Enzyme and Microbial Technology*, 3(2), 119-122. doi:10.1016/0141-0229(81)90069-7

Klibanov, A. M. (1983). Approaches to enzyme stabilization. *Biochemical Society Transactions*, 11(1), 19-20. Doi: 10.1042/bst0110019

Kulshrestha, Y., and Husain, Q. (2007). Decolorization and degradation of acid dyes mediated by salt fractionated turnip (*Brassica rapa*) peroxidases. *Toxicological and Environmental Chemistry*, 89(2), 255-267

Lade, H., Govindwar, S., & Paul, D. (2015). Mineralization and detoxification of the carcinogenic azo dye congo red and real textile effluent by a polyurethane foam immobilized microbial consortium in an upflow column bioreactor. *International Journal of Environmental Research and Public Health*, 12(6), 6894-6918. doi:10.3390/ijerph120606894

Larson, R. A., and Weber, E. J. (1994). *Reaction mechanisms in environmental organic chemistry*. USA, CRC press.

Li, W., Zhang, Y., Zhao, J., Yang, Y., Zeng, R. J., Liu, H., and Feng, Y. (2013). Synergetic decolorization of reactive blue 13 by zero-valent iron and anaerobic sludge. *Bioresource Technology*, 149, 38-43. doi:10.1016/j.biortech.2013.09.041

Lokesh, K. N., and Sivakiran, R. R. (2014). Biological methods of dye removal from textile effluents-A review. *Journal of Biochemical Technology*, 3(5), 177-180

López, C., Valade, A. -, Combourieu, B., Mielgo, I., Bouchon, B., & Lema, J. M. (2004). Mechanism of enzymatic degradation of the azo dye orange II determined by ex situ ¹H nuclear magnetic resonance and electrospray ionization-ion trap mass spectrometry. *Analytical Biochemistry*, 335(1), 135-149. doi:10.1016/j.ab.2004.08.037

Maguire, R. J. (1992). Occurrence and persistence of dyes in a canadian river. *Water Science and Technology*, 26(12), 265-270. Retrieved from www.scopus.com

Mantha, R., Biswas, N., Taylor, K. E., and Bewtra, J. K. (2002). Removal of nitroaromatics from synthetic wastewater using two-step zero-valent iron reduction and peroxidase-catalyzed oxidative polymerization. *Water Environment Research*, 74(3), 280-287. Doi: 10.2175/106143002X140017

Marechal, A. M. -, Slokar, Y. M., and Taufer, T. (1997). Decoloration of chlorotriazine reactive azo dyes with H₂O₂/UV. *Dyes and Pigments*, 33(4), 281-298. Doi: 10.1016/s0143-7208(96)00057-5

Matto, M., & Husain, Q. (2007). Decolorization of direct dyes by salt fractionated turnip proteins enhanced in the presence of hydrogen peroxide and redox mediators. *Chemosphere*, 69(2), 338-345. doi:10.1016/j.chemosphere.2007.03.069

Mazloun, S. (2014). Soybean Peroxidase Catalysis in Removal of Anilines and Azo-Dyes from Water. 7Doctoral dissertation), retrieved from: University of Windsor

Melgoza, A. M., Cruz, A., & Buitrón, G. (2004). Anaerobic/aerobic treatment of colorants present in textile effluents. *Water Science Technology*, 50(2),149-155.

Michniewicz, A., Ledakowicz, S., Ullrich, R., & Hofrichter, M. (2008). Kinetics of the enzymatic decolorization of textile dyes by laccase from cerrena unicolor. *Dyes and Pigments*, 77(2), 295-302. doi:10.1016/j.dyepig.2007.05.015

Minitab 17 support (a). Contour plots and 3D surface plots. Retrieved from: <http://support.minitab.com/en-us/minitab/17/topic-library/modeling-statistics/using-fitted-models/graphs/contour-plots-and-3d-surface-plots>

Minitab 17 support (b). Nonlinear regression. Retrieved from: <http://support.minitab.com/en-us/minitab/17/topic-library/modeling-statistics/regression-and-correlation/basics/nonlinear-regression/>

Minitab 17 support (c) (2016). What is a response surface design? Retrieved from: <http://support.minitab.com/en-us/minitab/17/topic-library/modeling-statistics/doe/response-surface-designs/what-is-a-response-surface-design/>

Minitab 17 support (d) (2016). What is the response optimization? Retrieved from: <http://support.minitab.com/en-us/minitab/17/topic-library/modeling-statistics/using-fitted-models/response-optimization/what-is-response-optimization/>

Mohan, S. V., Rao, N. C., Prasad, K. K., and Karthikeyan, J. (2003). Erratum: Treatment simulated reactive yellow 22 (azo) dye effluents using spirogyra species (waste management (2002) 22:6 (575-582) PII: S0956053X02000302). *Waste Management*, 23(2), 195. doi:10.1016/S0956-053X(03)00017-5

Montgomery, C. and Runger G., (2010). *Probabilidad y estadística aplicadas a la Ingeniería*. México: Limusa Wiley.

Myers R., Montgomery D., Anderson-Cook C., 2016. *Response surface methodology*. USA. Wiley

Nakamoto, S., and Machida, N. (1992). Phenol removal from aqueous solutions by peroxidase-catalyzed reaction using additives. *Water Research*, 26(1), 49-54. doi:10.1016/0043-1354(92)90110-P

Nam, S. (1998). Azo dye transformation by enzymatic and chemical systems. (Doctoral dissertation). Retrieved from: OHSU Digital commons

Nam, S., and Tratnyek, P. G. (2000). Reduction of azo dyes with zero-valent iron. *Water Research*, 34(6), 1837-1845. doi:10.1016/S0043-1354(99)00331-0

Natrella, M. (2010). NIST/SEMATECH e-handbook of statistical methods. (E-Reader Version). Retrieved from : <http://www.itl.nist.gov/div898/handbook/index.htm>

- Neifar, M., Jaouani, A., Kamoun, A., Ellouze-Ghorbel, R., and Ellouze-Chaabouni, S. (2011). Decolorization of solophenyl red 3BL polyazo dye by laccase-mediator system: Optimization through response surface methodology. *Enzyme Research*, 2011(1) doi:10.4061/2011/179050
- Nicell, J. A. (2003). Enzymatic treatment of waters and wastes. In *Chemical Degradation Methods for Wastes and Pollutants: Environmental and Industrial Applications*. CRC Press.
- Nicell J.A., Al-Kassim, L., Bewtra, J. K., and Taylor, K. E. (1993, March). Wastewater treatment by enzyme catalysed polymerization and precipitation. In *Biodeterioration Abstracts*, 7 (1), 1-8
- Onder, S., Celebi, M., Altikatoglu, M., Hatipoglu, A., & Kuzu, H. (2011). Decolorization of naphthol blue black using the horseradish peroxidase. *Applied Biochemistry and Biotechnology*, 163(3), 433-443. doi:10.1007/s12010-010-9051-8
- Oren A, Gurevich P, Henis Y. (1991) Reduction of nitrosubstituted aromatic compounds by the halophilic anaerobic eubacteria *Haloanaerobium praevalens* and *Sporohalobacter marismortui*. *Applied and Environmental Microbiology*, 57(11), 3367–3370
- Orth, W. S., and Gillham, R. W. (1995). Dechlorination of trichloroethene in aqueous solution using Fe⁰. *Environmental Science and Technology*, 30(1), 66-71.
- Pandey, A., Singh, P., and Iyengar, L. (2007). Bacterial decolorization and degradation of azo dyes. *International Biodeterioration and Biodegradation*, 59(2), 73-84. doi:10.1016/j.ibiod.2006.08.006
- Papadopoulou, K., Kalagona, I. M., Philippoussis, A., and Rigas, F. (2013). Optimization of fungal decolorization of azo and anthraquinone dyes via Box-Behnken design. *International Biodeterioration and Biodegradation*, 77, 31-38. doi:10.1016/j.ibiod.2012.10.008
- Patapas, J., Al-Ansari, M. M., Taylor, K. E., Bewtra, J. K., and Biswas, N. (2007). Removal of dinitrotoluenes from water via reduction with iron and peroxidase-catalyzed oxidative polymerization: A comparison between arthromyces ramosus peroxidase and soybeanperoxidase. *Chemosphere*, 67(8), 1485-1491.

Pereira, W. S., and Freire, R. S. (2006). Azo dye degradation by recycled waste zero-valent iron powder. *Journal of the Brazilian Chemical Society*, 17(5), 832-838. Retrieved from <http://dx.doi.org/10.1590/S0103-50532006000500003>

Puvaneswari, N., Muthukrishnan, J., and Gunasekaran, P. (2006). Toxicity assessment and microbial degradation of azo dyes. *Indian Journal of Experimental Biology*, 44(8), 618-626. Retrieved from www.scopus.com

Qiu, M., Shou, J., Ren, P., and Jiang, K. (2014). A comparative study of the azo dye reactive black 5 degradation by UV/TiO₂ and photo-fenton processes. *Journal of Chemical and Pharmaceutical Research*, 6(7), 2046-2051. ISSN : 0975-7384

Reardon, E. J. (1995). Anaerobic corrosion of granular iron: Measurement and interpretation of hydrogen evolution rates. *Environmental Science and Technology*, 29(12), 2936-2945. Doi: 10.1021/es00012a008

Rodriguez, E., Pickard, M. A., & Vazquez-Duhalt, R. (1999). Industrial dye decolorization by laccases from ligninolytic fungi. *Current microbiology*, 38(1), 27-32.

Roriz, M. S., Osma, J. F., Teixeira, J. A., and Rodríguez Couto, S. (2009). Application of response surface methodological approach to optimise reactive black 5 decolouration by crude laccase from *trametes pubescens*. *Journal of Hazardous Materials*, 169(1-3), 691-696. doi:10.1016/j.jhazmat.2009.03.150

Sadhanandam, P., Anumary, A., Ashokkumar, M., & Thanikaivelan, P. (2013). Probing horseradish peroxidase catalyzed degradation of azo dye from tannery wastewater. *SpringerPlus*, 2(1) doi:10.1186/2193-1801-2-341

Senthilkumar, S., Prabhu, H. J., and Perumalsamy, M. (2013). Response surface optimization for biodegradation of textile azo dyes using isolated bacterial strain *Pseudomonas sp.* *Arabian Journal for Science and Engineering*, 38(9), 2279-2291. doi:10.1007/s13369-012-0507-8

Senthilvelan, T., Kanagaraj, J., and Panda, R. C. (2014). Enzyme-mediated bacterial biodegradation of an azo dye (C.I. acid blue 113): Reuse of treated dye wastewater in post-tanning operations. *Applied Biochemistry and Biotechnology*, doi:10.1007/s12010-014-1158-x

Sessa, D. J. (2004). Processing of soybean hulls to enhance the distribution and extraction of value-added proteins. *Journal of the Science of Food and Agriculture*, 84(1), 75-82.

Steevensz, A., Cordova Villegas, L. G., Feng, W., Taylor, K. E., Bewtra, J. K., and Biswas, N. (2014). Soybean peroxidase for industrial wastewater treatment: a mini review. *Environmental Engineering Science*, 9(3), 181-186.

Silva, M. C., Corrêa, A. D., Amorim, M. T. S. P., Parpot, P., Torres, J. A., and Chagas, P. M. B. (2012). Decolorization of the phthalocyanine dye reactive blue 21 by turnip peroxidase and assessment of its oxidation products. *Journal of Molecular Catalysis B: Enzymatic*, 77, 9-14. doi:10.1016/j.molcatb.2011.12.006

Singh, A., Srivastava, A., Tripathi, A., and Dutt, N. N. (2016). Optimization of Brilliant Green Dye Removal Efficiency by Electrocoagulation Using Response Surface Methodology. *World Journal of Environmental Engineering*, 4(2), 23-29. doi: 10.12691/wjee-4-2-1

Sharma, P., Singh, L., & Dilbaghi, N. (2009). Optimization of process variables for decolorization of disperse yellow 211 by bacillus subtilis using box-behnken design. *Journal of Hazardous Materials* 164 (2-3), 1024-1029. Doi: 10.1016/j.hazmat.2008.08.104

Solís, M., Solís, A., Pérez, H. I., Manjarrez, N., and Flores, M. (2012). Microbial decolouration of azo dyes: A review. *Process Biochemistry*, 47(12), 1723-1748. doi:10.1016/j.procbio.2012.08.014

Spiess, A. N., and Neumeier, N. (2010). An evaluation of R^2 as an inadequate measure for nonlinear models in pharmacological and biochemical research: a Monte Carlo approach. *BMC pharmacology*, 10(1), 6.

Steevensz, A., Cordova Villegas, L. G., Feng, W., Taylor, K. E., Bewtra, J. K., & Biswas, N. (2014). Soybean peroxidase for industrial wastewater treatment: a mini review. *Environmental Engineering Science*, 9(3), 181-186.

Sudha, M., Saranya, A., Selvakumar, G., & Sivakumar, N. (2014). Microbial degradation of azo dyes: a review. *International Journal of Current Microbiology and Applied Sciences*, 3(2), 670-690.

Tizaoui, C., and Grima, N. (2011). Kinetics of the ozone oxidation of reactive orange 16 azo-dye in aqueous solution. *Chemical Engineering Journal*, 173(2), 463-473. doi:10.1016/j.cej.2011.08.014

Ulson de Souza, S. M. A. G., Forgiarini, E., and Ulson de Souza, A. A. (2007). Toxicity of textile dyes and their degradation by the enzyme horseradish peroxidase (HRP). *Journal of Hazardous Materials*, 147(3), 1073-1078. doi:10.1016/j.jhazmat.2007.06.003

United States Environmental Protection Agency. (2005) *Waste from the Production Of Dyes and Pigments Listed as Hazardous. National Service Center for Environmental Publications (NSCEP)*. Retrieved from US EPA website : <https://nepis.epa.gov>

United States Environmental Protection Agency. (2015). *Dyes Derived from Benzidine and Its Congeners*. Retrieved from US EPA website: https://www.epa.gov/sites/production/files/2015-09/documents/dcb_action_plan_06232010.noheader.pdf

United States Environmental Protection Agency. (1980,June). *Preliminary Risk Assessment: Phase I. Benzidine, its congeners, and their derivative dyes and pigments. EPA-560/11-80-019*. Retrieved from US EPA website : <https://nepis.epa.gov>

United States Environmental Protection Agency. (2002) *Aniline; CASRN 62-53-3*. Retrieved from: https://cfpub.epa.gov/ncea/iris/iris_documents/documents/subst/0350_summary.pdf

United States Environmental Protection Agency (1997). *Profile of the Textile Industry: Sector Notebook*. Retrieved from US EPA website: <https://nepis.epa.gov>

USDA (2017), United States Department of Agriculture Foreign Agricultural Service. Retrieved from: <https://apps.fas.usda.gov/psdonline/app/index.html#/app/compositeViz>

Ventura-camargo, B.D.C. and Marin-morales, M.A., 2013. Azo Dyes : Characterization and Toxicity – A Review, *Textiles and Light Industrial Science and Technology*. 2(2), 85–103.

Weber, E. J. (1996). Iron-mediated reductive transformations: Investigation of reaction mechanism. *Environmental Science and Technology*, 30(2), 716-719. doi:10.1021/es9505210

Weisburger, J. H. (2002). Comments on the history and importance of aromatic and heterocyclic amines in public health. *Mutation Research - Fundamental and Molecular Mechanisms of Mutagenesis*, , 9 (20), 506-507. doi:10.1016/S0027-5107(02)00147-1

Zhang, Q., Jing, Y. H., Shiue, A., Chang, C., Chen, B., and Hsueh, C. (2012). Deciphering effects of chemical structure on azo dye decolorization/degradation characteristics: Bacterial vs. photocatalytic method. *Journal of the Taiwan Institute of Chemical Engineers*, 43(5), 760-766. doi:10.1016/j.jtice.2012.03.001

Zollinger, H. (2003). *Color chemistry: syntheses, properties, and applications of organic dyes and pigments*. Switzerland. John Wiley & Sons.

APPENDIX A. CALIBRATION CURVES

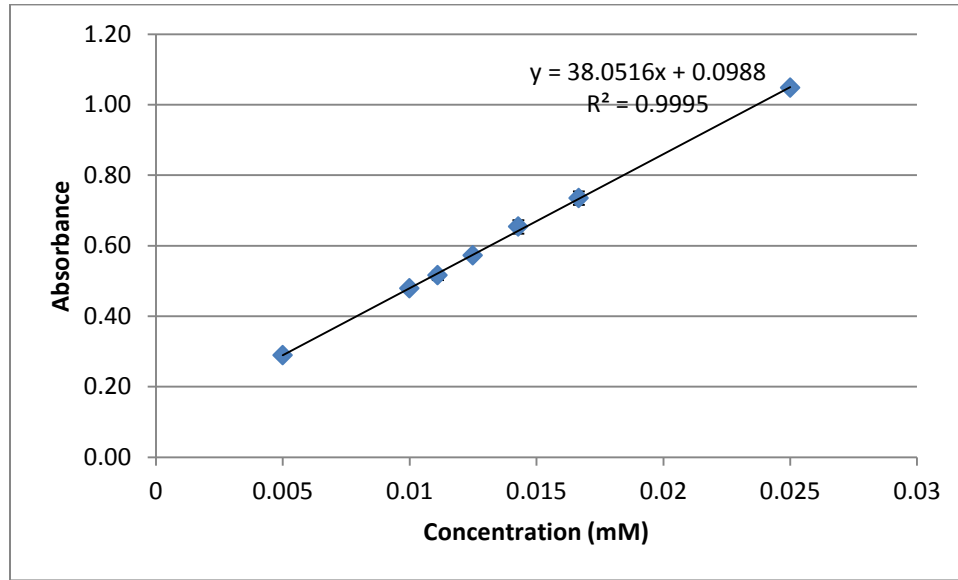


Figure A. 1 Calibration curve for AB113 at 565 nm (spectroscopy)

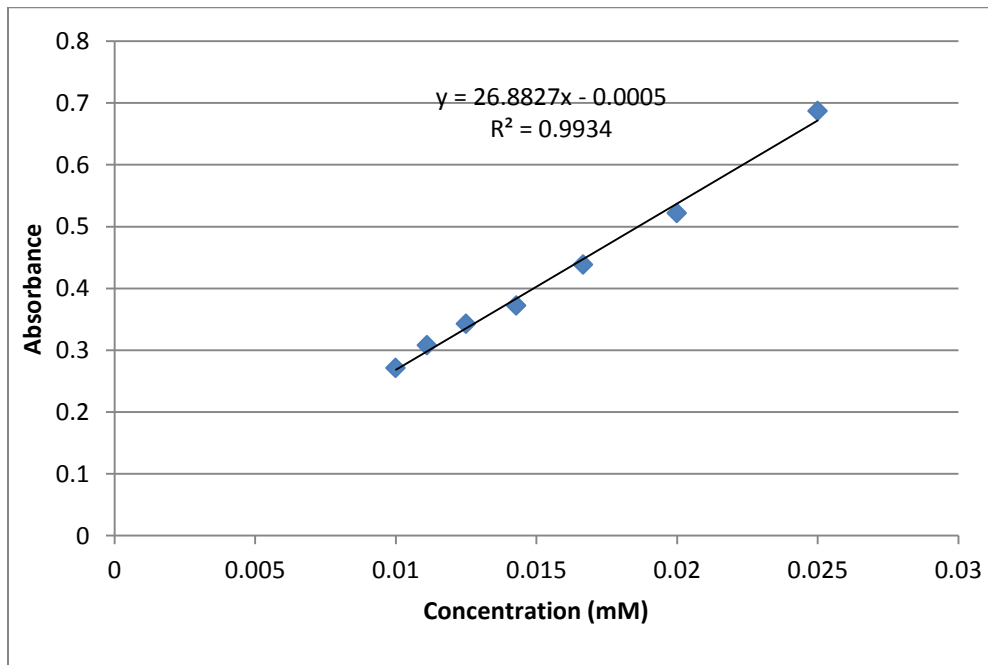


Figure A. 2 Calibration curve for AB11 at 536nm, pH 3.6 (spectroscopy)

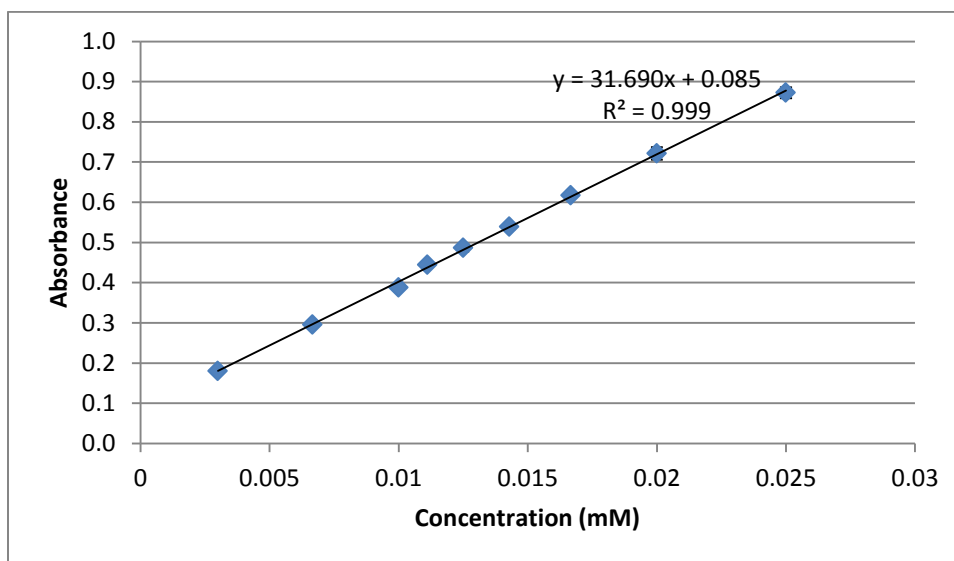


Figure A. 3 Calibration curve for DB38 at 520 nm (spectroscopy)

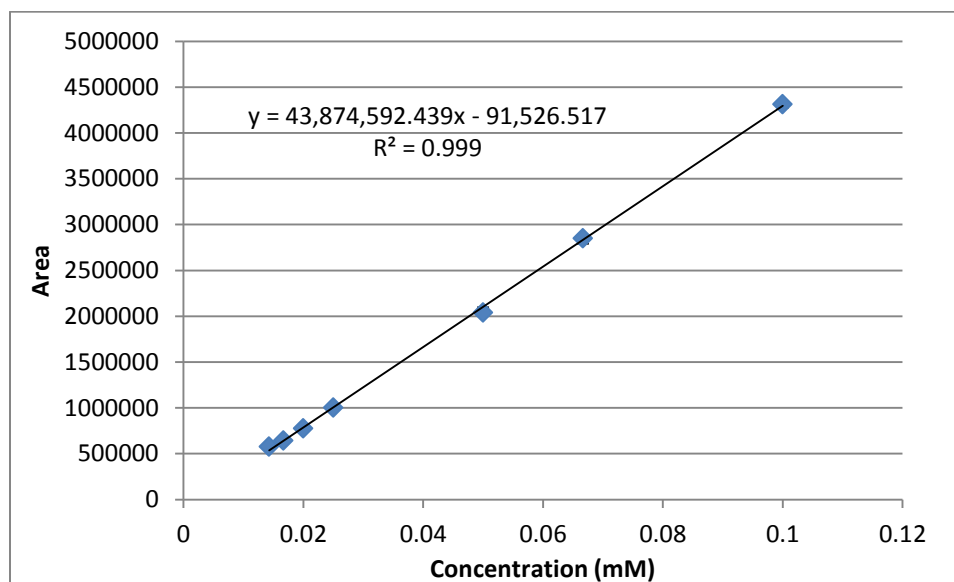


Figure A. 4 Calibration curve AB113 at 565 nm (HPLC)

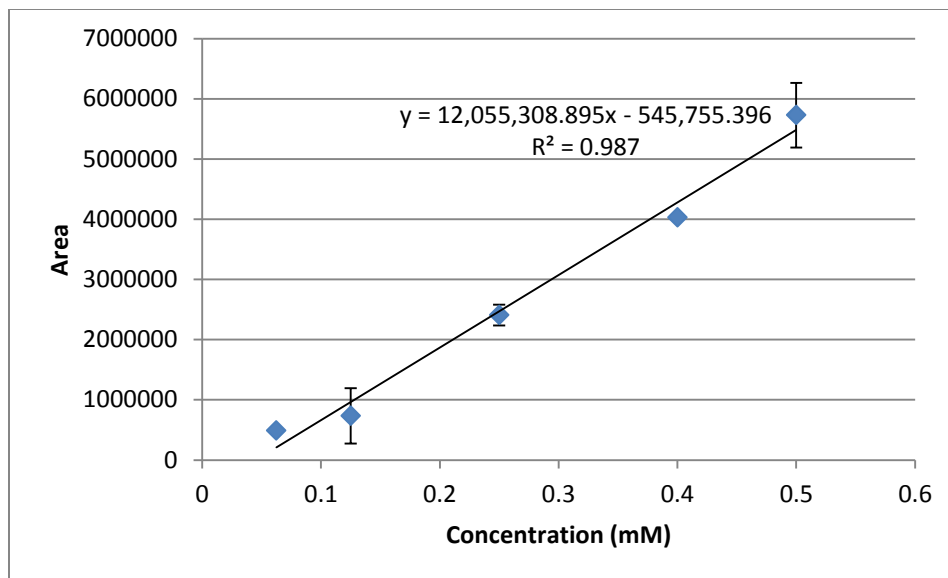


Figure A. 5 Calibration curve DB38 at 520nm (HPLC)

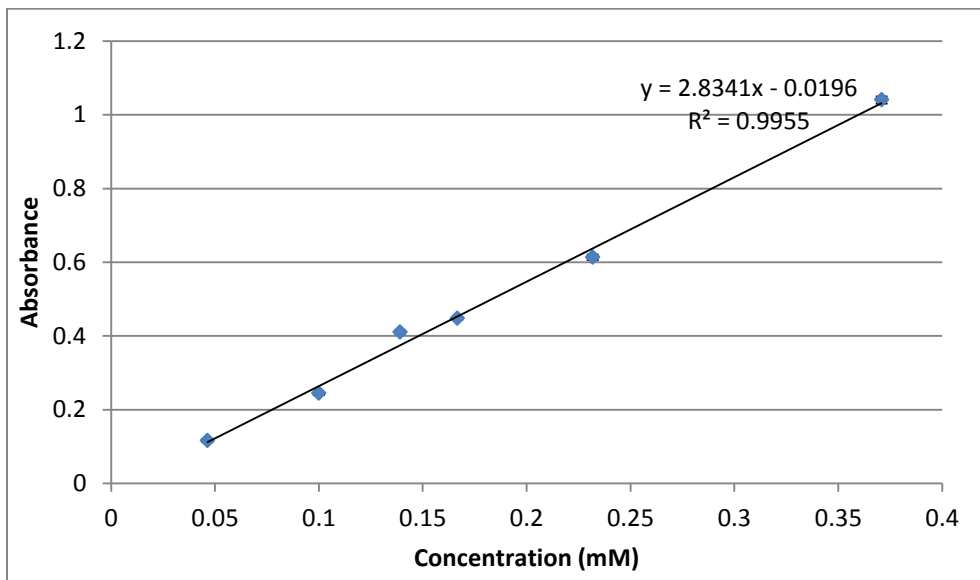


Figure A. 6 Calibration curve for total amine test as aniline at 440nm

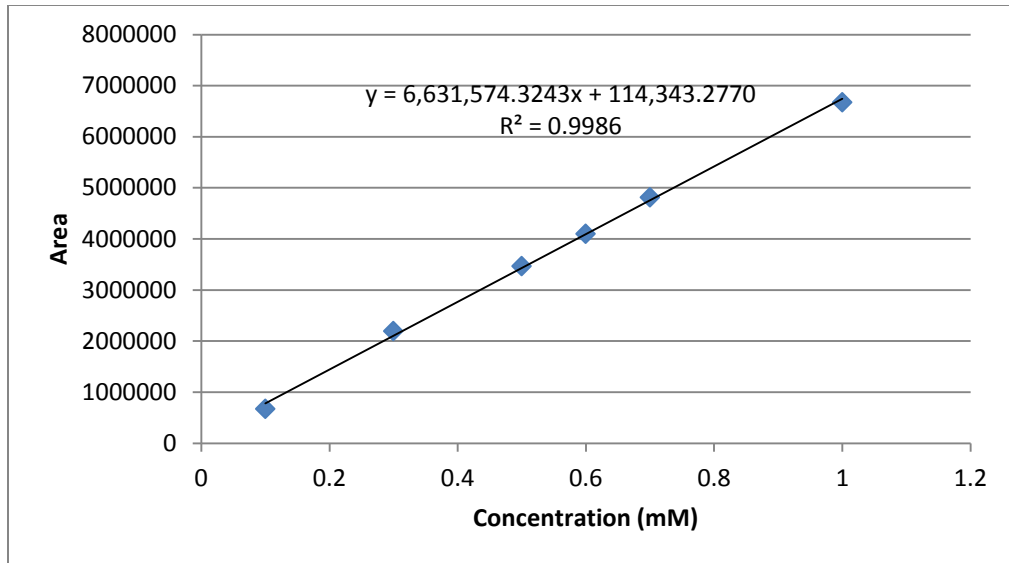


Figure A. 7 Calibration curve for 3-ABS at 235nm (spectroscopy)

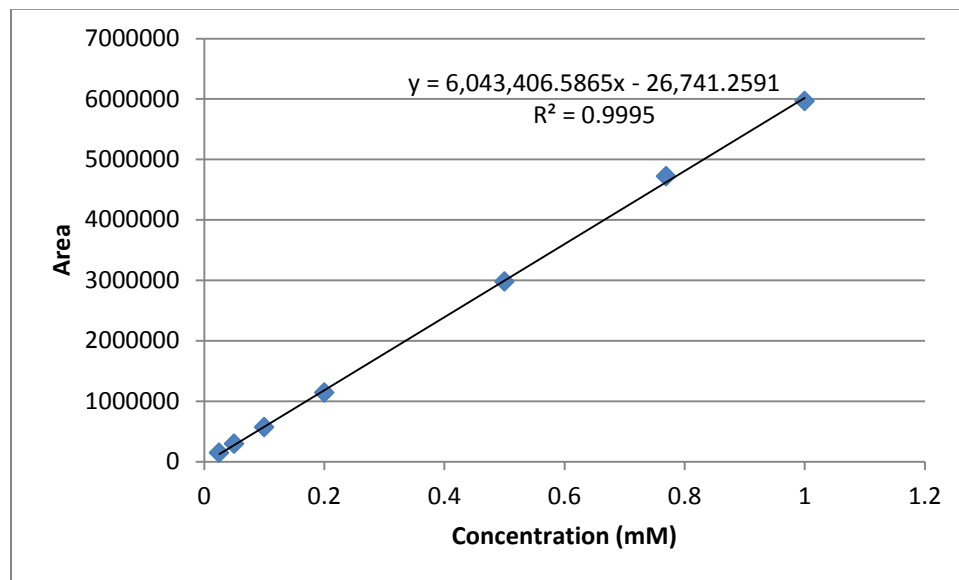


Figure A. 8 Calibration curve 3-ABS at 235nm (HPLC)

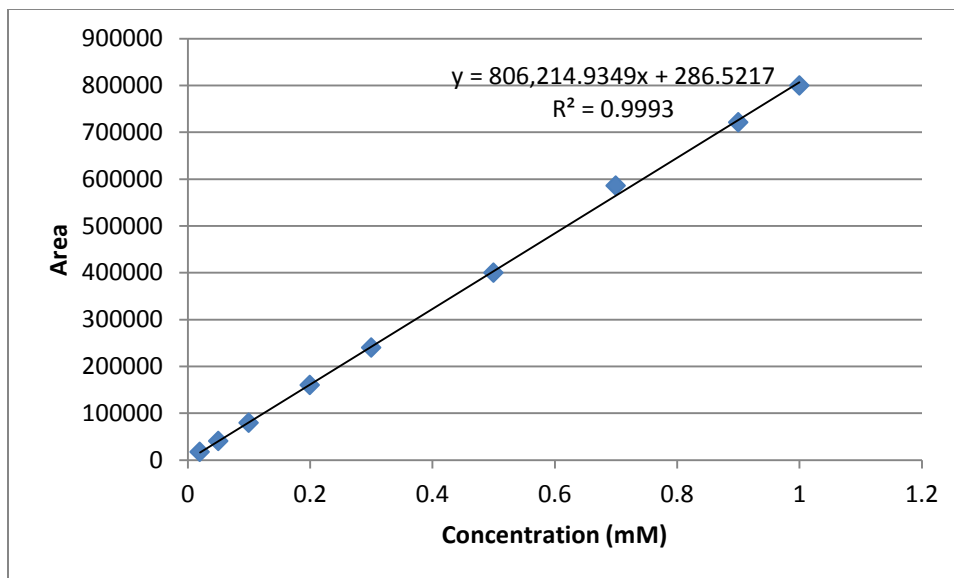


Figure A. 9 Aniline calibration curve at 280 nm (HPLC)

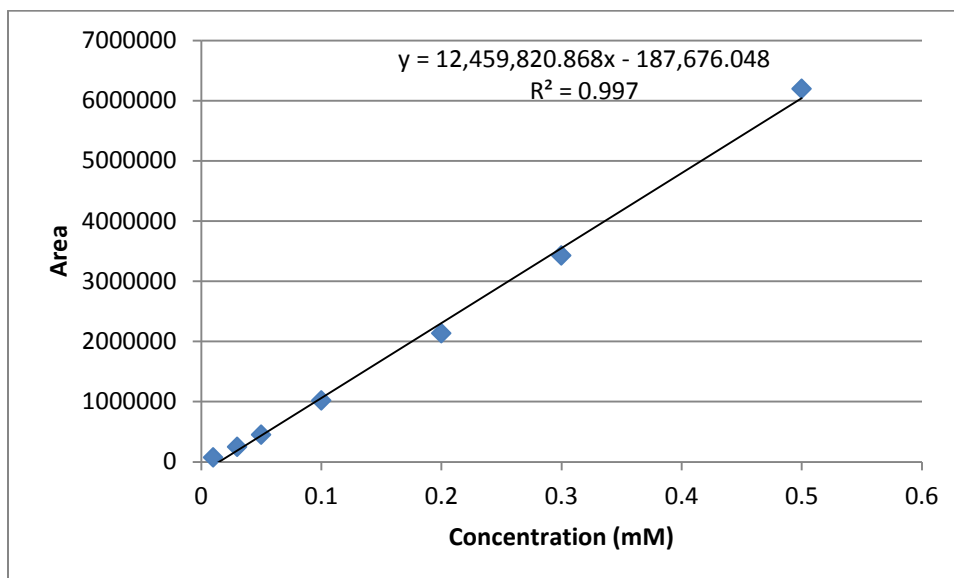


Figure A. 10 Benzidine calibration curve at 280 nm (HPLC)

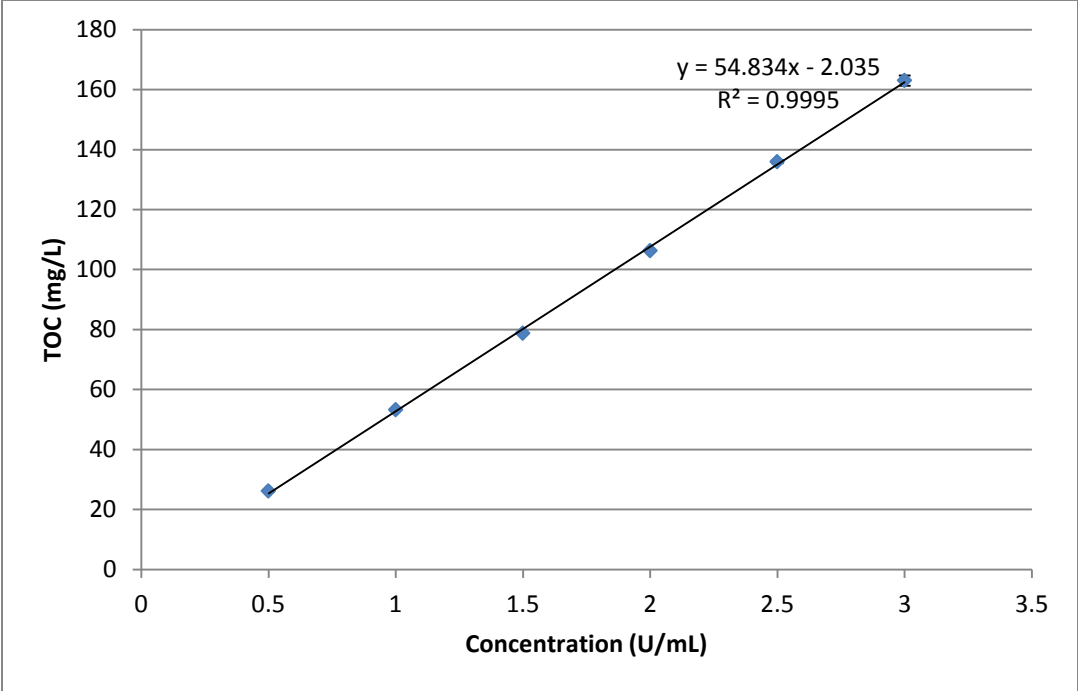


Figure A. 11 TOC (mg/L) for different enzyme concentrations (U/mL)

APPENDIX B. 3-ABS ENZYMATIC TREATMENT

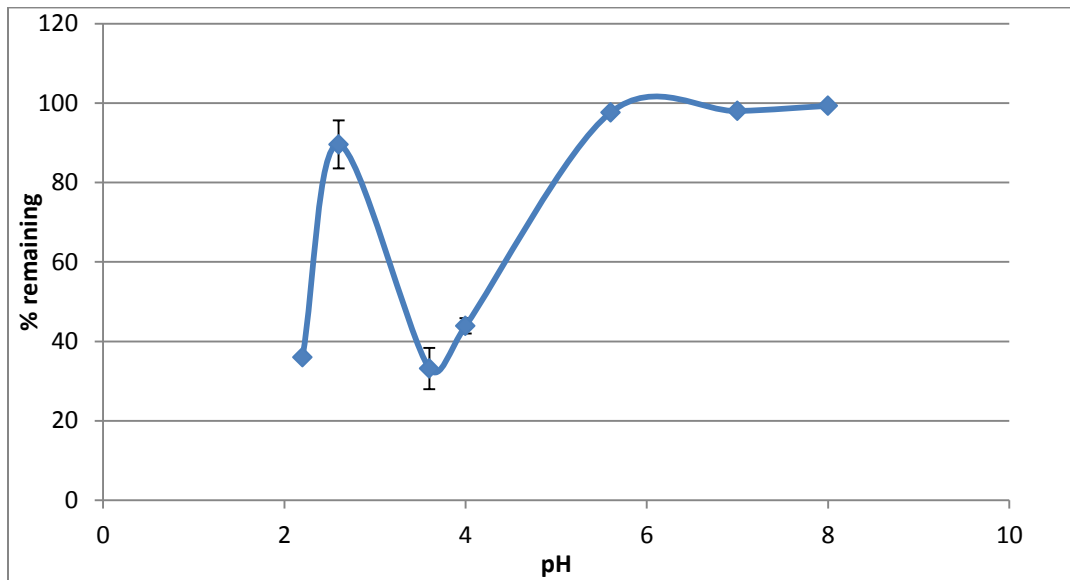


Figure B. 1 pH optimization of 1 mM 3-ABS with 1 mM H₂O₂ and 1 U/mL

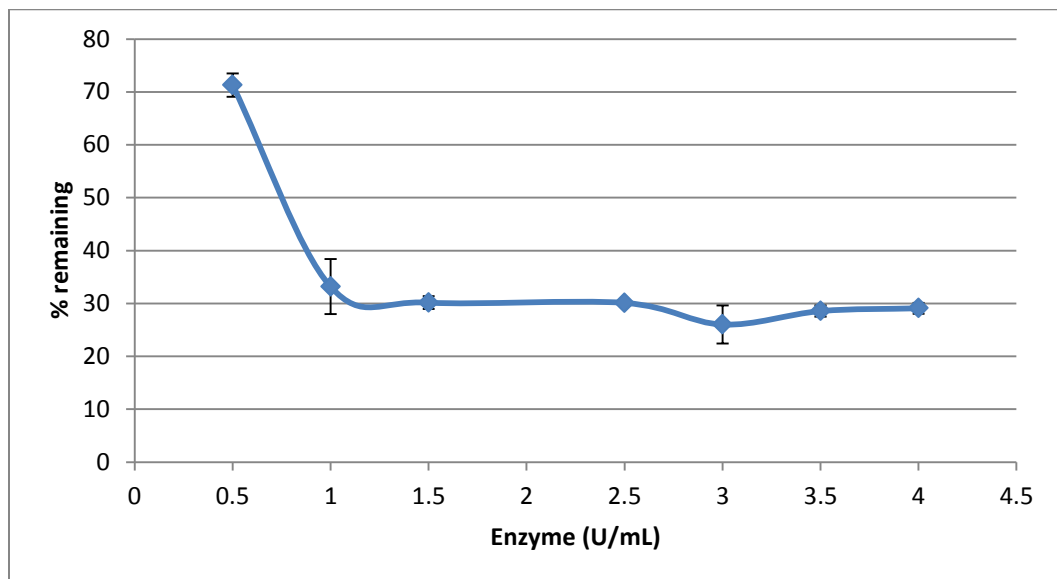


Figure B. 2 Enzyme optimization of 1 mM 3-ABS with 1 mM H₂O₂, pH 3.6

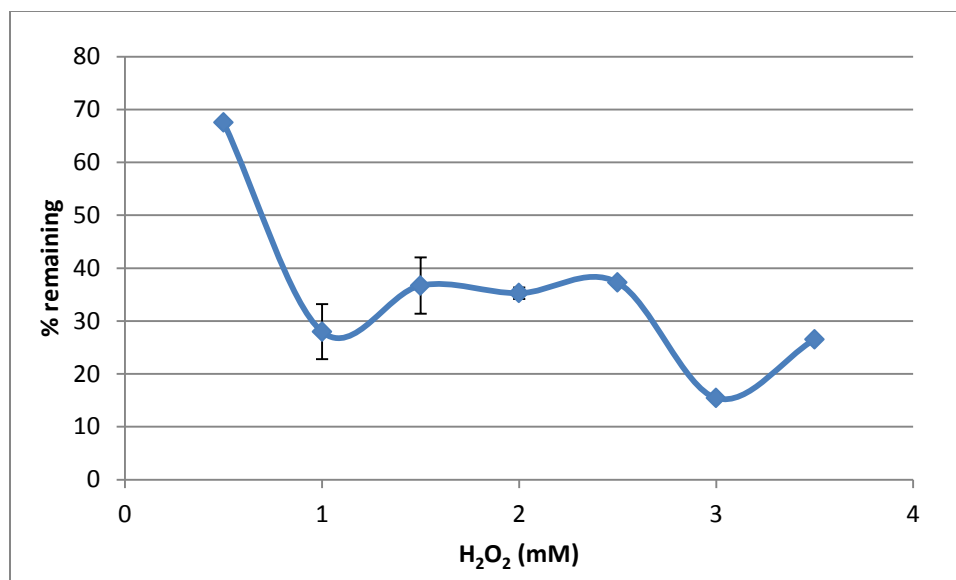


Figure B. 3 H₂O₂ optimization of 1 mM 3-ABS with 3 U/mL, pH 3.6

APPENDIX C. MINITAB EXPERIMENTAL RUNS

Table C. 1. Order for runs in first-order search for AB113

Run order	Central point	pH	H ₂ O ₂	enzyme
1	1	3.6	3.0	1.0
2	1	3.6	3.0	1.0
3	1	7.0	3.0	1.0
4	1	7.0	1.0	2.0
5	1	3.6	1.0	1.0
6	0	5.3	2.0	1.5
7	1	3.6	1.0	1.0
8	1	3.6	3.0	2.0
9	1	3.6	1.0	2.0
10	1	7.0	1.0	1.0
11	0	5.3	2.0	1.5
12	1	7.0	1.0	1.0
13	1	3.6	3.0	2.0
14	1	7.0	3.0	2.0
15	1	7.0	1.0	2.0
16	1	7.0	3.0	1.0
17	1	7.0	3.0	2.0
18	1	3.6	1.0	2.0
19	0	5.3	2.0	1.5

Table C. 2. Order for runs in Box-Behnken design with two replicates for AB113

Run order	pH	H ₂ O ₂	enzyme
1	5.3	2.0	1.5
2	7.0	2.0	2.0
3	5.3	1.0	1.0
4	5.3	2.0	1.5
5	5.3	2.0	1.5
6	5.3	3.0	1.0
7	5.3	2.0	1.5
8	5.3	3.0	2.0
9	3.6	2.0	1.0
10	3.6	3.0	1.5
11	7.0	3.0	1.5
12	7.0	2.0	2.0
13	5.3	1.0	2.0
14	3.6	1.0	1.5
15	7.0	3.0	1.5
16	5.3	2.0	1.5
17	7.0	2.0	1.0
18	3.6	2.0	2.0
19	3.6	2.0	2.0
20	3.6	1.0	1.5
21	7.0	2.0	1.0
22	3.6	2.0	1.0
23	3.6	3.0	1.5
24	7.0	1.0	1.5
25	5.3	1.0	2.0
26	5.3	3.0	2.0
27	5.3	2.0	1.5
28	5.3	1.0	1.0
29	5.3	3.0	1.0
30	7.0	1.0	1.5

Table C. 3. Order for runs in first-order search for AB113, second approach

Run order	Central point	pH	H ₂ O ₂	enzyme
1	1	3.60	3.00	1.00
2	1	4.45	2.00	1.50
3	1	5.30	3.00	2.00
4	1	5.30	3.00	1.00
5	1	5.30	3.00	1.00
6	0	3.60	3.00	1.00
7	1	5.30	3.00	2.00
8	1	5.30	1.00	1.00
9	1	4.45	2.00	1.50
10	1	3.60	1.00	2.00
11	0	4.45	2.00	1.50
12	1	5.30	1.00	2.00
13	1	5.30	1.00	1.00
14	1	3.60	3.00	2.00
15	1	5.30	1.00	2.00
16	1	3.60	1.00	2.00
17	1	3.60	3.00	2.00
18	1	3.60	1.00	1.00
19	0	3.60	1.00	1.00

Table C. 4. Order for runs in Box- Behnken design with two replicates for AB113, second approach

Run order	pH	H ₂ O ₂	enzyme
1	4.45	1.00	1.00
2	5.30	1.00	1.50
3	5.30	2.00	2.00
4	4.45	1.00	2.00
5	5.30	2.00	1.00
6	3.60	1.00	1.50
7	3.60	1.00	1.50
8	4.45	3.00	2.00
9	4.45	3.00	1.00
10	5.30	2.00	1.00
11	4.45	1.00	1.00
12	4.45	1.00	2.00
13	3.60	2.00	2.00
14	4.45	2.00	1.50
15	5.30	2.00	2.00
16	3.60	3.00	1.50
17	4.45	2.00	1.50
18	4.45	3.00	2.00
19	3.60	3.00	1.50
20	4.45	3.00	1.00
21	5.30	3.00	1.50
22	5.30	1.00	1.50
23	3.60	2.00	1.00
24	4.45	2.00	1.50
25	5.30	3.00	1.50
26	4.45	2.00	1.50
27	3.60	2.00	2.00
28	4.45	2.00	1.50
29	4.45	2.00	1.50
30	3.60	2.00	1.00

Table C. 5. Order for runs first-order search for DB38

RunOrder	pH	H ₂ O ₂	Enzyme
1	3.00	3.00	3.00
2	3.00	3.00	1.50
3	4.00	2.25	2.25
4	3.00	1.50	1.50
5	3.00	3.00	1.50
6	5.00	1.50	3.00
7	3.00	1.50	3.00
8	5.00	3.00	1.50
9	5.00	3.00	3.00
10	5.00	1.50	1.50
11	4.00	2.25	2.25
12	5.00	3.00	3.00
13	5.00	1.50	3.00
14	3.00	3.00	3.00
15	5.00	1.50	1.50
16	3.00	1.50	1.50
17	3.00	1.50	3.00
18	5.00	3.00	1.50

Table C. 6 Order for runs in Box-Behnken design with two replicates for DB38

Run order	pH	Enzyme	H ₂ O ₂
1	3.00	2.25	1.50
2	4.00	2.25	2.25
3	4.00	2.25	2.25
4	5.00	3.00	2.25
5	4.00	2.25	2.25
6	3.00	2.25	1.50
7	4.00	1.50	1.50
8	4.00	2.25	2.25
9	4.00	1.50	3.00
10	3.00	3.00	2.25
11	5.00	2.25	3.00
12	4.00	1.50	1.50
13	4.00	3.00	3.00
14	3.00	3.00	2.25
15	3.00	2.25	3.00
16	3.00	1.50	2.25
17	5.00	1.50	2.25
18	4.00	3.00	1.50
19	4.00	2.25	2.25
20	5.00	2.25	3.00
21	5.00	2.25	1.50
22	4.00	1.50	3.00
23	3.00	2.25	3.00
24	3.00	1.50	2.25
25	4.00	3.00	3.00
26	5.00	3.00	2.25
27	4.00	2.25	2.25
28	5.00	2.25	1.50
29	5.00	1.50	2.25
30	4.00	3.00	1.50

Table C. 7. Order for runs first-order search for DB38, second approach

Run order	Central point	pH	H ₂ O ₂	enzyme
1	1	3	3.5	2.5
2	1	4	3	3
3	1	3	3.5	3.5
4	1	4	3	3
5	1	5	3.5	2.5
6	0	3	2.5	3.5
7	1	3	2.5	2.5
8	1	3	3.5	3.5
9	1	5	2.5	2.5
10	1	5	2.5	2.5
11	0	4	3	3
12	1	3	2.5	3.5
13	1	5	3.5	3.5
14	1	3	2.5	2.5
15	1	5	2.5	3.5
16	1	5	3.5	2.5
17	1	3	3.5	2.5
18	1	5	3.5	3.5
19	0	5	2.5	3.5

Table C. 8. Order for runs in Box- Behnken design with two replicates for DB38, second approach

Run order	pH	H ₂ O ₂	enzyme
1	4	3	3
2	4	3	3
3	5	3	2.5
4	4	2.5	2.5
5	4	2.5	2.5
6	3	3.5	3
7	3	3	3.5
8	4	3	3
9	5	3	3.5
10	4	3.5	2.5
11	3	3	2.5
12	4	3	3
13	5	3	3.5
14	4	3.5	3.5
15	5	2.5	3
16	5	2.5	3
17	4	2.5	3.5
18	3	2.5	3
19	4	3	3
20	3	3	2.5
21	4	3.5	2.5
22	3	2.5	3
23	5	3.5	3
24	3	3.5	3
25	4	3.5	3.5
26	5	3.5	3
27	4	2.5	3.5
28	5	3	2.5
29	3	3	3.5
30	4	3	3

VITA AUCTORIS

NAME: Laura Gabriela Cordova Villegas

PLACE OF BIRTH: Chihuahua, México

YEAR OF BIRTH: 1987

EDUCATION: Chihuahua Autonomous University (UACH), B.Eng
Chihuahua, México 2009

CIMAV , M.Sc., Chihuahua, México 2013